THE JOURNAL
OF
CHEMICAL PHYSICS

VOLUME 17, NUMBER 3 MARCH, 1949

Thermodynamics of Crystallization in High Polymers. IV. A Theory of Crystalline States and Fusion in Polymers, Copolymers, and Their Mixtures with Diluents*

PAUL J. FLORY**
Research Laboratory, Goodyear Tire and Rubber Company, Akron 16, Ohio
(Received March 29, 1948)

The configurational entropy of a mixture of solvent and polymer molecules composed of segments connected by flexible bonds has been derived for the case in which the lattice they occupy contains limited regions of perfect order (i.e., the crystallites), which are reserved for occupancy by polymer segments exclusively. Although the derivation is carried out primarily for polymer chains of uniform length, modifications required for the treatment of heterogeneous polymers are included. An expression for the free energy of fusion ΔF_f of the semicrystalline mixture of polymer and solvent is derived assuming a vanLaar heat of mixing term.

The equilibrium (average) crystallite length ζ_e, derived by differentiation of ΔF_f, depends principally on the "nucleation parameter" D which, though it evades explicit evaluation from theory, represents the relative ease with which the first layer of a crystallite tends to form; ζ_e may depend to a lesser extent on the degree of crystallinity. The equilibrium degree of crystallinity, similarly deduced, depends primarily on the temperature. Fusion is predicted to occur over a range of temperatures, but the temperature T_m (the "melting point") at which crystallinity totally disappears is sharply defined. The melting range is predicted to be narrower the greater the chain length. If the degree of polymerization is greater than 100, the range (depending on the heat of fusion) for equilibrium melting should be quite narrow, as much as 75 percent of the fusion occurring within a few degrees of T_m. The dependence of the melting point on chain length is expressed approximately by a proportionality between the temperature depression given by $\Delta T_m = T_m^0 - T_m$, where T_m^0 is the melting point for infinite chain length and the reciprocal of the degree of polymerization.

Incorporation of a diluent should markedly broaden the melting range. If the degree of polymerization is very great, ΔT_m should be proportional to the number of moles of diluent per unit volume.

Extension of the treatment to random copolymers yields

$$1/T_m - 1/T_m^0 = (R/h_u)[-\ln X_A - \mu'(1-v_A)^2],$$

where h_u is the heat of fusion, μ' is the heat of mixing parameter, and X_A and v_A are the "mole" fraction and volume fraction, respectively, of the crystallizing structural unit in the copolymer. This expression is the exact analog of the freezing point relationship for "regular" binary mixtures of monomeric substances. Crystallinity in an ordered copolymer (the partial analog of an "irregular" solution) in which the structural units of a given type are arranged in long sequences should disappear at a temperature only slightly below T_m for the pure polymer. The phase rule cannot be applied to the crystal-amorphous transformation in polymers since the free energy per unit amount of the amorphous "phase" is not a unique function of the composition. Copolymers should melt over a wider temperature range and their crystallinity-temperature relationship is predicted to be sigmoid in character.

I. INTRODUCTION

AT the outset of the present series of investigations, crystallization induced by stretching polymers (such as vulcanized rubber) having a network structure seemed to be peculiarly amenable to theoretical attack in consideration of simplifications which enter as a result of the parallel orientation of crystallites formed under these circumstances. The first paper[1] of this series dealt with this problem. More recently, application of statistical-thermodynamical procedures to the general problem of crystallization in unoriented polymers has led to results which

* The work presented in this paper comprises a part of a program of fundamental research on rubber and plastics being carried out under contract between the Office of Naval Research and the Goodyear Tire and Rubber Company. Presented before the High Polymer Forum at the 112th Meeting of the American Chemical Society, New York, New York, September 16, 1947.
** Present address: Department of Chemistry, Cornell University, Ithaca, New York.

[1] Paul J. Flory, J. Chem. Phys. 15, 397 (1947).

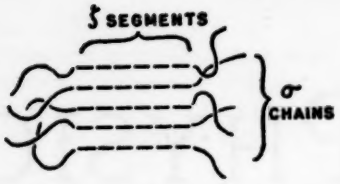

FIG. 1.

appear to be of considerably broader importance.[2] This latter investigation is the subject of the present paper. The generalizations which have been deduced suggest that a quantitative thermodynamic approach analogous to that universally employed in treating fusion and solubility behavior of simple molecules may be applied similarly to polymers and copolymers and to their mixtures with diluents.

As is clearly shown by the results of x-ray studies, the regularly repeating structural unit of a polymer plays a role in the crystalline state which is analogous to that of the monomeric molecule in its crystal lattice. The unit cell for a given crystalline polymer is occupied by a small number of structural units. The purposes of the present treatment can be accomplished without specifying the particular type of unit cell or the disposition of units within it. It is sufficient to consider merely that the structural units are arranged with perfect regularity (aside from normal fluctuations about their mean positions) in the crystallites so that the configurational entropy may be regarded as zero.

All crystalline high polymers (certain proteins excepted) retain some amorphous material interspersed with the crystallites. The breadth of the layer lines in x-ray diffraction patterns for crystalline polymers of high molecular weight indicate that the crystallites often are much shorter in length than the polymer molecules. A single molecule may therefore pass through several crystallites separated by amorphous regions. The formation of a molecular lattice in which the ends of molecules occur in regularly situated planes quite clearly cannot be expected for high polymers, owing to the non-uniformity of the chain length and its great (average) magnitude.

The essential features of the crystallite as required for the present treatment are shown schematically in Fig. 1. The state of the unoriented semicrystalline polymer will be defined by the percentage crystallinity and the average dimensions of the crystallites. Lateral dimensions of a crystallite should be independent of the molecular size and regularity of the polymer chain; they may be expected to depend principally on the kinetic factors governing crystallite growth and, under ideal crystallization conditions, they may be relatively very large. The longitudinal dimension, however, will depend on the structural regularity, i.e., on the regularity with which the crystallizing unit is repeated successively along the chain. The specific variables chosen to characterize the semicrystalline state of the polymer are, therefore, the degree of crystallinity $(1-\lambda)$ and the crystallite length (ζ).

An attempt to treat the general problem of crystallization in polymers was presented several years ago by Frith and Tuckett.[3] Their theoretical development, in common with the one given in this paper, was based on the lattice treatment[4,5] of polymer configurations. They erred, however, in employing relationships for the entropy of the amorphous chain elements which failed to take into consideration the fact that these elements are attached to the ends of crystallites. The same basic error persists in the extension of this treatment presented by Richards.[6] Their results, however, bear nominal similarity to certain of the deductions included here.

II. PRINCIPAL THEORETICAL DERIVATIONS

The primary exposition of the theory will be concerned with linear polymers composed exclusively of identical structural units, which will be designated as "A units." In a later section of the paper the theory will be extended to include copolymers containing both A and B units, the latter being incapable of entering the crystal lattice characteristic of the A units. In any case, x will represent the total number of structural units in a polymer molecule. Although all polymer molecules are assumed to be of equal length, it will be evident that the essentials of the theory may be applied also to non-homogeneous poly-

[2] A preliminary note pertaining to melting point relationships derived by a simplified version of the present treatment has been published: Paul J. Flory, J. Chem. Phys. 15, 684 (1947).

[3] E. M. Frith and R. F. Tuckett, Trans. Faraday Soc. 40, 251 (1944).

[4] Maurice L. Huggins, J. Phys. Chem. 46, 151 (1942); Ann. N. Y. Acad. Sci. 43, 1 (1942).

[5] Paul J. Flory, J. Chem. Phys. 10, 51 (1942); 12, 425 (1944).

[6] R. B. Richards, Trans. Faraday Soc. 41, 127 (1945).

mers, the number average degree of polymerization $\bar{x}_n$ replacing x.

Definitions and Assumptions

The structure of the polymer is adequately specified by the number and kinds of repeating units, but the configuration of the chain in the liquid state, and hence the entropy change associated with fusion, depends also on their size and flexibility. In analogy with accepted statistical-thermodynamical treatments of rubber elasticity, of chain configurations, and properties of polymer solutions, it is convenient to treat the configurational problem in terms of segments. The segment length l is to be so chosen that a hypothetical chain of the same over-all length, but comprised of rigid segments of this length l connected together by completely flexible bonds, would duplicate as closely as possible the configuration of the actual chain. The configurational segment will not correspond in general to the repeating structural unit. In decamethylene adipate, the repeating structural unit of which possesses eighteen chain atoms, for example, the segment surely will be much smaller than the unit. It will be necessary, therefore, to distinguish configurational segments from repeating structural units.

Primed symbols will be used to denote segments; e.g., x' will represent the number of segments per molecule. Letting z represent the number of segments per structural unit,

$$x' = zx.$$

A liquid solvent may be present with the amorphous polymer, but it is assumed to be excluded from the crystallites. The volume fraction of polymer in the composite of crystallites and amorphous material (including solvent) will be represented by v_2. The ratio of the molar volume of the solvent to the volume of a segment (or lattice cell) will be represented by z_s.

Further definitions are as follows:

n = number of solvent molecules.
$n' = z_s n$ = number of lattice (cf. seq.) cells occupied by solvent molecules.
N = number of polymer molecules.
ν = number of crystallites.
σ = number of chains in a cross section of a crystallite.
$m = \nu\sigma$ = total number of crystalline sequences.
ζ = length (average) of crystallite in number of units.
$\zeta' = z\zeta$ = length of a crystallite in number of segments.
$m\zeta$ = total number of crystalline units.
$v_1 = n'/(n'+x'N)$ = volume fraction of solvent in the entire mixture (i.e., disregarding exclusion of solvent from crystalline regions).
$v_2 = x'N/(n'+x'N)$ = volume fraction of polymer.
$\lambda = (xN-\zeta m)/xN$ = fraction of the polymer in the amorphous, or liquid, state.

Principal assumptions are the following:

(a) It is assumed that the properties of the liquid polymer can be described in terms of a pseudo-lattice having a coordination number γ, each cell of the lattice being of a size to accommodate one segment. The lattice, of course, is employed as a convenient artifice. Most of the ultimate deductions appear to be largely independent of the physical reality of the liquid lattice itself. In particular, the mixing law[5]

$$\Delta S_{\text{mixing}} = -R[n \ln v_1 + N \ln v_2] \qquad (1)$$

is assumed to apply. If solvent is present, solutions are assumed to be not so dilute as to cause serious departures from this relationship.[7]

(b) Entropies associated with the subdivision of the crystalline material into numerous crystallites and with their random orientation are neglected.

(c) Chain ends are assumed to be excluded from the crystal lattice. This assumption is an arbitrary one, the principal justification for which is the apparent lack of any other tangible means of introducing the influence of finite molecular weight (see Discussion). Doubtless it is violated in many cases.[8] Its significance obviously vanishes for high molecular weight polymers.

(d) Crystalline and amorphous regions are assumed to be sharply differentiable in the equilibrium state. Intermediate arrangements of the structural units in a semi-ordered condition of the type discussed by Baker and Fuller[9] are considered to represent non-equilibrium situations. This is the most important postulate and probably also the one most open to question on

[7] Paul J. Flory, J. Chem. Phys. 13, 453 (1945).
[8] R. D. Evans, H. R. Mighton, and P. J. Flory, J. Chem. Phys. 15, 685 (1947).
[9] W. O. Baker and C. S. Fuller, J. Am. Chem. Soc. 65, 1120 (1943); Baker, Fuller, and Pape, *ibid.* 64, 776 (1942).

the basis of concepts current at the present time regarding the nature of crystallinity in high polymers.

The Entropy of Fusion for Molecules of Uniform Length

The configurational entropy is derived in a manner paralleling the lattice treatment of polymer solutions.[4,5,10] At the outset, let all of the polymer and solvent molecules be joined together in random sequence to form a single linear chain. The number of different arrangements of the n solvent and N polymer molecules in the chain will be[11]

$$(n+N)!/n!N!$$

which corresponds to an entropy

$$S_1=k\{-n\ln[n/(n+N)] - N\ln[N/(n+N)]\}. \quad (2)$$

The solvent molecules are assumed to be of such a nature that their structures can be approximated by one or more linearly connected segments of the same size as the polymer chain segments. Before inserting the above chain into the lattice, certain regions of the lattice are set aside for accupancy by crystalline polymer. The entropy associated with the random locations and orientations of the crystallites is neglected, in accordance with assumption (b).

The above chain is then introduced into the lattice, one segment at a time, each segment being free to occupy any vacant cell surrounding the cell occupied by the preceding segment of the chain, *except in the regions reserved for the crystallites* where a special set of rules must be applied. A chain may enter (or leave) a crystalline region only at the ends, i.e., at the faces of the crystallite which are transverse to the chain axes. When, in the course of introducing successive segments of the continuous chain into the lattice, a segment falls in an unoccupied cell of the end layer of cells reserved for a crystallite, the succeeding $\zeta'-1$ segments of the chain must be assigned to the linear sequence of cells extending to the opposite end of the crystallite. No choice of location is allowed these $\zeta'-1$ segments and, according to the above rule, no previously added segments will be encountered in this sequence. On reaching the opposite end of the crystallite, the chain is again free to meander randomly through the amorphous region until another (or the same) crystallite is encountered, etc.

The entropy arising from the numerous configurations available in the lattice to the single chain (which fills the entire lattice) can be deduced according to the methods employed in the previously published lattice treatments[5] of liquid polymers and their mixtures.[12] For each segment which is situated in a region of the lattice where its location relative to that of its immediate predecessor is not predetermined, there will be an entropy contribution amounting to $k\ln[(\gamma-1)/e]$, where γ is the lattice coordination number. All segments enjoy this freedom except those beyond the first within a crystalline sequence. Hence, the configurational entropy of the continuous chain will be

$$S_2=k[n'+x'N-(\zeta'-1)m]\ln[(\gamma-1)/e]. \quad (3)$$

A given arrangement of the above chain will be acceptable only in the event that every crystalline sequence is filled exclusively by polymer segments, and that the ends of polymer molecules do not in any case occur within a crystallite. If the repeating unit is composed of more than one segment ($z>1$), all of the cells in a given layer of a crystallite must be occupied by corresponding segments. If, for example, the unit possesses regularly occurring polar groups, these must be arranged in planes in the manner prescribed by the nature of the crystal lattice.

The probability W_3 that the above conditions are fulfilled will equal the ratio of the total number of ways m sequences ζ units in length may be assigned to the N independent polymer molecules divided by the total number of all possible arrangements of the m sequences along the single chain comprised of all polymer and solvent molecules. The latter number is easily expressed as a ratio of factorials, but the former consists of an unwieldy sum of products difficult to evaluate in closed form. An acceptable approximation to W_3 may be deduced as follows. The probability that the first cell of a given crystalline sequence of cells is occupied by

[10] W. J. C. Orr, Trans. Faraday Soc. **40**, 320 (1944); **43**, 12 (1947).

[11] The individual polymer molecules are considered to be indistinguishable, in harmony with usual practice in statistical mechanics. While this convention is essentially arbitrary, its adoption permits subsequent use of Eq. (8) for the entropy of the totally liquid mixture previously derived (see reference 5) under the same convention.

[12] See, in particular, J. Chem. Phys. **10**, 53 (1942), Eq. (7), in which the total number N of polymer molecules is to be set equal to zero.

polymer and that it is occupied by the proper segment of the structural unit of the polymer will equal the volume fraction v_2 of polymer divided by the number z of segments per structural unit. Assuming that $m \ll x'N$, the probability that the initial cell of every crystal sequence is so occupied will be given by $(v_2/z)^m$.

Having established that the end cell of a sequence is occupied by a proper polymer segment, the probability that the end of the molecule involved does not occur within the sequence (although it may coincide with the end of the sequence) will be given by

$$(x-\zeta+1)/x.$$

In the present approximation, the probability P_3 that the same is true for *all* of the crystal sequences is assumed to be equal to this quantity raised to the power m; i.e.,

$$P_3=[(x-\zeta+1)/x]^m. \tag{4}$$

This expression is accurate, however, only when the degree of crystallinity is small. The probability that a given sequence does not contain the end of a molecule is not altogether independent of the status of other sequences; if a large fraction of the polymer is known to occupy certain crystalline regions in the required manner, the probability that some other sequence of cells through a crystallite is similarly occupied will be less than $(x-\zeta+1)/x$. Hence, Eq. (4) is strictly valid only at incipient crystallization; it may be presumed to afford a satisfactory approximation up to moderate degrees of crystallinity, however.

The over-all probability that the crystallites are suitably occupied by polymer molecules will be given by

$$W_3=(v_2/z)^m P_3.$$

Substituting the appropriate expression for v_2 and the above approximation for P_3,

$$S_3=km\{\ln[x'N/(n'+x'N)z] + \ln[(x-\zeta+1)/x]\}. \tag{5}$$

In order to achieve the state corresponding to the actual semicrystalline solution, it remains to sever the temporary linkages between the molecules comprising the continuous chain which occupies the entire lattice. Existence of the chain imposes the requirement that each end of a molecule (polymer or solvent) shall occupy a lattice cell adjacent to another end of a molecule. After these connections are removed, the ends of molecules are free to assume independent locations within the amorphous region.

We shall consider the probability of the reverse process, namely, the pairing off of ends of molecules. The probability that the set of molecular ends, which are free to assume any distribution of lattice sites, will spontaneously occur in a configuration in which every end of a molecule is paired with the end of another molecule, the two ends occupying adjacent lattice sites, is [13]

$$W_4^{-1}=\left[\frac{(n+N-1)(\gamma-1)}{n'+x'N-\zeta'm}\right]\left[\frac{(n+N-2)(\gamma-1)}{n'+x'N-\zeta'm}\right] \cdots \left[\frac{(\gamma-1)}{n'+x'N-\zeta'm}\right] \cong (n+N)! \times[(\gamma-1)/(n'+x'N-\zeta'm)]^{(n+N)}.$$

Hence,

$$S_4=-k\{(n+N)\ln[(\gamma-1)/e] + (n+N)\ln[(n+N)/(n'+x'N-\zeta'm)]\}. \tag{6}$$

The configurational entropy S_c of the semicrystalline polymer-solvent mixture is obtained by combining Eqs. (2), (3), (5), and (6).

$$\begin{aligned} S_c &= S_1+S_2+S_3+S_4 \\ &= k\{-n\ln[n/(n'+x'N-\zeta'm)] \\ &\quad -N\ln[N/(n'+x'N-\zeta'm)]+[n(z_s-1) \\ &\quad +N(x'-1)-m(\zeta'-1)]\ln[(\gamma-1)/e] \\ &\quad +m\ln[(x-\zeta+1)/x]+m\ln[x'N/(n' \\ &\qquad +x'N)z]\}. \end{aligned} \tag{7}$$

The entropy S_l of the totally non-crystalline solution obtained by setting $m=0$ is identical with the previously derived[5] expression for solvent-polymer mixtures, i.e.,

$$\begin{aligned} S_l &= k\{-n\ln[n/(n'+x'N)] \\ &\quad -N\ln[N/(n'+x'N)]+[n(z_s-1) \\ &\quad +N(x'-1)]\ln[(\gamma-1)/e]\}. \end{aligned} \tag{8}$$

The entropy difference between the totally liquid solution and the semicrystalline mixture, this difference being referred to somewhat er-

[13] Here we consider that the two ends of each molecule are differentiable, i.e., the symmetry number is 1 rather than 2. In the pairing of chain ends to form a continuous chain, ends of opposite character are assumed to be selected for each pair. Otherwise, each molecule could occur with two alternate orientations in the chain, and an inconsequential term $R(n+N)\ln 2$ would be added to the entropy.

roneously (cf. seq.) as the entropy of fusion ΔS_f, can be expressed as follows:

$$\Delta S_f = S_l - S_c = \zeta m s_u - k\{(n+N)\ln[(n'+x'N - \zeta' m)/(n'+x'N)] + m\ln[Dx'N/(n'+x'N)] + m\ln[(x-\zeta+1)/x]\}, \quad (9)$$

where

$$s_u = kz\ln[(\gamma-1)/e] \quad (10)$$

and

$$D = (\gamma-1)/ze. \quad (11)$$

A term-by-term examination of Eq. (9) suggests certain extensions and generalizations. The first term, wherein s_u represents an entropy of fusion per structural unit, ordinarily will dominate all others in magnitude. In deriving Eq. (9) the entire entropy change has been assumed to be configurational. Entropy contributions from changes in internal motions of the structural units and their oscillations with respect to their neighbors should be included. Since the magnitude of these contributions to the entropy of fusion can be assumed to be proportional to the number of structural units melted, they may be included in Eq. (9) merely by redefining s_u as follows:

$$s_u = kz\ln[(\gamma-1)/e] + s_i, \quad (12)$$

where s_i represents the non-configurational entropy changes. Terms other than the first in Eq. (9) vanish for low degrees of crystallinity in the absence of solvent if both the molecules and the crystallites are exceedingly long (i.e., $1 \ll \zeta \ll x$). Under these conditions s_u represents the total entropy of fusion per structural unit.

The second term in Eq. (9) expresses the entropy gain from the increased volume available after melting to the (n) solvent molecules and the ends of the (N) polymers.

The third term, which may be written $-km\ln(v_2D)$, represents an entropy of nucleation (rather, the negative thereof); the parameter D will be referred to as the nucleation constant. This becomes evident from a consideration of the formation within the totally non-crystalline solution of a crystallite nucleus consisting of *m equivalent* segments of adjacent molecules, these segments occupying a planar array of contiguous lattice sites. The probability of the spontaneous occurrence of such a constellation is $(v_2/z)^m$ as previously pointed out in deriving S_3. It is to be noted further that in the derivation of S_2 the occupation of the first lattice site of each crystalline sequence is implicitly considered to impose no configurational order on the form of the molecule. Hence, owing to the manner in which s_u has been defined, a term $km\ln[(\gamma-1)/e]$ remains. On combining this residue with $k\ln[(v_2/z)^m]$, the third term in Eq. (9) is obtained.

The tacit assumption (see also assumption (d)) that the internal order changes abruptly from crystalline to complete randomness within one layer of lattice cells at the end of a crystallite is inherently fallacious. Such a sharp disappearance of order cannot occur in the lattice model, and this aspect of the model probably holds for the actual polymer as well. Some degree of order may persist for several layers beyond the end of a crystallite. Neglecting the probable further dependence of this tendency on dilution, the entropy of fusion should on this account be corrected by the amount

$$km\ln d,$$

where d is some constant greater than unity. This correction can be incorporated in the entropy of fusion function through the following redefinition of D:

$$D = (\gamma-1)/zed. \quad (11')$$

It is to be noted that if the polymer contains regularly occurring polar groups such as may tend to associate in the liquid state, the probability of the nuclear array is likely to be greater than $(v_2/z)^m$. The effects of such departures from random disorder in the liquid state may be taken into account by altering z in Eq. (11'). With these various qualifications, it is apparent that the parameter D is beyond the scope of prediction according to the present theory. It is, however, a convenient repository for many of the expected deviations from the inevitable simplifications introduced in a treatment of this sort. The product v_2D, as will be shown later, assumes critical importance in regard to crystallite length at equilibrium.

The fourth term in Eq. (9) expresses the principal consequence of the requirement (assumption (c)) that the ends of molecules shall be excluded from the crystallites.

On re-defining n, N, m, and s_u to represent molar quantities, the entropy of fusion can be expressed in terms of the volume fraction v_2 of polymer, the fractional amount λ of the polymer

which is in the amorphous condition and the crystallite length ζ.

$$\Delta S_f/xN=(1-\lambda)s_u-R[(z/z_s)(1-v_2)/v_2 +1/x]\ln[1-v_2(1-\lambda)]-R[(1-\lambda)/\zeta] \times\{\ln(v_2D)+\ln[(x-\zeta+1)/x]\}. \quad (13)$$

Both melting and dilution are involved in the process covered by ΔS_f, to which the term "entropy of fusion" is somewhat inaccurately applied. Solvent occurs in admixture with the polymer in both initial and final states; hence, the conventional segregation of the melting and the dissolving processes cannot be applied here. In a more literal sense, the entropy of *fusion* of the semicrystalline polymer is represented by Eq. (13) when n (and n') is zero. Even so, ΔS_f is not a unique characteristic of the substance, but depends on the degree of crystallinity and the dimensions of the crystallites.

Effects of Non-Uniformity in Chain Length and Crystallite Length

If the molecules vary in length according to the "most probable distribution"[14] defined by

$$w_x=x(1-p)^2p^{x-1}, \quad (14)$$

where w_x is the weight fraction of species composed of x units, and p is a parameter representing the probability of continuation of the chain from one unit to the next, P_3 as defined by Eq. (4) requires revision; other terms in the previous development require no alteration. The probability that the ζ units occupying a given sequence of lattice cells running through one of the crystallites are connected in a continuous chain uninterrupted by the termination of a molecule is $p^{\zeta-1}$. If the extent of crystallization is very small, the same probability can be employed for every sequence, and

$$P_3=p^{m(\zeta-1)}. \quad (4')$$

Larger molecules are selectively chosen to occupy the sequences of cells within crystallites. Hence, as the degree of crystallization advances, the probability that an additional crystalline sequence is properly occupied may decrease substantially below $p^{\zeta-1}$, and Eq. (4') is no longer valid. Indiscriminate use of Eq. (4') for higher degrees of crystallinity is tantamount to the assumption that the molecules may share their units with one another through a re-shuffling process so as to accommodate an excessive number of long sequences. If this erroneous assumption were employed, Eq. (14) would, in effect, merely govern the probability of various distortions of the distribution and not the distribution itself.

For low degrees of crystallinity and for values of ζ not much larger than the average of x, the above expression for P_3 should be satisfactory. The entropy of fusion of the heterogeneous polymer conforming to the above distribution may then be written

$$\Delta S_f/xN=(1-\lambda)s_u-R[(z/z_s)(1-v_2)/v_2 +1/\bar{x}_n]\ln[1-v_2(1-\lambda)]-R[(1-\lambda)/\zeta] \times[\ln(v_2D/p)+\zeta\ln p]. \quad (13')$$

The correspondence between this equation and Eq. (13) for homogeneous polymers becomes evident by substituting

$$p=1-1/\bar{x}_n$$

which follows from the distribution (14), $\bar{x}_n$ representing the number average degree of polymerization. Then, for $(\zeta-1)\ll\bar{x}_n$,

$$\zeta\ln p=\ln(1-1/\bar{x}_n)^\zeta\cong\ln[(\bar{x}_n-\zeta+1)/\bar{x}_n].$$

Substitution of this expression in Eq. (13') yields an entropy equation equivalent to (13) with x replaced by $\bar{x}_n$. Thus, in the case of sufficiently short crystallites the two entropy expressions are equivalent to one another.

Non-uniformity in crystallite length affects none of the terms entering into the derivation of Eqs. (9) and (13) except P_3. All other considerations depend merely on the number m of crystalline sequences or on the total number ζm of crystalline units. So far as these terms are concerned, ζ and ζ' could be replaced with their number averages. For polymers of uniform chain length, P_3 is not easily formulated if the crystallites are of random length. If the chains are of random length, Eq. (4') is applicable regardless of the crystallite length distribution. We may conclude that no serious departures from the theory may be expected to arise from non-uniformity of crystal length, provided the degree of crystallinity is not large.

The Free Energy of Fusion

The heat change accompanying disappearance of crystallinity in the semicrystalline mixture of polymer and solvent consists of two parts: the

[14] Paul J. Flory, J. Am. Chem. Soc. 58, 1877 (1936); 64, 2205 (1942).

heat of fusion proper, $\Delta H_{f'}$, referring solely to the melting of the crystallites and the heat of mixing, ΔH_m, of the previously crystalline polymer segments with the surrounding polymer solution. As a first approximation, $\Delta H_{f'}$ might be assumed to be proportional to the number of crystalline units, i.e.,

$$\Delta H_{f'} = \zeta_m h_u,$$

where h_u is the heat of fusion per structural unit. No account would then be taken of the lower interaction energy which in general can be expected between units occurring in terminal layers of the crystallites, nor of a possible contribution (presumably opposite in magnitude) to the heat of fusion arising from the persistence of order extending somewhat beyond the ends of the crystallites (see above). A better approximation is afforded by

$$\Delta H_{f'} = \zeta m h_u - m h_e, \tag{15}$$

where h_e represents the deficiency per terminal layer unit in the heat of fusion.

If the heat of dilution of the liquid polymer with solvent can be expressed in the van Laar form,

$$\Delta H_m = BV(z_s/z)n(v_2 - v_2'),$$

where B is the "cohesive energy density" constant, V is the molar volume of a polymer structural unit ($z_s V/z$ being the molar volume of the solvent), and v_2' is the volume fraction concentration of polymer in the amorphous regions prior to fusion, i.e.,

$$v_2' = v_2\lambda/(1 - v_2 + v_2\lambda),$$

then

$$\Delta H_m = BV(nz_s/z)v_2(1-v_2) \times (1-\lambda)/(1-v_2+v_2\lambda) \tag{16}$$

and

$$\Delta H_f/xN = (\Delta H_{f'} + \Delta H_m)/xN = (1-\lambda)(h_u - h_e/\zeta) + BV(1-v_2)^2(1-\lambda)/(1-v_2+v_2\lambda). \tag{17}$$

The free energy change accompanying the fusion process will be given by

$$\Delta F_f = \Delta H_f - T\Delta S_f. \tag{18}$$

Substituting in Eq. (18) from Eqs. (13) and (17),

$$\Delta F_f/xN = (1-\lambda)(h_u - Ts_u) + RT\{[(z/z_s) \times (1-v_2)/v_2 + 1/x]\ln[1-v_2(1-\lambda)] + [(1-\lambda)/\zeta][\ln(v_2 D) + \ln((x-\zeta+1)/x)] + \mu(1-v_2)^2(1-\lambda)/(1-v_2+v_2\lambda)\}, \tag{19}$$

where [15]

$$\mu = BV/RT,$$

and D has again been redefined, this time as follows:

$$D = (\gamma - 1)/zde^{1+h_e/RT}. \tag{11''}$$

Thus the crystallite end correction in ΔH_f as expressed by Eq. (15) can be conveniently incorporated in the parameter D along with other uncertain quantities.

The free energy of fusion for the heterogeneous polymer will differ from that given by Eq. (19) in that x is replaced by $\bar{x}_n$ and the second term in brackets must be replaced by

$$[(1-\lambda)/\zeta][\ln(v_2 D/p) + \zeta \ln p]$$

in accordance with Eq. (13') for the entropy of fusion. This term alternatively may be written with negligible approximation except when $\bar{x}_n$ is small (i.e., except when p is considerably less than unity) as follows:

$$[(1-\lambda)/\zeta][\ln(v_2 D) - (\zeta - 1)/\bar{x}_n].$$

III. DEDUCTIONS FROM THE FREE ENERGY OF FUSION FUNCTION

Equilibrium Crystallite Length

The free energy of fusion, ΔF_f, may be regarded as the negative of the free energy of the semicrystalline polymer relative to the totally liquid state. The most stable semicrystalline state, therefore, is that for which ΔF_f assumes its *maximum* value, subject to such restraints as may be imposed on the system. For the purpose of exploring the dependence of ΔF_f on the crystallite length ζ, the function for homogeneous polymers (Eq. (19)) may be differentiated as follows:

$$(1/xN)(\partial \Delta F_f/\partial\zeta)_\lambda = -RT[(1-\lambda)/\zeta^2] \times \{\ln(v_2 D) + \ln[(x-\zeta+1)/x] + \zeta/(x-\zeta+1)\}. \tag{20}$$

Setting the derivative equal to zero in order to locate maxima and minima in ΔF_f, there is

[15] The above definition of μ differs somewhat from that previously employed in polymer solution theory (references 4 and 5. In particular, V represents the molar volume of a polymer *unit* and not the molar volume of the solvent.

obtained

$$-\ln(v_2D)=\zeta_e/(x-\zeta_e+1)+\ln[(x-\zeta_e+1)/x] \quad (21)$$

$$=(1/x)\left[1+\left(\frac{\zeta_e-1}{x}\right)\left(\frac{\zeta_e+1}{2}\right)+\left(\frac{\zeta_e-1}{x}\right)^2\left(\frac{2\zeta_e+1}{3}\right)+\cdots\right] \quad (21')$$

$$\cong 1/x+(\tfrac{1}{2})(\zeta_e/x)^2+(\tfrac{2}{3})(\zeta_e/x)^3\cdots, \quad (21'')$$

where ζ_e represents the equilibrium value of the crystallite length. Failure of the degree of crystallinity $1-\lambda$ to appear in Eq. (21) is a consequence of the approximate expression employed for S_3 in the derivation of ΔS_f above. Further consideration of the nature of the errors involved in this approximation indicates that ζ_e should be substantially independent of λ for low degrees of crystallinity, but that it may change markedly at very high degrees of crystallization. This limitation on the use of Eq. (21) may be more abstract than real, for achievement of true equilibrium conditions experimentally at high degrees of crystallization is likely to be prohibitively difficult. In any event, Eq. (21) is exact at incipient crystallization (within the limitations of other approximations employed in the present theory), and it should afford a satisfactory approximation generally up to moderate degrees of crystallinity.

If v_2D is less than unity,[16] Eq. (21) possesses a single solution in the physically significant range, $1\leqq\zeta\leqq x$. This solution represents a maximum in ΔF_f, corresponding to a condition of maximum stability. In Fig. 2 the equilibrium crystallite length ζ_e computed from Eq. (21) is plotted against v_2D for $x=100$. The value of ζ_e is increased by either a decrease in the nucleation parameter D, or an increase in the dilution (decrease in v_2). The nature of the dependence of ζ_e on x for a given value of v_2D is evident from the series expansions shown in Eqs. (21') and (21''); ζ_e is approximately proportional to x for large values of x.

If v_2D exceeds unity, $(\partial\Delta F_f/\partial\zeta)_\lambda$ as given by Eq. (20) is negative throughout the permissible range of ζ. Hence, it is indicated that the "crystallites" will assume the shortest possible length, i.e., $\zeta_e=1$. This degenerate crystalline condition, in which longitudinal order has all but disappeared and only lateral order remains, probably never is realized in actual polymers. Random association of segments doubtless would supersede such a state in cases where statistical and energy factors do not favor longitudinal order. We conclude, therefore, that the polymer will remain non-crystalline at equilibrium if circumstances are such as to make ΔF_f larger for $\zeta=1$ than for any other permissible value.

Differentiating the modified free energy expression for heterogeneous polymers having the most probable distribution,

$$(1/xN)(\partial\Delta F_f/\partial\zeta)_\lambda=-RT[(1-\lambda)/\zeta^2]\ln(v_2D/p)\cong -RT[(1-\lambda)/\zeta^2][\ln(v_2D)+1/\bar{x}_n]. \quad (20')$$

If v_2D is less than unity, Eq. (20') predicts that ζ_e shall be infinite. We conclude that the first crystals formed from the heterogeneous polymer will be extremely long at equilibrium. Since the polymer contains only a limited proportion of molecules many times larger than $\bar{x}_n$, the occurrence of appreciable degrees of crystallinity will necessitate diminution of ζ to a value not more than several times $\bar{x}_n$. If v_2D exceeds unity (more accurately, if v_2D/p exceeds unity), ζ_e will assume the value unity as in the case of homogeneous polymers.

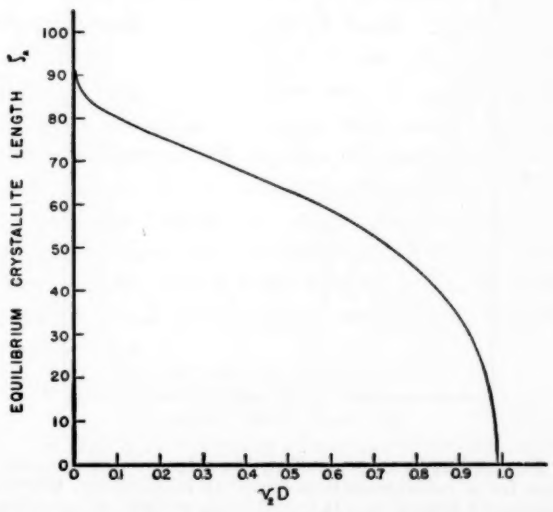

FIG. 2. Equilibrium crystallite length at incipient crystallization as a function of v_2D for chains of uniform chain length ($x=100$).

[16] Accurately stated, for $v_2D<\exp(-1/x)$ Eq. (21) possesses a single solution in the physically significant range. The statement in the text above is made on the presumption that x is very large.

Equilibrium Degree of Crystallinity

The free energy function (19) for homogeneous polymers possesses at most a single maximum with respect to λ within the permitted range $0 \leqq \lambda \leqq 1$; no minima are encountered. Differentiating the function with respect to λ,

$$(1/xN)(\partial \Delta F_f/\partial \lambda)_\xi = -(h_u - Ts_u) + RT\left\{\left[\frac{(z/z_s)(1-v_2)+v_2/x}{1-v_2(1-\lambda)}\right] - (1/\zeta)\ln(v_2 D) - (1/\zeta)\ln[(x-\zeta+1)/x] - \mu\left[\frac{1-v_2}{1-v_2(1-\lambda)}\right]^2\right\}, \quad (22)$$

which through substitution from Eq. (20) may be converted to the convenient alternate form,

$$(1/xN)(\partial \Delta F_f/\partial \lambda)_\xi = -(h_u - Ts_u) + RT\left\{\frac{(z/z_s)(1-v_2)+v_2/x}{1-v_2(1-\lambda)} + 1/(x-\zeta+1) - \mu\left[\frac{1-v_2}{1-v_2(1-\lambda)}\right]^2\right\} + [\zeta/(1-\lambda)xN](\partial \Delta F_f/\partial \zeta)_\lambda. \quad (23)$$

Equating to zero and letting

$$h_u/s_u = T_m^0,$$

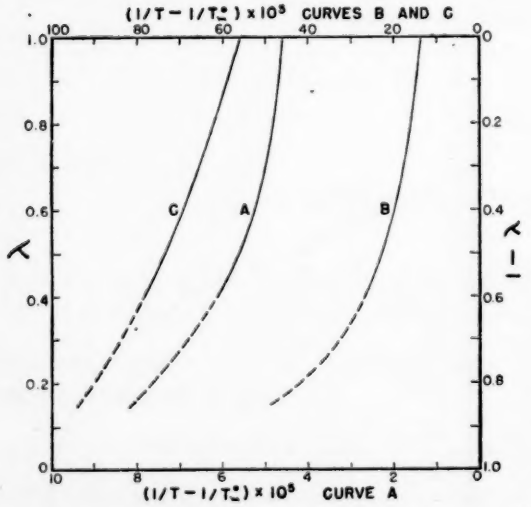

FIG. 3. Degree of crystallinity as a function of temperature for a homogeneous polymer at equilibrium. Curves calculated from Eqs. (24) or (25) for $x=100$, $R/h_u=10^{-3}$, $\mu=0$, and $D=0.50$; $v_2=1.00$, 0.90, and 0.50 for curves A, B, and C, respectively. Lower ordinate scale applies to the curve for undiluted polymer (A); the upper scale applies to the mixtures (B and C) with diluent.

where T_m^0 represents the melting point for the pure polymer of infinite chain length in the absence of diluent,

$$1/T - 1/T_m^0 = (R/h_u)\left\{\frac{(z/z_s)(1-v_2)+v_2/x}{1-v_2(1-\lambda)} + 1/(x-\zeta+1) - \mu\left[\frac{1-v_2}{1-v_2(1-\lambda)}\right]^2\right\} + (1/h_u T)[\zeta/(1-\lambda)xN](\partial \Delta F_f/\partial \zeta)_\lambda, \quad (24)$$

which reduces for $v_2=1$ to

$$1/T - 1/T_m^0 = (R/h_u)[1/x\lambda + 1/(x-\zeta+1)] + (1/h_u T)[\zeta/(1-\lambda)xN](\partial \Delta F_f/\partial \zeta)_\lambda. \quad (25)$$

If the crystallite length assumes its equilibrium value, i.e., if total equilibrium prevails, $(\partial \Delta F_f/\partial \zeta)_\lambda = 0$ and the last term vanishes in each of Eqs. (23), (24), and (25). The equilibrium value of ζ specified by Eq. (21) must then be employed.

In Fig. 3 the equilibrium fraction λ of amorphous material in a homogeneous polymer for which $x=100$ is plotted against the temperature function $1/T - 1/T_m^0$ as calculated from Eqs. (24) and (25) using the following values for the parameters involved: $R/h_u = 10^{-3}$, $\mu=0$, and $D=0.50$ with $v_2=1.00$, 0.90, and 0.50 for curves A, B, and C, respectively. In computing these curves equilibrium values of ζ, calculated from $v_2 D$ using Eq. (21), were substituted in Eqs. (24) and (25) with $(\partial \Delta F_f/\partial \zeta)_\lambda = 0$. The lower abscissa scale applies to the curve (A) for the undiluted polymer and the upper scale to the curves (B and C) representing polymer-diluent mixtures. Abscissa scales are approximately proportional to the temperature depression below T_m^0; if $T_m^0 = 316$ K, the numerals represent actual degrees centigrade below T_m^0 (for small depressions). Lower portions of the curves are dashed as a reminder of the approximate nature of the calculation for higher degrees of crystallization.

In the absence of diluent it is indicated that most of the fusion should take place within an interval of at most a few degrees. A change in D (while D remains less than unity) merely shifts the curve horizontally. According to Eq. (25), the melting range should be narrower the greater the chain length (x). These predictions are relevant, of course, only to the transformation carried out at equilibrium, which may not be realized under ordinary experimental conditions.

In the presence of even small amounts of diluent (curve B, for example) the melting range is markedly broadened. (Note the tenfold difference in ordinate scales.) In these calculations the size of the solvent molecule and of the structural unit of the polymer have been set equal to each other ($z_s=z$). If the molecular size of the diluent is increased, the broadening of the melting range for a given proportion of diluent should be diminished according to Eq. (24).

Employing the modification for heterogeneous polymers having the distribution given by Eq. (14), there is obtained in place of Eq. (24)

$$1/T-1/T_m^0\cong(R/h_u)\left\{\frac{(z/z_s)(1-v_2)+v_2/\bar{x}_n}{1-v_2(1-\lambda)}-(1/\zeta)\ln(v_2D)+(1-1/\zeta)/\bar{x}_n-\mu\left[\frac{1-v_2}{1-v_2(1-\lambda)}\right]^2\right\}, \quad (24')$$

which reduces for $v_2=1$ to

$$1/T-1/T_m^0=(R/h_u)[1/\bar{x}_n\lambda-(1/\zeta)\ln D+(1-1/\zeta)/\bar{x}_n]. \quad (25')$$

If v_2D is less than unity, the first crystals formed at equilibrium will be very long, justifying neglect of the second terms in Eqs. (24′) and (25′). As already noted, however, molecular species acceptable for very long crystallites are limited in abundance. When the proportion of such species remaining in the amorphous regions falls appreciably below the weight fraction indicated by Eq. (14), the temperature must be reduced in order to induce these remaining species to crystallize. A reduction of temperature also permits shorter crystallites (smaller ζ) to be formed from the smaller molecules which are present. The breadth of the melting range (assuming $\mu=0$ or that $v_2=1$) will be determined by the increases occurring in both the first and second terms in Eqs. (24′) and (25′) as crystallization progresses. The first term contains $1-\lambda$ directly; the second term will increase with increase in degree of crystallinity owing to the concurrent decrease in ζ. The lower the molecular weight, the greater the magnitude of the first term and the greater the decrease in ζ with degree of crystallization. Hence, both terms will act to make the melting range broader the lower the molecular weight. It is to be noted further that the melting range for a homogeneous polymer should be somewhat less than that for a heterogeneous polymer of the same number average chain length.

If the chain length is very large, the equilibrium crystallite length, also very large (assuming $D<1$), may be difficult to attain experimentally. In this case no distinction between heterogeneous and homogeneous polymers is required, and it is appropriate to set Eq. (22) equal to zero without specifying that ζ shall assume its equilibrium value. In the limit of indefinitely long chains for which it is legitimate to let $x=\infty$, there is obtained

$$1/T-1/T_m^0=(R/h_u)\left\{(z/z_s)/[1+v_2\lambda/(1-v_2)]-(1/\zeta)\ln(v_2D)-\mu\left[\frac{1-v_2}{1-v_2(1-\lambda)}\right]^2\right\}, \quad (26)$$

which reduces in the absence of diluent to

$$1/T-1/T_m^0=-(R/h_u)(\ln D)/\zeta. \quad (27)$$

The depression in the melting temperature below T_m^0 then depends entirely on ζ, being smaller the larger the value of ζ. At a given temperature depression below T_m^0, crystallization will continue until possibilities for further formation and growth of crystallites of length ζ specified by Eq. (27) are exhausted, without the imposition of undue configurational distortions on the residual amorphous portions of molecules.[1,17] Formation of smaller crystallites will require a lowering of the temperature. Thus, the temperature interval over which crystallization occurs (and likewise the interval of fusion) will depend on kinetic factors governing the degree of departure from the ultimate state of perfect crystallinity. Specifically, the breadth of the crystallization interval will depend on the number and arrangement of crystal nuclei within the matrix of polymer chains. In the experimentally unattainable limit of very large crystallites formed from chains substantially infinite in length, total crystallization should occur at a sharply defined temperature.

The Melting Point

Although the process of fusion in actual crystalline high polymers will invariably take place over a range of temperatures, total disappearance of crystallinity should occur at a sharply defined

[17] T. Alfrey and H. Mark, J. Phys. Chem. 46, 112 (1942).

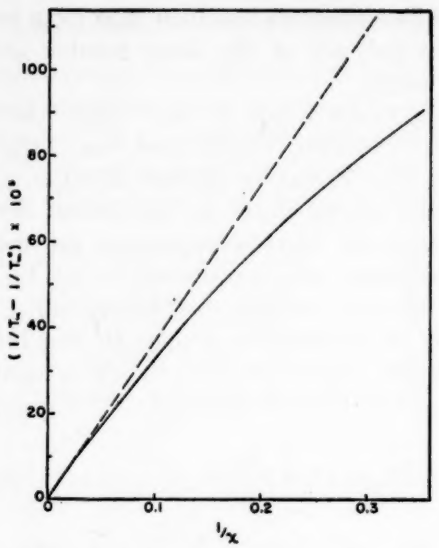

FIG. 4. Dependence of melting point on chain length for homogeneous polymers. $R/h_u = 10^{-3}$, $v_2 = 1$, and $D = \frac{1}{2}$. The straight dashed line represents the approximation in which b is constant.

temperature, i.e., $(\partial\lambda/\partial T)_{\lambda=1} \neq 0$. This temperature may therefore be referred to appropriately as a "melting point" T_m, bearing in mind, of course, that it does not, as with simple substances, represent an invariant temperature throughout the solid-liquid transition.

Setting $\lambda = 1$ in Eq. (24), ζ being assumed to have its equilibrium value as specified by Eq. (21) such that $(\partial \Delta F_f/\partial\zeta)_\lambda = 0$,

$$(1/T_m - 1/T_m^0) = (R/h_u)\{(z/z_s)(1-v_2) + (1/x)[v_2 + x/(x-\zeta_e+1)] - \mu(1-v_2)^2\}, \quad (28)$$

which expresses the melting temperature for homogeneous polymers as a function of the chain length x and the proportion of diluent. The relationship is not explicit, however, inasmuch as ζ_e for a given value of v_2D depends on x according to Eq. (21). As pointed out previously, $(\zeta_e - 1)/x$ approaches a constant limiting value as x increases (for the given value of v_2D). Hence the melting point relationship may be conveniently written

$$1/T_m - 1/T_m^0 = (R/h_u)[(z/z_s)(1-v_2) + (v_2+b)/x - \mu(1-v_2)^2], \quad (29)$$

where

$$b = [1 - (\zeta_e - 1)/x]^{-1}. \quad (30)$$

The quantity b depends on the value of $(\zeta_e - 1)/x$ specified by Eqs. (21) or (21′); unless x is small, it may be assumed that b is approximately constant for a given value of v_2D.

In the absence of diluent $(v_2 = 1)$[18]

$$1/T_m - 1/T_m^0 = (R/h_u)(1+b)/x, \quad (31)$$

which represents the dependence of the melting temperature on chain length for the pure polymer, subject, of course, to assumption (c) according to which chain ends are excluded from the crystallites. The predicted influence of chain length on T_m calculated from Eq. (31) when $v_2 = 1$ and $D = \frac{1}{2}$ is shown in Fig. 4.

Introducing the condition $\lambda = 1$ correspondingly into Eq. (24′) for heterogeneous polymers,

$$1/T_m - 1/T_m^0 = (R/h_u)[(z/z_s)(1-v_2) + v_2/\bar{x}_n - (1/\zeta)\ln(v_2D) + (1-1/\zeta)/\bar{x}_n - \mu(1-v_2)^2], \quad (28')$$

which in the absence of diluent reduces to

$$1/T_m - 1/T_m^0 \cong (R/h_u)[2/\bar{x}_n - (\ln D)/\zeta]. \quad (31')$$

According to the above discussion, ζ at incipient equilibrium crystallization should be infinite. Hence, terms in $1/\zeta$ in the above equations should be vanishingly small, the latter equation reducing to the simple expression

$$1/T_m - 1/T_m^0 = 2R/\bar{x}_n h_u. \quad (31'')$$

Owing to the limited supply of very large species as discussed above, the occurrence in practice of a detectable amount of crystallization (even at equilibrium) may require a value of ζ sufficiently small so that these terms in $1/\zeta$ are not quite negligible. The observed "melting point" for the heterogeneous polymer will not be absolutely sharp and may depend slightly on the particular method of observation employed, therefore. On the other hand, it remains true that theory predicts final disappearance of the last traces of crystallinity at a sharply defined temperature T_m deduced by setting $\zeta = \infty$ in the above equation. The aberration in the melting point as observed by a method of given sensitivity to crystallinity should increase with decrease in average chain length, just as the magnitude of the range over which fusion occurs increases with decrease in molecular weight. A similar situation is discussed in greater detail in the section on crystallization in copolymers.

If x, or $\bar{x}_n$, is very large, the influence of the chain length vanishes and Eqs. (28) and (28′)

[18] This expression replaces Eq. (5) of reference (2), which was somewhat incorrectly deduced by a simplified procedure.

reduce to

$$1/T_m - 1/T_m^0 = (R/h_u)[(z/z_s)(1-v_2) - \mu(1-v_2)^2], \quad (32)$$

which expresses the predicted dependence of T_m on the proportion of diluent. Since μ contains the temperature T_m, it is preferable to express Eq. (32) as follows:

$$(1/T_m - 1/T_m^0)/(1-v_2) = (R/h_u)(z/z_s) - (BV/h_u)(1-v_2)/T_m. \quad (33)$$

Thus, a plot of the quantity on the left of Eq. (33) against $(1-v_2)/T_m$ should be linear according to the assumptions (including, in particular, the assumption of a vanLaar heat of mixing term), with a slope dependent on the cohesive energy density constant B. If $B=0$, the temperature depression $1/T_m - 1/T_m^0$ should be proportional to the volume fraction of diluent. The constant of proportionality depends on the heat of fusion per structural unit and on the ratio of the molar volumes of structural unit and solvent. The depression is predicted to be less the higher the molecular weight of the solvent. A high polymeric diluent should therefore exert no appreciable depression, unless B (and μ) is sufficiently negative and the proportion $(1-v_2)$ of diluent is large enough to render the heat term occurring in Eqs. (32) and (33) significant.

IV. CRYSTALLIZATION IN COPOLYMERS

Random Copolymers

A linear copolymer composed of units of type A capable of crystallizing and other units, B, incapable of occupying the lattice characteristic of A, the two types of units occurring in random sequence, will be considered. The following alterations of the above derivation of the free energy of fusion are required for the treatment of such polymers and their mixtures with diluents: (i) allowance must be made for a difference in the sizes of the two types of units; (ii) the requirement that all of the polymer units occupying a given sequence of lattice sites running through a crystallite shall be of type A must be imposed; and (iii) the heat of mixing term must be modified. These revisions will be considered below. For simplicity the following discussion is limited to polymers of uniform chain length.

(i) The previous expressions for S_1, S_2, S_3, and S_4 may be employed provided the following definitions are introduced:

X_A = mole fraction of structural units of type A.
x = total number of units of both types (A and B) per polymer molecule.
x' = total number of segments per polymer molecule.
z_A = number of segments in an A unit.
z_B = number of segments in a B unit.
$\bar{z} = z_A X_A + z_B(1-X_A)$ = average number of segments per unit.
$x' = \bar{z}x$.
$\zeta' = z_A\zeta$.

(ii) The probability that all of the m sequences, each of ζ units selected from the hypothetical continuous chain composed of all of the polymer molecules (see above), consist exclusively of A units will be given, in the limit of very low degrees of crystallinity, by[19]

$$W_5 = X_A^{\zeta m},$$

which leads to the additional entropy term

$$S_5 = R\zeta m \ln X_A. \quad (34)$$

(iii) The heat of mixing the initially crystalline A units with the liquid mixture consisting of initially non-crystalline polymer (consisting of both A and B units) and solvent can be expressed as

$$\Delta H_m = B' V_A[n(z_s/z_A) + xN(\bar{z}/z_A - X_A)](v_A - v_A'). \quad (35)$$

Here V_A is the molar volume of the structural unit A, v_A is the volume fraction of A units occurring in the system, and v_A' their volume fraction in the amorphous regions of the semicrystalline polymer. The cohesive energy density "constant" B' will depend on the composition of the "solvent medium" which, in this case, consists of the diluent plus the B units; i.e., B' will depend on the ratio of diluent to B units in the mixture. Substituting

$$v_A = v_2 X_A(z_A/\bar{z})$$

[19] If $z_A \neq z_B$, the probability that the segment occupying the initial site of a sequence of cells of a crystalline region belongs to an A unit is given by the volume fraction of A units, $(z_A/\bar{z})X_A$. The probability relating to succeeding units is given by the mole fraction X_A. Hence, the above expression for W_5 should be replaced by

$$[(z_A/\bar{z})X_A^{\zeta}]^m.$$

Usually $z_A/\bar{z}$ may be replaced by unity without much error, and in any case it can be incorporated in D if desired.

and

$$v_A' = v_2(z_A/\bar{z})[X_A - (1-\lambda)]/[1 - v_2(z_A/\bar{z})(1-\lambda)]$$

in Eq. (35),

$$\Delta H_m/xN = B' V_A (1 - v_2 X_A z_A/\bar{z})^2 (1-\lambda)/ [1 - v_2(z_A/\bar{z})(1-\lambda)], \quad (36)$$

where λ refers to the fractional number of units of the total polymer which are amorphous, i.e., $\lambda = (xN - \zeta m)/xN$.

Incorporation of the revisions given under (i) and (iii), and the added term given in paragraph (ii) above, in the previous derivation leads to the following expression for the free energy of fusion of the semicrystalline copolymer containing diluent.

$$\Delta F_f/xN = (1-\lambda)(h_u - Ts_u) + RT\Big\{\Big[(\bar{z}/z_s) \times \Big(\frac{1-v_2}{v_2}\Big) + \frac{1}{x}\Big] \ln[1 - v_2(z_A/\bar{z})(1-\lambda)] + \Big(\frac{1-\lambda}{\zeta}\Big)\Big[\ln(v_2 D) + \ln\Big(\frac{x-\zeta+1}{x}\Big)\Big] + (1-\lambda)\ln X_A + \mu'(1 - v_2 X_A z_A/\bar{z})^2 (1-\lambda)/ [1 - v_2(z_A/\bar{z})(1-\lambda)]\Big\}, \quad (37)$$

where

$$\mu' = B' V_A/RT.$$

Eq. (37) is obviously similar to Eq. (19), aside from the added term $(1-\lambda)\ln X_A$.

The derivative of ΔF_f of Eq. (37) with respect to ζ is identical with the previous expression, Eq. (20).

Differentiating Eq. (37) with respect to λ and equating to zero, there is obtained in analogy to Eq. (24)

$$1/T - 1/T_m^0 = (R/h_u)\Big\{\frac{(z_A/z_s)(1-v_2) + v_2 z_A/x\bar{z}}{1 - v_2(1-\lambda)(z_A/\bar{z})} + 1/(x-\zeta+1) - \ln X_A - \mu'(1 - v_2 X_A z_A/\bar{z})^2/ [1 - v_2(z_A/\bar{z})(1-\lambda)]^2 + [\zeta/(1-\lambda)xNRT](\partial \Delta F_f/\partial\zeta)_\lambda\Big\}. \quad (38)$$

In the absence of diluent

$$1/T - 1/T_m^0 = (R/h_u)\Big\{(1/x)/[\lambda + (\bar{z}/z_A) - 1] + 1/(x-\zeta+1) - \ln X_A - \mu'(1 - X_A z_A/\bar{z})^2/ [1 - (z_A/\bar{z})(1-\lambda)]^2 - (1/\zeta)\Big[\ln D + \zeta/(x-\zeta+1) + \ln\Big(\frac{x-\zeta+1}{x}\Big)\Big]\Big\}. \quad (39)$$

For reasons which will appear below, $(\partial \Delta F_f/\partial\zeta)_\lambda$ has been replaced by substituting from Eq. (20). If the crystallites are of equilibrium length ζ_e defined by Eq. (21), the last term occurring in both Eqs. (38) and (39) is zero. It is to be noted that in the absence of diluent, B' and μ' should assume values characteristic of the pair of structural units, A and B, and independent of the composition.

Incipient crystallization temperatures T_m, or "melting points," may be derived as previously. The discussion included here will be confined to copolymers containing no diluent. Setting $\lambda = 1$ in Eq. (39) and assuming $\zeta = \zeta_e$,

$$1/T_m - 1/T_m^0 = (R/h_u)\{[(z_A/\bar{z}) + b]/x - \ln X_A - \mu'(1 - v_A)^2\}, \quad (40)$$

where $v_A = X_A z_A/\bar{z}$ and b retains the definition stated by Eq. (30). If x is very large

$$1/T_m - 1/T_m^0 = (R/h_u)[-\ln X_A - \mu'(1 - v_A)^2]. \quad (41)$$

The heat of interaction of the copolymerized units contributes a term exactly equivalent, within the vanLaar approximation, to that for polymer-diluent mixtures (compare Eq. (32)); the entropy terms bear no similarity. Equation (41) is identical in form with the freezing point depression relationship for regular binary mixtures of simple molecules. If $\mu' = 0$, the result previously derived is obtained.[20]

If D is appreciably less than unity, then according to Eq. (21), which as pointed out above applies also to the copolymers, ζ_e may be a large fraction of the value of x. For high molecular weight copolymers, the crystallites first formed at $T = T_m$ may tend to be quite long therefore. If X_A is much less than unity (e.g., if $X_A < 0.8$), long sequences of A type units will occur in the

[20] See Eq. (4) of reference 2.

polymer chains only rarely, and formation of crystallites of the "equilibrium" length must be correspondingly limited. Appreciable degrees of crystallinity are possible only through the formation of much shorter crystallites. In analogy with crystallization in heterogeneous polymers of limited average chain length as discussed above, the formation of shorter crystallites requires a further lowering of the temperature, since the last term in Eq. (39) makes a positive contribution for $\zeta<\zeta_e$. If the temperature at which crystallization occurs in detectable amount is significantly lower than T_m on this account, the melting point may appear to be ill-defined and highly dependent on the method of determination.

The magnitude of this effect can be illustrated by comparing the temperature T at which crystallites of a length ζ will form with the fraction of the A units occurring in sequences of length greater than ζ. For this purpose let $\lambda=1$ in Eq. (39) while $\zeta<\zeta_e$. Subtracting the temperature T so defined from T_m of Eq. (40),

$$-\Delta T=T_m-T\cong-(RT_m^2/h_u)(1/\zeta)\{\ln D+\zeta/(x-\zeta+1)+\ln[(x-\zeta+1)/x]\}, \quad (42)$$

which represents the temperature depression below T_m required to bring about incipient formation of crystallites of length $\zeta<\zeta_e$.

The fraction of the A units of the random copolymer which may be included in crystal sequences ζ units in length can be estimated as follows. The number of continuous sequences of y units of type A is

$$\nu_{yA}=\nu_A(1-X_A)^2X_A^{y-1},$$

where ν_A is the number of A units. The number of sequences for which $x\geqq\zeta$ is

$$\nu_{\geq\zeta}=\sum_{y=\zeta}^{\infty}\nu_{yA}=\nu_A(1-X_A)X_A^{\zeta-1}.$$

Overlooking the fact that some of the sequences for which $y>2\zeta$ may occupy more than one crystallite (the error so introduced being small when $X_A^{\zeta}\ll1$), we may consider that each of the $\nu_{\geq\zeta}$ sequences may occupy only one of the sequences of cells through a crystallite. The maximum (approximate) fraction of the A units which may occupy crystallites of length ζ is therefore

$$q_\zeta=\zeta\nu_{\geq\zeta}/\nu_A=\zeta(1-X_A)X_A^{\zeta-1}. \quad (43)$$

In Table I values of ΔT and q_ζ calculated from Eqs. (42) and (43), respectively, are given as functions of ζ for the values of D and X_A indicated. Values of other parameters are as follows: $x=100$, $R/h_u=10^{-3}$, $T_m=316°$K, i.e., $(RT_m^2/h_u)=10^2$. The conclusions to be drawn are trivially altered for all $\zeta\ll\zeta_e$ if $x=\infty$. As is shown by the figures in the last two columns of Table I, the amount of crystallization which may occur at $T=T_m$ (i.e., $\Delta T=0$, where ζ is required to equal ζ_e) is insignificant for $X_A=0.8$. If $X_A=0.8$, about 0.9 percent of the A units may form crystallites thirty units long. Incipient formation of crystallites of this length requires a depression of the temperature below T_m as predicted by Eq. (40), or by (41), by 2°C (for the above values of the parameters) if $D=\frac{1}{2}$, or by 4.3° if $D=\frac{1}{4}$. Furthermore, an approach to the maximum extent of crystallization q_ζ, which in this case is 0.009, will not be realized without a further lowering of the temperature; the ΔT values calculated from Eq. (42) and shown in Table I represent the temperature depressions for *incipient* formation of crystallites of length $\zeta=30$. Approximate calculations indicate, however, that a rather large fraction (30 to 50 percent perhaps) of the maximum extent of crystallization q_ζ may be realized with a further depression of only a few degrees (for large x).

From a theoretical point of view, the incipient crystallization temperature, or melting point, T_m, of a copolymer is sharply defined. The amount of crystallization which occurs within a fraction of a degree below T_m may, however, be too small to detect experimentally. Hence, the experimentally observed, or apparent, melting point may be appreciably below T_m and it is likely to depend on the sensitivity of the method employed for detecting traces of crystallinity. According to the calculations shown in Table I, a change of one degree may bring about a change of an order of magnitude or more in the degree of crystallinity in the range where it is very small. It follows that what may appear to be a fairly well defined melting point (according to a given sensitive method) may actually be located several degrees below T_m for the copolymer.

It is apparent also that the dependence of λ on T over the entire range through which melting occurs will differ markedly from the relationship shown in Fig. 3 for polymers. In the first place, the curve can be expected to be sigmoid in character, $d\lambda/dT$ passing through a maximum

at a temperature well below T_m, then decreasing to a very small value as T_m is approached. Secondly, melting should occur over a much broader range than for pure polymers. For example, referring again to the calculations shown in Table I for $D=\frac{1}{2}$ and $X_A=0.8$, retention of 25 percent crystallinity requires a temperature some 10° below T_m; according to Fig. 3, a half-degree depression should be sufficient for the same degree of crystallinity in the pure polymer. This broadening of the melting range and the associated obscuring of the incipient crystallization temperature T_m increases with decrease in D (for $D<1$) and with decrease in X_A.

Crystallization in Vinyl Copolymers

Whereas condensation copolymers usually are of the random type, the structural units of vinyl copolymers generally tend to alternate to a greater extent than a purely random arrangement would allow.[21] The character of the arrangement is dependent upon relative values of the rate constants for the reaction of each of the two kinds of radicals with each of the two monomers, and on the proportions of the comonomers.[22–24] According to copolymerization theory, the probability that a given A unit of an addition polymer is succeeded by an A unit is given by

$$p_A=r_1(m_A/m_B)/[1+r_1(m_A/m_B)], \qquad (44)$$

where m_A and m_B are the respective monomer concentrations in the polymerizing mixture (assuming low conversion) and r_1 is a ratio of velocity constants for the addition of monomers A and B to an A radical.[25] The probability that the A unit is preceded by another A unit in the chain can also be shown to be equal to p_A. Then

$$W_\zeta=[X_A p_A^{\zeta-1}]^m \qquad (45)$$

and

$$S_\zeta=R\zeta m \ln p_A+Rm \ln(X_A/p_A). \qquad (46)$$

The first term of Eq. (46) corresponds to the random copolymer term given in Eq. (34), X_A having been replaced by p_A; the last term, which is of minor importance, may be incorporated with the $\ln v_2 D$ term. Hence, the development of the preceding section can be extended to include non-random vinyl copolymers merely by replacing X_A with p_A, and by replacing $\ln(v_2 D)$ with $\ln(v_2 X_A D/p_A)$. Owing to the tendency toward alternation of structural units in most vinyl copolymers, p_A usually will be less than X_A. Hence, the melting points of vinyl copolymers generally should be less than those of the hypothetical random copolymers of the same composition.

TABLE I. Effect of crystallite length on crystallization temperature and the abundance of sequences of adequate length in the copolymer.

ζ	$-\Delta T$°C For $D=\frac{1}{2}$	$-\Delta T$°C For $D=\frac{1}{4}$	q_ζ For $X_A=0.8$	q_ζ For $X_A=0.6$
5	13.6	27.5	0.41	0.26
10	6.8	13.7	0.27	0.040
20	3.2	6.7	0.058	4.9×10^{-4}
30	2.0	4.3	0.009	4.4×10^{-6}
40	1.3	3.1	1.3×10^{-3}	3.5×10^{-8}
50	0.8	2.2	1.7×10^{-4}	2.7×10^{-10}
63*	0.0		1.0×10^{-6}	2.7×10^{-13}
73.5**		0.0	1.1×10^{-7}	1.4×10^{-15}

* For $D=\frac{1}{2}$, $\zeta_e=63$.
** For $D=\frac{1}{4}$, $\zeta_e=73.5$.

Crystallization in Ordered Copolymers

Copolymers in which the crystallizing units A tend to occur in abnormally long sequences also may be prepared.[26] In order to illustrate the effect on crystallinity of this type of deviation from random arrangement in copolymers, the extreme case of fairly long sequences of A units interspersed among complementary B sequences will be considered. For simplicity, let the A sequences be assumed to be uniformly y units in length. The probability that a given structural unit is an A unit and that it is succeeded by $\zeta-1$ additional A units, thus affording a group of ζ consecutive A units acceptable for occupancy of a sequence of ζ' cells running through a crystallite, is

$$W_\zeta=X_A{}^m[(y-\zeta+1)/y]^m$$

and

$$S_\zeta=Rm \ln X_A+Rm \ln[(y-\zeta+1)/y]. \qquad (47)$$

[21] F. M. Lewis, F. R. Mayo, and W. F. Hulse, J. Am. Chem. Soc. 67, 1701 (1945); F. R. Mayo, F. M. Lewis, and C. Walling, *ibid.* 70, 1529 (1948).
[22] T. Alfrey and G. Goldfinger, J. Chem. Phys. 12, 205 (1944).
[23] F. R. Mayo and F. M. Lewis, J. Am. Chem. Soc. 66, 1594 (1944).
[24] F. T. Wall, J. Am. Chem. Soc. 66, 2050 (1944).
[25] T. Alfrey, F. R. Mayo, and F. T. Wall, J. Poly. Sci. 1, 581 (1946).
[26] Examples are afforded by cellulose derivatives formed by partial substitution of native cellulose under conditions such that attack of the reagent is limited to localized minute regions within the fiber structure, and by copolyamides formed by limited interchange between two previously prepared polyamides (see M. M. Brubaker, D. D. Coffman, and F. C McGrew, U. S. Patent 2,339,237 (1944)).

The ΔF_f function for the ordered copolymer may be obtained by introducing Eq. (47) instead of (34) in the above treatment of random copolymers. For simplicity, let x approach infinity. Then it can be shown that the condition $(\partial \Delta F_f/\partial \zeta)_\lambda = 0$ leads to

$$-\ln(v_2 D X_A) = \zeta_e/(y-\zeta_e+1) + \ln[(y-\zeta_e+1)/y] \quad (48)$$

which replaces Eq. (21). Introduction of the condition $(\partial \Delta F_f/\partial \lambda)_\zeta = 0$ yields

$$1/T - 1/T_m^0 = (R/h_u)\{(z_A/z_s)(1-v_2)/[1-v_2(1-\lambda)(z_A/\bar{z})] + 1/(y-\zeta+1) - \mu'(1-v_2 X_A z_A/\bar{z})^2/[1-v_2(z_A/\bar{z})(1-\lambda)]^2 + [\zeta/(1-\lambda)xNRT](\partial \Delta F_f/\partial \zeta)_\lambda\}. \quad (49)$$

In these relationships y occupies a role corresponding to x for polymers of finite length, except that no term in $1/y$ appears in Eq. (49).

The melting point in the absence of diluent is given by

$$1/T_m - 1/T_m^0 = (R/h_u)[1/(y-\zeta_e+1) - \mu'(1-X_A z_A/\bar{z})^2]. \quad (50)$$

If $\mu' = 0$, the melting point is predicted to depend on the composition only through the influence of X_A on ζ_e according to Eq. (48). Thus, if the sequence length y is sufficiently large, the melting point of the ordered copolymer is predicted to be independent of the mole fraction X_A of A units.

V. DISCUSSION

Detailed features of the above treatment doubtless exceed the bounds of validity inherent in the lattice model. The lattice model has been interpreted literally in an effort to make the treatment comprehensive, without particular regard for probable inaccuracies in some of the relationships which have been derived. The extent of their validity remains to be established through appropriate experiments.

The naive representation of all molecular species, polymer and solvent, as chains of one or more spatially and configurationally equivalent segments is particularly vulnerable to criticism. Results which depend critically on the ratio of z to z_s probably should not be accepted literally. On the other hand, the deduction from Eq. (32) that high molecular weight solvents will depress the melting point less than analogous solvents of low molecular weight is believed to be qualitatively correct. Similarly, the precise formulation of the numbers of segments in the different units of copolymers may be only partially justified, but it serves to indicate the probable consequences of a large disparity in the sizes of the units.

The complete exclusion of chain ends from the crystallites in accordance with assumption (c) can be justified only on the grounds of steric considerations. If the terminal units of the chains are of such a size that they cannot possibly occupy the lattice even if somewhat distorted, then this assumption should afford a good approximation. Otherwise assumption (c) calls for refinement.

The opposite assumption, namely, that chain ends are uniformly partitioned between amorphous and crystalline regions, is even less attractive. Even in the absence of steric difficulties with the end units themselves, those which choose to occupy sites in the crystallites will be obliged to occur in pairs in end-to-end juxtaposition; any other arrangement will introduce a flaw in the array which may be more objectionable than a big end group. Hence, the chain ends will naturally gravitate to the greater freedom of the amorphous regions, although some of them, particularly if the molecular weight is low so that the end group population is large, will suffer the inhibitions of the paired relationship to which they are subject in the crystallites. In consideration of the manifest difficulties of devising a general treatment of such a complex situation which depends critically on the nature of individual cases, we have clung to the invariant simplicity of assumption (c). Melting point and temperature depressions as deduced probably are somewhat too large, particularly if the molecular weight is low. If the molecular weight is very high, the assumption obviously is of no consequence.

Attempts to apply the phase rule to transformations involving semicrystalline polymers inevitably lead to difficulties.[26a] These are especially evident in the case of copolymers. Partial crystallization of a random copolymer results in selective utilization of long sequences of the crystallizable A units in the formation of crystallites. In the remaining amorphous polymer the proportion of A units occurring in sequences of length ζ or greater will differ, in general, from

[26a] R. B. Richards, Trans. Faraday Soc. 42, 10 (1946).

that in a random copolymer of the same composition as the amorphous portion. Hence, the properties of the amorphous "phase" are not determined uniquely by the composition; specifically, the temperature below which further crystallization will commence is not a unique function of the phase composition (and temperature and pressure). The phase rule is based on the premise that a property such as the molar free energy may be so expressed. It follows at once that the phase rule is inherently inapplicable to the crystal-liquid transformation in copolymers.

The free energy of the amorphous portions of a polymer composed of a single structural unit likewise may not be expressed (accurately) as a unique function of the temperature and pressure; it depends also to some extent on the proportion of the other "phase." This obstruction to the utilization of the phase rule would not be eliminated if the polymer were composed of a single molecular species, unless, of course, these molecules were to form a molecular lattice, an unlikely circumstance in the absence of a point of exceptionally strong interaction at a characteristic place along the chain such as the end group. It is true that infinitely long polymer molecules in the absence of diluent are predicted to pass from $\lambda=1$ to 0 over an infinitesimal temperature range *at equilibrium*, and the phase rule may be applicable in principle here. However, such a transformation presupposes infinitely long crystallites, which in practice may never be approached sufficiently to warrant retention of the phase rule for this special case.

The analogy to regular solutions presented by random copolymers is interesting, although in the light of the above paragraphs the analogy must not be pushed too far. Regardless of the interaction energies between like and unlike units, they are maintained in random order, in one dimension at any rate, by the primary valence connections. Clustering of like units on the one hand or association of unlike units on the other, such as commonly leads to deviations from regularity in solutions of simple molecules, is severely restricted by the existence of the primary valence chains. After some of the longer sequences of A units have been converted to crystalline polymer, however, the same valence connections prevent the units of the amorphous portions of the chains from assuming a random distribution consistent with the altered composition. After partial crystallization has occurred, the amorphous portion of a random copolymer is neither random nor the precise analog of a regular solution.

Similarly, a non-crystalline vinyl copolymer in which the units tend to alternate may be regarded as the analog of an irregular solution in which the unlike molecules tend to associate. Ordered copolymers are analogs of irregular solutions in which the like molecules prefer to cluster together; pairs of simple liquids for which this tendency is pronounced are immiscible.

The solution of the free energy equations for which $\zeta_e=1$ is especially intriguing, for it suggests that while interaction forces and chain regularity are necessary for crystallinity they are not always sufficient conditions. The forces of interaction between regularly occurring polar groups may sometimes be satisfied to better advantage through random association. Such association differs from crystallinity in that the individual chains do not assume a specified configuration (e.g., fully extended) nor do they occur in parallel bundles.

Extension of the above treatment to nonlinear polymers is obvious. Branching centers or points of cross linkage are merely to be regarded as copolymeric constituents. The chain ends of such structures may be introduced by redefining x as the ratio of the total number of chain units divided by twice the number of ends.

The Absorption Spectrum of Ethylene Oxide in the Vacuum Ultraviolet

TA-KONG LIU* AND A. B. F. DUNCAN
Department of Chemistry, University of Rochester, Rochester, New York
(Received July 6, 1948)

The spectrum of ethylene oxide was investigated from the visible down to about 600A, with high resolution in the vacuum region. No discontinuous absorption was found above 1713A. Two Rydberg series, beginning at 1435 and 1382A were found, which converge to the same ionization potential at about 10.81 ev. Two non-Rydberg transitions were found, with origins apparently at 1713.4 and 1572.4A. An analysis and discussion is made of the spectrum. It is concluded that the Rydberg transitions arise by excitation from a molecular bonding orbital, very similar to one responsible for Rydberg series in ethylene and related compounds.

INTRODUCTION

THE electronic spectra of ethylene oxide vapor have not been reported, in spite of the fact that the structure and chemical properties of this compound are interesting and important. It appears from the present work that these spectra lie entirely in the vacuum ultraviolet region. Some recent discussion of the electronic structure of this molecule has been published.[1–9] The infra-red and Raman spectra of the molecule are fairly well understood, and are consistent with a symmetry group C_{2v}.[10] Electron diffraction measurements[11,12] show that the two carbons and oxygen are on the corners of an isosceles triangle which is almost equilateral. We have investigated the absorption spectrum with high resolving power and dispersion in the vacuum region. The results are presented here, with some interpretation and discussion.

EXPERIMENTAL DETAILS AND RESULTS

The best samples of ethylene oxide usually contain enough acetaldehyde, even after several vacuum fractionations, to show the strong bands of the latter. A specially purified sample** was used and found satisfactory. After repeatedly outgassing the sample, it was fractionated twice in vacuum and only the middle fraction was used.

Exploratory measurements were made with a Cario and Schmidt-Ott vacuum fluorite spectrograph, which covered the visible and ultraviolet regions down to about 1400A with low dispersion. The ethylene oxide was in a cell 40 cm long with lithium fluoride windows, waxed between a conventional hydrogen discharge tube and the spectrograph. The pressure range covered was from 730 down to 0.05 mm. Exposures were usually for three minutes on Eastman III-0 u.v. sensitized plates. Long exposures led to the appearance of a group of bands at 1815A, identified as strong bands of acetaldehyde formed in a photochemical reaction. Under these conditions no discontinuous absorption was observed above about 1713A. At high pressures continuous absorption extended up to about 2120A, possibly due to the broadening of the 1713.4A transition.

The structure below 1713A was examined in a vacuum grating spectrograph, with a four inch, 120000 line, two-meter radius of curvature grating, used at about normal incidence. This gave a dispersion of about 4.1A/mm in the first order. The vapor was admitted into the spectrograph, which served as the absorbing column, and the pressure was read with a calibrated thermocouple gauge. The Lyman continuum, used as a source, was produced in a tube described by Worley.[13] About 500 flashes, made once or twice a second, from the discharge of an 8-microfarad capacitor charged to about 3000 volts, was sufficient to give good blackening on Eastman III-0 u.v. sensitized plates. Helium (Ohio Chemical Company, 96 percent purity) at 0.5–2-mm pressure was used in the discharge. The slit width was 0.08 mm. The pressure range investigated under these conditions was from 0.5 to 0.005 mm. The whole system of bands was well developed within this range.

The spectral regions from 2200–1200 and 1600–600A were covered in two settings of the grating. A number of plates were measured, with a precision

* Part of a dissertation presented to the Faculty of the Graduate School of the University of Rochester in partial fulfillment of the requirements for the degree of Doctor of Philosophy.

[1] A. D. Walsh, Nature **159**, 165 (1947).
[2] See reference 1, p. 712.
[3] A. D. Walsh, Nature **160**, 903 (1947).
[4] R. Robinson, Nature **159**, 400 (1947).
[5] R. Robinson, Nature **160**, 162 (1947).
[6] R. Robinson, Nature **161**, 176 (1948).
[7] J. W. Linnett, Nature **160**, 162 (1947).
[8] T. M. Sugden, Nature **160**, 367 (1947).
[9] H. A. Skinner, Nature **160**, 902 (1947).
[10] Gerhard Herzberg, *Infrared and Raman Spectra of Polyatomic Molecules* (D. Van Nostrand and Company, New York, 1945), p. 340.
[11] P. G. Ackermann and J. E. Mayer, J. Chem. Phys. **4**, 377 (1936).
[12] R. Wierl, Ann. d. Physik **13**, 453 (1932).
** Obtained by Dr. W. D. Walters from Dr. D. R. Stull of Dow Chemical Company.
[13] R. E. Worley, Rev. Sci. Inst. **13**, 67 (1942).

TABLE I. Absorption spectrum of ethylene oxide.*

Wave number	Relative intensity	Assignment
58362(1713.4A)	58	V_I
59157	39	$V_I+\nu_5$
63597(1572.4A)	36	V_{II}
64722	31(U)	$V_{II}+\nu_3$
69684(1435.0A)	9	$R_I(2)$
70462	8	$R_I(2)+\nu_5$
70811	19	$R_I(2)+\nu_3$
70986	0	$R_I(2)+\nu_2$ (or $2\nu_5$)
71988	0	substructure of $R_{II}(3)$
72123	0	ditto
72347(VE)(1382.2A)	100	$R_{II}(3)$
72656	6	$R_{II}(3)+\nu_3-\nu_5$ (or $R_I(2)+\nu_1$)
73026(VE)	14(U)	$R_{II}(3)+\nu_5$
73486(VE)	27	$R_{II}(3)+\nu_3$
73554	1	$R_{II}(3)+2\nu_5$ (or ν_2)
73750	5	$R_{II}(3)+\nu_3$?
74170(VE)	0	$R_{II}(3)+\nu_3+\nu_5$
74609(VE)	2	$R_{II}(3)+2\nu_3$
75005	3	$R_{II}(3)+2\nu_7$ (or $2\nu_{10}$ or ν_1)
75209	3	—
75427	1	—
75670	0	$R_{II}(3)+3\nu_3$
77108	1	—
78211	12	$R_I(3)$
78712	2	$R_I(3)+\nu_5$
79318	6	$R_I(3)+\nu_3$
79510	6	$R_I(3)+\nu_2$
80730	38(U)	$R_{II}(4)$
81896	8	$R_I(4)$
82138	7	$R_I(4)+\nu_5$
82476	1	$R_I(4)+\nu_3$
82967	23	$R_{II}(5)$
83492	3	$R_I(5)$
84101	19	$R_{II}(6)$
84621	2	$R_I(6)$
84976	7	$R_{II}(7)$
85230	1	$R_I(7)$
85474	3	$R_{II}(8)$
85732	1	$R_I(8)$
86000(1162.8A)	1	$R_I(9)$

* Explanation of Table I. $R_I(n)$ and $R_{II}(n)$ indicate members of Rydberg series I and II. V_I and V_{II} are non-Rydberg transitions, possibly of type $N\rightarrow V$. ν_i are vibrations, in the notation of Herzberg (reference 10). (VE) indicates that the violet edge is sharper. (U) indicates uncertainty because of overlapping source line.

comparator, employing the following standards:[14] O IV 1338.603,1343.507; O V 1371.287; C IV 1548.214,1550.790 with other secondary standards identified from Boyce and Moore's Tables. The error in measurement of comparatively sharp bands does not exceed 5 cm^{-1}, but may be 10 cm^{-1} or a little more for some diffuse bands. A few very weak diffuse bands were measured from microphotometer tracings, with about the same accuracy as could be obtained from comparator measurements.

Wave numbers of the absorption bands are found in Table I, with relative intensity estimates, obtained from microphotometer tracings. We did not attempt any absolute intensity measurements. The strongest band at 72347 cm^{-1} was assigned an intensity of 100. Some representative microphotometer tracings are shown in Fig. 1. Some weak absorption bands may have been missed because of the presence of the usual emission and absorption lines in the source used. None of the bands in Table I can be ascribed to any impurities which might conceivably be present.

[14] J. C. Boyce and J. T. Moore, "Provisional Wavelength Identification Tables for the Vacuum Ultraviolet." (Mimeographed for private distribution, 1941.)

DISCUSSION

A qualitative examination of the spectrum as a whole shows these essential features. The two longest wave-length regions are diffuse, with origins apparently at 58362 and 63597 cm^{-1}. These are without doubt two separate electronic transitions. There is only one vibrational transition accompanying each of these electronic transitions. The two transitions as a whole are narrow, but broaden symmetrically with increase in pressure.

The remainder of the spectrum from 69684 up is stronger and the structure is sharper. Some of the bands are shaded definitely to the red. Most of this spectrum appears at 0.025 mm, and the strongest bands at 0.005 mm. There is apparently little continuous absorption in this pressure range below 83000 cm^{-1}. Above this it is possible that some very weak bands may be obscured by the weak continuum. Strong continuous absorption begins at about 87200 and nothing more can be seen at higher wave numbers, even at the lowest pressures. It will be convenient to discuss the spectrum above and below 69684 cm^{-1} separately.

The spectrum at wave numbers greater than 69684 is thought to arise mainly from two series of Rydberg transitions accompanied by few vibrational transitions, as is usual. An exception is the transition at 72374 which shows a moderately elaborate vibrational pattern. This transition, assigned as the first member of Rydberg Series II, also departs notably from the series formula. This shows probably that an equilibrium distance is changed from its normal state value more in this transition than in the others.

The two series appear to converge to essentially the same ionization potential (about 10.81 ev), and fit the following formulas:

$$\nu_0{}^n-87236=R/(n+0.45)^2=R_I(n) \quad n=2,3\cdots$$
$$\nu_0{}^n-87175=R/(n+0.05)^2=R_{II}(n) \quad n=3,4\cdots.$$

The agreement of observed and calculated terms, based on these ionization potentials is shown in Table II. This table shows also experimental terms in acetylene and ethylene taken from the data of Price.[15] A comparison of terms in acetylene series *I* with terms in ethylene oxide I is very striking, indicating, of course, about the same Rydberg denominator in the two cases. Agreement of ethylene oxide II with acetylene II and with

[15] W. C. Price, Phys. Rev. **47**, 444 (1935).

ethylene is less good, particularly with more recent results on ethylene.[16] We believe that these comparisons are significant.

Further comparison of terms in other molecules[17] containing carbon-carbon double and triple bonds with terms of molecules containing C=0 shows that generally the former have Rydberg series formulas with denominators approximately $(n+0.45)^2$ and $(n+0.05)^2$ while carbonyl compounds have $(n+0.3)^2$ and $(n+0.6)^2$. This leads us to conclude that the Rydberg spectra of ethylene oxide have little resemblance to comparable spectra of carbonyl compounds, where a $2p(0)$ non-bonding electron is excited. A similar comparison with water,[18] shows that its Rydberg spectrum is not like that of ethylene oxide. It also appears probable, although not certain, that $2p(0)$ in ethylene oxide might have a higher ionization potential (as in water) than in carbonyl compounds, and higher than that of an unsaturation orbital in ethylene.

The electron structure and molecular orbitals of ethylene oxide have been discussed recently.[1-3, 8] We do not propose to enter this discussion, especially not in its relation to the chemical properties and reactivity of the compound. We believe, how-

TABLE II. Experimental terms (in cm^{-1}).

n	Ethylene Oxide I (Observed)	Ethylene Oxide I (Calculated)	Acetylene I (Price) (Observed)
2	17552	18282	17560
3	9025	9220	8936
4	5340	5542	5411
5	3744	3695	3645
6	2615	2638	2612
7	2006	1977	—
8	1504	1537	1516
9	1236	1229	1216

n	Ethylene Oxide II (Observed)	Ethylene Oxide II (Calculated)	Acetylene II (Price) (Observed)	Ethylene (Price, 1935) (Observed)
2	—	26112	26160	27040
3	14828	11797	11834	12230
4	6445	6690	6724	6820
5	4208	4304	4314	4340
6	3074	2998	3004	3020
7	2199	2208	2207	2220
8	1701	1693	1690	—
9	—	1340	1340	—

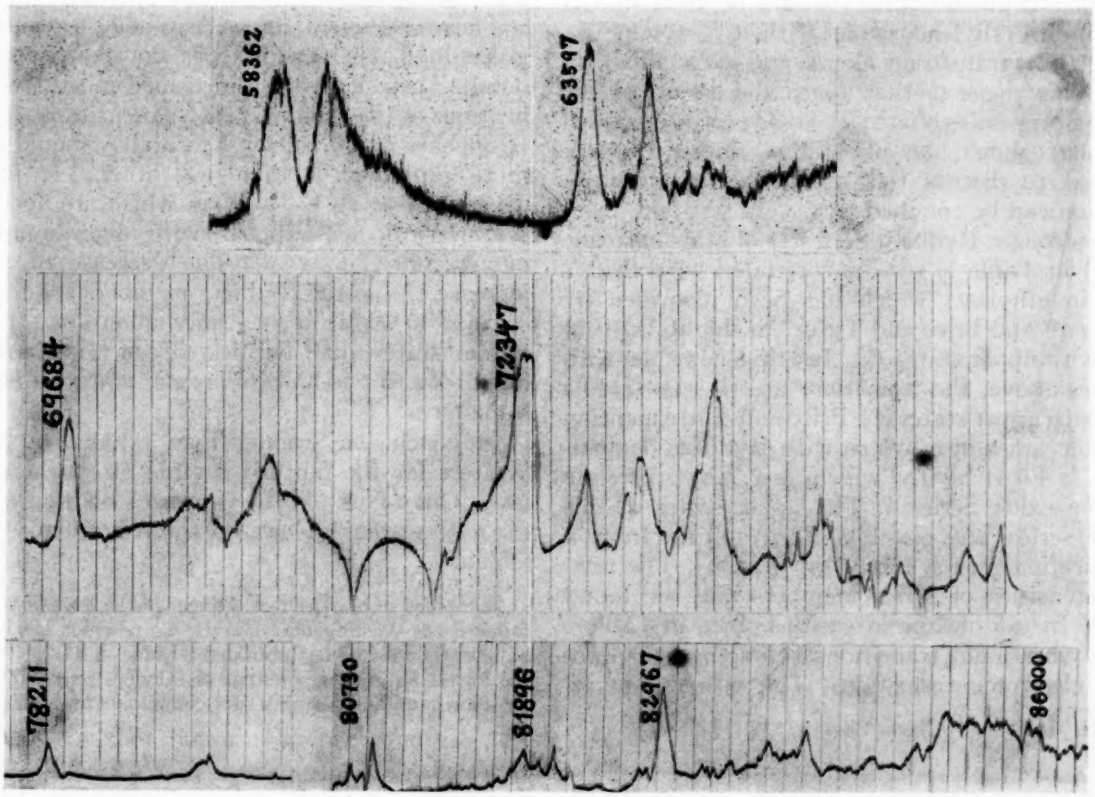

FIG. 1. Microphotometer tracings of the spectrum of ethylene oxide.

[16] W. C. Price and W. T. Tutte, Proc. Roy. Soc. (London) **A174**, 207 (1940).
[17] W. C. Price and A. D. Walsh, Trans. Faraday Soc. **41**, 381 (1945), methyl acetylene; W. C. Price and A. D. Walsh, Proc. Roy. Soc. (London) **A174**, 220 (1940), conjugated dienes; W. C. Price, J. Chem. Phys. **3**, 256 (1935), formaldehyde; A. D. Walsh, Proc. Roy. Soc. (London) **A185**, 176 (1946), acetaldehyde; A. D. Walsh, Trans. Faraday Soc. **41**, 498 (1945), acrolein.
[18] W. C. Price, J. Chem. Phys. **4**, 147 (1936).

ever, that the ideas of Walsh can very well be used to account for most of the features of the electronic spectra, especially the similarity of these to ethylene and acetylene.

For ethylene oxide with symmetry C_{2v}, it is appropriate to take the z axis along the symmetry axis and y in the plane of CCO perpendicular to z. With this choice, the unsaturation orbitals of ethylene are called (z_1+z_2) rather than (x_1+x_2) in the following discussion. From (z_1+z_2) of ethylene and $2p(0)$ we can construct a semilocalized bonding molecular orbital of ethylene oxide, written in LCAO form, coefficients omitted, as

$$\chi_{CCO}=(z_1+z_2+2p(0)).$$

The two non-bonding 0 electrons are in a $2p_z$ orbital; the other two 0 electrons are not distinguished in direction in a plane perpendicular to x, and are written $2p(0)$, as are their orbitals. The two carbons in ethylene are held together by a σ-bonding orbital also, which may be approximated in a localized treatment as $(t_y(1)+t_y(2))$, where $t_y(1)$ is the trigonal orbital of carbon (1) in the CC bond direction. (In the same localized treatment the other trigonal orbitals would be used in CH bonds.) In ethylene oxide with C_{2v} symmetry, $(t_y(1)+t_y(2))$ transforms like A_1 and so can mix with χ_{CCO}. This suggests that for a discussion of the bonding properties of ethylene oxide a non-localized treatment should be used. But since it is not intended to discuss this aspect of the problem, attention can be confined to χ_{CCO} as written.

The stronger Rydberg Series II of ethylene oxide ($R_{II}(n)$ in Table I) can be correlated with Price's series in ethylene, which has been identified by Mulliken[19] and Price and Tutte[16] as due to $(x_1+x_2)\rightarrow ns$, with upper states B_{3u}. In ethylene oxide, with the axes above, the transitions are $(z_1+z_2+2p(0))\rightarrow ns$, with upper states A_1. Price and Tutte mention a weaker series in ethylene with Rydberg denominator $(n+0.4)^2$ with which we may correlate ethylene oxide Series I. The upper states of this second series are possibly B_2, resulting from a configuration $(z_1+z_2+2p(0))np$ (or nd). The relative intensities of series members may be found roughly by adding the intensities given in Table I of the vibrational transitions belonging to appropriate electronic transitions. The decrease in intensity from low to high members of a series appears normal.

The transitions at smaller wave numbers than 69684 are believed to arise by excitation of an electron from $(z_1+z_2+2p(0))^2$ to one of the antibonding forms of this orbital. There will be a number of these, formulated $(z_1+z_2-2p(0))$, $(z_1-z_2+2p(0))$, $(z_1-z_2-2p(0))$, of which the first transforms like A_1 and the others like B_2. The $N\rightarrow V$ transition in ethylene (Mulliken's notation)[19] is between states A_{1g} and $(B_{3u})(B_{2g})=B_{1u}$. In ethylene oxide this is equivalent to a transition A_1 to B_2. The orbitals $(z_1-z_2\pm 2p(0))$ fulfill this requirement.

The experimental term value of $N\rightarrow V$ lies at about 28800 cm^{-1} below the ionization potential of (x_1+x_2) in ethylene. If it is assumed that $N\rightarrow V$ in ethylene oxide will lie about as far below the ionization potential of $(z_1+z_2+2p(0))$, the transition should occur at about 58400 cm^{-1}. The transition observed at 58362 may very probably arise from $(z_1+z_2+2p(0))^2\rightarrow(z_1+z_2+2p(0))(z_1-z_2+2p(0))$; $N\rightarrow V$. It is possible that the other non-Rydberg transition at 63597 is another $N\rightarrow V$ transition, possibly to $(z_1+z_2-2p(0))$.

The assignment of vibrational transitions is given in Table I and needs not be discussed in detail. These have been identified mostly as modifications of the normal state frequencies ν_3, ν_5, ν_2, ν_1. It appears reasonable that ν_3 and ν_5 should appear more prominently than the others. It may be expected that ν_7, ν_{10}, and ν_{12}, which are not totally symmetrical, will appear with even number of quanta only, if at all. The decrease of ν_3 with increase of n in the Rydberg members is quite large so that in $R_I(4)$ it has only about one-third its normal state value. The decrease of ν_5 is less marked but drops to one-half its normal state value in the same term.

In conclusion, we wish to thank Dr. W. D. Walters for the purified sample of ethylene oxide used. One of us (TKL) expresses his appreciation for a Research Fellowship from Academia Sinica, China.

Note added in proof: Dr. A. Langer of the Research Laboratories of the Westinghouse Electric Corporation has informed us recently that he has obtained a value of 11.2±0.5 ev for the lowest ionization potential of ethylene oxide. We thank Dr. Langer and his associates for communicating this information.

[19] R. S. Mulliken, J. Chem. Phys. **3**, 518 (1935).

The Normal Vibrations of Polyatomic Molecules as Treated by Urey-Bradley Field

TAKEHIKO SIMANOUTI
Chemical Institute, Faculty of Science, Tokyo University, Tokyo, Japan

(Received July 6, 1948)

A method of setting up the vibrational secular equation for polyatomic molecules of "Urey-Bradley field" type is described. By this method the vibration frequencies of CCl_4, CBr_4, CH_4, CD_4, CCl_3Br, CCl_2Br_2, $CClBr_3$, CCl_3H, CCl_2H_2, $CClH_3$, CCl_3D, CCl_2D_2, $CClD_3$, CH_3D, CH_2D_2, and CHD_3 molecules have been calculated. The 102 fundamental frequencies calculated using 28 distinct force constants are in satisfactory agreement with the observed, with a mean deviation of 1.4 percent.

WHEN the simple valence force field or the central force field is used as the potential function, the vibration frequencies of polyatomic molecules often cannot be calculated satisfactorily. In such cases it is most adequate to use the Urey-Bradley field, which contains both force constants related to changes in the distances between non-bonded atoms and force constants associated with changes in bond lengths and bond angles. In the present paper, the frequencies of the normal vibrations of numerous methane derivatives are calculated using this type of potential field.

POTENTIAL ENERGY

Pentatomic methane derivative molecules CXYZU are dealt with (Fig. 1). The Urey-Bradley field type of potential function is expressed as

$$V=\sum_{i=1}^{4}[K_i'r_i\Delta r_i+\tfrac{1}{2}K_i(\Delta r_i)^2]+\sum_{i<j}[H_{ij}'r_{ij}^2\Delta\alpha_{ij}+\tfrac{1}{2}H_{ij}(r_{ij}\Delta\alpha_{ij})^2]+\sum_{i<j}[F_{ij}'q_{ij}\Delta q_{ij}+\tfrac{1}{2}F_{ij}(\Delta q_{ij})^2], \quad (1)$$

where r's are the bond lengths, α's the bond angles, q's the distances between atoms not bonded directly, and r_{ij} represents $(r_ir_j)^{\frac{1}{2}}$. K', K, H', H, F', and F are the force constants, the last two of which are the repulsion constants between non-bonded atoms.

Through the relation

$$q_{ij}^2=r_i^2+r_j^2-2r_ir_j\cos\alpha_{ij}, \quad (2)$$

we can represent Δq_{ij} by Δr_i, Δr_j, and $\Delta\alpha_{ij}$:

$$\Delta q_{ij}=s_{ij}\Delta r_i+s_{ji}\Delta r_j+(t_{ij}t_{ji})^{\frac{1}{2}}(r_{ij}\Delta\alpha_{ij})+\{t_{ij}^2(\Delta r_i)^2+t_{ji}^2(\Delta r_j)^2-s_{ij}s_{ji}(r_{ij}\Delta\alpha_{ij})^2-2t_{ij}t_{ji}(\Delta r_i)(\Delta r_j)+2t_{ij}s_{ji}(\Delta r_i)(r_j\Delta\alpha_{ij})+2t_{ji}s_{ij}(\Delta r_j)(r_i\Delta\alpha_{ij})\}/2q_{ij}, \quad (3)$$

where

$$s_{ij}=(r_i-r_j\cos\alpha_{ij})/q_{ij},\quad s_{ji}=(r_j-r_i\cos\alpha_{ij})/q_{ij},\quad t_{ij}=r_j\sin\alpha_{ij}/q_{ij},\quad t_{ji}=r_i\sin\alpha_{ij}/q_{ij}. \quad (4)$$

In these equations, r_i, r_j, α_{ij}, and q_{ij} denote equilibrium values. From Eqs. (1) and (2) the potential energy is obtained as a function of valence-force coordinates:

$$V=\sum_i\left[K_i'r_i+\sum_{j(\neq i)}F_{ij}'s_{ij}q_{ij}\right](\Delta r_i)+\sum_{i<j}[H_{ij}'r_{ij}+F_{ij}'q_{ij}(t_{ij}t_{ji})^{\frac{1}{2}}](r_{ij}\Delta\alpha_{ij})+\frac{1}{2}\sum_i\left[K_i+\sum_{j(\neq i)}(t_{ij}^2F_{ij}'+s_{ij}^2F_{ij})\right](\Delta r_i)^2+\frac{1}{2}\sum_{i<j}[H_{ij}-s_{ij}s_{ji}F_{ij}'+t_{ij}t_{ji}F_{ij}](r_{ij}\Delta\alpha_{ij})^2+\sum_{i<j}[-t_{ij}t_{ji}F_{ij}'+s_{ij}s_{ji}F_{ij}](\Delta r_i)(\Delta r_j)+\sum_{i\neq j}[t_{ij}s_{ji}F_{ij}'+t_{ji}s_{ij}F_{ij}]\times(r_j/r_i)^{\frac{1}{2}}(\Delta r_i)(r_{ij}\Delta\alpha_{ij}). \quad (5)$$

In this equation all Δr's are independent variables, but all $\Delta\alpha$'s are not and the relation among the latter is not simple. When it is assumed, however, that all the bond angles are tetrahedral in the equilibrium position, the following relation among six $\Delta\alpha$'s can be obtained, neglecting

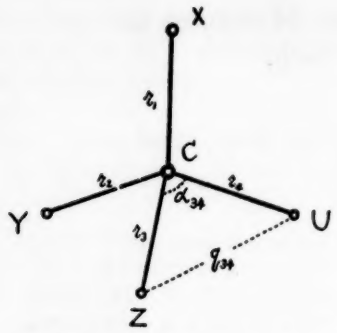

FIG. 1. Coordinates used.

higher terms of $\Delta\alpha$'s.

$$\sum_{i<j}(\Delta\alpha_{ij})+(\sqrt{2}/8)\left\{3\sum_{i<j}(\Delta\alpha_{ij})^2+4\sum_{i\neq j\neq k}(\Delta\alpha_{ij})(\Delta\alpha_{ik})\right\}=0. \quad (6)$$

As the atoms are in equilibrium position, from Eqs. (5) and (6) are obtained:

$$r_i K_i'+\sum_{j(\neq i)} s_{ij}q_{ij}F_{ij}'=0, \quad (7)$$

$$r_{ij}^2 H_{ij}'+r_{ij}q_{ij}(t_{ij}t_{ji})^{\frac{1}{2}}F_{ij}'+\kappa=0, \quad (8)$$

where κ is a new molecular constant which may appropriately be called "intramolecular tension." Finally, the potential energy can be expressed as follows:

$$\begin{aligned}V=&-\frac{1}{2}\sum_i\left[K_i+\sum_{j(\neq i)}(t_{ij}^2F_{ij}'+s_{ij}^2F_{ij})\right](\Delta r_i)^2\\&+\frac{1}{2}\sum_{i<j}[H_{ij}-s_{ij}s_{ji}F_{ij}'+t_{ij}t_{ji}F_{ij}\\&\qquad+(3\kappa/\sqrt{8}r_{ij}^2)](r_{ij}\Delta\alpha_{ij})^2\\&+\sum_{i<j}[-t_{ij}t_{ji}F_{ij}'+s_{ij}s_{ji}F_{ij}](\Delta r_i)(\Delta r_j)\\&+\sum_{i\neq j}[t_{ij}s_{ji}F_{ij}'+t_{ji}s_{ij}F_{ij}]\\&\qquad\times(r_j/r_i)^{\frac{1}{2}}(\Delta r_i)(r_{ij}\Delta\alpha_{ij})\\&+\sum_{i\neq j\neq k}(\kappa/\sqrt{2}r_{ij}r_{ik})(r_{ij}\Delta\alpha_{ij})(r_{ik}\Delta\alpha_{ik}). \quad (9)\end{aligned}$$

TABLE I. Observed frequencies[a,b] and force constants of CX_4 molecules.

	Frequencies (cm^{-1})				Force constants* (10^5 dynes/cm)			
	A	E	T	T	K	H	F'	F
CCl_4	458	218	314	776	1.76	0.080	−0.097	0.656
CBr_4	269	122	183	667	1.43	0.045	−0.078	0.493
CH_4	2914	1499	1306	3018				
CD_4	2085	1036	997	2259	4.79	0.41	0	0.077

[a] A. Langseth, Zeits. f. Physik **72**, 350 (1931).
[b] See reference 10.
* As the anharmonicity and liquid perturbation are neglected, the force constants mean the effective values. In the case of CH_4 and CD_4 the force constants are determined so that the calculated frequencies agree with the observed as well as possible.

SECULAR EQUATION

To express the vibrational kinetic energy with the valence-force coordinates, the method developed by E. B. Wilson[1] is used and the normal vibrations can be calculated from the secular equation

$$|\mathbf{GF}-\mathbf{E}\lambda|=0. \quad (10)$$

TETRAHEDRAL MOLECULES, CX_4

For the four frequencies, A, E, and two T's, of CX_4 molecules, the following **F** and **G** matrices are obtained:

$$\left.\begin{aligned}\mathbf{G}_A&=\mu,\\ \mathbf{F}_A&=K+4F,\end{aligned}\right\} \quad (11)$$

$$\left.\begin{aligned}\mathbf{G}_E&=3\mu,\\ \mathbf{F}_E&=H-\tfrac{1}{3}F'+\tfrac{1}{3}F,\end{aligned}\right\} \quad (12)$$

$$\left.\begin{aligned}\mathbf{G}_T&=\begin{pmatrix}\mu+\frac{4}{3}\mu_0, & -\frac{8}{3}\mu_0\\ -\frac{8}{3}\mu_0, & 2\mu+\frac{16}{3}\mu_0\end{pmatrix},\\ \mathbf{F}_T&=\begin{pmatrix}K+\frac{4}{3}F'+\frac{4}{3}F, & \frac{2}{3}(F'+F)\\ \frac{2}{3}(F'+F), & H-\frac{5}{3}F'+\frac{1}{3}F\end{pmatrix},\end{aligned}\right\} \quad (13)$$

where μ and μ_0 are the reciprocals of the masses of the X atom and C atom, respectively. This result is in good agreement with those of Rosenthal[2] and Urey and Bradley.[3]

From four observed frequencies four force constants, K, H, F', and F, are calculated. The other constants can be expressed with F'; that is, K' is expressed with Eq. (7) and κ with Eq.

TABLE II. Force constants (10^5 dynes/cm).

H_{ClCBr} =	0.0303
F'_{ClBr} =	−0.0872
F_{ClBr} =	0.575

TABLE III. The vibration frequencies of chlorobromomethanes (cm^{-1}). ($r_{CCl}=1.77$A, $r_{CBr}=1.92$A, α = the tetrahedral angle.)

	CCl_3Br				CCl_2Br_2				$CClBr_3$		
	Obs.	Calc.	Δν per-cent		Obs.	Calc.	Δν per-cent		Obs.	Calc.	Δν per-cent
A_1	710	714	0.6	A_1	720	727	1.0	A_1	734	724	1.4
	418	422	1.0		370	383	3.5		326	333	2.1
	243	246	1.2		230	242	5.2		210	210	0.0
E	765	758	0.9		141	150	6.4	E	674	671	0.4
	289	294	1.7	B_1	759	740	2.5		210	211	0.5
	187	184	1.6		252	259	2.8		139	137	1.4
				B_2	672	674	0.3				
					230	226	1.7		266	Overtone	
				A_2	164	164	—				
					318	Overtone					

[1] E. Bright Wilson, Jr., J. Chem. Phys. **7**, 1047 (1939); **9**, 76 (1941).
[2] Jenny E. Rosenthal, Phys. Rev. **45**, 538 (1934).
[3] H. C. Urey and C. A. Bradley, Phys. Rev. **38**, 1969 (1931).

(8), since H' is considered to be zero in this molecule. In this case Eq. (7) becomes

$$\kappa = -r_{ij}^2 F_{ij}' \sin\alpha_{ij}. \qquad (14)$$

The results of calculation are given in Table I. The negative values of F' show that the forces between non-bonded atoms are repulsive, as pointed out by Urey and Bradley.[3] The magnitude of the values of F' and F are found to be reasonable when some of them are compared with the interatomic forces of argon, krypton, and the like.[4,5]

CCl_3Br, CCl_2Br_2, AND $CClBr_3$

In the case of CX_3Y and CX_2Y_2 molecules, the **F** and **G** matrices are factored because of the symmetry properties, the details of which have been already given.[1,6-8] Of the twelve necessary constants, the values of K_{CCl}, H_{ClCCl}, F'_{ClCl}, F_{ClCl}, K_{CBr}, H_{BrCBr}, F'_{BrBr}, and F_{BrBr} are assumed to be the same as those of CCl_4 and CBr_4. For the values of F'_{ClBr}, F_{ClBr}, and κ, the arithmetical means of those of CCl_4 and CBr_4 are used. The remaining constant H_{ClCBr} is calculated from the frequency 164 cm^{-1} of CCl_2Br_2 molecule. The force constants thus obtained are given in Table II. Table III gives the calculated frequencies using these constants. The observed frequencies are taken from the Raman spectra measured by Lecomte and collaborators,[9] but the assignments are somewhat different.

TABLE IV. The vibration frequencies of deuteromethanes (cm^{-1}).

CH_3D				CH_2D_2				CHD_3			
	Obs.	Calc.	Δν per-cent		Obs.	Calc.	Δν per-cent		Obs.	Calc.	Δν per-cent
A_1	2982	2958	0.8	A_1	2974	2983	0.3	A_1	2992	3005	0.2
	2205	2204	0.0		2139	2160	1.0		2141	2115	1.2
	1306	1315	0.7		1450	1407	3.0		1046	1010	3.4
E	3030	3026	0.1		1036	1022	1.3	E	2269	2253	0.7
	1477	1435	2.8	B_1	3020	3026	0.2		1299	1265	2.6
	1156	1164	0.7		1090	1101	1.0		982	1022	4.1
				B_2	2255	2254	0.0				
					1235	1241	0.5				
				A_2	1286	1285	0.1				

[4] Y. Morino, I. Watanabe, and S. Mizushima, Sci. Pap. I. P. C. R. (Tokyo) **39**, 348 (1942).
[5] Takehiko Simanouti, Bull. I. P. C. R. (Tokyo) **23**, 314 (1944).
[6] J. E. Rosenthal and H. H. Voge, J. Chem. Phys. **4**, 134 (1936).
[7] J. Wagner, Zeits. f. physik. Chemie **B45**, 69 (1940).
[8] Takehiko Simanouti, Bull. I. P. C. R. (Tokyo) **21**, 825 (1942).
[9] Lecomte, Volkringer, and Tchakirian, Comptes Rendus **204**, 1927 (1937).

TABLE V. Force constants (10^5 dynes/cm).

K_{CCl} =1.75	K_{CH}=4.8(CH_4), 4.5(CH_3—), 4.2(CH_2—), 3.9(CH—)	
H_{ClCCl}=0.1	H_{HCH}=0.4	H_{ClCH}=0.05
F'_{ClCl} =−0.1	F'_{HH} =0.0	F'_{ClH} =−0.05
F_{ClCl} =0.65	F_{HH} =0.1	F_{ClH} =0.8

CH_3D, CH_2D_2, AND CHD_3

In calculating the frequencies of these molecules the force constants necessary are only four, which are given in Table I. The calculated values are compared (Table IV) with the observed which have been reviewed by Dennison[10] and Halverson.[11]

CCl_3H, CCl_2H_2, $CClH_3$, CCl_3D, CCl_2D_2, AND $CClD_3$

In these molecules the bond angles deviate from tetrahedral by several degrees.[12] In the present calculation the tetrahedral angles are assumed, and in consequence some deviations are unavoidable. In view of this approximation, only rounded values of force constants are assumed (Table V). The values of K_{CH}, H_{ClCH}, F'_{ClH}, and F_{ClH} are determined so that the

TABLE VI. The vibrational frequencies of chloro- and deuterochloromethanes (cm^{-1}).*

		Obs.	Calc.	Δν per-cent
CCl_4	A	458	456	0.4
	E	218	224	2.7
	T	314	318	1.3
		776	787	1.4

		Obs.	Calc.	Δν per-cent			Obs.	Calc.	Δν per-cent
CCl_3H	A_1	364	357	1.9	CCl_3D	A_1	367	357	2.7
		667	670	0.5			651	659	1.2
		3033	2988	1.5			2256	2170	3.8
	E	260	267	2.7		E	262	266	1.5
		760	745	2.0			738	728	1.4
		1205	1252	3.9			908	922	1.5
CCl_2H_2	A_1	283	292	3.2	CCl_2D_2	A_1	—	290	—
		704	718	2.0			—	694	—
		1429	1439	0.8			—	1053	—
		2984	2992	0.3			—	2162	—
	B_1	899	847	5.8		B_1	—	677	—
		3048	3015	1.1			—	2216	—
	B_2	737	715	3.0		B_2	—	705	—
		1266	1302	2.8			—	957	—
	A_2	1155	1127	2.4		A_2	—	802	—
$CClH_3$	A_1	732	724	1.1	$CClD_3$	A_1	701	706	0.7
		1355	1367	0.9			1029	1011	1.7
		(2920)	2981	2.1			2161	2134	1.3
	E	1020	966	5.2		E	775	731	5.7
		1460	1433	1.8			1081	1036	4.2
		3047	3028	0.6			2300	2239	2.6
CH_4	A	2916	2960	1.5	CD_4	A	2085	2093	0.4
	E	1499	1480	1.3		E	1036	1047	1.1
	T	1306	1324	1.4		T	997	996	0.1
		3018	3037	0.6			2259	2259	0.0

* For the recently observed frequencies in Tables IV and VI the writer is indebted to the reviewer of the Journal of Chemical Physics, to whom he wishes to express his thanks.

[10] David M. Dennison, Rev. Mod. Phys. **12**, 208 (1940).
[11] Frederick Halverson, Rev. Mod. Phys. **19**, 100 (1947).
[12] Y. Morino and M. Kimura, private communication.

calculated values agree with the observed as well as possible. Four values of K_{CH}, 4.8, 4.5, 4.2, and 3.9×10^5 dynes/cm, are those of CH_4, $CClH_3$, CCl_2H_2, and CCl_3H, respectively. Those values can be used successfully also in the calculation of the vibration frequencies of ethane ($K_{CH}=4.5$) and polyethylene ($K_{CH}=4.2$).[13] That the K_{CH} force constant is different in these molecules seems to be due to the difference of CH bond length.[14] For the values of κ, the weighted means of those obtained from Eq. (14) and the values of F' in Table V are taken. The calculated and the observed frequencies are compared in Table VI. The frequencies of CCl_4, CH_4, and CD_4 are recalculated using these force constants. The observed frequencies of the other molecules are taken from the Raman and the infra-red data (liquid state).[15]

CONCLUSION

Taking into account that the assumptions are very simple and that the assumed force constants are only 28 (strictly speaking 20), the results obtained for 102 frequencies are satisfactory. As the anharmonicity, liquid state frequency shift, and bond angle deviation from tetrahedral are neglected, the difference of several percent between the calculated and the observed values is unavoidable.

Thus we can conclude that the Urey-Bradley field is an adequate type of potential function to explain the vibration frequencies of polyatomic molecules and, therefore, the repulsive forces between non-bonded atoms are not negligible compared with the bond stretching or bending forces.

By means of almost the same method, Sanichiro Mizushima, Yonezo Morino, and the author have already calculated the skeletal vibrational frequencies of propane, *n*-butane, *n*-pentane, *n*-hexane, other normal long-chain paraffins,[16] and the rotational isomers of dichloroethane.[17] The vibrations of ethane, hexahalogenoethanes, acetate ion, glycine, and polyethylene (including its deutero and fluoro derivatives) are also calculated. All these calculations have given good results, the details of which will be reported in the near future.

The author wishes to express his sincere thanks to Professor S. Mizushima for helpful suggestions and advice, and also to Professor Y. Morino for the constant interest he has shown throughout the research.

[13] Takehiko Simanouti, unpublished work.
[14] T. Simanouti and H. Baba, unpublished work.
[15] George Herzberg, *Infrared and Raman Spectra of Polyatomic Molecules* (D. Van Nostrand Company, Inc., New York, 1945).
[16] S. Mizushima and T. Simanouti, Proc. Imp. Acad. Tokyo **20**, 86 (1944).
[17] S. Mizushima, Y. Morino, and T. Simanouti, Sci. Pap. I. P. C. R. (Tokyo) **40**, 87 (1942).

The Planar Vibrations of Benzene

BRYCE L. CRAWFORD, JR.
School of Chemistry, University of Minnesota, Minneapolis, Minnesota

AND

FOIL A. MILLER*
Department of Chemistry, University of Illinois, Urbana, Illinois

(Received June 7, 1948)

A normal coordinate treatment has been carried out for the planar vibrations of benzene and its deuterium derivatives. By using the latest assignments of Ingold and co-workers, eighteen of the twenty-six harmonic force constants have been determined.

INTRODUCTION

IN an earlier paper[1] the authors have reviewed previous work on the normal vibrations of benzene, and have treated the nonplanar vibrations in some detail. It was mentioned at that time that a satisfactory normal coordinate treatment of the planar vibrations awaited more experimental data which were needed to provide a satisfactory and complete assignment. A great step in this direction has been made by Ingold and his co-workers in their 1946 series of papers.[2] We have now used their assignments in an attempt to calculate the force constants for the planar vibrations of benzene.

A number of workers have carried out such calculations before,[3] but always with assignments which were more or less incomplete. Although the assignments of Ingold *et al.* are still open to question in a few details, they represent a significant advance. Therefore, it seems worth while to bring the force constants up to date. At the same time the secular equation will be presented in the form of Wilson's **F** and **G** matrices. This will serve a twofold purpose. (i) Equations will be readily available for re-evaluating the force constants, if that should be demanded by any future change in the assignments. (ii) The secular equation for benzene or for *any* of its deuterium derivatives can be written down immediately from these matrices.

TABLE I. Symmetry properties and notation for the planar vibrations of benzene.

D_{6h}	z C_3	z C_2	y C_2	i	No.	Ring	Notation Hyd. str.	Notation Hyd. bend
A_{1g}	+	+	+	+	2	ν_1	ν_2	
A_{2g}	+	+	−	+	1			ν_3
B_{1u}	+	−	+	−	2	ν_{12}	ν_{13}	
B_{2u}	+	−	−	−	2	ν_{14}		ν_{15}
E_{1g}	e	+	+	+	4	ν_{6a}, ν_{8a}	ν_{7a}	ν_{9a}
E_{1g}	e	+	−	+	4	ν_{6b}, ν_{8b}	ν_{7b}	ν_{9b}
E_{2u}	e	−	+	−	3	ν_{19a}	ν_{20a}	ν_{18a}
E_{2u}	e	−	−	−	3	ν_{19b}	ν_{20b}	ν_{18b}

MATHEMATICAL METHODS

The general procedure is the same as that used for the non-planar vibrations. The reader is referred to our earlier paper[1] for many details which will not be repeated here.

Benzene has twenty-one fundamental planar vibrations. Of these, seven are non-degenerate and seven are doubly degenerate, giving fourteen distinct frequencies in all. Their symmetry properties and notation are shown in Table I. We have

Species	VFSC	Coefficient for $j=$ 1	2	3	4	5	6	N	VFC
A_{1g}	S_1	1	1	1	1	1	1	$6^{-1/2}$	ΔR_j
	S_2	1	1	1	1	1	1	$6^{-1/2}$	Δr_j
A_{2g}	S_3	1	1	1	1	1	1	$6^{-1/2}$	$r_0\beta_j$
B_{1u}	S_{12}	−1	1	−1	1	−1	1	$6^{-1/2}$	$R_0\alpha_j$
	S_{13}	−1	1	−1	1	−1	1	$6^{-1/2}$	Δr_j
B_{2u}	S_{14}	−1	1	−1	1	−1	1	$6^{-1/2}$	ΔR_j
	S_{15}	−1	1	−1	1	−1	1	$6^{-1/2}$	$r_0\beta_j$
E_{1g}	S_{6a}	−2	1	1	−2	1	1	$12^{-1/2}$	$R_0\alpha_j$
	S_{7a}	−2	1	1	−2	1	1	$12^{-1/2}$	Δr_j
	S_{8a}	−1	2	−1	−1	2	−1	$12^{-1/2}$	ΔR_j
	S_{9a}	0	−1	1	0	−1	1	1/2	$r_0\beta_j$
E_{1g}	S_{6b}	0	−1	1	0	−1	1	1/2	$R_0\alpha_j$
	S_{7b}	0	−1	1	0	−1	1	1/2	Δr_j
	S_{8b}	−1	0	1	−1	0	1	1/2	ΔR_j
	S_{9b}	2	−1	−1	2	−1	−1	$12^{-1/2}$	$r_0\beta_j$
E_{2u}	S_{18a}	0	1	1	0	−1	−1	1/2	$r_0\beta_j$
	S_{19a}	−1	0	1	1	0	−1	1/2	ΔR_j
	S_{20a}	−2	−1	1	2	1	−1	$12^{-1/2}$	Δr_j
	S_{7a}	−2	−1	1	2	1	−1	$12^{-1/2}$	$R_0\alpha_j$
E_{2u}	S_{18b}	2	1	−1	−2	−1	1	$12^{-1/2}$	$r_0\beta_j$
	S_{19b}	1	2	1	−1	−2	−1	$12^{-1/2}$	ΔR_j
	S_{20b}	0	1	1	0	−1	−1	1/2	Δr_j
	S_{7b}	0	1	1	0	−1	−1	1/2	$R_0\alpha_j$

FIG. 1. Elements of the transformation **U: VFSC=U** $\times$**VFC.** N is the normalization constant. Thus in species $E_{1g}b$, $S_{7b}=(1/2)(-\Delta r_2+\Delta r_3-\Delta r_5+\Delta r_6)$.

* This work was initiated while the junior author was a National Research Fellow at the University of Minnesota in 1942–44. Present address: Department of Research in Chemical Physics, Mellon Institute, Pittsburgh, Pennsylvania.

[1] F. A. Miller and B. L. Crawford, Jr., J. Chem. Phys. **14**, 282 (1946). In the present paper we have changed slightly our designation of the symmetry species; we now follow the usage of G. Herzberg, *Infrared and Raman Spectra* (D. Van Nostrand and Company, Inc.), which has been generally accepted by molecular spectroscopists.

[2] C. K. Ingold *et al.*, J. Chem. Soc. (London), 222–333 (1946).

[3] Reference 1 reviews the earlier work.

Class	VFSC	S_1	S_2	S_3	S_{12}	S_{13}	S_{14}	S_{15}	S_{4a}	S_{7a}	S_{8a}	S_{9a}
A_{1g}	S_1	$1/M$	$-1/M$									
	S_2	$-1/M$	$(1/M)+A$			B				G		
A_{2g}	S_3			$[(\rho+1)^2/M]+A$				B				I
B_{1u}	S_{12}				$12/M$	$12^{\frac{1}{2}}/M$						
	S_{13}				$12^{\frac{1}{2}}/M$	$(1/M)+A$				$-H$		
B_{2u}	S_{14}						$3/M$	$-3^{\frac{1}{2}}/M$				
	S_{15}						$-3^{\frac{1}{2}}/M$	$(1/M)+A$				$-J$
$E_{\rho a}{}^{+}$	S_{4a}								$15/2M$	$27^{\frac{1}{2}}/2M$	$-27^{\frac{1}{2}}/2M$	$-3^{\frac{1}{2}}(5\rho+2)/4M$
	S_{7a}								$27^{\frac{1}{2}}/2M$	$(1/M)+E$	$-1/2M$	$-3\rho/4M$
	S_{8a}								$-27^{\frac{1}{2}}/2M$	$-1/2M$	$5/2M$	$3(\rho+2)/4M$
	S_{9a}								$-3^{\frac{1}{2}}(5\rho+2)/4M$	$-3\rho/4M$	$3(\rho+2)/4M$	$[(5\rho^2+4\rho+8)/8M]+C$
$E_{\rho b}{}^{+}$	S_{6b}											
	S_{7b}											
	S_{8b}											
	S_{9b}											
$E_{ua}{}^{-}$	S_{18a}											
	S_{19a}											
	S_{20a}											
$E_{ub}{}^{-}$	S_{18b}											
	S_{19b}											
	S_{20b}											

(Symmetric)

FIG. 2. G matrix for planar vibrations of the deuterobenzenes. M = mass of carbon in atomic weight units; m = mass of hy- $+1/m_4+1/m_5+1/m_6]$; $B=1/6[-1/m_1+1/m_2-1/m_3+1/m_4-1/m_5+1/m_6]$; $C=1/4[1/m_2+1/m_3+1/m_5+1/m_6]$; $D=1/4\times$ $-1/m_6]$; $G=(2^{\frac{1}{2}}/12)[-2/m_1+1/m_2+1/m_3-2/m_4+1/m_5+1/m_6]$; $H=(2^{\frac{1}{2}}/12)[-2/m_1-1/m_2+1/m_3+2/m_4+1/m_5-1/m_6]$; $L=(3^{\frac{1}{2}}/12)[1/m_2+1/m_3-1/m_5-1/m_6]$.

followed Wilson[4] and Langseth and Lord[5] in numbering the vibrations and in defining the coordinate axes. The z axis is taken to be perpendicular to the plane of the molecule; the y axis is in the plane of the molecule and passes through carbon atoms one and four.

Wilson's technique[6] was used to obtain the secular equation. The following four types of valence force coordinates (VFC) were employed:

1. Δr_i, the change in length of the ith C−H bond.
2. ΔR_i, the change in length of the ith C−C bond.
3. $R_0\alpha_i$, where α_i is the change in the ith C−C−C angle and R_0 is the equilibrium C−C distance.
4. $r_0\beta_i$, where β_i is the angle between the ith C−H bond and the exterior bisector of the C−C−C angle centered on the ith carbon, and r_0 is the equilibrium C−H bond distance.

[4] E. Bright Wilson, Jr., Phys. Rev. **45**, 706 (1934).
[5] A. Langseth and R. C. Lord, Jr., Kgl. Danske Vid. Sels. Math.-Fys. Medd. **16**, 6 (1938).
[6] E. Bright Wilson, Jr., J. Chem. Phys. **7**, 1047 (1939); **9**, 76 (1941).

It is important to note that the ΔR_i have a different symmetry with respect to the x and y axes than do the other three types of VFC. The ΔR_i have the symmetry of the carbon-carbon bonds, whereas the remaining VFC have the symmetry of the atoms.

Symmetry factoring was obtained by using valence force symmetry coordinates ($VFSC$), which are orthonormal combinations of the VFC. The matrix **U** for the transformation $\mathbf{VFSC}=\mathbf{U}\times\mathbf{VFC}$ is given in a condensed form in Fig. 1. The various $VFSC$ are designated as S_1, S_2, $\cdots$ corresponding to normal vibrations ν_1, ν_2, $\cdots$. Three redundant coordinates appear among the $VFSC$ as a consequence of the fact that benzene is a ring molecule. The necessity of ring closure imposes three restrictions on the various possible normal vibrations. The redundant coordinate in A_{1g} was easily eliminated at the start. The remaining two were kept in the **U** matrix. They are designated S_{ra} and S_{rb} of species E_{2ua} and E_{2ub}. These two coordinates were carried through to the **G** matrix and were then

S_{8b}	S_{7b}	S_{2b}	S_{9b}	S_{18a}	S_{19a}	S_{20a}	S_{18b}	S_{19b}	S_{20b}
	I					H			J
			$-G$	J			$-H$		
	$-J$					$-G$			$-I$
			H	$-.$			G		
	K					F			L
			$-K$	D			$-L$		
$15/2M$	$27^{\frac{1}{2}}/2M$	$-27^{\frac{1}{2}}/2M$	$-3^{\frac{1}{2}}(5\rho+2)/4M$						
$27^{\frac{1}{2}}/2M$	$(1/M)+C$	$-1/2M$	$-3\rho/4M$			L			D
$-27^{\frac{1}{2}}/2M$	$-1/2M$	$5/2M$	$3(\rho+2)/4M$						
$-3^{\frac{1}{2}}(5\rho+2)/4M$	$-3\rho/4M$	$3(\rho+2)/4M$	$[(5\rho^2+4\rho+8)/8M]+E$	$-L$			F		
				$[(9\rho^2+12\rho+8)/8M]+C$	$-6^{\frac{1}{2}}(3\rho+2)/4M$	$3\rho/4M$	$-K$		
				$[-6^{\frac{1}{2}}(3\rho+2)/4M]$	$3/M$	$-6^{\frac{1}{2}}/2M$			K
				$3\rho/4M$	$-6^{\frac{1}{2}}/2M$	$(1/M)+E$			
							$[(9\rho^2+12\rho+8)/8M]+E$	$-6^{\frac{1}{2}}(3\rho+2)/4M$	$3\rho/4M$
							$-6^{\frac{1}{2}}(3\rho+2)/4M$	$3/M$	$-6^{\frac{1}{2}}/2M$
							$3\rho/4M$	$-6^{\frac{1}{2}}/2M$	$(1/M)+C$

drogen in atomic weight units; $\rho=r_0/R_0=$C$-$H equilibrium distance/C$-$C equilibrium distance; $A=1/6[1/m_1+1/m_2+1/m_3$ $[-1/m_2+1/m_3+1/m_5-1/m_6]$; $E=1/12[4/m_1+1/m_2+1/m_3+4/m_4+1/m_5+1/m_6]$; $F=1/12[4/m_1-1/m_2+1/m_3-4/m_4+1/m_5$ $I=(6^{\frac{1}{2}}/12)[-1/m_2+1/m_3-1/m_5+1/m_6]$; $J=(6^{\frac{1}{2}}/12)[1/m_2+1/m_3-1/m_5-1/m_6]$; $K=(3^{\frac{1}{2}}/12)[-1/m_2+1/m_3-1/m_5+1/m_6]$;

removed by applying the transformations

$$\tilde{\mathbf{L}}\times\mathbf{G}'(E_{2ua})\times\mathbf{L}=\mathbf{G}(E_{2ua})$$

and

$$\tilde{\mathbf{L}}\times\mathbf{G}'(E_{2ub})\times\mathbf{L}=\mathbf{G}(E_{2ub})$$

where $\mathbf{L}$ is the matrix:

L	S_{18}	S_{19}	S_{20}	S_r
S_{18}	1	0	0	0
S_{19}	0	$2^{-1/2}$	0	$2^{-1/2}$
S_{20}	0	0	1	0
S_r	0	$-2^{-1/2}$	0	$2^{-1/2}$

$\tilde{\mathbf{L}}$ is the transpose of $\mathbf{L}$, $\mathbf{G}'(E_{2ua})$ is the $\mathbf{G}$ matrix for symmetry block E_{2ua} containing the redundant coordinate, and $\mathbf{G}(E_{2ua})$ is the $\mathbf{G}$ matrix for block E_{2ua} with the redundant coordinate removed.

The final $\mathbf{G}$ matrix is given in Fig. 2. The outlined blocks indicate the way the matrix factors for D_{6h} symmetry. Terms outside these blocks are interaction terms which are zero for benzene and benzene-d_6, but which may be different from zero in the intermediate deuterium derivatives of lower symmetry. By leaving the results in this form, the secular equation for any deuterium derivative of benzene can be obtained with very little trouble.[1] The reader is referred to Wilson's first paper on the subject[6] for the method of reducing the matrices to the explicit equations.

We now turn to the potential function. The $\mathbf{F}$ matrix for the *VFSC* is given in Fig. 3. One will note that it includes all the possible interaction constants for the planar vibrations that are compatible with the symmetry of benzene—twenty-six in all. The scheme of notation for these force constants (hereafter termed "Greek" constants) is outlined in Table IIA.

The force constants for the *VFSC* can be expressed in terms of the constants for the *VFC* (hereafter termed "Latin" constants). The notation for the latter is indicated in Table IIB. For example, the diagonal force constant for $\Delta r_i\times\Delta r_i$ is termed E, while the interaction constants for the various $\Delta r_i\times\Delta r_j (i\neq j)$ are termed e_o, e_m, and e_p.

Species	*VFSC*	S_1	S_2	S_3	S_{12}	S_{13}	S_{14}	S_{15}	S_{6a}	S_{7a}	S_{8a}	S_{9a}	S_{6b}	S_{7b}	S_{8b}	S_{9b}	S_{18a}	S_{19a}	S_{20a}	S_{18b}	S_{19b}	S_{20b}
A_{1g}	S_1	A_1	ξ_1																			
	S_2	ξ_1	Ω_1																			
A_{2g}	S_3			Γ_1																		
B_{1u}	S_{12}				Σ_2	ψ_2																
	S_{13}				ψ_2	Ω_2																
B_{2u}	S_{14}						A_2	μ_2														
	S_{15}						μ_2	Γ_2														
E_{1ga}	S_{6a}								Σ_3	ψ_3	χ_3	π_3										
	S_{7a}								ψ_3	Ω_3	ξ_3	τ_3										
	S_{8a}								χ_3	ξ_3	A_3	μ_3										
	S_{9a}								π_3	τ_3	μ_3	Γ_3										
E_{1gb}	S_{6b}												Σ_3	ψ_3	χ_3	π_3						
	S_{7b}												ψ_3	Ω_3	ξ_3	τ_3						
	S_{8b}												χ_3	ξ_3	A_3	μ_3						
	S_{9b}												π_3	τ_3	μ_3	Γ_3						
E_{2ua}	S_{18a}																Γ_4	μ_4	τ_4			
	S_{19a}																μ_4	A_4	ξ_4			
	S_{20a}																τ_4	ξ_4	Ω_4			
E_{2ub}	S_{18b}																			Γ_4	μ_4	τ_4
	S_{19b}																			μ_4	A_4	ξ_4
	S_{20b}																			τ_4	ξ_4	Ω_4

FIG. 3. **F** matrix for planar vibrations of the deuterobenzenes.

The subscripts *o*, *m*, and *p* refer to the ortho, meta, and para positions. Thus e_o is the constant for interaction between the stretching of two C−H bonds which are ortho to each other. Similarly, the various *l*'s are interaction constants between hydrogen stretchings and hydrogen bendings. Interaction constants bearing no subscripts refer to immediately adjacent positions. For example, l itself is the constant for interaction between the stretching of a given C−H bond and the bending of that same bond—for $\Delta r_1 \times r_0\beta_1$, $\Delta r_2 \times r_0\beta_2$, etc.

Just as for the non-planar vibrations, there are fewer Greek constants (26) than Latin constants (37).[7] The Greek constants are the ones which are evaluated from the experimental frequencies. Even if they could all be determined (which is not the case at present), it would be impossible to evaluate the harmonic *valence force* potential function completely. However, the terms for hydrogen stretching and hydrogen bending motions can be determined, since there are four Greek constants and four Latin constants in each case. The relations are:

[7] Several of these thirty-seven Latin constants may be shown to be equal to zero by symmetry. Examples are $n=n_o=0$. Nevertheless, there are still fewer Greek than Latin constants because of the redundancy relations among the *VFC* mentioned above.

Hydrogen stretching:

$$\Omega_1 = E + 2e_o + 2e_m + e_p.$$
$$\Omega_2 = E - 2e_o + 2e_m - e_p.$$
$$\Omega_3 = E - e_o - e_m + e_p.$$
$$\Omega_4 = E + e_o - e_m - e_p.$$

Hydrogen bending:

$$\Gamma_1 = G + 2g_o + 2g_m + g_p.$$
$$\Gamma_2 = G - 2g_o + 2g_m - g_p.$$
$$\Gamma_3 = G - g_o - g_m + g_p.$$
$$\Gamma_4 = G + g_o - g_m - g_p.$$

The problem, then, is to evaluate the twenty-six Greek force constants from the assigned frequencies of light and heavy benzene (and intermediate deuterium derivatives if necessary). For this purpose the assignments of Ingold and co-workers[8] were employed. They are given later in Table V.

The following numerical values were used in the calculations:

m = mass of hydrogen (or deuterium) = 1.008 (or 2.016) atomic weight units.

M = mass of carbon = 12.01 atomic weight units.

r_0 = C−H and C−D equilibrium distance = 1.08A.

R_0 = C−C equilibrium distance = 1.39A.

$\rho = r_0/R_0 = 0.777$.

ν = frequency in wave numbers = const. $\times \lambda^{\frac{1}{2}}$, where λ is a root of the secular equation. When masses are in atomic weight units and force constants are 10^{-5} times their value in dynes/cm, the constant is 1302.9.

EVALUATION OF THE FORCE CONSTANTS

Species $A_{1g}(\nu_1, \nu_2)$

The two vibrations in this species are the totally symmetrical C−H and C−C stretching modes (the "breathing" frequencies). It is often assumed that the interactions between C−H stretching vibrations and other modes are negligible. If we assume this by putting the interaction constant ξ_1 equal to zero, we can evaluate the two constants Λ_1 and Ω_1 from the two frequencies of benzene or from those of benzene-d_6. The results will not quite agree because of differing degrees of anharmonicity in the two molecules. We find:

	Benzene	Benzene-d_6	Average
Λ_1	7.617	7.623	6.620
Ω_1	5.085	5.154	5.119
ξ_1	(0)	(0)	(0)

[8] Reference 2, p. 332.

TABLE II.

A. Notation for force constants for *VFSC*.

	Ring stretch	Hyd. stretch	Ring bend	Hyd. bend
Ring stretch	A	ξ	χ	μ
Hydrogen stretch		Ω	ψ	τ
Ring bend			Σ	π
Hydrogen bend				Γ

B. Notation for force constants for *VFC*.

	Ring stretch ΔR_i	Hyd. stretch Δr_i	Ring bend $R_0\alpha_i$	Hyd. bend $r_0\beta_i$
Ring stretch ΔR_i	D, d_o, d_m, d_p	h_o h_m h_p	i_o i_m i_p	j_o j_m j_p
Hyd. stretch Δr_i		E e_o e_m e_p	k k_o k_m k_p	l l_o l_m l_p
Ring bend $R_0\alpha_i$			F f_o f_m f_p	n n_o m_m m_p
Hyd. bend $r_0\beta_i$				G g_o g_m g_p

It is to be remembered that the force constants must be multiplied by 10^5 to convert to dynes/cm.

A more exact procedure is to use the two frequencies of benzene and the two for benzene-d_6 to provide three independent equations from which Λ_1, Ω_1, and ξ_1 may be evaluated. It is noteworthy that one gets only three, rather than four, independent equations from these four frequencies. The equation of highest degree for each of the two molecules has the form $f(k\text{'s}) = \lambda_1 \cdot \lambda_2 \times f(\text{masses})$. When one substitutes the known values for the λ's and for the masses of benzene and benzene-d_6, the equations become identical (except for anharmonic effects). This is a general result for any symmetry species.[9] Hence, if a species has n genuine normal vibrations, the frequencies of the original molecule and its completely substituted isotopic derivative give only $2n-1$ independent equations for evaluating the force constants.

For species A_{1g} of benzene this procedure furnishes two sets of roots, but only the following set is physically reasonable.

Λ_1	7.832	(Ring stretch)
Ω_1	5.003	(Hyd. stretch)
ξ_1	−0.4198	(Interaction)

It is clear that the usual neglect of interactions between C−H stretching and other vibrations is not justified in terms of accurate values of force constants. However, the frequency values (as well as the diagonal force-constant values) are relatively insensitive to these particular interaction constants, so that for the purpose of calculating frequencies they may be neglected—particularly in view of uncertainties due to anharmonicity. This is exemplified by the results in Table III.

[9] Use is made of it in the derivation of the Teller-Redlich product rule. O. Redlich, Zeits. f. physik. Chemie **28B**, 371 (1935).

TABLE III. Calculated values for the A_{1g} frequencies.

		Observed	Calc. ($\xi_1=0$)*	Calc. ($\xi_1\neq 0$
Benzene	ν_1	992	992	996
	ν_2	3062	3072	3061
Benzene-d_6	ν_1	943	943	939
	ν_2	2293	2285	2294

* The average values of A_1 and Ω_1 were used.

Species $A_{2g}(\nu_3)$

There is only one frequency and one force constant in this species. One finds:

	Benzene	Benzene-d_6	Average
Γ_1	0.8253	0.8347	0.8300

Species $B_{1u}(\nu_{12}, \nu_{13})$

This species contains a hydrogen stretching and a ring bending vibration. Again we calculate two sets of values by first omitting the interaction constant and then including it.

	Benzene	Benzene-d_6	Average
Ω_2	5.076	5.131	5.104
Σ_2	0.6587	0.6636	0.6612
ψ_2	(0)	(0)	(0)

If one includes ψ_2, one finds two sets of roots.

	Set 1	Set 2	
Ω_2	5.002	5.002	(Hyd. stretch)
Σ_2	0.6768	2.467	(Ring bend)
ψ_2	0.1064	−2.994	(Interaction)

Both sets are physically possible, but set 1 is more plausible because it contains an interaction constant which is smaller in magnitude than the diagonal constant Σ_2, and because the absolute value of Σ_2 is more reasonable.

Species $B_{2u}(\nu_{14}, \nu_{15})$

The assignment of ν_{14} is still in considerable doubt. We shall use Ingold's values of 1648 cm^{-1} in benzene and 1571 cm^{-1} in benzene-d_6 to calculate provisional values for the force constants. Neither ν_{14} nor ν_{15} is a C−H stretching mode, so the interaction constant is important and we do not attempt to set it equal to zero. Again two sets of roots are obtained.

	Set 1	Set 2	
Γ_2	0.94993	0.9493	(Hyd. bend)
Λ_2	6.724	4.989	(Ring stretch)
μ_2	1.299	−0.2030	(Interaction)

It is hard to choose a preferred set in this case, and we make no attempt to do so, because the assignments may well be incorrect. It seems more useful to give the explicit equations for this species so that any different assignment can be readily used to obtain the corresponding force constants. The equations are

$$\lambda_1+\lambda_2=(1/M)[3\Lambda_2+\Gamma_2-12^{\frac{1}{2}}\mu_2]+\Gamma_2/m.$$
$$\lambda_1\cdot\lambda_2=(3/mM)[\Lambda_2\Gamma_2-\mu_2^2].$$

Species $E_{2u}(\nu_{18}, \nu_{19}, \nu_{20})$

The spectra of light and heavy benzene furnish a total of six frequencies in E_{2u}, but as pointed out earlier there are only five independent equations for solving for the force constants. The complete potential function contains six force constants. Obviously, a complete solution is impossible. Two possible alternatives suggest themselves. (i) One can assume that the value of the C−H stretching constant, Ω_4, is the same as in species A_{1g} and B_{1u} (5.003 and 5.002, respectively). This can be inserted in the equations, giving five equations in five unknown force constants. The assumption is probably good, but the solution promises to be formidable. (ii) One can assume some of the interaction constants are zero. The logical choices are τ_4 and ξ_4, the interactions between C−H stretching and the other two forms of motion involved. One then has five equations in four unknowns. Since, in practice, the most important use of force constants is in calculating frequencies, the most desirable procedure is one in which as few constants as possible are used consistent with results of the requisite accuracy. This suggests that the dropping of the two interaction constants is not only easier but also more practical. Consequently this method was used. Again one obtains two sets of roots.

	Set 1	Set 2
Ω_4	5.147	5.147
Γ_4	0.8698	0.8698
Λ_4	6.143	3.917
μ_4	1.399	0.1393
ξ_4	(0)	(0)
τ_4	(0)	(0)

It was found that the calculated force constants varied rather appreciably, depending upon just how the equations were solved for them. There are several reasons for this. First, anharmonicities are different for benzene and benzene-d_6, and this is ignored in the process of solution. Second, the method of solution sometimes involves taking small differences between large numbers. Consequently, we do not claim that the values of the above constants express accurate physical reality. They will, however, give moderately good calculated values for the frequencies (Table V).

The reader may have noticed that in every symmetry class the values of the diagonal constants for C−H stretching and C−H bending are determined uniquely. Only for the ring stretching and bending constants, and for the interaction constants, are two sets of roots obtained. This is because constants of the first type are readily evaluated by comparing the equations for benzene with those of benzene-d_6. For the evaluation of the remaining force constants, however, it was found that it was not as helpful to have two sets of equations as we had expected. This is due to the fact that the potential function is anharmonic, and the anharmonicity has a larger effect on the experimental frequencies of benzene than on those of benzene-d_6. Hence the two sets of equations are not actually satisfied by a common set of values for the force constants. For the same reason it is not helpful to introduce the equations for deuterium derivatives of lower symmetry. Therefore, after first evaluating the diagonal C−H stretching and bending constants, we confined ourselves wherever possible to the equations for one isotopic molecule.

Species $E_{1g}(\nu_6, \nu_7, \nu_8, \nu_9)$

In this species benzene and benzene-d_6 furnish eight frequencies, or seven independent equations, from which to evaluate ten force constants. Obviously, the values of at least three constants must be assumed. A reasonable procedure is to set the constants for interaction with C−H stretching equal to zero: $\psi_3=\xi_2=\tau_3=0$. One can then evaluate Ω_3 and Γ_3 without much trouble by comparing the resulting equations for benzene and those of benzene-d_6. One finds $\Omega_3=5.044$, $\Gamma_3=0.8491$. With these values introduced, the relation between force constants and the sum of the frequency parameters is identically the same for benzene and benzene-d_6; thus one has six equations to determine the five remaining constants. To do this, we first assumed the three interaction constants π_3, μ_3, and χ_3 to be small, and neglected second-order terms; we could then solve for the diagonal constants, and found $\Lambda_3=5.66$ and $\Sigma_3=0.741$. (There was also a second pair of roots, not physically reasonable.) Using these values, we adjusted the interaction constants by a least-squares procedure, and found $\pi_3=0.241$, $\chi_3=-0.181$, with μ_3 negligible. These values gave frequencies in good agreement with the observed, except for ν_6; to improve this, we readjusted Σ_3 by a least-squares procedure, and found $\Sigma_3=0.810$. With the set of constants so obtained, we calculated the frequencies shown in Table V, in satisfactory agreement with the observed values.

This completes the determination of the force constants. For convenience the results have been gathered together in Table IV, where the various sets are arranged in order of decreasing preference.

FURTHER RESULTS

One can now use the force constants to calculate the vibrational frequencies. Table V gives the results. The preferred set of force constants has been used in each case. For benzene and benzene-d_6, we have merely calculated back the frequencies used in evaluating the force constants, but a few independent checks can be obtained from symbenzene-d_3 as shown. In principle all the planar frequencies for the various deutero-benzenes should be calculable, but the symmetry blocks are so large that the labor is prohibitive. It may be noted that the calculated and observed values agree within 1.0 percent in all but six cases, with a maximum error of 2.2 percent.

It is now also possible to evaluate the valence force potential constants for the hydrogen stretching and bending motions. One finds, by use of Eqs. (1) and (2):

$$E=5.065 \qquad G=0.8695$$
$$e_o=0.017 \qquad g_o=-0.0164$$
$$e_m=-0.031 \qquad g_m=+0.0101$$
$$e_p=-0.034 \qquad g_p=-0.0268$$

We do not attach much significance to these results because the hydrogen vibrations are especially subject to anharmonicity, and hence so are the

TABLE IV. Values of the force constants ($k\times10^{-5}$ dyne/cm).

Species	Force constant	1st preference	2nd preference
A_{1g}	Λ_1	7.83	7.62
	Ω_1	5.00	5.12
	ξ_1	−0.420	0*
A_{2g}	Γ_1	0.830	
B_{1u}	Ω_2	5.00	5.10
	Σ_2	0.677	0.661
	ψ_2	0.106	0*
B_{2u}	Γ_2	0.949	0.949
	Λ_2	6.72	4.99
	μ_2	1.30	−0.203
E_{2u}	Ω_4	5.15	5.15
	Γ_4	0.870	0.870
	Λ_4	6.14	3.92
	μ_4	1.40	0.139
	ξ_4	0*	0*
	τ_4	0*	0*
E_{1g}	Ω_3	5.04	
	Γ_3	0.849	
	Σ_3	0.810	
	Λ_3	5.66	
	ψ_3	0*	
	χ_3	0.181	
	π_3	0.241	
	ξ_3	0*	
	τ_3	0*	
	μ_3	0	

* Assumed to be zero.

TABLE V. Calculated *vs.* assigned frequencies (cm^{-1}).

Species	Freq. no.	Benzene Calc.	Benzene Assigned	Benzene % Diff.	sym-benzene-d_3 Calc.	sym-benzene-d_3 Assigned	sym-benzene-d_3 % Diff.	Benzene-d_6 Calc.	Benzene-d_6 Assigned	Benzene-d_6 % Diff.
A_{1g}	1	996	992	+0.4	948	956	−0.8	939	943	−0.4
	2	3061	3062	0.0	3065	3053	+0.4	2294	2293	0.0
A_{2g}	3	1323	1326	−0.2	1245	1230±2%	—	1034	1037	+0.3
B_{1u}	12	1017	1010	+0.7	1006	1004	+0.2	960	963	−0.3
	13	3058	3060	0.0	2289	2282	+0.3	2291	2290	0.0
B_{2u}	14	1647	1648	0.0	1614	1600	+0.9	1572	1571	+0.1
	15	1112	1110	+0.2	900	920	−2.2	824	825	−0.1
E_{2u}	18	1053	1037	+1.3				815	813	+0.2
	19	1469	1485	−1.1				1320	1333	−1.0
	20	3082	3080	+0.1				2301	2294	+0.3
E_{1g}	6	599	606	−1.2				568	577	−1.6
	7	3050	3047	+0.1				2280	2265	+0.7
	8	1617	1596	+1.3				1561	1552	+0.6
	9	1180	1178	+0.2				869	867	+0.2

Greek constants from which these values are calculated.

ACKNOWLEDGMENT

We acknowledge with gratitude the assistance of Dr. C. E. Sun, and financial support from Contract N5ori-147, T.O. II, with the Office of Naval Research, on some of the final calculations.

One of us (F.A.M.) wishes to express his appreciation to the National Research Council for the grant of a fellowship.

THE JOURNAL OF CHEMICAL PHYSICS VOLUME 17, NUMBER 3 MARCH, 1949

Internal Rotation I

A Product Rule for *Cis*- and *Trans*-Isomers

H. J. BERNSTEIN
National Research Council, Ottawa, Canada

(Received July 12, 1948)

The assumption of equal force constants in the potential functions of *cis*- and *trans*-forms leads to a product rule for the planar vibrations of rotational isomers.
The rotational isomers of symmetrical dichloro- and dibromoethane are *trans*- and "gauche."

IF the potential energy of a molecule is expressed as the most general quadratic function of the displacements from the equilibrium configuration, it has been shown[1] that the product of the frequencies of the normal modes of vibration belonging to the same symmetry class can be expressed as the product of two functions. One of these is a function of the force constants only, and the other a function of the masses of the atoms and internuclear distances in the molecule. If some of the atoms of a molecule are replaced by their isotopes the potential energy of the isotopic molecule involves the same force constants as that for the original molecule since isotopic substitution does not change the internal field. Consequently the ratio of the product of the frequencies of a molecule to the product of the frequencies belonging to the same symmetry class of the isotopic molecule is the ratio of the two functions involving masses and internuclear distances only. The Teller-Redlich[2] product rule expresses this ratio in terms of molecular weights and moments of inertia.

TABLE I.

Cis-C_{2v} Type	No. of vib'ns	Non-genuine vib'ns	*Trans*-C_{2h} Type	No. of vib'ns	Non-genuine vib'ns
A_1	5	T_y	A_g	5	R_z
B_1	4	T_xR_z	B_u	4	T_xT_y
A_2	2	R_y	A_u	2	T_z
B_2	1	T_zR_x	B_g	1	R_xR_y

To obtain a product rule for rotational isomers it is necessary as a first approximation to assume that the force constants appearing in the potential function of the two isomers are the same.[3] This will be true to a very good approximation for all planar force constants[4] but need not be true for out-of-plane constants where in general the rotational isomers have different activation energies and thus different curvatures of the potential function at their respective minima. Even for the in-plane vibrations the interaction constants between groups or atoms on neighboring atoms will in general be quite different for *cis*- and *trans*-configurations. However, to a good first approximation, the interaction constants between atoms whose internuclear distance is independent of azimuthal angle will not be very

[1] E. B. Wilson, Jr., J. Chem. Phys. **7**, 1047 (1939); **9**, 76 (1941).

[2] E. Teller, quoted in W. R. Angus *et al.*, J. Chem. Soc. (1936), p. 971; O. Redlich, Zeits. f. physik. Chemie **B28**, 371 (1935).

[3] E. L. Pace, J. Chem. Phys. **15**, 528 (1947), has obtained a product rule for the E_g and E_u vibrations of an X_2Y_6 molecule by assuming the force constants to be the same and that the interaction constants of the XY_3 groups may be neglected.

[4] J. A. A. Ketelaar, Rec. Trav. Chim. **58**, 266 (1939); J. Sherman and J. A. A. Ketelaar, Physica **6**, 572 (1939). Both valence bond and molecular orbital treatments of *cis*- and *trans*-dichloroethylenes gave the same C−Cl bond length. This means that the bond constants are the same.

different for *cis-* and *trans*-forms. When the internuclear distance changes as a function of azimuthal angle the interaction constants will be different but very small since these interactions are between substituents on non-adjacent atoms.

Inspection of the expressions[5] for the product of the frequencies of vibrations in corresponding symmetry classes for two molecules with *cis-* and *trans*-configurations shows that the ratio of the product of the *trans*-frequencies to that of the *cis-* is given by:

$$\frac{\Pi^T}{\Pi^C}=\left\{\left(\frac{m_1{}^C}{m_1{}^T}\right)^{\alpha}\left(\frac{m_2{}^C}{m_2{}^T}\right)^{\beta}\cdots\frac{(M^T)^a}{(M^C)^b}\cdot\frac{(I_x)^{\delta_x{}^T}(I_y)^{\delta_y{}^T}(I_z)^{\delta_z{}^T}}{(I_x)^{\delta_x{}^C}(I_y)^{\delta_y{}^C}(I_z)^{\delta_z{}^C}}\cdot\left(\frac{4}{d^2}\right)^{\delta_x{}^T+\delta_y{}^T+\delta_z{}^T}\cdot\left(\frac{d^2}{4}\right)^{\delta_x{}^C+\delta_y{}^C+\delta_z{}^C}\right\}^{\frac{1}{2}} \quad (1)$$

where the superscripts C, T indicate *cis-* and *trans-* respectively and $m_1m_2\cdots\alpha, \beta, \cdots M, I_x, I_y, I_z$, have the same significance as in the Teller-Redlich product rule (see G. Herzberg, *Infrared and Raman Spectra of Polyatomic Molecules* (D. Van Nostrand and Company, New York, 1945), p. 232); a, b are the number of translations of the symmetry type considered; $\delta_x{}^T$, $\delta_y{}^T$, $\delta_z{}^T$, $\delta_x{}^C$, $\delta_y{}^C$, $\delta_z{}^C$, are 1 or 0 depending on whether or not the rotation about the x, y, z axis is a non-genuine vibration of the symmetry type considered; d is the internuclear distance in A° between the two atoms lying on the rotation axis (x axis) about which *cis-* and *trans-*configurations may be obtained by rotation; the moments of inertia and molecular weights are expressed in atomic units and the xy plane is the plane of the molecule.

As an example one may consider *cis-* and *trans-*dichloroethylene. The symmetry types and non-genuine vibrations are given in Table I.

It is readily seen for the totally symmetric classes of *trans-* and *cis-* since R_z and T_y are the only non-genuine vibrations that appear, that $a=0$ and $b=1$, and $\delta_x{}^T=\delta_y{}^T=\delta_x{}^C=\delta_y{}^C=\delta_z{}^C=0$ and $\delta_z{}^T=1$.

If there is no isotopic substitution $m_1{}^T=m_1{}^C$ etc. so that relation (1) becomes

$$\Pi A_g/\Pi A_1=\left\{\frac{I_z{}^T}{M}\cdot\frac{4}{d^2}\right\}^{\frac{1}{2}}.$$

Table II lists various product ratios for *cis-* and *trans*-dichloroethylene, dibromoethylene, and butene-2.

The agreement over a wide range of product ratios is quite satisfactory and indicates that this ratio may be used to an accuracy of within 10 percent.

[5] F. Lechner, S. B. Akad. Wiss. Wien (IIA) **141**, 633 (1932); A. Verleysen, Ann. Bruxelles **59**, 267 (1939).

TABLE II.

Product ratio	Molecule	Ratio calc. from (1)	Observed ratio	Percent diff.
$\Pi A_g/\Pi A_1$	$C_2H_2Cl_2$[a]	2.70	2.57	5.1
$\Pi A_g/\Pi A_1{}^{(i)}$*		5.35	5.03	6.3
$\Pi A_g{}^{(i)}/\Pi A_1$		1.36	1.36	—
$\Pi A_g{}^{(i)}/\Pi A_1{}^{(i)}$		2.69	2.66	1.1
$\Pi B_u/\Pi B_1$		0.436	0.422	3.3
$\Pi B_u/\Pi B_1{}^{(i)}$		0.861	0.822	4.5
$\Pi B_u{}^{(i)}/\Pi B_1$		0.224	0.227	−1.3
$\Pi B_u{}^{(i)}/\Pi B_1{}^{(i)}$		0.435	0.442	−1.6
$\Pi A_g/\Pi A_1$	$C_2H_2Br_2$[b]	3.1	2.8	10.0
$\Pi A_g/\Pi A_1$	$CH_3CH=CHCH_3$[c]	2.3	2.1	11.0

* The superscript (i) designates the completely deuterated molecule.

[a] Bond distances from L. R. Maxwell (reference 7). B_u and B_1 frequencies from H. J. Bernstein and D. A. Ramsay (to be published); A_g and A_u frequencies from T. Wu (reference 8).

[b] Bond distances from L. R. Maxwell (reference 7); frequencies are those of A. Dadieu, A. Pongratz, and K. W. F. Kohlrausch, Monats. f. Chem. **60**, 221 (1932).

[c] Bond distances from L. R. Maxwell (reference 7); frequencies are those given by Kohlrausch, *Ramanspektren* (Edwards Brothers, Inc., Ann Arbor, Michigan, 1945).

Structure of the Rotational Isomers of 1,2-Dichloro- and 1,2-Dibromoethane

Equation (1) may be applied to the rotational isomers of substituted ethanes which have a plane of symmetry. Because of the lack of free rotation about the C−C bond in dihalogen substituted ethanes two rotational isomers are present.[6] It is known definitely that the more stable isomer has a *trans*-(C_{2h}) configuration[6] but whether the other isomer is *cis-* or "gauche" has not been established. The "gauche" form is one in which the halogens are at an intermediate position, between *cis-* and *trans-*. If the other isomer has C_{2v} symmetry then the computed product ratio from Eq. (1) should agree to within 10 percent with the observed ratio. From the known bond distances[7] and angles, the value computed for $\Pi A_g/\Pi A_1$ for 1,2-dichloroethane and 1,2-dibromoethane are 2.36 and 2.76 respectively. The observed ratios[8] are 1.46 and 1.90 respectively. These large differences between observed and computed ratios are strong evidence that the configuration of the less stable rotational isomer in these halogenated ethanes is "gauche."

It is unsafe to extend the use of this rule to calculate the azimuthal angle that the "gauche" forms make with the *trans*-configuration since out-of-plane vibrations are involved and the approximation of equality of force constants would not be valid.

[6] S. Mizushima and Y. Morino, Proc. Ind. Acad. Sci. **8A**, 315 (1938).

[7] L. R. Maxwell, J. Opt. Soc. Am. **30**, 374 (1940).

[8] The frequencies used to compute the observed ratios are taken from T. Y. Wu, *Vibrational Spectra and Structure of Polyatomic Molecules* (Edwards Brothers, Inc., Ann Arbor, Michigan, 1946).

Internal Rotation II

The Energy Difference between the Rotational Isomers of 1,2-Dichloroethane

H. J. BERNSTEIN
National Research Council, Ottawa, Canada
(Received July 12, 1948)

From the variation of the intensities of infra-red bands with temperature the value of ΔH^0 for the reaction C_{2h} dichloroethane $\rightarrow C_2$ dichloroethane is found to be 1250 ± 50 cals. per mole. The probable energy difference between the isomers is 1100 ± 50 cal. per mole. A tentative assignment of all the fundamentals has been made.

Peak intensities and integrated intensities yield the same results within the limits of the experimental error. The ratio of the number of C_2 molecules to the number of C_{2h} molecules at room temperature is 0.29.

IT is well known[1] that 1,2-dichloroethane is an equilibrium mixture of two rotational isomers. One isomer has the structure C_{2h} (a pure *trans*-form)[2] and the other is very likely C_2 or "gauche" in which the azimuthal angle between the C – Cl bonds is 60°.[3] Since at low temperatures the *trans*-form only is present,[2] the C_2 form is the less stable isomer and the potential energy as a function of azimuthal angle is as shown in Fig. 1. The potential barrier corresponds to the ordinate at $\phi=\pm60°$ and the ordinate at $\phi=\pm120°$ is the energy difference between the isomers, $(\Delta E_0{}^0)$, neglecting the small difference in zero-point vibrational energy between the two forms.

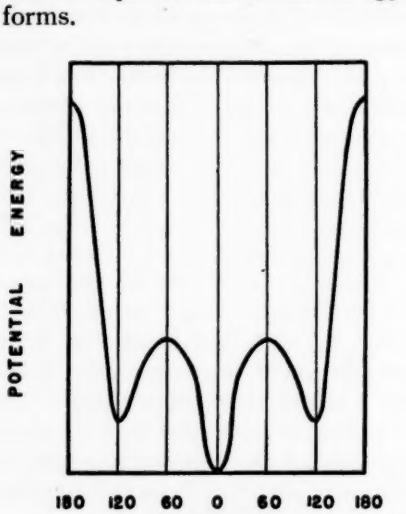

FIG. 1. Potential energy of 1,2-dichloroethane as a function of azimuthal angle.

A direct method for obtaining $\Delta E_0{}^0$ is to study the temperature dependence of the ratio of the intensities of Raman lines[4] or infra-red bands belonging to the two isomers. This method is rigorously true only when applied to the gaseous state, and the previous results[4] obtained in the liquid state are not to be taken as gas values. As Gerding[5] has pointed out, the temperature variation of the intensity ratio of two Raman lines in the liquid may be altogether different from that in the gas, and indeed may be taken as a measure of the molecular interactions in the liquid state. A spectrographic method in the gas phase however can be applied successfully so long as at least two lines or bands corresponding to the two isomers in equilibrium do not overlap.

It was the purpose of this investigation to find the temperature dependence of the ratio of the intensities of two infra-red bands of the isomers of 1,2-dichloroethane in the gas phase; and evaluate ΔH^0, for the reaction C_{2h} dichloroethane$\rightarrow C_2$ dichloroethane and also $\Delta E_0{}^0$, the difference in energy between the C_{2h} and C_2 forms.

If I_0 is the intensity of the incident radiation and I that of the transmitted radiation, the integrated intensity A over the band width is given by[6]

$$A=\int \ln\frac{I_0}{I}d\nu=\frac{8\pi^3N\nu|M^2|}{3hc}$$

where N is the number of molecules per cc, ν is the frequency of the band, M is the dipole moment term, and h and c have their usual meaning.

[1] K. W. F. Kohlrausch, *Ramanspektren* (Edwards Brothers, Inc., Ann Arbor, Michigan, 1945).
[2] S. Mizushima and Y. Morino, Proc. Ind. Acad. Sci. **8A**, 315 (1938).
[3] G. Glockler, Rev. Mod. Phys. **15**, 111 (1943). The product rule for rotational isomers [See J. Chem. Phys. **17**, 256 (1949)] excludes C_{2v} as the configuration of the other rotational isomer.
[4] A. Langseth and H. J. Bernstein, J. Chem. Phys. **8**, 410 (1940).
[5] H. Gerding and P. G. Meerman, Rec. Trav. Chim. **61**, 523 (1942).
[6] E. B. Wilson, Jr., J. Chem. Phys. **14**, 578 (1946). As pointed out in this paper $\int \ln(I_0/I)d\nu$ is the integrated intensity at infinite resolution. In this work slit widths of the order of 5 cm^{-1} are used so there is a small correction for finite slit widths to be applied to the experimental A's. However, since the ratio of two band intensities is always used, these corrections tend to cancel one another and measured intensity ratio is not appreciably different from the absolute ratio.

For a particular band A is proportional to $N\nu$, and for a band belonging to the C_2 isomer $A_{C_2}=K_{C_2}N_{C_2}\nu_{C_2}$, and for one belonging to the C_{2h} isomer $A_{C_{2h}}=K_{C_{2h}}N_{C_{2h}}\nu_{C_{2h}}$. The ratio of the intensities of the two bands is

$$\frac{A_{C_2}}{A_{C_{2h}}}=\text{const.}\frac{N_{C_2}}{N_{C_{2h}}} \tag{1}$$

when the same two bands are always compared.

Since the *trans*-form is more stable the equilibrium constant is

$$K=\frac{N_{C_2}}{N_{C_{2h}}}=\text{const. }\exp(-\Delta H^0/RT) \tag{2}$$

where ΔH^0 is positive and R is the gas constant, and both are measured in cal./mole.

Substituting from Eq. (1) in (2)

$$\frac{A_{C_2}}{A_{C_{2h}}}=\text{const. }\exp(-\Delta H^0/RT). \tag{3}$$

When the L.H.S. is known for several temperatures a least square method for $\log A_{C_2}/A_{C_{2h}}$ and $1/RT$ gives the best value of ΔH^0.

The methods of statistical thermodynamics[7] show moreover that for an isomeric equilibrium of the type *trans*-⇌*cis*- that

$$K=\frac{N_{cis\text{-}}}{N_{trans\text{-}}}=\frac{f_{cis\text{-}}}{f_{trans\text{-}}}\cdot\exp(-\Delta E_0^0/RT)$$

where $f_{cis\text{-}}$, $f_{trans\text{-}}$ are the partition functions of the *cis*- and *trans*-molecules respectively.

In the case of 1,2-dichloroethane where the isomeric forms are C_{2h} and C_2 with twice as many potential minima for the C_2 as for the C_{2h} the equilibrium constant is given by

$$K=\frac{N_{C_2}}{N_{C_{2h}}}=\frac{2f_{C_2}}{f_{C_{2h}}}\cdot\exp(-\Delta E_0^0/RT). \tag{4}$$

ΔE_0^0 is the energy difference at 0°K between the two isomers. Assuming the rigid rotator and harmonic oscillator approximations[8]

$$\frac{f_{C_2}}{f_{C_{2h}}}=\left[\frac{(I_AI_BI_C)_{C_2}}{(I_AI_BI_C)_{C_{2h}}}\right]^{\frac{1}{2}}\cdot\frac{\Pi_{C_{2h}}}{\Pi_{C_2}}$$

where $(I_AI_BI_C)_{C_2}$ is the product of the principal moments of inertia of the C_2 molecule and $(I_AI_BI_C)_{C_{2h}}$ that for the C_{2h} molecule; and

$$\Pi_{C_{2h}}=(1-\exp(-h\nu_1/kT))\times(1-\exp(-h\nu_2/kT))\cdots(1-\exp(-h\nu_{18}/kT))$$

where $\nu_1\nu_2\cdots\nu_{18}$ are the frequencies of the fundamental modes of vibration of the C_{2h} molecule; and

$$\Pi_{C_2}=(1-\exp(-h\omega_1/kT))\times(1-\exp(-h\omega_2/kT))\cdots(1-\exp(-h\omega_{18}/kT))$$

where $\omega_1\omega_2\cdots\omega_{18}$ are the frequencies of the fundamentals of the C_2 molecule.

Substituting for $f_{C_2}/f_{C_{2h}}$ in Eq. (4)

$$\frac{N_{C_2}}{N_{C_{2h}}}=2\left[\frac{(I_AI_BI_C)_{C_2}}{(I_AI_BI_C)_{C_{2h}}}\right]^{\frac{1}{2}}\cdot\frac{\Pi_{C_{2h}}}{\Pi_{C_2}}\cdot\exp(-\Delta E_0^0/RT). \tag{5}$$

Since we are interested only in the temperature dependent terms, from (1) and (5)

$$\frac{A_{C_2}}{A_{C_{2h}}}=\text{const.}\frac{\Pi_{C_{2h}}}{\Pi_{C_2}}\cdot\exp(-\Delta E_0^0/RT). \tag{6}$$

Again a least squares solution for

$$\log\left(\frac{A_{C_2}}{A_{C_{2h}}}\cdot\frac{\Pi_{C_2}}{\Pi_{C_{2h}}}\right)$$

and $1/RT$ gives the best value of ΔE_0^0.

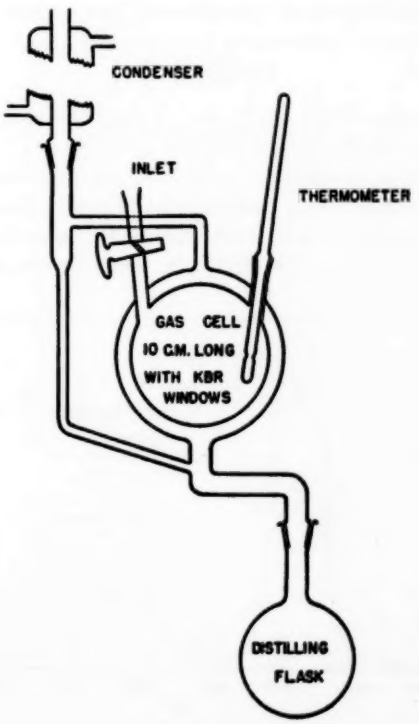

FIG. 2.

[7] Fowler and Guggenheim, *Statistical Thermodynamics* (The MacMillan Company, New York, 1939), p. 157.

[8] G. Herzberg, *Infrared and Raman Spectra of Polyatomic Molecules* (D. Van Nostrand Company, New York, 1945).

EXPERIMENTAL AND RESULTS

The 1,2-dichloroethane was the Eastman Kodak product distilled through a 60 cm Stedman column: b.p. = 82.9±0.1°C at normal pressure. The infra-red spectra were obtained in the laboratory of Dr. R. N. Jones on a Perkin Elmer spectrometer with a Brown recorder, by Dr. D. A. Ramsay and Mr. D. Keir. A 10-cm long absorption cell with KBr windows was used. Vapor from a constant boiling liquid condensing on the walls of the cell served to heat the contents. In this way the temperature was kept quite steady (±1°) and was read from a thermometer (which penetrated the cell). See Fig. 2.

A preliminary run showed that two bands at 1235 cm^{-1} and 1291 cm^{-1} whose intensity ratio A_{1235}/A_{1291} decreased with temperature, would be suitable because of practically no overlapping.

Figure 3 shows a $\log I_0/I/cm^{-1}$ plot for the two bands at room temperature and 424°K.

In Table I the complete I. R. spectrum of 1,2-dichloroethane at room temperature (10-cm cell at 80 mm Hg) is given. The assignment is given in the last column where ν's are for the C_{2h} form and the ω's for the C_2 form. The intensity is designated in column 2 in the ordinary way and in column 3 the separations between peaks are given, where measured. Column 4 indicates the contour of the band.

In Table II the integrated intensities A of the bands in arbitrary units at 5 different temperatures are given. At each of the first 3 temperatures 3 runs were taken and at the last 2 only 2 runs were obtained. The last column gives the material used in the distilling flask to obtain the various temperatures.

DISCUSSION

From the data in Table II and Eq. (3) a least squares solution gives $\Delta H^0 = 1250 \pm 50$ cal. per mole. In order to evaluate ΔE_0^0 the frequencies of the fundamentals have to be known. In the temperature range investigated, frequencies greater than 1000 cm^{-1} contribute very little to the vibrational partition function and can be neglected in evaluating the Π's.

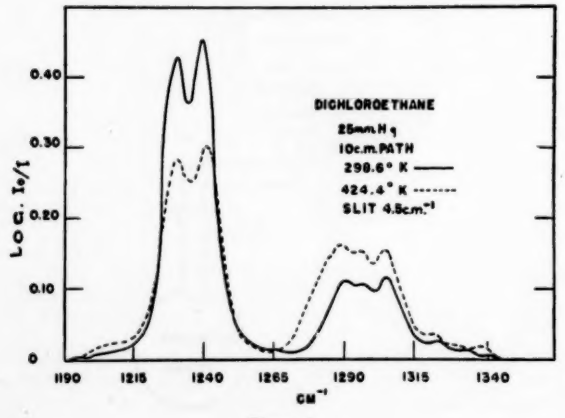

FIG. 3.

The assignment made in Table I is comparatively straightforward. The modes of vibration in the B_u class of the C_{2h} molecules give rise to bands which are doublets[9] and those in the A_u class give singlets.[9] Since the variation in electric moment is not parallel to any of the principal axes of inertia of a C_2 molecule, the bands are hybrid. However, since the gauche form is only 60° out of plane from the C_{2v} form, the modes antisymmetric with respect to the two-fold axis would be expected to give triplets;[10] the modes symmetric with respect to the two-fold axis would be expected to give doublets. The latter seem to appear very weakly in the infra-red.

In Table III the Raman and infra-red data are collected and a tentative assignment of all fundamentals is given. In the table ν_1 to ν_6 inclusive are A_g vibrations, ν_7 to ν_{11} inclusive are B_u vibrations, ν_{12} to ν_{15} inclusive are A_u vibrations, ν_{16} to ν_{18} inclusive are B_g vibrations, and ω_1 to ω_6 and ω_{12} to ω_{15} are A vibrations, and ω_7 to ω_{11} and ω_{16} to ω_{18} are B vibrations.

On the whole this assignment seems probable and is consistent with the Raman and infra-red data in all points except one (see reference c to Table III). Whether the line at 124 cm^{-1} is polarized or depolarized however only affects the assignment and not the determination of ΔE_0^0 for which only the magnitude of the frequency is significant.*

TABLE I. Infra-red spectrum of 1,2-dichloroethane (10-cm path, 80 mm of Hg).

Absorption band in cm^{-1}	Intensity	Separation in cm^{-1}	Contour	Assignment
543	m.			$\nu_1+\nu_7$
695	m.	13	triplet	ω_7
*728	s.	9	doublet	ν_8
772	w.		singlet	ν_{13}
832	v.w.			$\nu_2+\nu_{12}$
890	m.	15	triplet	ω_8
946	m.	13	doublet	ν_9
993	w.			$\nu_2+\nu_7$
1027	w.			ω_4
1124	w.			ω_9
1235	s.	10	doublet	ν_{10}
1291	s.	12	triplet	ω_{10}
1319	w.			ν_{14}
1460	m.	11	doublet	ω_{14}
1531	w.			$\nu_1+\nu_{10}$
2881	m.			ω_6
3029	s.			ν_{11}

* This band was resolved at a pressure of 5 mm of Hg.

[9] T. Y. Wu, J. Chem. Phys. **5**, 392 (1937).

[10] T. Y. Wu, *Vibrational Spectra and Structure of Polyatomic Molecules* (Edwards Brothers, Inc., Ann Arbor, Michigan, 1946), p. 122.

* Recently W. D. Gwinn and K. S. Pitzer, J. Chem. Phys. **16**, 303 (1948), have estimated the vibrational heat capacity using Wu's (see reference 10) choice of fundamentals. These authors also consider the line at 124 cm^{-1} to be polarized. They use Raman data of Mizushima *et al.*, Bull. Chem. Soc. (Japan) **17**, 94 (1942), for $\nu_7 = 223$ cm^{-1}.

TABLE II.

T°K	A_{1235} cm^{-1}	A_{1291} cm^{-1}	$\frac{A_{1291}}{A_{1235}}$	Av. value of $\frac{A_{1291}}{A_{1235}}$	Distilling material
298.6	27.95	10.83	0.387		
	29.12	10.74	0.369	0.376±0.008	
	27.92	10.35	0.371		
347.7	27.30	13.31	0.488		Carbon
	27.24	13.38	0.491	0.487±0.004	tetra-
	27.05	13.00	0.481		chloride
368.3	27.30	15.32	0.561		
	28.69	16.03	0.559	0.558±0.003	H_2O
	27.89	15.42	0.553		
387.4	26.46	15.98	0.604	0.586±0.017	C_2Cl_4
	25.17	14.33	0.569		
424.4	23.25	16.90	0.727	0.718±0.010	C_2HCl_5
	21.61	15.29	0.708		

With the above fundamentals the II's of Eq. (6) may be calculated and ΔE_0^0 evaluated, whence $\Delta E_0^0 = 1100 \pm 50$ cal. per mole. Of course the value of ΔE_0^0 is dependent on the frequencies chosen for the unobserved fundamentals ν_1, ν_{12} and ν_{13} of Table III. To make ΔE_0^0 very different from 1000 cal. the values of these frequencies would indeed have to be extreme. In no case, however, can the value of ΔE_0^0 exceed its upper limit of $\Delta H^0 = 1250$ cal.

Using the electron diffraction data[11] for the dimensions of $C_2H_4Cl_2$ and assuming tetrahedral angles the product of the principal moments of inertia for the C_{2h} and C_2 forms may be evaluated. It is found[12] that

$$\left[\frac{(I_A I_B I_C)_{C_2}}{(I_A I_B I_C)_{C_{2h}}}\right]^{\frac{1}{2}} = 1.355.$$

Using this value of 1.355 for the moment of inertia factor and the II's computed for the above choice of fundamentals the ratios $N_{C_2}/N_{C_{2h}}$ at 298.6°K, 347.7°K, 368.3°K, 387.4°K, and 424.4°K are found to be 0.290, 0.374, 0.417, 0.451, 0.574 respectively.

If peak intensities are used throughout instead of areas it is found that $\Delta H^0 = 1325 \pm 50$ cal. per mole and $\Delta E_0^0 = 1140 \pm 50$ cal. per mole. There seems to be no significant difference in the results obtained whether peak intensities or integrated intensities are used.

[11] L. R. Maxwell, J. Opt. Soc. Am. **30**, 374 (1940).
[12] See reference 8, p. 509.

TABLE III. Vibrational assignment of C_2 and C_{2h} 1,2-dichloroethane.

	Trans C_{2h}			C_2	
ν	Raman*	I. R.**	ω	Raman*	I. R.**
1	301		1	264	
2	753		2	653	
2	991		3	943	
4	1054		4	1032	1027
5	1302		5	1205	
6	2956		6	2873	2881
7		243[a]	7	676	696
8		725	8	881	890
9		950	9	1143	1124
10		1235	10		1291
11		3029	11		3000
12		80[b]	12	124[c]	
13		772	13	454	
14		1319	14		1460
15		3000	15	3000	3000
16	1263		16	410	
17	1442		17	1428	
18	3002		18	3000	

* Raman data from Kohlrausch (liquid) (reference 1).
** Infra-red data from this work (gas).
[a] Obtained from the observed band at 544 by difference. 544 = 243 + 301.
[b] Obtained from the observed band at 833. 833 = 80 + 753.
[c] This line is given as depolarized in the literature whereas in its present assignment it should be polarized. Measurements of depolarization in the region close to the exciting line are very difficult, however, and it is possible that the data have been misinterpreted.

ACKNOWLEDGMENT

Thanks are due Mr. P. Langevin for the figures and Miss E. Miller for assistance with the computations.

Internal Rotation III

The Potential Barrier in 1, 2-Dichloroethane

H. J. BERNSTEIN
National Research Council, Ottawa, Canada

(Received July 12, 1948)

The potential energy as a function of azimuthal angle has been computed on the basis of an inverse fifth power of the distance law for the energy of interaction. Suitable corrections for second order interactions were also made. A three minima potential curve is obtained of the form

$$V=0.733(1-\cos\phi)+1.123(1-\cos 3\phi)+0.197(1-\cos\phi)(1-\cos 3\phi) \text{ K cal./mole.}$$

The barrier is computed to be 2.81 K cal./mole.

ONE of the rotational isomers of 1,2-dichloroethane has a *trans*-(C_{2h}) configuration[1] and the other very probably C_2 with an azimuthal angle between the CH_2Cl groups of 60°.[2] Furthermore the *trans* is the more stable isomer[1] with potential energy of 1100 cals.[3] per mole lower than the C_2 form. The potential energy curve as a function of azimuthal angle has 3 potential minima; one due to *trans* at $\phi=0°$ and 2 identical ones at $\phi=120°$ corresponding to the C_2 forms. The energy at $\phi=120°$ is then 1100 cal. greater than that at $\phi=0°$. The potential barrier is the ordinate at $\phi=60°$. See Fig. 1 of the preceding article.

Various attempts have been made to evaluate the potential barrier between the isomers of dichloroethane from the temperature dependence of the dipole moment.[4] The dipole measurements have hitherto been interpreted in terms of a potential function which allows only one isomeric form to be present, such as $V=A/2(1+\cos\phi)$, $V=A/\pi(\pi-\phi)$, $V=A/\pi^2(\pi^2-\phi^2)$ used by Beach and Stevenson,[4] or in terms of *cis* and *trans* forms such as $V=V_1\cos\phi+V_2\cos 2\phi$ used by Altar.[4] Further, the rotational and vibrational contributions to the phase integral have usually been neglected.[5] In view of these gross approximations it seems unlikely that the interpretation of the dipole moment data has yielded as yet a reliable figure for the magnitude of the potential barrier. Recently, however, Gwinn and Pitzer[6] have reinterpreted Zahn's[4] data using a potential energy function of the form $V=A(1-\cos\phi)+B(1-\cos 3\phi)$, making suitable estimates of the rotational and vibrational contributions to the phase integral. These authors also obtained gas heat capacities. It was found that the above potential function could be used over the range $0\leq\phi\leq 130°$ but for $\phi>130°$ $V=\infty$ had to be used. Gwinn and Pitzer[6] state that, "it is impossible to find a potential function of the above type for which calculated values are in agreement with all of the experimental values of the dipole moment, entropy, and gas heat capacity."

Since the interpretation of the dipole moment/temperature and gas heat capacity/temperature data depends on the kind of potential function used and since those used to date have been inadequate it seems worth while proposing the following method of computing the potential function.

Lassettre and Dean[7] have shown that the interaction due to quadrupoles gives a barrier of ~1.85 K cal./mole for ethane. This corresponds to an interaction energy which is proportional to the inverse 5th power of the interatomic distance. Eyring *et al.*[8] and Penney[9] have shown that the repulsive energy between atoms is of the form

$$E_R=\text{const.}\{2e^{-a(R-R_0)}-e^{-2a(R-R_0)}\}$$

in which a, R_0 have the same significance as in the Morse potential function.[10] Estimating the constant from quantum mechanical considerations for H atoms[11] the barrier in ethane is computed as ~1.00 K cal./mole. It would seem that the sum of these interactions would account for the observed barrier of 2.7 K cal./mole in ethane. Since the shape of the Morse curve in the region $R\geq 3R_0$ is

[1] S. Mizushima and Y. Morino, Proc. Ind. Acad. Sci. **8A**, 315 (1938).
[2] G. Glockler, Rev. Mod. Phys. **15**, 111 (1943); H. J. Bernstein, J. Chem. Phys. **17**, 256 (1949).
[3] H. J. Bernstein, J. Chem. Phys. **17**, 258 (1949).
[4] C. T. Zahn, Phys. Rev. **38**, 521 (1931); E. W. Green and J. W. Williams, *ibid.* **42**, 119 (1932); W. Altar, J. Chem. Phys. **3**, 460 (1935); J. Y. Beach and D. P. Stevenson, *ibid.* **6**, 635 (1938).
[5] W. Altar, J. Chem. Phys. **3**, 460 (1935), takes the rotational contribution into account but neglects the vibrational contribution.
[6] W. D. Gwinn and K. S. Pitzer, J. Chem. Phys. **16**, 303 (1948).
[7] E. N. Lassettre and L. B. Dean, Jr., J. Chem. Phys. **16**, 151 (1948); Errata, **16**, 553 (1948).
[8] H. Eyring, J. Walter, G. E. Kimball, *Quantum Chemistry* (John Wiley & Sons, Inc., New York, 1946).
[9] W. G. Penney, *The Quantum Theory of Valency* (Methuen & Company, London, 1935).
[10] P. M. Morse, Phys. Rev. **57**, 34 (1929).
[11] J. O. Hirschfelder, J. Chem. Phys. **9**, 645 (1941).

practically identical with a R^{-5} curve the total interaction may be represented rather closely by an inverse 5th power energy law. This has been borne out by Aston and collaborators[12] who find that an empirical relation of the form* $E=A/R^5$ is obtained to fit the experimental barriers in hydrocarbons.

The repulsive energy of dichloroethane as a function of the internuclear distances may be represented then by

$$E=\frac{A_{H_2}}{R_{HH}{}^5}+\frac{A_{HCl}}{R_{HCl}{}^5}+\frac{A_{Cl_2}}{R_{ClCl}{}^5},$$

where A_{H_2}, A_{HCl}, A_{Cl_2} are the constants for HH, HCl, and ClCl interaction and R_{HH}, R_{HCl} and R_{ClCl} are the interatomic distances between hydrogen, hydrogen and chlorine, and chlorine atoms, respectively.

In addition to this repulsive energy there are interactions due to dipole-dipole, induction, and dispersion. These may be estimated in the approximate manner given below, and since the dipole-dipole interaction is repulsive and the other two attractive there is considerable cancellation of effects. The dipole-dipole interaction may be estimated by placing a charge of $q=\mu/R$ (μ is the dipole moment of the bond and R the bond distance) at the nuclei and computing the electrostatic interaction as a function of interatomic distance.

The dispersion effect may be evaluated from the expression[13]

$$-\frac{3}{2}\cdot\frac{I_1I_2}{I_1+I_2}\cdot\frac{\alpha_1\alpha_2}{R^6},$$

where I_1, I_2 are the ionization potentials of the two atoms and α_1, α_2 their polarizabilities and R the distance between them.

The induction energy is given by[14]

$$-\frac{\alpha}{2}\frac{\mu^2}{R^6}(2\cos\theta_1\cos\theta_2-\sin\theta_1\sin\theta_2\cos\phi)^2$$

where α is the polarizability of the C–C bond, μ the bond moment; R the distance from the center of electrical gravity at which the infinitesimal dipole is placed and the center of the C–C bond; and the angles are as shown in Fig. 1. In these calculations the C–Cl dipole was placed at a distance $\frac{1}{3}$ the bond distance from the chlorine atom and the C–H dipole in the middle of the C–H bond.[15]

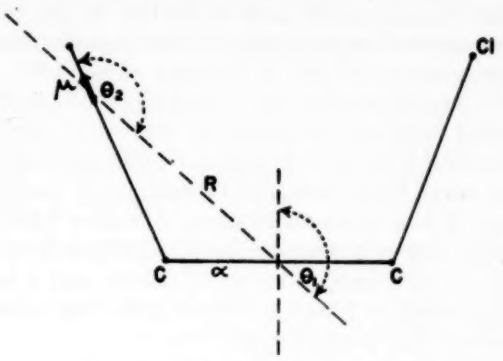

FIG. 1.

Using the barrier of 2700 cal.[16] in ethane and the spectroscopic bond distances,[16] A_{H_2} is 4.65×10^5. To evaluate the HCl interaction constant the barrier of 2700 cal./mole in CH_3CCl_3 was used[16] and the bond distances C–C = 1.54A, C–Cl = 1.76A, C–H = 1.09A. This gives $A_{HCl}=6.35\times10^5$. Using these values for A_{H_2}, A_{HCl}, and the experimental value for the energy difference between C_2 dichloroethane and C_{2h} dichloroethane of 1100 cal./mole[3] the value of A_{Cl_2} is found to be 8.55×10^5.

The energies for several configurations were calculated with these constants with second order corrections and are shown in Table I. The computed barrier is found to be 2.81 K cal./mole, and where Gwinn and Pitzer found they had to use $V=\infty$, the curve rises to a value of 4.50 K cal./mole for the cis-trans energy difference. This energy curve compares rather favorably with that of Gwinn and Pitzer in the region $0\leq\phi\leq130°$. Their values are 1.37 K cal./mole for the C_{2h}, C_2 energy difference and 2.70 K cal./mole for the barrier.

A suitable potential function covering the entire range would be a 3 constant expression of the form $V=A(1-\cos\phi)+B(1-\cos2\phi)+C(1-\cos\phi)\times(1-\cos3\phi)$ where $A=0.733$ K cal./mole, B

TABLE I.

		Potential Energy in K cal. per mole					
ϕ	Configuration	Repulsion	Induction	Dispersion	Dipole-dipole	Net P.E.	Pot. energy referred to $\phi=0$
0	*Trans* C_{2h}	26.66	0.0	−1.97	−0.99	23.70	0.0
60		29.81	−0.28	−2.39	−0.63	26.51	2.81
120	Gauche C_2	27.38	−0.82	−2.42	0.66	24.80	1.10
180	*Cis* C_{2v}	31.58	−1.10	−3.90	1.62	28.20	4.50

[12] J. G. Aston, S. Isserow, G. J. Szasz, and R. M. Kennedy, J. Chem. Phys. **12**, 336 (1944).

* In this expression the constant is evaluated for R in A and E in calories per mole.

[13] K. W. Wolfe, *Theoretische Chemie* (Edwards Brothers, Michigan, 1944), p. 465.

[14] The energy of induction

$$E_{ind}=-\frac{\mu\mu_e}{R^3}(2\cos\theta_1\cos\theta_2-\sin\theta_1\sin\theta_2\cos\phi)$$
$$=-\mu_eF$$

but $E_{ind}=-\frac{1}{2}\alpha F^2$. Elimination of F gives the induction energy in terms of the polarizability.

[15] L. Meyer, Zeits. f. physik. Chemie **B8**, 27 (1930).

[16] G. Herzberg, *Infrared and Raman Spectra* (D. Van Nostrand Company, New York, 1945).

$=1.123$ K cal./mole, and $C=0.197$ K cal./mole. The minimum corresponding to the C_2 configuration is computed at $\phi=117.1°$ instead of $\phi=120°$, and the force constants for the C_2 and C_{2h} configurations obtained from the curvature of the potential function are $9B+13.5C-A/2$ and $A+9B$, respectively.

For small amplitudes of vibration the potential energy of C_{2h} dichloroethane is $V=(A+9B/2)\cdot\phi^2$ and the kinetic energy is $T=2\times\frac{1}{2}\times(I)/(2)\cdot\dot{\theta}^2$ where I is the least moment of inertia and $\dot{\theta}$ is the angular velocity about the least axis. The relation between θ and ϕ is given by

$$\theta=\phi\left\{\frac{\sin\beta}{\tan(\pi/2-\beta)}+\cos\beta\right\}$$

where β is the angle the axis of least moment of inertia makes with the C−C axis $=49°\,25'$. Although the torsion vibration occurs in a symmetry class with three other vibrations its frequency may be evaluated approximately from

$$\omega^2=\frac{4(A+9B)}{I}\,\frac{1}{\left\{\dfrac{\sin\beta}{\tan(\pi/2-\beta)}+\cos\beta\right\}^2}.$$

Assuming tetrahedral angles and the values of the internuclear distances given above, it is found that $I=34.3\times10^{-40}$ c.g.s. The torsion frequency is then calculated as $\nu_{12}=101$ cm^{-1}. This agrees as well as can be expected with the value chosen (80 cm^{-1}) for this frequency from the experimental data.[3]

Gwinn and Pitzer have calculated the torsion frequency of the C_2 molecule from the curvature of their potential function and found 79 cm^{-1}. Since the frequency is proportional to the square root of the force constant, use of the potential function constants in this paper leads to the calculated frequency of $\nu=(12.40/9.95)^{\frac{1}{2}}\times79=88$ cm^{-1}. This compares as well as can be expected with the observed value of 124 cm^{-1}.**

Other halogen substituted ethanes are being treated in the same manner.

** Recently Gordon and Giauque (J. Am. Chem. Soc. 70, 1506 (1948)) have given the barrier for ethyl chloride as 4700 cal. for entropy data. Using this value to obtain the magnitude of the constant for HCl interaction gives $A_{HCl}=20.0\times10^5$. With $A_{H_2}=4.65\times10^5$ and $A_{HCl}=20.0\times10^5$ the A_{Cl_2} constant is calculated as 63.3×10^5. This leads to values of A, B, C, in the potential function equal to 0.76, 1.48, 3.67 K cal./mole respectively.

The force constant for C_2 dichloroethane calculated from the curvature of the potential function with these values of the constants leads to a value for $\nu=(62.3/9.95)^{\frac{1}{2}}\times79=198$ cm^{-1}. This frequency is much higher than that observed at 124 cm^{-1} and serves as a suitable criterion to reject these high values for A, B, C. It would seem that the observed barrier of 4700 cal. for C_2H_5Cl is too high. Using the constants obtained from the barrier in CH_3CCl_3 the computed barrier in C_2H_5Cl (after suitable correction for the second order interaction) is 2700 cal./mole.

THE JOURNAL OF CHEMICAL PHYSICS VOLUME 17, NUMBER 3 MARCH, 1949

The Dipole Moments of Fulvene and Azulene*

G. W. WHELAND AND D. E. MANN**
Department of Chemistry, University of Chicago, Chicago, Illinois
(Received August 24, 1948)

The dipole moments of fulvene and azulene have been calculated theoretically by the LCAO MO method, and have been obtained from experimental data. The experimental results support the theoretical predictions.

ON the basis of the molecular-orbital (MO) calculations of Coulson and Longuet-Higgins,[1] fulvene (Fig. 1, with $R'=R''=H$) should have a dipole moment of about 4.7 D, and azulene (Fig. 2) should have a dipole moment of about 6 D. (In Figs. 1 and 2, the negative end of the dipole is indicated by the head of the arrow.) Refinements in the calculations, which are described in the mathematical appendix to this paper, reduce the predicted moment of fulvene to about 1.5–2 D. (See column 4 of Table VI, below.) These refinements, if applied to

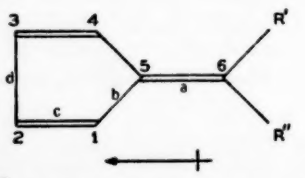

FIG. 1.

TABLE I. 6,6-Dimethylfulvene in benzene at 23.7°C.

w	ϵ_{12}	d_{12}	ρ_{12} (cc/g)	P_2 (cc)
0.0	2.275	0.8743	0.3412	—
0.02608	2.340	0.8744	0.3530	84.4
0.03250	2.355	0.8744	0.3559	84.3
0.03926	2.372	0.8742	0.3589	84.1

* The material in this paper is taken from the dissertation submitted by D. E. Mann to the Division of the Physical Sciences of the University of Chicago in partial fulfillment of the requirements for the degree of Doctor of Philosophy.

** Du Pont Predoctoral Fellow (1946–1948). Present address: School of Chemistry, University of Minnesota, Minneapolis, Minnesota.

[1] C. A. Coulson and H. C. Longuet-Higgins, Rev. Sci. Inst. 85, 927 (1947).

TABLE II. 6,6-Diethylfulvene in benzene at 23.7°C.

w	ϵ_{12}	d_{12}	p_{12} (cc/g)	P_2 (cc)
0.0	2.275	0.8743	0.3412	——
0.02412	2.319	0.8743	0.3493	91.0
0.02752	2.325	0.8742	0.3504	90.6
0.03268	2.333	0.8742	0.3519	89.8
0.03968	2.346	0.8741	0.3542	90.0
0.04283	2.351	0.8741	0.3553	90.0

azulene, would probably reduce its moment (given above) to about 1–2 D. Since even the revised moments are unusually large for hydrocarbons, it was desirable to obtain experimental evidence in support of the theoretical results. Moreover, these experimental data provide a test of the validity[2] of the results obtained by the application of the MO method to the calculation of charge distributions and related quantities.

Since fulvene itself has not been obtained in a pure state,[3] it is necessary to estimate its probable experimental moment from the moments of various substituted fulvenes. The fulvenes used for this purpose are 6,6-dimethylfulvene, 6,6-diethylfulvene, and 6,6-diphenylfulvene. Their moments were measured by the optical-solution method,[4] and were found to be respectively 1.48±0.03 D, 1.44±0.03 D, and 1.34±0.04 D. If it is assumed that these solution moments are 10–20 percent lower than the corresponding "true" or vapor-phase moments, and if it is assumed that the moments of 6,6-dimethyl-, 6,6-diethyl-, and 6,6-diphenylfulvene are a few tenths of a Debye unit larger than the moment of fulvene itself, then we may assume that 1.2 D is a reasonable, vapor-phase moment for fulvene. The agreement between this probable experimental value and the theoretical result given above is better than we have a right to expect. It has also been shown that the negative end of the fulvene dipole resides in the five-membered ring. This conclusion, which is predicted by the MO treatment, follows at once from a consideration of the vector relationships of the dipole moments in the 6,6-diphenylfulvene, 6,6-bis-(*p*-chlorophenyl)fulvene, and chlorobenzene molecules. (It is assumed that the phenyl-carbon-phenyl angle in the diaryl fulvenes is the same as that reported for 1,1-diphenylethylene.[5]) Unfortunately, however, there seems to be no way in which either the numerical results of the MO calculations or the measured moments can be explained *nonmathematically* in terms of resonating structures or otherwise.

TABLE III. 6,6-Diphenylfulvene in benzene at 23.7°C.

w	ϵ_{12}	d_{12}	p_{12} (cc/g)	P_2 (cc)
0.0	2.275	0.8743	0.3412	——
0.02456	2.306	0.8784	0.3453	117
0.03319	2.317	0.8800	0.3467	117
0.04915	2.337	0.8826	0.3493	117

TABLE IV. 6,6-bis-(*p*-chlorophenyl)fulvene in benzene at 23.7°C.

w	ϵ_{12}	d_{12}	p_{12} (cc/g)	P_2 (cc)
0.0	2.275	0.8743	0.3412	——
0.02560	2.288	0.8811	0.3409	98.6
0.02612	2.290	0.8812	0.3412	102
0.03314	2.292	0.8833	0.3409	99.2
0.04013	2.296	0.8850	0.3408	99.4
0.04023	2.297	0.8851	0.3410	100

The dipole moment of azulene has been measured by the optical-solution method, and is 1.0±0.05 D. This result, taken together with the fulvene results given above, makes clear the verification and substantiation of the MO predictions for these molecules.

EXPERIMENTAL

The fulvenes were prepared by the general method of Thiele.[3] A few minor modifications of the general procedure were required in order to prepare 6,6-bis-(*p*-chlorophenyl)fulvene, which has not been reported in the literature. It was prepared from *p,p'*-dichlorobenzophenone and freshly distilled cyclopentadiene, with sodium ethoxide as condensing agent. Dioxane, instead of absolute alcohol,[3] was used as solvent. The crude fulvene was recrystallized first from 30–60°C petroleum ether, and then six or seven times from 1:1 methanol-ether, from which it separates in the form of red plates. The melting point (by the usual capillary-tube method) of purified 6,6-bis-(*p*-chlorophenyl)fulvene varies widely (95–110°C) with the rate and duration of heating. Its melting point is estimated* to be 116±1°C. Analytical:—Calculated for $C_{18}H_{12}Cl_2$: C, 72.1 percent; H, 4.0 percent; Cl, 23.7 percent; M.W., 299.2. Found: C, 72.3 percent; H, 4.2 percent; Cl, 23.7 percent;[6] M.W., 307.

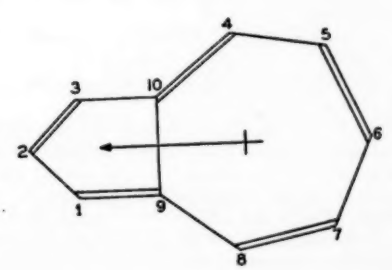

FIG. 2.

[2] C. A. Coulson and G. S. Rushbrooke, Proc. Camb. Phil. Soc. 36, 198 (1940).
[3] J. Thiele, Ber. d. D. chem. Ges. **33**, 671 (1900); J. Thiele and H. Balhorn, Ann. d. Chim. **348**, 5 (1908).
[4] See for example, R. W. J. Le Fèvre, *Dipole Moments* (Methuen and Company, Ltd., London, 1938).
[5] G. E. Coates and L. E. Sutton, J. Chem. Soc. (2), p. 567 (1942).
[6] All analyses were performed by Mr. W. Saschek.

TABLE V. Azulene in benzene at 23.7°C.

w	ϵ_{12}	d_{12}	p_{12} (cc/g)	P_2 (cc)
0.0	2.275	0.8743	0.3412	——
0.01565	2.296	0.8765	0.3442	68.5
0.02143	2.303	0.8775	0.3451	67.0
0.03291	2.317	0.8789	0.3472	67.1

Azulene was prepared by the method of Plattner and Wyss.[7] It was shown spectroscopically[8] that there is no more than 0.5 percent of naphthalene present in our samples of purified azulene. This amount of impurity is negligible so far as this investigation is concerned. The methods and apparatus used to determine the dipole moments have been described by Goldsmith and Wheland.[9] The molar refractions, R_2^D, of 6,6-dimethylfulvene and 6,6-diethylfulvene are literature values[10,11] which were checked in this laboratory. The values of R_2^D for 6,6-diphenylfulvene and 6,6-bis-(*p*-chlorophenyl)fulvene were computed from atom and group refractions,[12,13] with the assumption of an exaltation of 2 cc. The molar refraction of azulene is assumed to be that of naphthalene.

6,6-Dimethylfulvene (b.p. 72°C at 38 mm).[14]—The experimental data for this substance are given in Table I, where w is the weight fraction of solute, ϵ_{12} is the dielectric constant of the solution, p_{12} is the specific polarization of the solution, and P_2 is the total molar polarization of the solute. The data $P_2^\infty = 85 \pm 1$ cc, $R_2^D = 38.2 \pm 1$ cc, and $T = 296.9°K$ lead to $\mu = 1.48 \pm 0.03$ D.

6,6-Diethylfulvene (b.p. 77°C at 17 mm).—The data $P_2^\infty = 92 \pm 1$ cc, $R_2^D = 47 \pm 1$ cc, and $T = 296.9°K$ lead to $\mu = 1.44 \pm 0.03$ D. (Cf. Table II.)

6,6-Diphenylfulvene (m.p. 80–81°C).—The data $P_2^\infty = 117 \pm 1$ cc, $R_2^D = 76.5 \pm 1$ cc, and $T = 296.9°K$ lead to $\mu = 1.34 \pm 0.04$ D. (Cf. Table III.)

6,6-Bis-(p-chlorophenyl)fulvene (m.p. 116±1°C, but see above).—The data $P_2^\infty = 100 \pm 1$ cc, $R_2^D = 87 \pm 1$ cc, and $T = 296.9°K$ lead to $\mu = 0.68 \pm 0.1$ D. (Cf. Table IV.)

Azulene (m.p. 97–98°C).—The data $P_2^\infty = 68 \pm 1$ cc, $R_2^D = 44.4 \pm 1$ cc, and $T = 296.9°K$ lead to $\mu = 1.0 \pm 0.05$ D. (Cf. Table V.)

TABLE VI. Charge distribution in fulvene.[a]

Atom[b]	1	2	2a	3	3a	3b	4[c]
6	+0.378	+0.251	+0.213	+0.061	+0.138	+0.043	+0.135
5	−0.047	−0.036	−0.032	+0.057	−0.025	+0.042	+0.008
1, 4	−0.092	−0.058	−0.048	−0.043	−0.022	−0.035	−0.0415
2, 3	−0.073	−0.049	−0.042	−0.016	−0.035	−0.007	−0.030
μ	4.7 D	3.1 D	2.6 D	1.1 D	1.8 D	0.7 D	1.9 D

[a] The charge distribution is given in terms of net charge (in e.u.) for each atom of the conjugated system in fulvene. At the head of each column of figures is given the number of the calculation to which the figures apply, and at the left of each row is given the number of the atom to which the net charge refers.
[b] The numbering of the atoms in fulvene is that given in Fig. 1.
[c] The figures in this column refer to the results of the so-called self-consistent first order perturbation calculation.

TABLE VII. Bond orders in fulvene.

Bond[a]	1	2	2a	3	3a	3b	4
a	1.759	1.835	1.857	1.674	1.700	1.708	——
b	1.449	1.381	1.358	1.206	1.204	1.189	——
c	1.778	1.838	1.858	1.676	1.703	1.706	——
d	1.520	1.440	1.409	1.244	1.240	1.222	——

[a] The designation of the bonds in fulvene is given in Fig. 1. It should also be noted that the figures given here are for total bond orders, which are defined by $(1 + p_{rs})$ (see reference 18).

TABLE VIII. Bond lengths[a] in fulvene.

Bond	1	2	2a	3	3a	3b	4
a	1.37	1.36	1.355	1.39	1.38	1.38	——
b	1.43	1.44	1.45	1.48	1.48	1.49	——
c	1.37	1.36	1.355	1.39	1.38	1.38	——
d	1.42	1.43	1.44	1.47	1.47	1.48	——

[a] Bond lengths were read from Coulson's curve, and are given in angstrom units.

TABLE IX. First order perturbation calculation of the variation of charge distribution in fulvene.[a]

δ_6	+0.213	+0.061	+0.1	−0.1	+1	−1	+0.135
δ_5	−0.035	+0.057	0.0	0.0	0	0	+0.008
$\delta_1 = \delta_4$	−0.048	−0.043	0.0	0.0	0	0	−0.0415
$\delta_2 = \delta_3$	−0.042	−0.016	0.0	0.0	0	0	−0.030
$r = 6$[b]	+0.077	+0.194	+0.159	+0.268	−0.333	+0.759	+0.135
5	+0.047	−0.034	+0.001	−0.064	+0.293	−0.357	+0.008
1, 4	−0.043	−0.036	−0.047	−0.049	−0.036	−0.060	−0.0415
2, 3	−0.016	−0.044	−0.0325	−0.052	+0.057	−0.142	−0.030
μ	1.2 D	2.4 D	2.0 D	3.2 D	−3.7[c] D	9.1 D	1.9 D

[a] In each column of figures is listed a given set of δ_r's (rows 1–4), then the net charges (in e.u.) derived from this set of δ_r's (rows 5–8), and last, the dipole moment calculated with the use of the net charges given in rows 5–8.
[b] The numbering of the atoms in fulvene is that given in Fig. 1.
[c] The minus sign on the dipole moment indicates that the direction of the moment is the opposite of that given in Fig. 1.

[7] Joachim Wyss, Thesis, *Synthesen Einfacher Azulene* (Zürich, 1941), p. 27 ff.

[8] By Drs. J. R. Platt and H. B. Klevens, who used the 2205Å naphthalene peak for identification purposes. Cf. also E. Heilbronner and K. Wieland, Helv. Chim. Acta **30**, 951 (1947).

[9] M. Goldsmith and G. W. Wheland, J. Am. Chem. Soc. **70**, 2632 (1948).

[10] K. v. Auwers and F. Eisenlohr, J. prakt. Chem. (2) **84**, 53 (1911).

[11] R. Willstätter and M. Heidelberger, Ber. d. D. chem. Ges. **46**, 522 (1913).

[12] Whereas the dialkyl fulvenes do not appear to absorb close enough to the region of the sodium *D* lines to give abnormal exaltations, solutions of the diaryl fulvenes probably absorb close to this region since exaltations of the order of magnitude of 7 cc are observed. For 6,6-dimethylfulvene the observed exaltation is about 2.7 cc, and for 6,6-diethylfulvene the exaltation is about 2 cc.

[13] A. Weissberger, *Physical Methods of Organic Chemistry* (Interscience Publishers, Inc., New York, 1945), p. 673.

[14] All melting and boiling points are uncorrected.

MATHEMATICAL APPENDIX

The jth MO for fulvene is $\psi=\sum_n c_n\theta_n$, where the c's are numerical coefficients, and the functions θ_n are defined in terms of the atomic orbitals as follows:[15] $\theta_1=\phi_6$, $\theta_2=\phi_5$, $\theta_3=(\phi_1+\phi_4)$, $\theta_4=(\phi_2+\phi_3)$, $\theta_5=(\phi_1-\phi_4)$, $\theta_6=(\phi_2-\phi_3)$. The secular equation for fulvene has the form[16]

$$\begin{vmatrix} (\zeta_6 y+\delta_6) & \rho_{56} & 0 & 0 & 0 & 0 \\ \rho_{56} & (\zeta_5 y+\delta_5) & 2\rho_{15} & 0 & 0 & 0 \\ 0 & \rho_{15} & (\zeta_1 y+\delta_1) & \rho_{12} & 0 & 0 \\ 0 & 0 & \rho_{12} & (\zeta_2 y+\delta_2+\rho_{23}) & 0 & 0 \\ 0 & 0 & 0 & 0 & (\zeta_1 y+\delta_1) & \rho_{12} \\ 0 & 0 & 0 & 0 & \rho_{12} & (\zeta_2 y+\delta_2-\rho_{23}) \end{vmatrix}=0.$$

The corresponding 10×10 secular equation for azulene is set up in the same way.

Calculation 1.—In the simplest treatment (given by Coulson and Longuet-Higgins[1]) all ζ's$=1$, all δ's$=0$, and all ρ's$=1$. The results of this and the following calculations are given in Tables VI–X.

Calculation 2.—The preceding calculation for fulvene is refined by taking into account, by the Lennard-Jones method,[17] the variation of the bond integrals with bond length. The bond lengths are determined from the Coulson curve,[18] with the aid of the bond orders obtained from Calculation 1. All δ's and overlap integrals are set equal to zero.

Calculation 2a.—To refine the preceding calculation, new bond lengths are determined from the Coulson curve, with the aid of the revised bond orders obtained from Calculation 2. These revised bond lengths are used to calculate new values of the ρ's. The other assumptions are the same as before.

Calculation 3.—In this calculation the bond lengths are determined from the bond orders obtained from the preceding calculation. It is assumed that the δ's *are equal* to the *net* charges (in electron units) on the corresponding atoms. The net charges actually used are those obtained from Calculation 2a. It is easily seen that the δ-values thus obtained are of a reasonable order of magnitude, and show the correct qualitative dependence[16] on the electron affinities of the corresponding unsaturated carbon atoms in fulvene. Furthermore, the assumption which leads to these values is simple and easy to apply.

TABLE X. Charge distribution in azulene.

Atom[a]	q_r	Net charge (in e.u.)
2	1.047	−0.047
1, 3	1.173	−0.173
9, 10	1.027	−0.027
4, 8	0.855	+0.145
5, 7	0.986	+0.014
6	0.870	+0.130

[a] The numbering of the atoms is that given in Fig. 2.

[15] The subscripts on the ϕ's, and the subscripts used in the secular equation below, refer to the numbering system given in Fig. 1.

[16] The methods and nomenclature are given by G. W. Wheland, J. Am. Chem. Soc. **64**, 900 (1942).

[17] J. E. Lennard-Jones, Proc. Roy. Soc. (London), **A158**, 280 (1937).

[18] C. A. Coulson, Proc. Roy. Soc. (London), **A169**, 423 (1939).

Calculation 3a.—Here the charge distribution and bond orders obtained from Calculation 3 are used to determine respectively the δ's and the ρ's for the secular equation.

Calculation 3b.—The results of the preceding calculation are used to evaluate the δ's and the ρ's for the secular equation.

Calculation 4.—The last refinement applied to the MO treatment of fulvene is a first order perturbation calculation, with the δ's as perturbation parameters. The unperturbed secular equation is taken as that of Calculation 2a. The q_r's[19] are thus obtained as linear functions of the four δ's, as follows.

$$q_6=0.78674+0.54620\delta_6-0.32466\delta_5-0.022832\delta_1-0.19870\delta_2,$$
$$q_5=1.03194-0.32468\delta_6+0.34922\delta_5-0.048968\delta_1+0.02436\delta_2,$$
$$q_1=q_4=1.04819-0.011414\delta_6-0.024486\delta_5+0.34087\delta_1-0.30495\delta_2,$$
$$q_2=q_3=1.04246-0.099346\delta_6+0.012186\delta_5-0.30494\delta_1+0.39208\delta_2.$$

Finally, the q_r's in these equations are replaced by the corresponding $(1-\delta_r)$ terms. (This substitution is equivalent to the assumption that the δ's are equal to the corresponding net charges in electron units.) The resulting set of four, linear, simultaneous equations is solved for δ_6, δ_5, δ_1, and δ_2. The values thus obtained are listed in the last column of Table IX. These δ's are now used to obtain the corresponding q_r's. This set of δ_r's and q_r's is then said to be *self-consistent*. The moment calculated from this self-consistent set is about 1.9 D. (Cf. the last column of Table IX.)

Calculation 5.—The calculation for azulene was not carried beyond the simple treatment of Coulson and Longuet-Higgins.[1] The results, which are

[19] The quantity q_r represents the average number of π-electrons on the rth carbon atom.

analogous to those obtained for fulvene by Calculation 1, are listed in Table X.

Finally, a word should perhaps be said in regard to the significance of calculated charge distributions, dipole moments, bond orders, and bond lengths which differ as markedly as do those listed in Tables VI–IX. In Table VI, for example, the numerical values given in columns 1, 2, $\cdots$4 represent successive approximations, with those in the last column presumably the most reliable. Table IX, which illustrates the application of the perturbation method, brings out two different points of interest. Thus, the δ_r's listed in rows 1–4 of the last column are indeed self-consistent (cf. the last column of Table VI) since they are respectively equal to the q_r's listed in rows 5–8. However, the δ's given in the six preceding columns are clearly not self-consistent. In the second place, it is seen that the use of unreasonable values for the δ's, as in columns 6 and 7, leads to unreasonable charge distributions and to unreasonable moments. This fact lends some support to the otherwise arbitrary fundamental assumption (see above) that the δ's are equal to the corresponding net charges.

THE JOURNAL OF CHEMICAL PHYSICS VOLUME 17, NUMBER 3 MARCH, 1949

The Thermodynamics of High Polymer Solutions. IV. Phase Equilibria in the Ternary System: Polymer—Liquid 1—Liquid 2*

ROBERT L. SCOTT‡
Department of Chemistry, University of California, Berkeley, California
(Received July 12, 1948)

Two approximate methods of calculating equilibrium phase diagrams in ternary systems of polymer and mixed liquids have been compared with exact phase diagrams based upon the Flory-Huggins equations. Both a "single liquid approximation" and a "complete immiscibility approximation" are worthless except for the crudest qualitative considerations. Analytical expressions for the plait points of such ternary systems (a maximum of ten) have been derived. A consideration of the solubility of polymers in mixed solvents leads to the conclusion that a polymer may be completely soluble in certain mixtures of non-solvents if its internal pressure (cohesive energy density) lies between those of the two liquids and if the two liquids are themselves completely miscible. The position of the phase boundary is nearly independent of the molecular weight of the polymer for molecular weights above 10,000. Osmotic pressures in mixed solvents are discussed, and Gee's suggestion that the osmotic pressure is zero at the critical solubility limit is confirmed.

INTRODUCTION

IN Articles I and II of this series[1,2] a first attempt was made to treat the multicomponent system involved in the fractionation of high polymers. In particular, we assumed that "solvent mixtures can be treated with a fair degree of accuracy assuming the mixture of two solvents to behave as a homogeneous liquid with respect to the polymer," this new "liquid" having average thermodynamic properties. We did not suppose this treatment, which we shall call the "single liquid approximation," to be very accurate, but used it to obtain valuable qualitative information concerning the fractionation of high polymers. The present paper attempts to consider in further detail the problem of phase equilibria in a three-component system consisting of a long-chain polymer and two ordinary liquids, with a view to determining, among other results, the limitations of such a "single liquid approximation."

THE HEAT OF MIXING OF A TERNARY SYSTEM

Van Laar,[3] Scatchard,[4] and Hildebrand[5] have shown that, in many cases, the heat absorbed in mixing two substances may be represented by the expression:

$$\Delta H_{12}{}^{M} = V_m A_{12} \phi_1 \phi_2, \quad (1)$$

when V_m is the volume of the mixture, ϕ_1 and ϕ_2 are the volume fractions of the respective components, and A_{12} is a constant characteristic of the system. Scatchard[6] has shown that if one makes entirely equivalent assumptions for a three-component system, one obtains

$$\Delta H_{123}{}^{M} = V_m(A_{12}\phi_1\phi_2 + A_{13}\phi_1\phi_3 + A_{23}\phi_2\phi_3), \quad (2)$$

where the A's are the constants for the corresponding binary systems.

Differentiation leads to the partial molal heats

* The major portion of the following work was done on a Frank B. Jewett Fellowship granted by the Bell Telephone Laboratories and first presented to the High Polymer Forum at the 111th meeting of the American Chemical Society at Atlantic City, New Jersey, April 14, 1947.
‡ Present address: Department of Chemistry, University of California, Los Angeles 24, California.
[1] R. L. Scott and M. Magat, J. Chem. Phys. **13**, 172 (1945).
[2] R. L. Scott, J. Chem. Phys. **13**, 178 (1945).
[3] J. J. van Laar, "Sechs Vortrage," Zeits. f. physik. Chemie **72**, 723 (1910).
[4] George Scatchard, Chem. Rev. **8**, 321 (1931).
[5] J. H. Hildebrand, *Solubility of Non-electrolytes* (Reinhold Publishing Corporation, New York, 1936).
[6] G. Scatchard, Trans. Faraday Soc. **33**, 160 (1937).

of mixing:

$$\Delta\bar{H}_1=\partial\Delta H_{123}/\partial N_1=V_1[A_{12}\phi_2^2+A_{13}\phi_3^2+(A_{12}+A_{13}-A_{23})\phi_2\phi_3], \quad (3a)$$

$$\Delta\bar{H}_2=\partial\Delta H_{123}/\partial N_2=V_2[A_{12}\phi_1^2+A_{23}\phi_3^2+(A_{12}+A_{23}-A_{13})\phi_1\phi_3], \quad (3b)$$

$$\Delta\bar{H}_3=\partial\Delta H_{123}/\partial N_3=V_3[A_{13}\phi_1^2+A_{23}\phi_2^2+(A_{13}+A_{23}-A_{12})\phi_1\phi_2]. \quad (3c)$$

If, in addition, we assume[3-5] that the interaction energy between unlike pairs of molecules is the geometric mean of those between like pairs, then:

$$A_{ij}=(\delta_i-\delta_j)^2, \quad (4)$$

where δ_i represents the square root of the internal pressure (or "cohesive energy density"), $(\Delta E_i^v/V_i)^{\frac{1}{2}}$, where ΔE_i^v is the energy of vaporization and V_i the molal volume of component i.

We may then rewrite Eqs. (2) and (3):

$$\Delta H_{123}^M=V_m[(\delta_1-\delta_2)^2\phi_1\phi_2+(\delta_1-\delta_3)^2\phi_1\phi_3+(\delta_2-\delta_3)\varphi_2\phi_3], \quad (5)$$

$$\Delta\bar{H}_1=V_1[(\delta_1-\delta_2)\phi_2+(\delta_1-\delta_3)\phi_3]^2, \quad (6a)$$

$$\Delta\bar{H}_2=V_2[(\delta_2-\delta_1)\phi_1+(\delta_2-\delta_3)\phi_3]^2, \quad (6b)$$

$$\Delta\bar{H}_3=V_3[(\delta_3-\delta_1)\phi_1+(\delta_3-\delta_2)\phi_2]^2. \quad (6c)$$

Each of these equations may be rearranged in a form which shows that the partial molal heat of mixing of liquid 1 with liquids 2 and 3 is equivalent to the heat of mixing of liquid 1 with a hypothetical new liquid whose δ is the volume fraction average of 2 and 3:

$$\Delta\bar{H}_1=V_1[\delta_1-(\phi_2\delta_2+\phi_3\delta_3)/(\phi_2+\phi_3)]^2(\phi_2+\phi_3)^2, \quad (7)$$

or

$$\Delta\bar{H}_1=V_1[\delta_1-\delta_0]^2\phi_0^2, \quad (8)$$

where

$$\delta_0=(\phi_2\delta_2+\phi_3\delta_3)/(\phi_2+\phi_3), \quad \phi_0=\phi_2+\phi_3.$$

Such a transformation may always be made and is frequently useful in dealing with one-phase systems. It should be just as valid for high polymer solutions as for those of small molecules.

FREE ENERGIES IN TERNARY SYSTEMS

Adding the equations of the previous section for the heat of mixing to the familiar expressions of Huggins,[7] Flory,[8] Miller,[9] and Guggenheim[10] for the entropy of high polymer solutions, we obtain the partial molal free energies of the three components in a ternary system. For a three-component system consisting of a long-chain polymer (subscript 3) and two liquids (subscripts 1 and 2) of equal molal volumes ($V_1=V_2=V_0$), we obtain:

$$\Delta\bar{F}_1=RT[\ln\phi_1+(1-(1/m))\phi_3+\mu_{12}\phi_2^2+\mu_{13}\phi_3^2+(\mu_{12}+\mu_{13}-\mu_{23})\phi_2\phi_3], \quad (9a)$$

$$\Delta\bar{F}_2=RT[\ln\phi_2+(1-(1/m))\phi_3+\mu_{12}\phi_1^2+\mu_{23}\phi_3^2+(\mu_{12}+\mu_{23}-\mu_{13})\phi_1\phi_3], \quad (9b)$$

$$\Delta\bar{F}_3=RT[\ln\phi_3-(m-1)(\phi_1+\phi_2)+m\mu_{13}\phi_1^2+m\mu_{23}\phi_2^2+m(\mu_{13}+\mu_{23}-\mu_{12})\phi_1\phi_2], \quad (9c)$$

where m is the ratio of molal volumes of polymer and liquid (V_3/V_0), or approximately the degree of polymerization, and the μ's are constants for the corresponding binary systems such that:

$$\mu_{12}=V_0A_{12}/RT, \quad (10a)$$

$$\mu_{13}=\mu^s+(V_0A_{13}/RT), \quad (10b)$$

$$\mu_{23}=\mu^s+(V_0A_{23}/RT). \quad (10c)$$

In these equations μ^s is a correction factor from the entropy. In the original Flory treatment,[8] certain second-order corrections in the statistical treatment were ignored, and μ^s, resultantly, was zero. In the more nearly accurate treatments of Huggins,[7] Miller,[9] and Guggenheim,[10] μ^s reduces to approximately $1/z$, where z is the coordination number of the quasi-lattice. Actually, we know from experiment and from recent theoretical studies[11,12] that μ^s is greater than $1/z$; for the purposes of this paper, we shall treat it as an empirical constant about 0.25 in magnitude.

If Eq. (4) holds, we may write:

$$\mu_{12}=(V_0/RT)(\delta_1-\delta_2)^2=(A+B)^2, \quad (11a)$$

$$\mu_{13}=\mu^s+(V_0/RT)(\delta_1-\delta_3)^2=\mu^s+A^2, \quad (11b)$$

$$\mu_{23}=\mu^s+(V_0/RT)(\delta_2-\delta_3)^2=\mu^s+B^2, \quad (11c)$$

where these equations are used to define new parameters A and B.

Using Eqs. (11abc), we may rewrite Eqs. (9abc):

$$\Delta\bar{F}_1=RT[\ln\phi_1+(1-(1/m))\phi_3+\mu^s\phi_3^2+([A+B]\phi_2+A\phi_3)^2], \quad (12a)$$

$$\Delta\bar{F}_2=RT[\ln\phi_2+(1-(1/m))\phi_3+\mu^s\phi_3^2+([A+B]\phi_1+B\phi_3)^2], \quad (12b)$$

$$\Delta\bar{F}_3=RT[\ln\phi_3+(m-1)(\phi_1+\phi_2)+m\mu^s(\phi_1+\phi_2)^2+m(A\phi_1-B\phi_2)^2]. \quad (12c)$$

We propose to calculate the equilibrium phase diagrams for ternary systems using the above equations. In any two-phase systems, the thermodynamic conditions for equilibrium require that the partial molal free energy of each component be

[7] M. L. Huggins, J. Chem. Phys. 9, 440 (1941), Ann. N. Y. Acad. Sci. 43, 1 (1942).
[8] P. J. Flory, J. Chem. Phys. 9, 660 (1941); 10, 51 (1942).
[9] A. R. Miller, Proc. Camb. Phil. Soc. 38, 109 (1942); 39, 154 (1943).
[10] E. A. Guggenheim, Proc. Roy. Soc. A183, 203 (1944).
[11] A. R. Miller, J. Chem. Phys. 16, 841 (1948).
[12] B. H. Zimm, Am. Chem. Soc. meeting in New York (Sept. 1947).

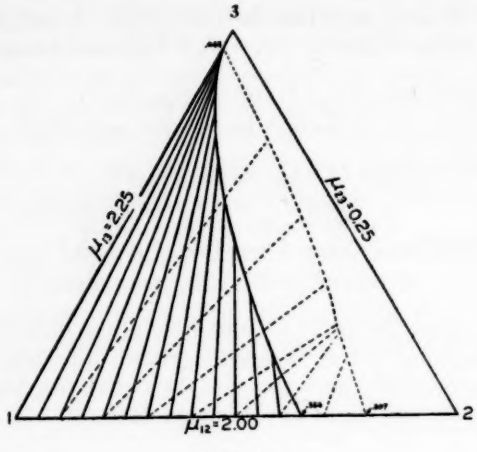

FIG. 1.

the same in both phases:

$$\Delta\bar{F}_1' = \Delta\bar{F}_1'', \tag{13a}$$

$$\Delta\bar{F}_2' = \Delta\bar{F}_2'', \tag{13b}$$

$$\Delta\bar{F}_3' = \Delta\bar{F}_3''. \tag{13c}$$

Upon substituting appropriate values for m, μ^s, A^2, and B^2 (or, in the more general case, m, μ_{12}, μ_{13}, and μ_{23}), one may determine the phase boundaries and the tie lines for any hypothetical system.

Before doing so, however, let us consider two approximation methods.

THE "SINGLE LIQUID" APPROXIMATION

The existence of equations of the form of (7) suggested[1,2] that one might solve the problem of a two-phase-three-component system in which one component is a high polymer by reducing it to that of a binary system: polymer plus hypothetical single liquid of average properties. Substitution of the equivalent of Eq. (8) into Eq. (12c) yields:

$$\Delta\bar{F}_3 = RT[\ln\phi_3 - (m-1)\phi_0 + m\mu_{30}\phi_0^2], \tag{14}$$

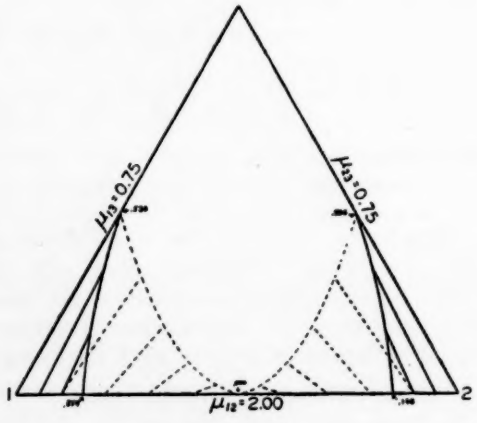

FIG. 2.

where

$$\phi_0 = \phi_1 + \phi_2 = 1 - \phi_3, \tag{15}$$

$$\mu_{30} = \mu^s + [A\phi_1 - B\phi_2/\phi_1+\phi_2]^2 = \mu_{13}(\phi_1/\phi_1+\phi_2) + \mu_{23}(\phi_2/\phi_1+\phi_2) - \mu_{12}(\phi_1\phi_2/(\phi_1+\phi_2)^2). \tag{16}$$

A corresponding equation for the hypothetical "single liquid" would be:

$$\Delta\bar{F}_0 = RT[\ln\phi_0 + (1-(1/m))\phi_3 + \mu_{30}\phi_3^2]. \tag{17}$$

For such a set of equations to be useful, we must assume that μ_{30} has the same value in both conjugate phases. With this assumption we may solve Eqs. (14) and (17) for a series of binary systems with varying values of μ_{30} (i.e., different ratios of 1 to 2, ϕ_1/ϕ_2) and obtain a complete phase diagram.

Of course, such a treatment will be rigorously accurate, if and only if the relative proportions of the two liquids are identical in the two conjugate phases; otherwise, μ_{30}' does not equal μ_{30}''. This requires that the extension of all tie lines pass through the vertex of 100 percent 3. That this condition is ever precisely satisfied (except in the trivial case that the two liquids have identical properties) is doubtful.

Figures 1 and 2 show the results of "single liquid" calculations for two simple cases, all chosen for the limit of infinite molecular weight polymer, $(m\to\infty)$.

Case I (Fig. 1), $m\to\infty$, $\mu^s=0.25$, $A^2=2.0$, $B^2=0$ (i.e., $\mu_{13}=2.25$, $\mu_{23}=0.25$, $\mu_{12}=2.00$). In this case liquid 2 has no heat of mixing with the polymer, and hence is the best possible solvent; liquids 1 and 2 are at their critical solution temperature. A real system which approximates such a situation would be polystyrene-benzene-methanol.

Case II (Fig. 2), $m\to\infty$, $\mu^s=0.25$, $A^2=0.50$, $B^2=0.50$ (i.e., $\mu_{13}=0.75$, $\mu_{23}=0.75$, $\mu_{12}=2.00$). In this case the two liquids are entirely equivalent in their solvent power for the polymer, and are again at their critical solution temperature. The "single liquid" approximation yields the interesting result that the polymer, while only partially miscible with either pure liquid, is miscible in all proportions with certain mixtures.

THE "COMPLETE IMMISCIBILITY" APPROXIMATION

A second kind of approximation is obtained if we assume arbitrarily that two of the three components are completely immiscible. If, for example, 1 and 3 are completely immiscible, the system will consist of a phase consisting of 1 and 2 only in equilibrium with a phase consisting of 2 and 3 only. Were this true, we would obtain the phase diagram (which consists of tie lines extending from the 1,2 edge of the triangle to the 2,3 edge) by equating the partial molal free energies of 2 in the two

phases:

$$RT[\ln\phi_2' + \mu_{12}(\phi_1')^2] = RT[\ln\phi_2'' + (1-(1/m))(\phi_3'') + \mu_{23}(\phi_3'')^2], \quad (18)$$

or

$$\ln\phi_2' + \mu_{12}(1-\phi_2')^2 = \ln\phi_2'' + (1-(1/m))(1-\phi_2'') + \mu_{23}(1-\phi_2'')^2. \quad (19)$$

Given a value of ϕ_2'', we may calculate ϕ_2' and hence determine the phase diagram. Common sense will dictate the choice of which pair to choose as completely immiscible.

Figure 3 shows the "complete immiscibility" approximation for Case I of the previous section, assuming the polymer (3) and the non-solvent (1) are completely immiscible. For Case II, the miscibility region is obviously so large as to render this approximation absurd.

Consideration of the assumptions involved will show that where the right pairs are chosen in each of the two approximate methods, they represent extreme cases, and the correct phase diagram will be intermediate. For example, the next section will show that the true phase diagram for Case I lies between those of Fig. 1 and Fig. 3.

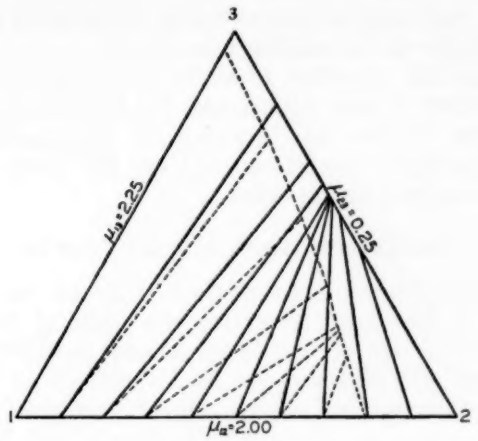

FIG. 3.

THE CORRECT PHASE DIAGRAMS

The exact calculation of the phase diagrams of a three-component system is extremely difficult without the aid of the preceding approximations. Since no analytical expression for the phase boundary and the tie lines exists, they must be determined by a laborious trial and error process. The amount of calculation is measurably reduced if the molecular weight is increased without limit ($m\to\infty$), for in this case, one conjugate phase necessarily contains no polymer ($\phi_3'=0$), and the tie lines end on the 1,2 edge of the triangle. Six such systems have been calculated ($m\to\infty$, $\mu^s=0.25$).

Case I. $A^2=2.0$, $B^2=0$ ($\mu_{12}=2.0$, $\mu_{13}=2.25$, $\mu_{23}=0.25$). (See Fig. 4.) As previously noted, this corresponds to a system in which a polymer of extremely high molecular weight is mixed with the best possible solvent with which there is no heat of mixing; the third component is a strong precipitant just miscible with the solvent. The plait point is at 79.3 percent solvent, 20.7 percent precipitant, not at 64.6 percent−35.4 percent, as predicted by the "single liquid" approximation, or at 100 percent solvent, as required by the "complete immiscibility" treatment. The failure of the latter was expected; the reason for the inadequacy of the former is also clear; the tie lines show that the proportions of solvent and non-solvent in the two conjugate phases are widely different.

Case IA. $A^2=1.0$, $B^2=0$ ($\mu_{12}=1.0$, $\mu_{13}=1.25$, $\mu_{23}=0.25$). (See Fig. 5.) This represents a system of polymer-solvent-precipitant in which the precipitant is not so effective, having a heat of mixing with the solvent only half that in Case I. The real system polystyrene-benzene-isopropanol should correspond roughly to that shown in Fig. 5.

Case 1B. $A^2=2.2$, $B^2=0$ ($\mu_{12}=2.2$, $\mu_{13}=2.45$, $\mu_{23}=0.25$). (See Fig. 6.) On the other hand, the solvent and non-solvent may be partially immiscible. In such a case, a three-phase region results, as shown in Fig. 6. A real system which might approach this behavior is polyisobutylene-cyclohexane-methanol.

Case II. $A^2=0.5$, $B^2=0.5$ ($\mu_{12}=2.0$, $\mu_{13}=0.75$, $\mu_{23}=0.75$). Figure 7 represents the hypothetical case of a polymer midway in internal pressure between two liquids at their critical solution temperature. The polymer is, in fact, completely miscible in all proportions with a 50–50 mixture of the two liquids, but the two-phase region is not nearly so large as that predicted by the single liquid approximation. Hence, as in Case I, the true phase diagram lies intermediate between the extremes of the two approximational methods.

Case IIA. $A^2=0.4$, $B^2=0.4$ ($\mu_{12}=1.6$, $\mu_{13}=0.65$, $\mu_{23}=0.65$). Figure 8 represents a situation similar

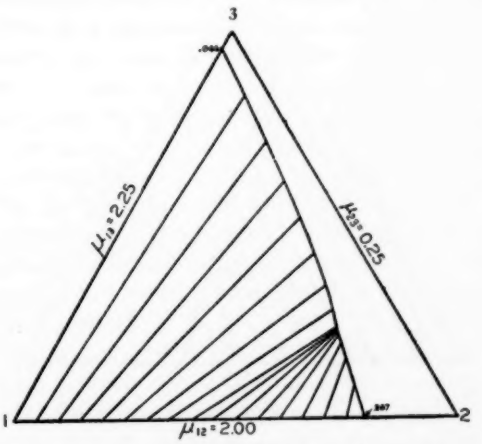

FIG. 4.

to II, but with a sizeable range of complete miscibility, due to the smaller heat effects.

Case IIB. $A^2=0.55$, $B^2=0.55$ ($\mu_{12}=2.2$, $\mu_{13}=0.80$, $\mu_{23}=0.80$). Figure 9 illustrates the analogous phase diagram for the case in which the two liquids are only partially miscible (as in Case IB). Here again a three-phase region exists.

DETERMINATION OF PLAIT POINTS

Exact determination of these diagrams for more than a few cases, even for the limit of infinite molecular weight, would be almost prohibitively difficult. Fortunately, one may obtain useful information by solving analytically for the plait point, which corresponds to the critical point in a binary system.

According to Gibbs,[13] one may obtain the coordinates of the plait point (or "critical phase" in his terminology) by solving two simultaneous equations, both expressed as secular determinants:

$$\begin{vmatrix} \dfrac{\partial^2 F}{\partial n_1^2} & \dfrac{\partial^2 F}{\partial n_1 \partial n_2} \\ \dfrac{\partial^2 F}{\partial n_1 \partial n_2} & \dfrac{\partial^2 F}{\partial n_2^2} \end{vmatrix} = U = 0, \tag{20}$$

$$\begin{vmatrix} \dfrac{\partial U}{\partial n_1} & \dfrac{\partial U}{\partial n_2} \\ \dfrac{\partial_2 F}{\partial n_1 \partial n_2} & \dfrac{\partial^2 F}{\partial n_2^2} \end{vmatrix} = V = 0, \tag{21}$$

where F in the above equation represents the total free energy of the system, and the n's numbers of molecules of the various components.

An entirely equivalent set of equations may be obtained in a perhaps more physically obvious manner as follows: If we consider first not the limiting case of the plait point, but two separate conjugate phases, we find that in addition to Eqs. (13abc), another condition (not independent of these) is satisfied. This is that if one plots the total free energy along the extended tie line connecting the two conjugate phases, the two conjugate phases may be identified as the points where a straight line is tangent simultaneously.

If we now approach the limit of the plait point, we find that the two points of tangency approach each other and finally become identical. Such a situation is mathematically equivalent to the coalescence of two points of inflection, a situation which requires that the second and third derivatives vanish. In the phase diagram there is at the plait point a line tangent to the phase boundary which we may regard as the extension of a limiting tie line. If we define a variable q as the coordinate of a point along this line, we may write:

$$d^2F/dq^2=0, \tag{21a}$$

$$d^3F/dq^3=0. \tag{21b}$$

We may replace the total free energy, without loss of generality, by that per mole:

$$F=x_1\Delta\bar{F}_1+x_2\Delta\bar{F}_2+x_3\Delta\bar{F}_3, \tag{22}$$

where the x's represent mole fractions, and we may write the familiar Gibbs-Duhem-Margules relation as:

$$x_1 d\Delta\bar{F}_1+x_2 d\Delta\bar{F}_2+x_3 d\Delta\bar{F}_3=0. \tag{23}$$

Using these relations, one may show that the conditions for the plait point are:

$$d\Delta\bar{F}_1/dq=0, \tag{24a}$$

$$d\Delta\bar{F}_2/dq=0, \tag{24b}$$

$$d\Delta\bar{F}_3/dq=0, \tag{24c}$$

$$(dx_1/dq)\cdot(d^2\Delta\bar{F}_1/dq^2)+(dx_2/dq)(d^2\Delta\bar{F}_2/dq^2) +(dx_3/dq)(d^2\Delta\bar{F}_2/dq^2)=0. \tag{25}$$

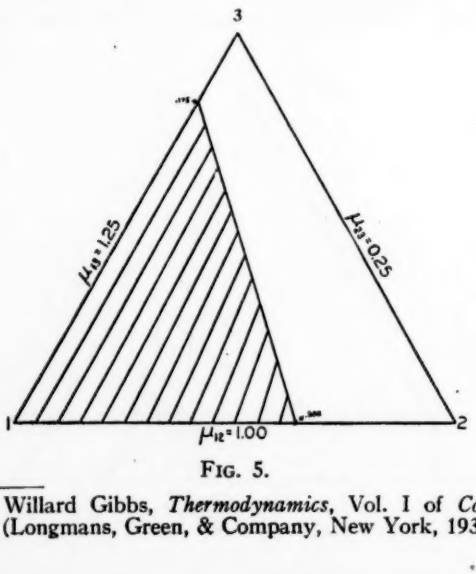

FIG. 5.

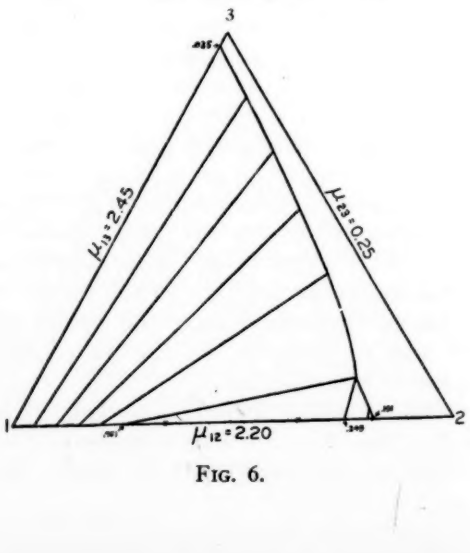

FIG. 6.

[13] J. Willard Gibbs, *Thermodynamics*, Vol. I of *Collected Works* (Longmans, Green, & Company, New York, 1931).

This gives us three independent equations[14] which permit us to solve for the coordinates of the plait point, and the slope of the tangent line.

By either method shown above, one is led upon substitution of Eqs. (9abc) to the following complicated expressions:

$$\phi_1+\phi_2+m\phi_3-2[\mu_{12}\phi_1\phi_2+m\mu_{13}\phi_1\phi_3+m\mu_{23}\phi_2\phi_3]+Qm\phi_1\phi_2\phi_3=0, \quad (26)$$

$$m\phi_3^2[(1-2\mu_{13}\phi_1)(1-\phi_1[\mu_{13}+\mu_{12}-\mu_{23}])+(1-2\mu_{23}\phi_2)(1-\phi_2[\mu_{23}+\mu_{12}-\mu_{13}])]-(1-2\mu_{12}\phi_1\phi_2)^2+\phi_3[\mu_{12}(\phi_1^2+4\phi_1\phi_2+\phi_2^2)+\mu_{13}(\phi_1^2-\phi_2^2)+\mu_{23}(\phi_2^2-\phi_1^2)-2(\phi_1+\phi_2)-1]=0, \quad (27)$$

where

$$Q=2\mu_{12}\mu_{13}+2\mu_{12}\mu_{23}+2\mu_{13}\mu_{23}-\mu_{12}^2-\mu_{13}^2-\mu_{23}^2. \quad (28)$$

If Eq. (4) holds true, Eqs. (11abc) for the μ's are valid, and on substitution of Eqs. (11abc) into Eq. (28), we obtain:

$$Q=4\mu^s(A+B)^2=4\mu^s\mu_{12}. \quad (29)$$

Since μ^s is positive, Q is necessarily positive unless Eq. (4) fails. Were μ^s zero (as in the original oversimplified Flory equation[7]), Q would vanish and Eqs. (26) and (27) would simplify. Negative values of Q are possible only if Eq. (4) is invalid. Since Eq. (4) is fairly satisfactory in the absence of dipoles, we shall expect to find negative values of Q only when one or more of the components, either polymer or liquid or both, are decidedly polar substances.

The set of simultaneous equations (26) and (27) have a maximum of twelve possible solutions, of which two are spurious.[15]

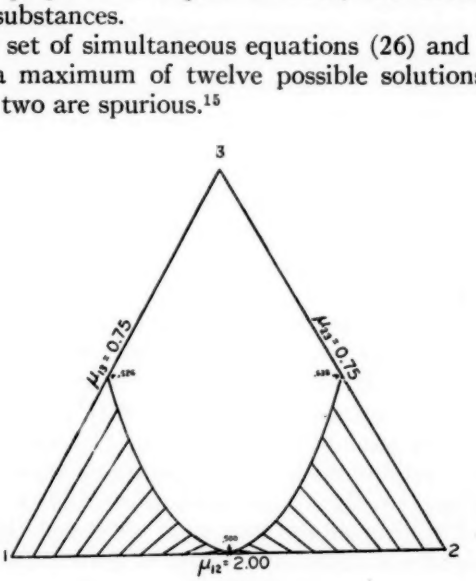

FIG. 7.

[14] Equations (24abc) are essentially the limiting case of Eqs. (13abc), but they do not represent at the limit, three independent equations, inasmuch as the third can be obtained from the other two by means of Eq. (23). Hence the need of Eq. (25).

[15] Two roots correspond to the points in the binary system 1,2 where the partial molal free energies are minima or maxima, and must be discarded. This does not exclude a real plait point if the binary system is at its critical solution temperature.

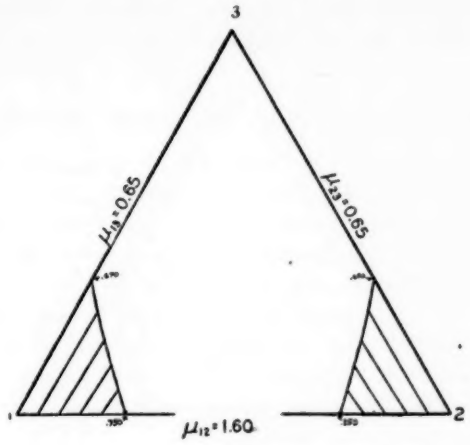

FIG. 8.

If $Q=0$, then there are only six possible solutions to the pair of simultaneous equations. This is not to say that in any real system there are ten (or six) different real roots. Some may be imaginary, and some degenerate. Others may be outside the triangular diagram and be without physical meaning.

For the moment, let us confine ourselves to the solutions of Eqs. (26) and (27) in the limit of extremely high molecular weight polymer ($m\rightarrow\infty$). Two of the solutions are degenerate at the limit of infinite molecular weight, leaving a maximum of eight different solutions (or five for the case $Q=0$), which are given in Appendix I. Of these eight, for any given set of μ's, only a few, never more than three, are of physical significance. The most important correspond to the two solutions of the equations:

$$1-2\mu_{13}\phi_1-2\mu_{23}\phi_2+Q\phi_1\phi_2=0, \quad (30)$$

$$\phi_3=0. \quad (31)$$

The plait points indicated by crosses in Figs. 5–10 are solutions of these equations.

SOLUBILITY IN MIXED SOLVENTS

When a sufficiently small amount of a non-solvent is added to a solution, no phase separation results. However, as one increases the amount of non-solvent, a point is reached at which two phases appear, one rich in polymer, and we speak of "precipitation." For high molecular weights, this point, which may be called a "precipitation threshold" or a "critical solubility limit," is very sharp and represents the boundary between a region of complete miscibility of polymer and solvent mixture and a region where the solubility of the polymer is extremely small. It is easily seen that these limits are identical with the plait points calculated in the previous section. We may therefore use Eqs. (30) and (31) to define these limits.

There are, in general, either two real or two imaginary solutions to Eqs. (30) and (31). When

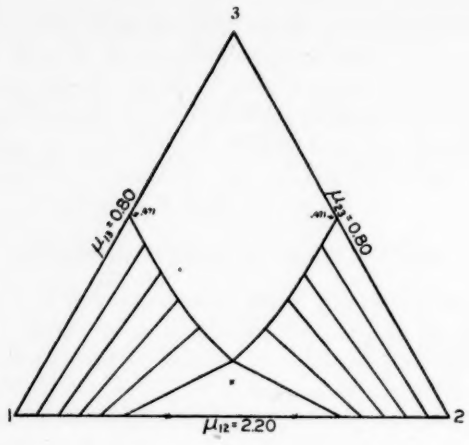

FIG. 9.

the roots are real, either or both may lie outside the diagram. Only real roots for which ϕ_1 and ϕ_2 lie between zero and one are of physical significance. The phase diagram will include two, one, or no critical solubility limits, depending on the number of such real roots.

Three different cases have to be distinguished, depending on the solvent properties of the two liquids.

(a) Both liquids solvents: Reference to the familiar problem of two components[8,16] shows that for both liquids to be solvents (i.e., miscible in all proportions with the polymer) the mathematical conditions are: $\mu_{13}<\frac{1}{2}$; $\mu_{23}<\frac{1}{2}$. For positive values of Q, there are no solutions between zero and one; which means the polymer is completely miscible with all possible solvent mixtures. If, however, $\mu_{12}>2$ (which corresponds to a negative Q), the two liquids are themselves immiscible, and there will be an intermediate two-phase region.[17]

(b) One solvent; one non-solvent: In this familiar solvent-precipitant system, $\mu_{13}<\frac{1}{2}$, $\mu_{23}>\frac{1}{2}$ or, conversely, $\mu_{13}>\frac{1}{2}$, $\mu_{23}<\frac{1}{2}$. Normally, there is one, and only one, root between zero and one, corresponding to the one physically necessary in a transition between a solvent and non-solvent. See, for example, Figs. 4 and 5. As before, if $\mu_{12}>2$, a region in which the two liquids are immiscible complicates the diagram, in one of several ways. For positive values of Q there is a three-phase region, as in Fig. 6. For negative values of Q, there may be two two-phase regions isolated from each other.

(c) Two non-solvents: For this system $\mu_{13}>\frac{1}{2}$, $\mu_{23}>\frac{1}{2}$. Under these conditions there are either zero or two solutions between zero and one. For negative Q's there are no such roots. For positive Q's there are two roots provided that:

$$\mu_{13}+\mu_{23}-1<\mu_{12}<2 \tag{32}$$

When $\mu_{12}>2$, the situation is again complicated by the immiscibility of the two liquids. The significant conclusion is essentially that already obtained from Figs. 7 and 8—namely, that under certain circumstances (namely, those defined by Eq. (32)) mixtures of two non-solvents may be good solvents (i.e., show complete miscibility with the polymer).[18] While the conclusions from the first two cases are physically obvious, this was not.

Very similar conclusions were reached in an earlier treatment by Gee[19] based upon an equation similar to, but different from, our Eqs. (30) and (31). The relation between the two treatments will be discussed in Appendix II.

Of great significance is the fact that Gee showed experimentally in six cases that rubbers could be dispersed in appropriate mixtures of non-solvents, in agreement with the theoretical conclusions.

POLYMERS OF FINITE MOLECULAR WEIGHT

The previous sections have dealt exclusively with polymers of extremely high molecular weight or, strictly speaking, the limiting case of infinite molecular weight. Let us now examine the effect of finite molecular weight upon the conclusions already arrived at. Calculation of detailed phase diagrams for any but infinite molecular weights would be almost impossibly difficult. One may expect, however, that for reasonably high molecular weights the phase diagrams will be very similar to the limiting ones. We may appraise the magnitude of the difference by determining several points on the phase diagram: the two conjugate phases (if any) in the binary systems, polymer-liquid 1, and polymer-liquid 2, and the plait points of the system. The extent to which these differ from the corresponding points for $m\rightarrow\infty$ will illuminate the problem.

We cannot explicitly solve Eqs. (26) and (27) for finite molecular weights, but we may expand around the solution for $m=\infty$ and obtain solutions as series expansion in inverse powers of m. If we expand about the roots of Eqs. (30) and (31), we obtain a power series of $m^{-\frac{1}{2}}$. For the particular case (corresponding to Fig. 5), $\mu_{12}=2.0$, $\mu_{13}=2.25$, $\mu_{23}=0.25$ ($Q=2.0$), we obtain four such solutions, three of which are outside the phase diagram. The one solution of physical significance is:

$$\phi_1=0.2071+(0.290/m^{\frac{1}{2}})+\cdots, \tag{33a}$$

$$\phi_2=0.7929-(0.730/m^{\frac{1}{2}})+\cdots, \tag{33b}$$

$$\phi_3=(0.440/m^{\frac{1}{2}})+\cdots. \tag{33c}$$

[16] M. L. Huggins, J. Am. Chem. Soc. **64**, 1712 (1942).

[17] In this case, the two solubility limits are not plait points; the plait point of the two-phase region is in the interior of the diagram corresponding to a different solution than those represented by Eqs. (30) and (31).

[18] This effect is not entirely precluded for $\mu_{12}>2$. Even here a small region of complete solubility may exist. The mathematical conditions for this are far more complicated.

[19] G. Gee, Trans. Faraday Soc. **40**, 468 (1944).

Using these equations for the plait point, the phase boundaries for various molecular weights have been estimated, and are shown in Fig. 10. As one can easily see, above molecular weights of 10,000 ($m=100$), the diagrams are almost indistinguishable from the limiting case. This is in agreement with the well-known features of fractional precipitation in which, after the precipitation threshold is reached, a few more drops of precipitant suffice to bring down successive fractions.

For Case IA a similar situation holds. Solving the equations, one finds for the plait point:

$$\phi_1=0.3660+(0.534/m^{\frac{1}{2}})+\cdots, \quad (34a)$$

$$\phi_2=0.6340-(1.173/m^{\frac{1}{2}})+\cdots, \quad (34b)$$

$$\phi_3=(0.639/m^{\frac{1}{2}})+\cdots. \quad (34c)$$

These are very similar to Eqs. (33abc), except that the change with molecular weight is greater, in agreement with the lowered sensitivity of milder precipitants.

The existence of expansions such as Eqs. (33) and (34) does not guarantee the existence of a plait point for all values of m; below certain values of m, the series may no longer converge—in which case the plait point does not exist. Equation (33) is a case in point; for very low values of m (below about 10), it does not converge.

THREE-PHASE REGIONS

We may regard a three-phase region as resulting from the overlapping of three two-phase regions, one corresponding to each side of the triangle. With each two-phase region is associated a plait point, so we may consider the existence of three real non-degenerate solutions to the plait point equation as a necessary (but not always sufficient) condition for a three-phase region. For $m=\infty$, a consideration of the eight possible solutions (Appendix I) shows that for there to be three real solutions, μ_{12} must exceed 2.0, corresponding to the physically obvious requirement that the two liquids 1 and 2 be only partially miscible. For finite molecular weights, however, a small three-phase region may persist for values of μ_{12} slightly less than 2.0. Since these regions are small and vanish rapidly[20] with decreasing μ_{12}, they may largely be ignored.

The existence of three real mathematical solutions to the plait point equation does not necessitate their existence as physically real plait points. Some, or all, may be inside the three-phase region. The three plait points required by a three-phase region are shown by crosses for Cases IB and IIB in Figs. 6 and 9.

[20] For example, consider the case $\mu_{12}=2$, $\mu_{13}=2$, $\mu_{23}=0$ ($Q=0$). For all values of m between 17.7 and ∞, there is a small three-phase region. If we let $\mu_{12}=\mu_{13}$ and decrease μ_{12}, these limits converge until the three-phase region vanishes absolutely at $\mu_{12}=\mu_{13}=1.984$ and $m=15.5$. Below this value of μ no three-phase region can exist for any value of m.

OSMOTIC PRESSURES IN MIXED SOLVENTS

The success of the theories of Huggins and Flory *et al.*[1-10] in explaining the osmotic pressures of high polymer solutions suggests that the treatment of three-component systems developed in the preceding pages be applied to the interpretation of osmotic pressures in mixed solvents.

Thermodynamic equilibrium is reached only when the partial molal free energy of each of the diffusible components is the same on both sides of the membrane. Mathematically, these conditions are expressed in Eqs. (35a) and (35b), where the zero superscript indicates the polymer-free phase:

$$\ln\phi_1^0+\mu_{12}(\phi_2^0)^2=\ln\phi_1+[1-(1/m)]\phi_3+\mu_{12}\phi_2^2 +\mu_{13}\phi_3^2+(\mu_{12}+\mu_{13}-\mu_{23})\phi_2\phi_3+(\pi V_0/RT), \quad (35a)$$

$$\ln\phi_2^0+\mu_{12}(\phi_1^0)^2=\ln\phi_2+[1-(1/m)]\phi_3+\mu_{12}\phi_1^2 +\mu_{23}\phi_3^2+(\mu_{12}+\mu_{23}-\mu_{13})\phi_1\phi_3+(\pi V_0/RT). \quad (35b)$$

No exact analytical expression for π can be obtained from equations of such a form, but we may obtain a solution in the form of a series expansion in powers of ϕ_3, the volume fraction of the non-diffusible polymer. Equation (36) gives the first two terms of such an expression (the derivation will be found in Appendix II).

$$\frac{\pi V_0}{RT}=\frac{\phi_3}{m} +\frac{1-2\mu_{13}\phi_1^0-2\mu_{23}\phi_2^0+Q\phi_1^0\phi_2^0}{2(1-2\mu_{12}\phi_1^0\phi_2^0)}\phi_3^2+\cdots. \quad (36)$$

At equilibrium the solvent ratios are not usually the same in both places. The relation between the two may be obtained again, as a series expansion in powers of ϕ_3:

$$\frac{\phi_1}{\phi_2}=\frac{\phi_1^0}{\phi_2^0}\left\{1-\phi_3\frac{[\mu_{13}-\mu_{23}+\mu_{12}(\phi_1^0-\phi_2^0)]}{(1-2\mu_{12}\phi_1^0\phi_2^0)}+\cdots\right\}. \quad (37)$$

We can see from this equation that true equilibrium requires the exchange of what may be rather considerable quantities of the two liquids. As Gee[21] has noted in a similar treatment to this one, it is hardly possible that the solvent distribution throughout the two cells of the osmometer reaches equilibrium in the short time required for a single osmotic pressure measurement. He suggests that equilibrium is set up between two thin layers in contact with the membrane. In such a situation, there would be a concentration gradient across the

[21] G. Gee, Trans. Faraday Soc. 40, 463 (1944).

cells of the osmometer which would be gradually reduced by slow exchange through the membrane. After this initial quasi-equilibrium is reached, the osmotic pressure will change only slightly. (Mathematical analysis indicates that the further change in π depends only on higher powers of ϕ_3 than the second.) An alternative, and perhaps less probable, hypothesis involves the assumption that the initial quasi-equilibrium is reached by gross flow of the solvent mixture through the membrane until the total free energy per "mole" of the mixed liquids is equal on both sides, followed by subsequent disproportionation through the membrane. In such a hypothesis, the initial quasi-equilibrium is obtained without alternation of the solvent ratio ($\phi_1^0/\phi_2^0=\phi_1/\phi_2$), and we have a "single liquid" approximation. With these assumptions we obtain an osmotic pressure π^*, which we designate by an asterisk to distinguish it from the true equilibrium osmotic pressure:

$$(\pi^* V_0/RT)=\ln(1-\phi_3)+[1-(1/m)]\phi_3 + (\mu_{13}\phi_1^0+\mu_{23}\phi_2^0-\mu_{12}\phi_1^0\phi_2^0)\phi_3^2. \quad (38)$$

Expanding in powers of ϕ_3 for comparison with Eq. (36), we find:[22]

$$\frac{\pi^* V_0}{RT}=\frac{\phi_3}{m} + \frac{1-2\mu_{13}\phi_1^0-2\mu_{23}\phi_2^0+2\mu_{12}\phi_1^0\phi_2^0}{2}\phi_3^2+\cdots. \quad (39)$$

We see that the first terms are identical and equivalent to van't Hoff's Law. The coefficients of the second term, while different, are, in both cases, essentially independent of molecular weight. Thus use of the familiar π/c *vs.* c extrapolation to determine the molecular weight is justified, whether π^* or the true osmotic pressure π is the measured quantity. For convenience we shall denote the coefficients of the second term in (36) and (39), a_2 and a_2^*, respectively, using the same convention as for π and π^*. Hence,

$$a_2=\frac{1-2\mu_{13}\phi_1^0-2\mu_{23}\phi_2^0+Q\phi_1^0\phi_2^0}{2(1-2\mu_{12}\phi_1^0\phi_2^0)}, \quad (40)$$

$$a_2^*=\frac{1-2\mu_{13}\phi_1^0-2\mu_{23}\phi_2^0+2\mu_{12}\phi_1^0\phi_2^0}{2}. \quad (41)$$

Figure 11 shows the variation of a_2 and a_2^* with the composition of the mixed solvent for the conditions of Case I ($\mu_{12}=2.0$, $\mu_{23}=0.25$, $\mu_{13}=2.25$). The differences are marked, and presumably appropriate experimental measurements could determine which represents the initial equilibrium. Measurement of the change in osmotic pressure over longer periods of times than those involved in the usual measurement would also be illuminating.

It should be noted that the numerator of a_2 is identical with (30), which defined the critical solubility limits for polymers of very high molecular weight. We may therefore conclude that at the critical solubility limit the osmotic pressure is zero (or, more accurately, that the second term, $a_2\phi_3^2$, is zero).

ACKNOWLEDGMENTS

The author wishes to thank Professors Joel H. Hildebrand and Bruno H. Zimm for many helpful suggestions and discussions.

APPENDIX I

The Ten Solutions of the Plait Point Equation

We have noted that there are ten possible solutions to the set of simultaneous equations (26) and (27). For $m=\infty$, these may be separated into various classes, as follows:

(1–4) For $m=\infty$ there are two solutions corresponding to the two roots of Eqs. (30) and (31), previously given:

$$1-2\mu_{13}\phi_1-2\mu_{23}\phi_2+Q\phi_1\phi_2=0, \quad (30)$$

$$\phi_3=0. \quad (31)$$

Each of these roots is doubly degenerate, and for finite molecular weights there are four roots. If one expands in powers of $m^{-\frac{1}{2}}$, there are two pairs; within each pair, even powers of $m^{-\frac{1}{2}}$ are identical; odd powers have the same coefficients but opposite signs. One member of each pair corresponds to a negative ϕ_3 (i.e., is outside the diagram) and may be disregarded.

The above roots are imaginary unless the following conditions are satisfied:

$$(Q-2\mu_{12})(Q-4\mu_{13}-4\mu_{23}+2\mu_{12})>0.$$

The conditions under which these solutions are of physical significance have been discussed in detail previously.

For $Q=0$ there are only two roots instead of four (or one at the limit $m=\infty$).

(5,6) Two more limiting solutions to the plait point equations are given by:

$$1-2\mu_{12}\phi_1\phi_2=0, \quad (43)$$

$$\phi_3=0. \quad (44)$$

We may obtain a solution for finite molecular weights by expanding in powers of m^{-1}. In so doing, we must avoid the spurious solutions (referred to in note 15) in which the solutions of Eqs. (43) and (44) are valid for all molecular weights, and all but the leading terms in the ex-

[22] If we apply the condition $V_1=V_2$ to Eq. (18) of Gee's paper,[21] we obtain Eq. (39) rather than Eq. (36), although he did not consciously introduce the single liquid approximation. This anomaly is explained in Appendix II.

pansion vanish. In the true solutions the m^{-1} terms of ϕ_3 vanish, leaving the first non-zero term that in m^{-2}. Equal and opposite terms in m^{-1} exist, however, for ϕ_1 and ϕ_2.

Values of μ_{12} between 0 and +2 give only imaginary solutions to Eqs. (43) and (44). Negative values of μ_{12} give plait points outside the triangular diagram which are without physical meaning. Only for $\mu_{12}>2$ are the plait points given by (43) and (44) of physical significance, and even then they are always inside a triangular three-phase region which they help to define.

(7–10) Four more solutions, for which, in general, ϕ_3 is not zero even in the limit $m=\infty$, correspond to the four possible sets of solutions to the equations:

$$1-2\mu_{13}\phi_1-2\mu_{23}\phi_2+Q\phi_1\phi_2=0, \tag{45}$$

$$(1-2\mu_{13}\phi_1)(1-\phi_1[\mu_{13}+\mu_{12}-\mu_{23}]) +(1-2\mu_{23}\phi_2)(1-\phi_2[\mu_{23}+\mu_{12}-\mu_{13}])=0. \tag{46}$$

One of the four may be expressed explicitly:

$$\phi_1=\frac{1}{\mu_{13}+\mu_{12}-\mu_{23}}, \tag{47a}$$

$$\phi_2=\frac{1}{\mu_{23}+\mu_{12}-\mu_{13}}, \tag{47b}$$

$$\phi_3=1-\frac{2\mu_{12}}{(\mu_{13}+\mu_{12}-\mu_{23})(\mu_{23}+\mu_{12}-\mu_{13})}. \tag{47c}$$

The other three solutions do not simplify except in special cases.

In the particular instance that $Q=0$, we may set $\mu_{12}=(A+B)^2$, $\mu_{13}=A^2$, $\mu_{23}=B^2$. There are six solutions, including one pair which is degenerate at $m=\infty$. We tabulate these solutions here for $m=\infty$:

	ϕ_1	ϕ_2	ϕ_3
1,2	$\frac{1-2B^2}{2(A^2-B^2)}$	$\frac{1-2A^2}{2(B^2-A^2)}$	0
5	$\frac{1+\left(1-\frac{2}{(A+B)^2}\right)^{\frac{1}{2}}}{2}$	$\frac{1-\left(1-\frac{2}{(A+B)^2}\right)^{\frac{1}{2}}}{2}$	0
6	$\frac{1-\left(1-\frac{2}{(A+B)^2}\right)^{\frac{1}{2}}}{2}$	$\frac{1+\left(1-\frac{2}{(A+B)^2}\right)^{\frac{1}{2}}}{2}$	0
7	$\frac{1}{2A(A+B)}$	$\frac{1}{2B(A+B)}$	$1-\frac{1}{2AB}$
8	$\frac{B}{2A^2(A+B)}$	$\frac{A}{2B^2(A+B)}$	$1-\frac{A^2-AB+B^2}{2A^2B^2}$.

APPENDIX II

Expansion of the Osmotic Pressure Equation

Given the thermodynamic equations for the partial molal free energies (Eq. (35ab)), we wish to obtain $\pi V_0/RT$ as a power series in ϕ_3:

$$\ln\phi_1^0+\mu_{12}(\phi_2^0)^2 =\ln\phi_1+\left(1-\frac{1}{m}\right)\phi_3+\mu_{12}\phi_2^2+\mu_{13}\phi_3^2 +(\mu_{12}+\mu_{13}-\mu_{23})\phi_2\phi_3+\frac{\pi V_0}{RT}, \tag{35a}$$

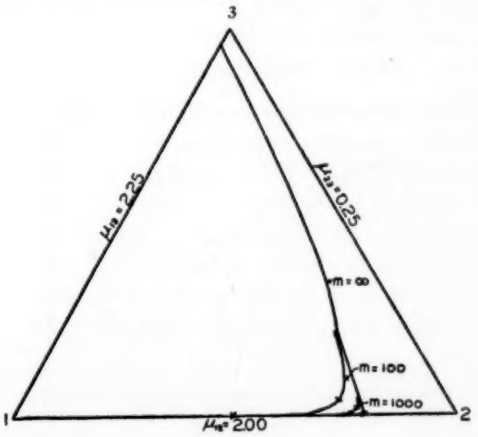

FIG. 10.

$$\ln\phi_2^0+\mu_{12}(\phi_1^0)$$

$$=\ln\phi_2+\left(1-\frac{1}{m}\right)\phi_3+\mu_{12}\phi_1^2+\mu_{23}\phi_3^2$$

$$+(\mu_{12}+\mu_{23}-\mu_{13})\phi_1\phi_3+\frac{\pi V_0}{RT}. \quad (35b)$$

We introduce a variable ϵ to relate the solvent ratios in the two cells, such that

$$\frac{\phi_1}{\phi_1+\phi_2}=\frac{\phi_1}{1-\phi_3}=\phi_1^0+\epsilon, \quad (48a)$$

$$\frac{\phi_2}{\phi_1+\phi_2}=\frac{\phi_2}{1-\phi_3}=\phi_2^0-\epsilon. \quad (48b)$$

We substitute in Eqs. (35ab) for ϕ_1 and ϕ_2, obtaining equations in terms of the variables π, ϕ_1^0, ϕ_2^0, ϕ_3, and ϵ.

$$\frac{\pi V_0}{RT}+\left(1-\frac{1}{m}\right)\phi_3+\ln(1-\phi_3)+\ln\left(1+\frac{\epsilon}{\phi_1^0}\right)$$

$$+\mu_{12}[(\phi_2^0-\epsilon)^2(1-\phi_3)^2-(\phi_2^0)^2]+\mu_{13}\phi_3^2$$

$$+(\mu_{12}+\mu_{13}-\mu_{23})(\phi_2^0-\epsilon)(1-\phi_3)\phi_3=0. \quad (49a)$$

$$\frac{\pi V_0}{RT}+\left(1-\frac{1}{m}\right)\phi_3+\ln(1-\phi_3)+\ln\left(1-\frac{\epsilon}{\phi_2^0}\right)$$

$$+\mu_{12}[(\phi_1^0+\epsilon)^2(1-\phi_3)^2-(\phi_1^0)^2]+\mu_{23}\phi_3^2$$

$$+(\mu_{12}+\mu_{23}-\mu_{13})(\phi_1^0+\epsilon)(1-\phi_3)\phi_3=0. \quad (49b)$$

We wish to eliminate ϵ and obtain π as a function of ϕ_1^0, ϕ_2^0, and ϕ_3. Anticipating that ϵ is proportional to ϕ_3 (and higher powers), as will later be shown, we expand Eqs. (49ab) in powers of ϕ_3 and ϵ, dropping powers higher than ϕ_3^2, $\phi_3\epsilon$, or ϵ^2:

$$\frac{\pi V_0}{RT}+\phi_3\left[(\mu_{12}+\mu_{13}-\mu_{23})\phi_2^0-2\mu_{12}(\phi_2^0)^2-\frac{1}{m}\right]$$

$$+\epsilon\left[\frac{1}{\phi_1^0}-2\mu_{12}\phi_2^0\right]+\phi_3^2[\mu_{13}\phi_1^0+\mu_{23}\phi_2^0$$

$$-\mu_{12}\phi_1^0\phi_2^0-\tfrac{1}{2}]+\phi_3\epsilon[4\mu_{12}\phi_2^0-(\mu_{12}+\mu_{13}-\mu_{23})]$$

$$+\epsilon^2\left[-\frac{1}{2(\phi_1^0)^2}+\mu_{12}\right]+\cdots=0. \quad (50a)$$

$$\frac{\pi V_0}{RT}+\phi_3\left[(\mu_{12}+\mu_{23}-\mu_{13})\phi_1^0-2\mu_{12}(\phi_1^0)^2-\frac{1}{m}\right]$$

$$-\epsilon\left[\frac{1}{\phi_2^0}-2\mu_{12}\phi_1^0\right]+\phi_3^2[\mu_{13}\phi_1^0+\mu_{23}\phi_2^0$$

$$-\mu_{12}\phi_1^0\phi_2^0-\tfrac{1}{2}]-\phi_3\epsilon[4\mu_{12}\phi_1^0-(\mu_{12}+\mu_{23}-\mu_{13})]$$

$$+\epsilon^2\left[-\frac{1}{2(\phi_2^0)^2}+\mu_{12}\right]+\cdots=0. \quad (50b)$$

If we multiply Eq. (50a) by ϕ_1^0, Eq. (50b) by ϕ_2^0, and add, we eliminate the term in ϵ:

$$\frac{\pi V_0}{RT}-\frac{\phi_3}{m}+\phi_3^2[\mu_{13}\phi_1^0+\mu_{23}\phi_2^0-\mu_{12}\phi_1^0\phi_2^0-\tfrac{1}{2}]$$

$$-\phi_3\epsilon[\mu_{13}-\mu_{23}+\mu_{12}(\phi_1^0-\phi_2^0)]$$

$$+\epsilon^2\left[\mu_{12}-\frac{1}{2\phi_1^0\phi_2^0}\right]+\cdots=0. \quad (51)$$

Alternatively, we substract Eq. (50b) from Eq. (50a), eliminating π:

$$\phi_3[\mu_{13}-\mu_{23}+\mu_{12}(\phi_1^0-\phi_2^0)]$$

$$+\epsilon\left[\frac{1}{\phi_1^0\phi_2^0}-2\mu_{12}\right]+\phi_3\epsilon[2\mu_{12}]$$

$$+\epsilon^2\left[\frac{\phi_1^0-\phi_2^0}{2(\phi_1^0)^2(\phi_2^0)^2}\right]+\cdots=0, \quad (52)$$

or

$$\epsilon=-\phi_3\frac{[\mu_{13}-\mu_{23}+\mu_{12}(\phi_1^0-\phi_2^0)]\phi_1^0\phi_2^0}{1-2\mu_{12}\phi_1^0\phi_2^0}+\cdots. \quad (53)$$

Since ϵ occurs only in square terms in Eq. (51), we need only use the first term of the expansion in Eq. (53). Substituting for ϵ in Eq. (51), we obtain the desired equation:

$$\frac{V_0}{RT}=\frac{\phi_3}{m}$$

$$+\frac{1-2\mu_{13}\phi_1^0-2\mu_{23}\phi_2^0+Q\phi_1^0\phi_2^0}{2(1-2\mu_{12}\phi_1^0\phi_2^0)}\phi_3^2+\cdots. \quad (36)$$

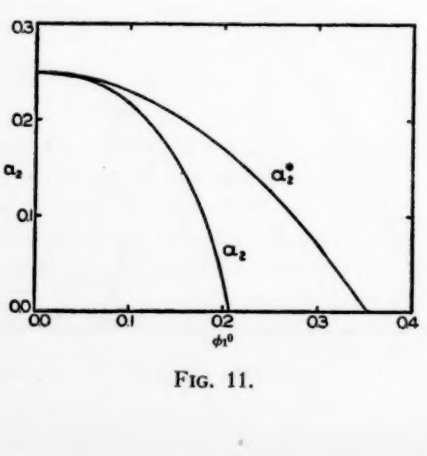

FIG. 11.

We may obtain ϕ_1, ϕ_2 and the ratio ϕ_1/ϕ_2 as functions of ϕ_1^0, ϕ_2^0, and ϕ_3:

$$\phi_1=(\phi_1^0+\epsilon)(1-\phi_3)=\phi_1^0 - \phi_3\left[\phi_1^0+\frac{\mu_{13}-\mu_{23}+\mu_{12}(\phi_1^0-\phi_2^0)}{1-2\mu_{12}\phi_1^0\phi_2^0}\right]+\cdots. \quad (54a)$$

$$\phi_2=(\phi_2^0-\epsilon)(1-\phi_3)=\phi_2^0 - \phi_3\left[\phi_2^0+\frac{\mu_{23}-\mu_{13}+\mu_{12}(\phi_2^0-\phi_1^0)}{1-2\mu_{12}\phi_1^0\phi_2^0}\right]+\cdots. \quad (54b)$$

$$\frac{\phi_1}{\phi_2}=\frac{\phi_1^0+\epsilon}{\phi_2^0-\epsilon}=\frac{\phi_1^0}{\phi_2^0} \times\left(1-\phi_3\frac{[\mu_{13}-\mu_{23}+\mu_{12}(\phi_1^0-\phi_2^0)]}{(1-2\mu_{12}\phi_1^0\phi_2^0)}+\cdots\right). \quad (37)$$

We have noted that Gee,[21] although starting with equations entirely equivalent to our Eq. (35ab) did not obtain an equation equivalent to our Eq. (39), but rather a single liquid approximation equivalent to our Eq. (36).

This discrepancy is apparently due to the introduction of a variable r (analogous to our ϵ), and in the subsequent expansion retaining no powers of r higher than the first. This is tantamount to dropping the $\phi_3\epsilon$ and ϵ^2 terms from Eq. (51). But since $\epsilon\sim\phi_3$, there is no justification for dropping these terms unless the ϕ_3^2 term is dropped also. If one solves Gee's Eq. (14), retaining terms in r^2, one obtains an equation entirely equivalent to our Eq. (36), if $V_1=V_2$ (i.e., setting Gee's variable $l=1$).

Gee's treatment of solubility [19] depends upon his assumption that the ϕ_3^2 term in π vanishes at the critical solubility limit (an assumption which we have proved to be correct). Since he inadvertently calculated a_2^*, rather than a_2, his results, while in qualitative agreement with ours, are not exactly equivalent, to the extent that $a_2^*\neq a_2$.

THE JOURNAL OF CHEMICAL PHYSICS VOLUME 17, NUMBER 3 MARCH, 1949

The Thermodynamics of High Polymer Solutions. V. Phase Equilibria in the Ternary System: Polymer 1—Polymer 2—Solvent*

ROBERT L. SCOTT‡
Department of Chemistry, University of California, Berkeley, California

(Received July 12, 1948)

A thermodynamic analysis of phase equilibria similar to that developed in Part IV when applied to the ternary system of two polymers and a solvent leads to an explanation of the usual incompatibility of different high polymers in solution. Unless their heat of mixing is virtually zero or negative, two high polymers are always immiscible in the absence of a solvent; the primary role of the solvent is non-specific, merely one of diluting the polymer mixture and decreasing the heat of interaction of the polymers. The recent experiments of Dobry and Boyer-Kawenoki show reasonable agreement with these theoretical conclusions. Osmotic pressures of mixed polymers are discussed; such measurements would permit determination of μ_{12}, the interaction constant of the two polymers.

INTRODUCTION

THE incompatibility of certain high polymers in solution is a phenomenon long familiar to polymer chemists, especially in the fields of paints and varnishes. Recently, Dobry and Boyer-Kawenoki[1] have examined phase separation for a large number of three-component systems, and find incompatibility of two polymers in the same solvent to be the normal situation. The application of thermodynamic analysis to the ternary systems involving one polymer and two liquids[2] suggests the extension of such a treatment to the corresponding system of two polymers and one solvent.

THE TWO POLYMER SYSTEM

First let us consider a mixture of two chain polymers in the absence of a solvent. (We ignore the mechanical problems involved and assume that equilibrium is reached somehow.) Flory,[3] Scott and Magat,[4] and Guggenheim[5] have derived expressions for the free energy of mixtures of polymers of different molecular weight. The equations of Flory and of Scott and Magat, although based

* The following research was done on a Frank B. Jewett Fellowship granted by the Bell Telephone Laboratories and first presented to the High Polymer Forum at the 111th meeting of the American Chemical Society at Atlantic City, New Jersey, April 14, 1947.

‡ Present address: Department of Chemistry, University of California, Los Angeles 24, California.

[1] A. Dobry and F. Boyer-Kawenoki, J. Polymer Sci. 2, 90 (1947).

[2] R. L. Scott, J. Chem. Phys. 17, 268 (1949).

[3] P. J. Flory, J. Chem. Phys. 12, 425 (1944).

[4] R. L. Scott and M. Magat, J. Chem. Phys. 13, 172 (1945) (Article I of this series).

[5] E. A. Guggenheim, Proc. Royal Soc. A183, 203, 213 (1944).

upon somewhat different assumptions, are in this particular case identical; to them we add a term for the heat of mixing of the two different polymers:

$$\Delta\bar{F}_1 = RT\left[\ln\phi_1 + \left(1-\frac{m_1}{m_2}\right)\phi_2 + m_1\mu_{12}\phi_2^2\right], \quad (1a)$$

$$\Delta\bar{F}_2 = RT\left[\ln\phi_2 + \left(1-\frac{m_2}{m_1}\right)\phi_1 + m_2\mu_{12}\phi_1^2\right], \quad (1b)$$

where ϕ_1 and ϕ_2 are volume fractions, and m_1 and m_2 are essentially degrees of polymerization, relating the molal volumes V_1 and V_2 of the polymers to a fictitious molal volume V_0 of one submolecule of polymer.

$$m_1 = V_1/V_0, \quad m_2 = V_2/V_0.$$

μ_{12} is a constant related to the heat of interaction of submolecules of the two polymers.

The introduction of the m's in terms of an arbitrary V_0 is unnecessary here, but will prove desirable later when we identify V_0 with the molal volume of the solvent in the three-component system. The constant μ_{12} is in this case entirely due to the heat interaction. The contribution of an entropy term, μ^s, while usually considerable, is for two long chains entirely negligible.

For long chains, and small values of μ_{12}, the more complex equations of Guggenheim[5] reduce to Eqs. (1a) and (1b).

We may obtain the critical conditions by the familiar requirement that the first and second derivatives of either $\Delta\bar{F}_1$ or $\Delta\bar{F}_2$ be zero. Solving such equations, we find that when the two polymers are at their critical solution temperatures:

$$(\mu_{12})_c = \tfrac{1}{2}\{(1/(m_1)^{\frac{1}{2}}) + (1/(m_2)^{\frac{1}{2}})\}^2, \quad (2)$$

$$(\phi_1)_c = (m_2)^{\frac{1}{2}}/\{(m_1)^{\frac{1}{2}} + (m_2)^{\frac{1}{2}}\}, \quad (3)$$

$$(\phi_2)_c = (m_1)^{\frac{1}{2}}/\{(m_1)^{\frac{1}{2}} + (m_2)^{\frac{1}{2}}\}. \quad (4)$$

In the "critical phase," the low molecular weight material predominates. For $m_1 = 1$, these equations reduce to the familiar ones for a polymer-solvent system[6-8] (in this case, however, μ_{12} includes a significant entropy term).

We see that for two polymers, both of high molecular weight, the critical value of μ_{12} is several orders of magnitude smaller than that for two normal liquids ($\mu_{12} = 2$) or for a polymer-solvent system ($\mu_{12} = \frac{1}{2}$). Polymers of infinite molecular weight would be incompatible if there were any positive heat of mixing (per submolecule) at all.

[6] M. L. Huggins, J. Chem. Phys. 9, 440 (1941); Ann. N. Y. Acad. Sci. 43, 1 (1942).
[7] P. J. Flory, J. Chem. Phys. 9, 660 (1941); 10, 51 (1942).
[8] R. L. Scott, J. Chem. Phys. 13, 178 (1945) (Article II of this series).

TWO POLYMERS—ONE SOLVENT

We may now proceed to consideration of the ternary system of two polymers and one solvent. For the partial molal free energies of the polymers (subscripts 1 and 2) and the solvent (subscript 0), we write:

$$\Delta\bar{F}_0 = RT[\ln\phi_0 + (1-(1/m_1))\phi_1 + (1-(1/m_2))\phi_2 + \mu_{10}\phi_1^2 + \mu_{20}\phi_2^2 + (\mu_{10}+\mu_{20}-\mu_{12})\phi_1\phi_2], \quad (5a)$$

$$\Delta\bar{F}_1 = RT[\ln\phi_1 + (1-m_1)\phi_0 + (1-(m_1/m_2))\phi_2 + m_1\{\mu_{10}\phi_0^2 + \mu_{12}\phi_2^2 + (\mu_{10}+\mu_{12}-\mu_{20})\phi_0\phi_2\}], \quad (5b)$$

$$\Delta\bar{F}_2 = RT[\ln\phi_2 + (1-m_2)\phi_0 + (1-(m_2/m_1))\phi_1 + m_2\{\mu_{20}\phi_0^2 + \mu_{12}\phi_1^2 + (\mu_{20}+\mu_{12}-\mu_{10})\phi_0\phi_1\}], \quad (5c)$$

where μ_{10} = the interaction constant for the binary system polymer 1—solvent.
μ_{20} = the interaction constant for the binary system polymer 2—solvent.
μ_{12} = the interaction constant for the binary system polymer 1—polymer 2.

μ_{12}, as noted for the two polymer system, is entirely a heat contribution, but μ_{10} and μ_{20} will have sizable contributions from entropy terms μ^s, as is normal for polymer-solvent systems.

If two phases exist at equilibrium, the free energies of each component must be the same in both phases. Denoting the two phases by single and double primes, we may write:

$$\Delta\bar{F}_0' = \Delta\bar{F}_0'', \quad (6a)$$

$$\Delta\bar{F}_1' = \Delta\bar{F}_1'', \quad (6b)$$

$$\Delta\bar{F}_2' = \Delta\bar{F}_2''. \quad (6c)$$

Normally these equations will be soluble only by long and tedious successive approximation methods. Fortunately, we shall be able to obtain useful qualitative results without such labor.

THE SPECIAL SYMMETRICAL CASE

For the special case in which $\mu_{10} = \mu_{20} = \mu$, $m_1 = m_2 = m$, the equations become symmetrical, and we may calculate a phase diagram without difficulty. Substituting the above conditions into Eqs. (5abc) and making the necessary substitutions into Eqs. (6abc), we obtain:

$$\ln\phi_0' + (1-(1/m))(1-\phi_0') + \mu(1-\phi_0')^2 - \mu_{12}\phi_1'\phi_2' = \ln\phi_0'' + (1-(1/m))(1-\phi_0'') + \mu(1-\phi_0'')^2 - \mu_{12}\phi_1''\phi_2'', \quad (7a)$$

$$\ln\phi_1' + (1-m)\phi_0' + m\{\mu(\phi_0')^2 + \mu_{12}(\phi_2')^2 + \mu_{12}\phi_0'\phi_2'\} = \ln\phi_1'' + (1-m)\phi_0'' + m\{\mu(\phi_0'')^2 + \mu_{12}(\phi_2'')^2 + \mu_{12}\phi_0''\phi_2''\}, \quad (7b)$$

$$\ln\phi_2' + (1-m)\phi_0' + m\{\mu(\phi_0')^2 + \mu_{12}(\phi_1')^2 + \mu_{12}\phi_0'\phi_1'\} = \ln\phi_2'' + (1-m)\phi_0'' + m\{\mu(\phi_0'')^2 + \mu_{12}(\phi_1'')^2 + \mu_{12}\phi_0''\phi_1''\}. \quad (7c)$$

A solution of these equations will be

$$\phi_0' = \phi_0'', \tag{8}$$

$$\phi_1' = \phi_2'', \tag{9a}$$

$$\phi_1'' = \phi_2'. \tag{9b}$$

Substituting these conditions into Eq. (7b), we obtain

$$\ln\phi_1' + m\mu_{12}\phi_2' = \ln\phi_2' + m\mu_{12}\phi_1'. \tag{10}$$

The identical equation is obtained from (7c), of course. Equation (10) is easily solved, but the nature of the solution will be clearer if we make a further substitution, defining a new variable θ, corresponding to the relative concentrations of the two polymers:

$$\theta_1' = \phi_1'/(\phi_1' + \phi_2') = \phi_1'/(1-\phi_0), \tag{11a}$$

$$\theta_2' = \phi_2'/(\phi_1' + \phi_2') = \phi_2'/(1-\phi_0) = 1-\theta_1'. \tag{11b}$$

Transforming Eq. (10) into the new variables, we find:

$$\ln\theta_1' + m\mu_{12}(1-\phi_0)(\theta_2')^2 = \ln\theta_2' + m\mu_{12}(1-\phi_0)(\theta_1')^2. \tag{12}$$

This is entirely equivalent to the solution of a binary system of two molecules of equal size.[9] We see, therefore, that the function of the solvent is merely that of diminishing the value of the heat constant μ_{12}. The tie lines of the ternary system are all parallel to the 1,2 axis, and we may regard each cross section as a binary system for which the constant is $m\mu_{12}(1-\phi_0)$. We may obtain the plait point by applying the familiar critical conditions for symmetrical binary systems.

$$m\mu_{12}(1-\phi_0) = 2, \tag{13}$$

$$\theta_1 = \theta_2 = \tfrac{1}{2}, \tag{14}$$

or, rearranging,

$$\phi_0 = 1-(2/m\mu_{12}), \tag{15}$$

$$\phi_1 = \phi_2 = 1/m\mu_{12}. \tag{16}$$

The striking feature of this calculation is that the position of the phase boundary is independent of the value of μ, the polymer-solvent interaction.[10] Figure 1 shows phase diagrams calculated for $m\mu_{12}=4$, 8, and 20. For an m of 1000 (molecular weight of polymer about 100,000), these would mean μ_{12}'s of 0.004, 0.008, and 0.02, very small indeed compared with normal heat interactions. We see, therefore, that for large molecular weight polymers, incompatibility should be the rule rather than the exception. Only when the two polymers are so nearly alike in chemical nature that μ_{12} is vanishingly small will they be compatible.

PLAIT POINTS

For the general case, no exact analytical solution is possible. Each individual system must be calculated after substituting particular values of the parameters, μ_{10}, μ_{20}, μ_{12}, m_1, and m_2. We may attempt to determine the plait point of the ternary system by the methods outlined in the preceding paper,[2] but even here we must approximate. Fortunately, a good approximation is available. If $|\mu_{10}-\mu_{20}| \ll 1$, and $m_1^{\frac{1}{2}} < m_2 < m_1^2$, as will usually be the case,[11] we may write:

$$\phi_0 \cong 1-(1/2\mu_{12})\{(1/m_1)^{\frac{1}{2}}+(1/m_2)^{\frac{1}{2}}\}^2, \tag{17a}$$

$$\phi_1 \cong (1/2\mu_{12})(m_2)^{\frac{1}{2}}/\{(m_1)^{\frac{1}{2}}+(m_2)^{\frac{1}{2}}\} \times\{(1/m_1)^{\frac{1}{2}}+(1/m_2)^{\frac{1}{2}}\}^2, \tag{17b}$$

$$\phi_2 \cong (1/2\mu_{12})(m_1)^{\frac{1}{2}}/\{(m_1)^{\frac{1}{2}}+(m_2)^{\frac{1}{2}}\} \times\{(1/m_1)^{\frac{1}{2}}+(1/m_2)^{\frac{1}{2}}\}^2, \tag{17c}$$

The tie lines are still nearly parallel to the 1–2 axis, and any dependence on the values of μ_{10} and μ_{20} shows up only in the higher terms of the approximation. For purposes of comparison, we transform Eq. (17abc) as follows:

$$\mu_{12} = \tfrac{1}{2}\{(1/m_1)^{\frac{1}{2}}+(1/m_2)^{\frac{1}{2}}\}^2\{1/(1-\phi_0)\}, \tag{18}$$

$$\theta_1 = (m_1)^{\frac{1}{2}}/\{(m_1)^{\frac{1}{2}}+(m_2)^{\frac{1}{2}}\}, \tag{19}$$

$$\theta_2 = (m_2)^{\frac{1}{2}}/\{(m_1)^{\frac{1}{2}}+(m_2)^{\frac{1}{2}}\}, \tag{20}$$

Comparison of Eqs. (18)–(20) with Eqs. (2)–(4) reveals a striking similarity. Here, as in the special symmetrical case, we conclude that the main contribution of the solvent is purely that of lowering

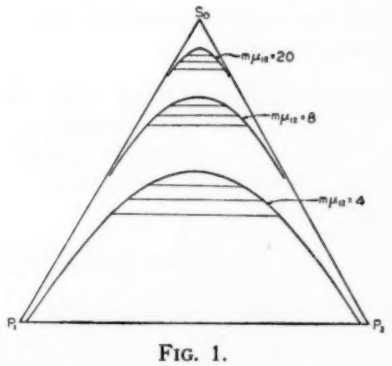

FIG. 1.

[9] See, for example, J. H. Hildebrand, *Solubility of Non-Electrolytes* (Reinhold Publishing Corporation, New York, 1936), second edition, pp. 51–54, 144–152.

[10] For values of μ large enough so that the polymers are immiscible with the liquid, this is, of course, not exactly true, since there are tie lines along the 1–0 and 2–0 axes. However, we confine ourselves here to the case where the liquid is a solvent for both polymers.

[11] The significance of these conditions is as follows: The entropy contribution, μ_s, to the polymer-solvent μ's is about 0.3, while if we required the liquid to be a solvent for both polymers, the μ's cannot exceed about 0.5; hence the maximum value for $|\mu_{10}-\mu_{20}|$ will be around 0.2, which is very much smaller than 1. The second condition is essentially that the polymer of shorter length be more like the other polymer in size than like the solvent.

the critical solution temperature by dilution; the exact nature of the solvent is of only secondary importance.

It remains to show the magnitude of the incompatibility. For many non-polar systems we may write:

$$\mu_{12} = V_0/RT(\delta_1-\delta_2)^2, \quad (21)$$

where V_0 is the molecular volume of the solvent, and the δ's are the square roots of the internal pressures or "cohesive energy densities" of polymers 1 and 2.

If we assume $V_0=100$ cc, $T=300°$K, $\Delta\delta=0.2$, $m_1=m_2=10{,}000$ (molecular weight about 1,000,000), then $\mu_{12}=0.0067$, and we find for the plait point:

$$\phi_1=\phi_2=0.015, \quad \phi_0=0.97.$$

Phase separation in such a case sets in at 3 percent total polymer; for molecular weights around 100,000, phase separation would occur around 30 percent total polymer.

A δ-difference of 0.2 is small (about the difference between benzene and toluene or between hexane and octane), and most polymer pairs, unless they are very similar in chemical composition, will exhibit much larger μ_{12}'s and correspondingly greater incompatibility than the case calculated above. Hence, it is not surprising that most polymer pairs are very incompatible even if the solvent is a "good" solvent for both.

THE DILUTION APPROXIMATION

The discovery that the main effect of the solvent is merely to dilute the polymer mixture, and in so doing decrease the heat interaction, encourages us to make an attempt to calculate the phase diagram by what we might call the "dilution approximation." We assume that the volume fraction of solvent ϕ_0 is the same in both conjugate phases, and that we may write by analogy to Eq. (12) for the symmetrical case:

$$\ln\theta_1'+(1-(m_1/m_2))\theta_2'+m_1\mu_{12}(1-\phi_0)(\theta_2')^2 = \ln\theta_1''+(1-(m_1/m_2))\theta_2''+m_1\mu_{12}(1-\phi_0)(\theta_2'')^2, \quad (22a)$$

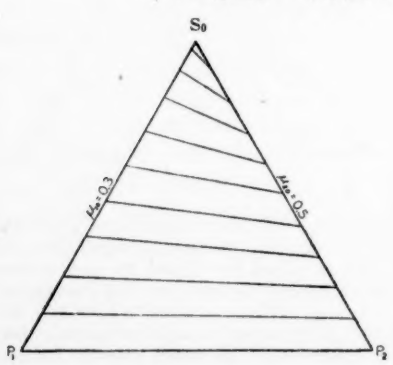

FIG. 2.

$$\ln\theta_2'+(1-(m_2/m_1))\theta_1'+m_2\mu_{12}(1-\phi_0)(\theta_1')^2 = \ln\theta_2''+(1-(m_2/m_1))\theta_1''+m_2\mu_{12}(1-\phi_0)(\theta_1'')^2. \quad (22b)$$

The problem essentially reduces, therefore, to a binary system of two polymers such as discussed in the first section, which is relatively easy to determine.[12] The tie lines of the ternary system are all parallel to the 1,2 axis, and each represents a binary system for which $\mu=\mu_{12}(1-\phi_0)$. As in the binary system, we expect displacement of the plait point and the whole solubility curve in the direction of the low molecular weight polymer (see Fig. 3).

THE COMPLETE IMMISCIBILITY APPROXIMATION

We may obtain another approximate idea of the phase diagram by the approximation of complete immiscibility introduced in the preceding article.[2] If we assume that one phase consists solely of solvent and polymer 1, and the other solely of solvent and polymer 2, we may equate the free energy of the solvent in the two phases:

$$\ln\phi_0'+(1-(1/m_1))(1-\phi_0')+\mu_{10}(1-\phi_0')^2 = \ln\phi_0''+(1-(1/m_2))(1-\phi_0'')+\mu_{20}(1-\phi_0'')^2. \quad (23)$$

For given values of the constants m_1, m_2, μ_{10} and μ_{20}, we can calculate conjugate values of ϕ_0' and ϕ_0''. Obviously this approximation is correct only when μ_{12} is very large, and it will be more nearly correct in those regions where the incompatibility of the polymers is largest,—i.e., at high polymer concentrations. Figure 2 shows such a diagram for the extreme case $m_1=100$; $\mu_{10}=0.3$; $m_2=10{,}000$; $\mu_{20}=0.5$. If we assume, in addition, $\mu_{12}=0.2$, the approximate equations (17abc) yield a plait point at $\phi_0\cong0.96975$, $\phi_1\cong0.0275$, $\phi_2\cong0.00275$. Shown in Fig. 3 is the dilution approximation for the same conditions (coordinates in volume percent —only upper part of diagram shown). The true diagram will lie somewhere between these extremes.

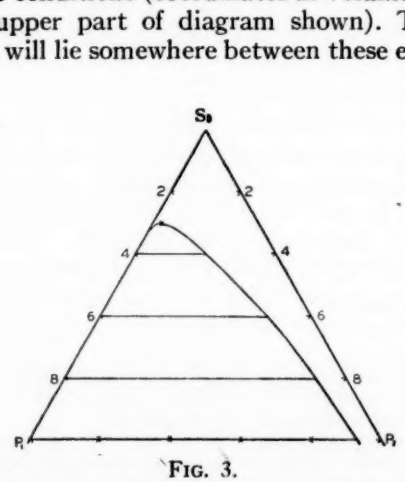

FIG. 3.

[12] It should be pointed out that Eqs. (22a) and (22b) are formally equivalent to a polymer-solvent system, as well.

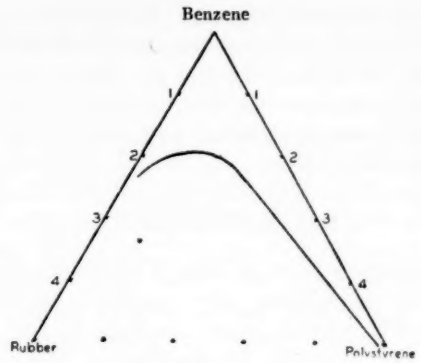

FIG. 4.
Coordinates in weight percent

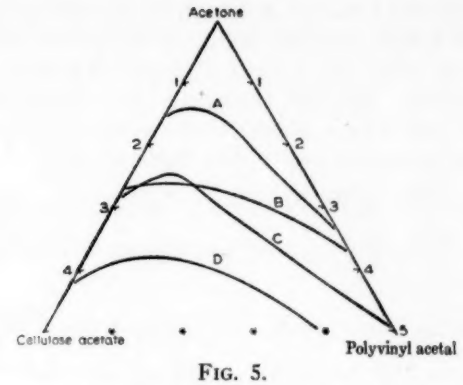

FIG. 5.
Coordinates in weight percent

COMPARISON WITH EXPERIMENT

Let us now examine the experimental data of Dobry and Boyer-Kawenoki[1] in the light of the preceding theory. Their conclusions may be summarized as follows:

(a) Of the 35 pairs of high polymers tested, only three or four (nitrocellulose-polyvinyl acetate, nitrocellulose-polymethyl methacrylate benzylcellulose and polystyrene, and perhaps nitrocellulose-cellulose acetate in acetic acid) do not show separation. In view of the stringent limits on μ_{12}, this is hardly surprising. With two polar polymers, of course, a negative μ_{12} is not excluded. Unfortunately, the only system investigated for which all three components were completely non-polar is the system polystyrene-rubber-benzene shown in Fig. 4.

(b) When two high polymers are incompatible in one solvent, they are generally incompatible in all other solvents. This is in agreement with our conclusion that the primary dependence is upon the molecular weights and the interaction constant μ_{12} of the two polymers, the exact nature of the solvent being only of secondary importance. The limit of phase separation appears to vary somewhat, the plait points in acetic acid, mesityl oxide, and dioxane being greater than for the others; this departure from the theoretical expectation may perhaps be attributed to specific interactions of the polar molecules.

(c) The molecular weight of the polymers is of great importance; the higher it is, the greater is the incompatibility. Figure 5 shows this effect for two fractions of cellulose acetate ($M=16{,}000$ and 56,000) and two fractions of polyvinyl acetal ($M=39{,}000$ and 97,000). In addition to the greater incompatibility with higher molecular weights, the theory predicts a displacement toward the lower molecular weight material (the cellulose acetate), the greatest asymmetry occurring for the 97,000–16,000 pair. All these qualitative conclusions are confirmed by Fig. 5.

(d) There is no obvious relationship between the compatibility of two polymers and the chemical nature of their monomers. The explanation probably rests upon a satisfactory treatment of the thermodynamics of polar solutions. Measurement of the heat of mixing of the corresponding monomer pairs would be instructive.

Unfortunately, only a few tie-lines were obtained, and no plait points. From theory one deduces that the plait points are close to the limits of phase separation (maximum ϕ_0), but experimental confirmation is lacking.

OSMOTIC PRESSURES WITH POLYMER MIXTURES

The problem of osmotic pressures with two polymers and one solvent is not the complicated one which we have encountered in the case of mixed solvent,[2] since only one component is diffusible. We may obtain the osmotic pressure of a solution of mixed polymers directly from Eq. (5a):

$$\pi V_0 = -\Delta\bar{F}_0 = -RT[\ln\phi_0+(1-(1/m_1))\phi_1 +(1-(1/m_2))\phi_2+\mu_{10}\phi_1^2+\mu_{20}\phi_2^2 +(\mu_{10}+\mu_{20}-\mu_{12})\phi_1\phi_2]. \quad (24)$$

With the use of the variables θ_1 and θ_2, we may transform Eq. (24):

$$\pi = -(RT/V_0)[\ln\phi_0+(1-(1/\bar{m}_n))(1-\phi_0) +\mu^*(1-\phi_0)^2], \quad (25)$$

where $\bar{m}_n$ is the number average m:

$$1/\bar{m}_n = (\theta_1/m_1)+(\theta_2/m_2), \quad (26)$$

and

$$\mu^* = \mu_{10}\theta_1+\mu_{20}\theta_2-\mu_{12}\theta_1\theta_2. \quad (27)$$

If we define a volume fraction of total polymer $\phi_p=\phi_1+\phi_2$, and expand Eq. (25) in powers of ϕ_p, we obtain

$$\pi = +(RT/V_0)[(\phi_p/\bar{m}_n)+(\tfrac{1}{2}-\mu^*)\phi_p^2+\cdots]. \quad (28)$$

This is the familiar equation for the osmotic pressure of a high polymer solution except for the substitution of $\bar{m}_n$ for m and μ^* for μ. We may transform from volume fractions to concentrations (grams per cc) by noting that $c=\phi\rho$ where ρ is the density in grams per cc. We then obtain:

$$\pi=RT[(c_p/\bar{M}_n)+(\tfrac{1}{2}-\mu^*/V_0\bar{\rho}^2)c_p^2+\cdots], \quad (29)$$

where $\bar{M}_n$ is the number average molecular weight, defined as

$$(c_p/\bar{M}_n)=(c_1+c_2/\bar{M}_n)=(c_1/M_1)+(c_2/M_2), \quad (30)$$

and $\bar{\rho}$ is the harmonic mean of the densities if expressed as a function of concentration, or the arithmetic mean taken as volume fractions:

$$\bar{\rho}=c_1+c_2/(c_1/\rho_1)+(c_2/\rho_2)=\phi_1\rho_1+\phi_2\rho_2/\phi_1+\phi_2 =\theta_1\rho_1+\theta_2\rho_2. \quad (31)$$

By the usual technique of plotting π/c against c, we may use the slope of the line to determine the coefficient of c^2 and, hence, μ^*. Since μ_{10} and μ_{20} are known, we can use the variation of μ^* with θ (Eq. (27)) to determine μ_{12}, which cannot be determined directly.

ACKNOWLEDGMENTS

The author wishes to thank Professor Bruno H. Zimm for suggesting the problem to him and Professor Hermann Mark, Editor of the Journal of Polymer Science, for supplying him with the proof of the Dobry and Boyer-Kawenoki article in advance of publication. In addition, the author acknowledges many helpful suggestions from and discussions with Professor Zimm and Professor Joel H. Hildebrand.

THE JOURNAL OF CHEMICAL PHYSICS VOLUME 17, NUMBER 3 MARCH, 1949

The Kinetics of the Thermal Decomposition of Propylene

M. SZWARC
Department of Chemistry, The University of Manchester, Manchester, England
(Received August 5, 1948)

The thermal decomposition of propylene was investigated for temperatures ranging from 680°C up to 870°C and with percentages of decomposition from 0.01 percent up to about 2 percent. The reaction was shown to be a homogenous gas reaction of the first order, the first-order constant being given by an expression $1.1\cdot10^{13}\exp-(72{,}000/RT)$. Two mechanisms are discussed, both of which account for the observed kinetics and products of decomposition. It is demonstrated that the first step in the thermal decomposition of propylene is the splitting of the C—H bond leading to the formation of H atoms and allyl radicals. The problem of the value of D(C—H) in propylene is discussed in the light of the two suggested mechanisms. An attempt is made to account for the variety of the reactions between H atoms and propylene molecules as observed by various investigators.

ALTHOUGH several investigations of the pyrolysis of propylene have been carried out within the last twenty years, we still lack a full understanding of the mechanism of this process. In particular, the first steps of this decomposition are not definitely known, and the present research was an attempt to clarify this problem. We shall start with a brief summary of the results obtained by previous investigations, confining our discussion to those processes which are homogenous gas reactions.*

Frey and Smith[1] studied the decomposition of propylene in a silica vessel at 575°C and atmospheric pressure, using a flow method and a time of contact of 1–4 minutes. They found that this process was a homogenous gas reaction. Analysis of the gases showed CH_4 and C_2H_4 to be the main products of the decomposition, in addition to smaller quantities of H_2, C_2H_6, and higher hydrocarbons. Assuming that the C_2H_6 resulted from the hydrogenation of a part of the originally formed C_2H_4, we find from the data of these authors that the CH_4/C_2H_4 ratio is 1:1 ($CH_4=10.7$ percent, $C_2H_4=8.0$ percent, and $C_2H_6=1.9$ percent). This is the ratio which we might expect on the basis of the mechanism suggested later in the discussion of our results. Assuming also that the hydrogenation of C_2H_4 to C_2H_6 and C_3H_6 to C_3H_8** consumed a part of the H_2 originally formed, we find the CH_4/total H_2 ratio as 2:1. This is the CH_4/H_2 ratio found in the present research.

Kinetic studies of the thermal decomposition of propylene were provided by Hurd and Meinert,[2] who investigated this reaction between 600°C and 700°C under atmospheric pressure in a flow system.

* A review of the earlier literature is given by G. Egloff and E. Wilson, Ind. Eng. Chem. **27**, 917 (1935).

[1] F. E. Frey and D. F. Smith, Ind. Eng. Chem. **20**, 948 (1928).

** Frey and Smith found, indeed, that under their experimental conditions the hydrogenation of C_2H_4 and C_3H_6 by H_2 occurs easily.

[2] C. D. Hurd and R. N. Meinert, J. Am. Chem. Soc. **52**, 4978 (1930).

They stated that the decomposition in a silica or Pyrex vessel was a homogenous, first-order gas reaction (proved by packing the reaction vessel and by diluting the propylene with nitrogen). They reported CH_4, C_2H_4, and H_2 to be the main products of the pyrolysis. The composition of the gases was changed only slightly by varying the temperature or time of contact. The CH_4/C_2H_4 ratio was 1:1 in agreement with the above-mentioned interpretation of Frey and Smith's results. In addition to gaseous products, they isolated liquid products of an aromatic character, resulting probably from the polymerization favored by the high pressure of propylene (the dilution of propylene by N_2 decreased the amount of these liquid products). Neither allene, nor products of its polymerization, were found in the pyrolyzed material. This point, which is in a sharp contradiction to our present finding, deserves special consideration, and we shall return to it later in the discussion.

The third work which should be mentioned is that of Tropsch, Parrish, and Egloff.[3] These authors used an extremely short time of contact (about 0.001 sec.), but unfortunately they chose such a high temperature of pyrolysis (1100°C–1400°C), that all the propylene was decomposed. Therefore, it is impossible to draw any conclusion about the mechanism of decomposition from their data.

EXPERIMENTAL

Apparatus and Technique

The apparatus and the technique were essentially the same as used previously for the pyrolytical studies of toluene and the xylenes.[4] The propylene was kept in a 25-l storage flask, and was introduced into a silica reaction vessel through a needle valve and a capillary. Adjustment of the needle valve made it possible to vary the pressure of propylene in the reaction vessel. The quantity of propylene passed into the reaction vessel was measured by the pressure drop in the storage flask. The pyrolyzed gas passed through a *U*-shaped trap, cooled to −80°C, and then through a large trap cooled by liquid air. Here all the undecomposed propylene was frozen out (as well as any other products of the decomposition, except CH_4 and H_2). The H_2 and CH_4 formed during the pyrolysis were continuously pumped out by a system of two mercury pumps into 1.5-l storage vessel as described in the previous communication.[4]

The extent of the pyrolysis was measured by the quantity of H_2 and CH_4 formed, it being assumed that each mole of H_2 or CH_4 corresponds to one mole of propylene decomposed originally. After the conclusion of a series of experiments the recovered propylene could be distilled in vacuum into a trap, from which it could be returned to the 25-l storage flask. In such a way the pyrolyzed material could be re-used. This arrangement made it possible to investigate the propylene previously pyrolyzed any required number of times.

TABLE I.

Run	Pretreatment of propylene. No. of previous pyrolyses	T°C	P·mm Hg	Time of contact: sec.	$K \cdot 10^3$ sec.$^{-1}$	$K_{780} \cdot 10^3$ sec.$^{-1}$*
4	First batch of propylene: Once at 780°C	778	8.4	0.149	14.5	15.7
5	Once at 780°C	778	8.3	0.148	15.0	16.2
6	Once at 780°C	781	8.3	0.151	16.6	16.0
7	Twice at 780°C	781	8.3	0.147	15.1	14.5
8	Twice at 780°C	780	8.3	0.147	14.5	14.5
9	Twice at 780°C	780	8.2	0.144	14.8	14.8
11	3 times at 780°C	780	8.3	0.144	15.8	15.8
59	Once at 830°C	781	8.9	0.127	14.9	14.3
60	Second batch of propylene: Once at 830°C	781	8.7	0.143	16.3	15.7
71	Second batch of propylene: Once at 780°C	781	8.7	0.150	14.8	14.3
75	Second batch of propylene: Twice at 780°C	785	8.9	0.148	18.1	14.1
						$K_{745} \cdot 10^3$ sec.$^{-1}$*
18	First batch of propylene: 4 times at 770°C	745	6.6	0.119	4.8	5.1
19	First batch of propylene: 4 times at 770°C	747	8.1	0.152	5.7	5.5
21	First batch of propylene: 5 times at 770°C	746	8.6	0.155	5.4	5.4
22	First batch of propylene: 5 times at 770°C	745	8.5	0.153	5.0	5.2
23	First batch of propylene: 5 times at 770°C	746	8.0	0.108	5.0	5.0
61	Second batch of propylene: Once at 830°C	748	8.9	0.154	5.7	5.3
93	Second batch of propylene: Once at 800°C	746	8.7	0.146	5.3	5.3

* This column gives the k interpolated to a constant temperature for the sake of comparison.

The Material Used for Pyrolysis

The propylene used in this study was generously supplied by Petrochemicals, Ltd., Manchester. Two samples from different batches were investigated in order to ascertain the reproducibility of the results and their independence of incidental impurities. The analysis of the gas showed that both batches contained over 99.3 percent of propylene. The propylene was further purified by vacuum distillation from −80°C into a trap cooled by liquid air and connected to a high vacuum pump. The condensed gas was evacuated for a couple of hours, before it was ultimately led into the 25-l storage flask.

In spite of these precautions it was found that the unpyrolyzed propylene decomposed at a rate slightly lower than that which had been pyrolyzed. However, one pyrolysis at a temperature not lower than 770°C yields a product which in any subsequent pyrolysis decomposed at a constant rate. This point was carefully examined. Table I demonstrates

TABLE II.

	Run	T°C	P·mm Hg	$K \cdot 10^3$ sec.$^{-1}$	Percent H_2	Percent CH_4
Not packed	50	810	8.3	46	28	72
Packed	105	813	8.4	57	—	—
Packed	106	808	8.4	45	30	70

[3] H. Tropsch, C. I. Parrish, and G. Egloff, Ind. Eng. Chem. 28, 581 (1936).
[4] M. Szwarc, J. Chem. Phys. 16, 128 (1948).

TABLE III.

Run	T°C	P·mm of Hg	Time of contact sec.	Percent of decomp.	$K \cdot 10^3$ sec.$^{-1}$	
			T round 717°C			$K_{717} \cdot 10^3$ sec.$^{-1}$
67	718	3.1	0.182	0.038	2.1	2.0
64	714	3.6	0.152	0.027	1.8	2.0
65	717	8.5	0.155	0.033	2.1	2.1
66	718	14.6	0.120	0.028	2.4	2.3
			T round 746°C			$K_{746} \cdot 10^3$ sec.$^{-1}$
63	746	4.5	0.180	0.102	5.6	5.6
61	746	8.9	0.154	0.088	5.7	5.7
62	746	13.6	0.137	0.079	5.8	5.8
			T round 780°C			$K_{780} \cdot 10^3$ sec.$^{-1}$
12	780	2.2	0.150	0.22	14.9	14.9
13	780	4.2	0.118	0.19	15.7	15.7
9	780	8.2	0.144	0.21	14.8	14.8
11	780	8.3	0.144	0.23	15.8	15.8
10	782	14.4	0.124	0.25	19.9	18.3
Longer time of contact 17	778	2.7	0.602	0.76	12.5	13.5
Longer time of contact 15	780	6.3	0.580	0.86	14.8	14.8
Longer time of contact 14	780	11.3	0.448	0.88	19.7	19.7

clearly that the rate of decomposition was independent of the number of previous pyrolyses and it did not depend on the temperature at which the previous pyrolyses had been performed (provided that at least one of the previous pyrolyses had been carried out at a temperature $\geqslant 770$°C). This constant rate was taken as the true rate of decomposition of propylene.

The inspection of the data presented in Table I proves that both batches of propylene decomposed at the same rate. It should be noted also that the reproducibility of the results was extremely good (the deviations from the average value were less than 10 percent).

The Kinetics of the Decomposition

The decomposition of propylene was shown to be a homogenous gas reaction of the first order. The homogenity was demonstrated by packing the reaction vessel with silica wool which increased the surface by factor of 6. The data for the packed and empty reaction vessel are given in Table II.

The first order of the reaction was demonstrated by varying the pressure of propylene by factor of 7 (from 2 mm of Hg up to 14 mm of Hg), and by varying the time of contact by factor of 6 (from 0.1 sec. up to 0.6 sec.). Table III contains the results obtained for various pressures of propylene and various times of contact.

The unimolecular k seems to be fairly constant, although a closer examination of the data reveals a trend with increasing pressure of propylene. This trend is most noticeable with longer times of contact (runs No. 17, 15, 14) amounting to about a 40 percent increase in k for a fourfold increase in the pressure of propylene.

The variation of the unimolecular k with temperature is recorded in Table IV, and the plot of log k against $1/T$ is given in Fig. 1. Each point in this graph represents the average of at least five experiments. It should be noted that the Arrhenius law is obeyed over the whole investigated range of temperatures from 680°C up to 870°C (i.e., over 190°C). Figure 1 enables us to estimate the energy of activation at 72.0 ± 3.0 kcal./mole and the frequency factor at $1.1 \cdot 10^{13}$.

The Products of Decomposition

The pyrolysis of propylene produced CH_4 and H_2 in a nearly constant proportion of about 2:1. Table V contains the results of analysis of the

TABLE IV.

Run	T°C	P·mm Hg	Time of contact sec.	Percent of decomp.	$K \cdot 10^3$ sec.$^{-1}$	
35	686	8.7	0.185	0.0067	0.36	
36	686	8.7	0.180	0.0063	0.35	Average for
37	685	8.6	0.185	0.0063	0.34	685°C
38	683	8.3	0.187	0.0056	0.30	$0.34 \cdot 10^{-3}$
39	685	8.7	0.192	0.0064	0.32	
29	698	8.7	0.210	0.021	0.99	
30	698	8.7	0.167	0.015	0.92	Average for
31	699	8.6	0.165	0.017	1.03	698°C
32	698	8.4	0.159	0.015	0.94	$0.95 \cdot 10^{-3}$
33	698	8.5	0.143	0.013	0.94	
24	723	8.5	0.157	0.033	2.12	
25	723	8.3	0.155	0.032	2.09	Average for
26	724	8.7	0.170	0.038	2.24	723°C
27	725	8.6	0.160	0.039	2.44	$2.12 \cdot 10^{-3}$
28	723	8.5	0.165	0.032	1.94	
18	745	6.6	0.119	0.058	4.9	
19	747	8.1	0.152	0.087	5.7	Average for
21	746	8.6	0.155	0.083	5.4	745°C
22	745	8.5	0.153	0.077	5.0	$5.05 \cdot 10^{-3}$
23	746	8.0	0.108	0.054	5.0	
4	778	8.4	0.149	0.22	14.5	
5	778	8.3	0.148	0.22	15.0	Average for
6	781	8.3	0.151	0.25	16.6	780°C
7	781	8.3	0.147	0.22	15.1	$15.5 \cdot 10^{-3}$
8	780	8.3	0.147	0.21	14.5	
9	780	8.2	0.144	0.21	14.8	
50	810	8.3	0.138	0.64	46	
51	811	8.1	0.135	0.65	48	Average for
52	810	8.4	0.139	0.66	47	810°C
53	811	8.5	0.135	0.58	43	$44.6 \cdot 10^{-3}$
54	811	8.4	0.132	0.59	45	
55	811	8.5	0.145	0.64	44	
44	857	8.4	0.149	1.95	131	
45	857	8.4	0.130	1.70	131	Average for
46	859	8.4	0.155	2.18	141	857°C
47	858	8.6	0.117	1.53	131	$128 \cdot 10^{-3}$
48	857	8.7	0.138	1.72	124	
56	872	9.2	0.138	3.54	256	

TABLE V.

Run	T°C	P·mm Hg	Per-cent H_2	Per-cent CH_4	Previous treatment
64	704	8.6	22	78	Once pyrolyzed at 830°C
65	707	8.5	26	74	Once pyrolyzed at 830°C
61	746	8.9	29	71	Once pyrolyzed at 830°C
10	782	14.4	28	72	3 times pyrolyzed at 780°C
75	785	8.9	30	70	2 times pyrolyzed at 780°C } Second
74	791	3.1	30	70	Once pyrolyzed at 780°C } batch
79	791	14.0	32	68	Once pyrolyzed at 780°C
50	810	8.3	28	72	2 times pyrolyzed at 850°C
54	811	8.4	28	72	3 times pyrolyzed at 850°C
57	830	8.6	32	68	Once pyrolyzed at 830°C
40	851	8.1	30	70	Not pyrolyzed
44	851	8.4	32	68	Once pyrolyzed at 850°C
69	868	9.1	32	68	3 times pyrolyzed at 870°C
56	872	9.1	32	68	3 times pyrolyzed at 850°C

CH_4+H_2 mixture. It should be noted that the ratio of CH_4/H_2 does not depend on the pressure of propylene, and is not influenced by the previous pyrolysis of the investigated sample of propylene. A very slight decrease in the CH_4/H_2 ratio was observed with increasing temperatures. The analysis of the gas formed in the decomposition at 710°C gave 74–78 percent of CH_4, whereas at 870°C the percentage of CH_4 in the gas dropped to 68–70 percent. On the assumption that the change of CH_4/H_2 ratio with temperature depends on the difference in the energies of activation of the processes leading to the formation of CH_4 and H_2, respectively, we conclude that

$$E_{act.H_2}-E_{act.CH_4}=2-4 \text{ kcal./mole.}$$

In order to get simple kinetics and to avoid all reactions due to the accumulation of products, we limited the percentage of decomposition to 0.01 percent–2 percent. The investigation of the products of decomposition other than H_2 and CH_4 was therefore feasible only for runs made at higher temperatures, and even in these cases the results were of a qualitative, rather than quantitative, nature. The other products of decomposition were found to be C_2H_4 and allene by fractional distillation on the Podbielniak type still of propylene pyrolyzed two or three times at 850°C–870°C. The allene fraction was identified by its boiling point (−33°C−−35°C) and by the reaction obtained with solution of $HgCl_2$ (white precipitate). The quantities suggested that one mole of C_2H_4 was produced for every mole of CH_4, and one mole of allene was produced for each mole of CH_4 or H_2.

Very small quantities of yellowish liquid were observed in propylene pyrolyzed repeatedly at highest temperature. The boiling point of this liquid was about 60°C, suggesting it was C_6 hydrocarbon. Its quantity was 10–15 mole percent of H_2+CH_4 (calculating it as C_6 hydrocarbon). No non-volatile or polymeric substances were observed.

In a further attempt to identify the products of reaction (other than H_2 and CH_4), the whole pyrolyzed propylene was brominated. The bromination product was carefully fractionated, and the high boiling fraction was collected separately. The typical analysis of this fraction was

	C	H	Br
High boiling fraction	11.4%	1.4%	87.1%
Theoretical $CH_2Br\cdot CBr_2\cdot CH_2Br$	10.0%	1.1%	88.9%
Theoretical $CH_2Br\cdot CHBr\cdot CH_2\cdot CH_2\cdot CHBr\cdot CH_2Br$	17.9%	2.5%	79.6%

This shows that the high boiling fraction consisted mainly of tetrabromallene with perhaps small quantities of tetrabromdiallyl. The quantities of these high boiling fractions indicated again the 1:1 ratio of (H_2+CH_4)/allene.

Influence of Addition of Diallyl and Allene

As our experimental technique is extremely sensitive to small amounts of impurities, it was desirable to find how the addition of diallyl and allene influences the rate of decomposition of propylene. It was demonstrated that addition of very small quantities of diallyl was without any effect (up to few tenths of percent). However, greater quantities (1 percent–4 percent) of diallyl increased considerably the rate of decomposition of propylene. The addition of 4 percent of diallyl also changed the composition of the H_2+CH_4 mixture. After this

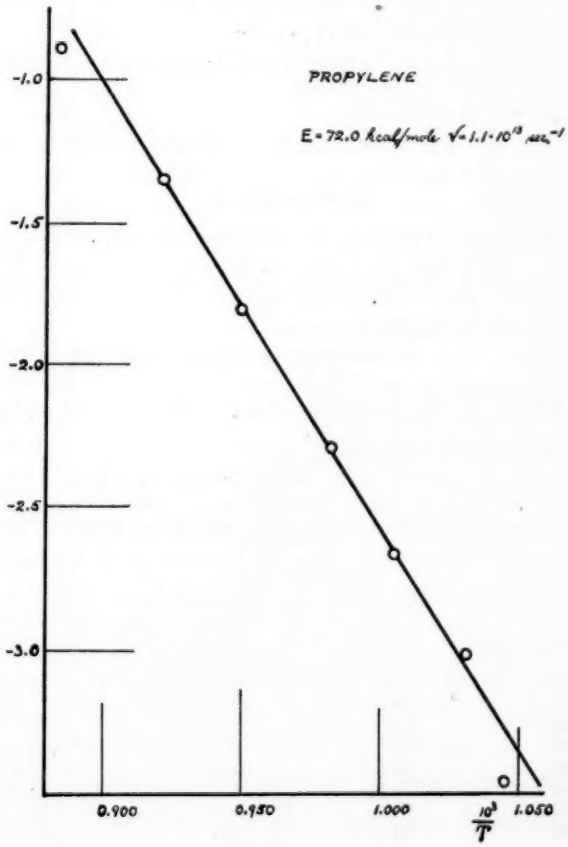

FIG. 1.

addition the rate of decomposition increased by a factor of 3, while the percent of H_2 increased from about 30 percent (observed for the pure propylene) to nearly 50 percent. The results of these experiments are given in Table VI.

We conclude from these results that diallyl is not the main product of decomposition of propylene, since samples of pyrolyzed propylene which contained about 6 percent of decomposition products still gave the same rate of decomposition on subsequent pyrolysis. Addition of allene (up to 8 percent) caused no appreciable change in the rate of decomposition of propylene.

DISCUSSION

Two distinct mechanisms of the decomposition of propylene can account for the observed facts. We shall start by formulating both mechanisms, then indicate how they account for the experimental data, and finally discuss how it is possible to decide which is the correct one.

Mechanism 1

$$CH_2=CH-CH_3 \rightarrow CH_2=CH-CH_2\cdot + H; \quad (1)$$

$$CH_2=CH-CH_3 + H \rightarrow CH_2=CH-CH_2\cdot + H_2; \quad (2)$$

$$\begin{cases} CH_2=CH-CH_3 + H \rightarrow C_2H_4 + CH_3\cdot; & (3a) \\ CH_2=CH-CH_3 + CH_3\cdot \rightarrow CH_2=CH-CH_2\cdot + CH_4; & (3b) \end{cases}$$

$$2CH_2=CH-CH_2\cdot \rightarrow CH_2=CH-CH_3 + CH_2=C=CH_2. \quad (4)$$

Mechanism 2

$$CH_2=CH-CH_3 \rightarrow CH_2=CH-CH_2\cdot + H; \quad (1)$$

$$CH_2=CH-CH_2\cdot \rightarrow CH_2=C=CH_2 + H; \quad (5)$$

$$CH_2=CH-CH_3 + H \rightarrow CH_2=CH-CH_2\cdot + H_2; \quad (2)$$

$$\begin{cases} CH_2=CH-CH_3 + H \rightarrow C_2H_4 + CH_3\cdot; & (3a) \\ CH_2=CH-CH_3 + CH_3\cdot \rightarrow CH_2=CH-CH_2\cdot + CH_4; & (3b) \end{cases}$$

$$CH_2=CH-CH_2\cdot + H \rightarrow CH_2=CH-CH_3. \quad (6)$$

TABLE VI.

Run	T°C	Percent diallyl.	$K\cdot10^3$ ·sec.$^{-1}$
82	810	0.00	45.1
83	811	0.05	43.7
84	812	0.2	45.3
85	812	0.2	45.5
86	812	1.0	85.0
87	812	1.0	75.0
89	812	4.0	140
90	812	4.0	142

Mechanism 1

This mechanism is essentially the one which was previously proposed to account for the decomposition of toluene, the xylenes,[4,5] the fluorotoluenes,[6] and the picolines.[7] Reaction 1 is the rate determining step which is followed by the rapid reactions (2), (3a), and (3b). The reactions (2) and (3a) represent the two ways in which the H atoms are removed from the system. The first leads to the formation of H_2, the second to that of CH_4 and C_2H_4. It is obvious from an inspection of reactions (3a) and (3b) that this mechanism requires the CH_4/C_2H_4 ratio to be 1:1. This ratio was deduced previously from the data of Frey and Smith,[1] and it was explicitly reported by Hurd and Meinert.[2] Our present experiments seem to confirm this 1:1 ratio, although no exact determination was possible owing to the extremely low percentages of decomposition at which we worked.

Since H_2 and CH_4 are alternative products of the same reaction

$$CH_2=CH-CH_3 + H \begin{cases} \nearrow CH_2=CH-CH_2\cdot + H_2 \\ \searrow C_2H_4 + CH_3\cdot, \end{cases}$$

the CH_4/H_2 ratio should be independent of the pressure of propylene. This was confirmed in runs 10, 75, 74, and 79. (See Table V.) The energies of activation for both reaction paths are certainly small, and therefore the CH_4/H_2 ratio which is dependent on their difference should be nearly independent of temperature (see Table V).

A further conclusion which can be drawn from the proposed mechanism is that the (H_2+CH_4)/allene ratio should be 1:1. Our data seem to confirm this conclusion. Allene was definitely found as one of the products of decomposition. Taking into account some losses caused by the polymerization of allene to the observed C^6 hydrocarbon, we find a fair agreement between the actually estimated quantity of allene and that calculated (equal to H_2+CH_4). For example, the calculated quantity of allene was 8 percent while the observed was 5 percent. Hurd and Meinert reported that the pyrolysis of allene[8] gave some liquid polymer as a main product of reaction, but they found, as previously noted, neither allene nor the above-mentioned liquid products in the pyrolysis of propylene.[2] The following explanation is suggested in order to reconcile these results with ours. Allene was indeed formed in the experiments

[5] M. Szwarc, Nature 160, 403 (1947).
[6] M. Szwarc and J. S. Roberts, J. Chem. Phys. 16, 609 (1948).
[7] J. S. Roberts and M. Szwarc, J. Chem. Phys. 16, 981 (1948).
[8] R. N. Meinert and C. D. Hurd, J. Am. Chem. Soc. 52, 4540 (1930).

of Hurd and Meinert, but it co-polymerized with propylene. Therefore, the resulting liquid products, which were found by Hurd and Meinert in pyrolysis of propylene, differed from the products of polymerization of pure allene.

Kinetically, mechanism 1 represents a true unimolecular reaction. Hence it accounts for the first-order decomposition and the 10^{13} frequency factor, which is theoretically required for true unimolecular reactions.[9]

Mechanism 2

This mechanism is a chain process in which reaction (1) is the chain initiation, reactions (5) and (2) or (5), (3a), and (3b) are alternative chain propagation, and, finally, reaction (6) is the chain termination.***

Inspection of the suggested reaction scheme shows that mechanism 2 also requires the ratio CH_4/C_2H_4 to be 1:1, the ratio CH_4/H_2 to be independent of pressure of propylene and only slightly dependent on temperature, and, finally, the (CH_4+H_2)/allene ratio to be 1:1 (on the same grounds as given before in the discussion of mechanism 1).

Using the stationary state method we obtain the following expression for the rate of reaction:

$$d(\text{gas})/dt=(k_1\cdot k_5\cdot k_2/k_6)^{\frac{1}{2}}\cdot(\text{propylene}).$$

For the sake of simplicity we considered in this expression only reactions (5) and (2) as the chain propagation, but the final result is not changed if we consider the alternative chain propagation, namely, reactions (5), (3a), and (3b).

Reactions (1) and (5) are unimolecular decompositions of the propylene and allyl radicals, respectively. Both, therefore, should have frequency factor of the order 10^{13}. The energy of activation of (1) is equal to $D(C-H)$ in propylene, that of (2) is equal or slightly greater than $D(C-H)$ in the allyl radical. The sum of $D(C-H)$ in propylene and $D(C-H)$ in the allyl radical is given by thermochemical data as the endothermicity of the following reaction:

$$CH_3-CH=CH_2\rightarrow CH_2=C=CH_2+2H-145 \text{ kcal.}$$

We see, therefore, that $(k_1\cdot k_5)^{\frac{1}{2}}\sim 10^{13}\cdot\exp(72.5/RT)$. Now, k_2 and k_6 are the rate constants for the bimolecular reactions $H+CH_3-CH=CH_2$ and $H+\cdot CH_2-CH=CH_2$, respectively. We should expect that both constants correspond to the same collision factor. Also, since the energy of activation of (2) is very small and that of (6) probably zero, we can assume in the first approximation $k_2\sim k_6$.

We came to the conclusion that the mechanism 2 gives first-order kinetics, with a frequency factor of the order 10^{13} and an energy of activation about 72 kcal./mole. Thus, mechanism 2 accounts for all observed features of the decomposition of propylene.

THE DISTINCTION BETWEEN MECHANISM 1 AND MECHANISM 2

As was shown in the previous paragraphs, both mechanisms require the same products of reaction, in the same proportions, the same order of decomposition with the same frequency factor and energy of activation. To distinguish between them we must use indirect methods. The most elegant way would be provided by a study of the decomposition of either or both deuterium compounds A and B.

$$\underset{A}{CH_2=CH-CD_3};\quad \underset{B}{CH_2=CD-CH_3}.$$

According to mechanism 1, A should give pure D_2, while B should give pure H_2. According to mechanism 2, both compounds should give a mixture of deuterium and hydrogen, and the amount of hydrogen in deuterium in case of A, or deuterium in hydrogen in case of B, would provide a measure of the length of the chain. Unfortunately, we are unable to obtain these compounds at present and therefore we must abandon this approach for the time being.

We turn, therefore, to the conclusions which can be drawn from the reported experimental facts, on the basis of the suggested mechanisms. Mechanism 1 demands that the observed energy of activation of 72 kcal./mole should be equal to the $D(C-H)$ in propylene (assuming as usual that the energy of activation for recombination of H atoms and radicals is zero). This is a surprisingly low value, although not quite impossible. There are good reasons to believe that the $D(C-H)$ in propylene is lower than $D(C-H)$ in toluene. Taylor and Smith[10] found that CH_3 radicals extract H atoms more easily from propylene than from toluene; Butler and Polanyi[11] found the rate of decomposition of allyl iodide to be greater than that of benzyl iodide and the same observation was made by Shaw and the present author[12] using a static method. The $D(C-H)$ in toluene was estimated at 77.5 kcal/mole.[4] It should be emphasized that in the case of toluene and its derivatives there is no ambiguity of interpretation such as is found in the case of propylene.

[9] M. Polanyi and E. Wigner, Zeits. f. physik. Chemie **A139**, 439 (1928).

*** The other chain terminations, i.e., $H+H+M\rightarrow H_2+M$, or $2CH_2=CH-CH_2\cdot\rightarrow CH_2=C=CH_2+CH_3\cdot CH=CH_2$ have been ruled out on the energetical basis. The former requires $Ea\sim\frac{1}{2}D(C-H)$, i.e., $D(C-H)$ in propylene would be $\sim$144 kcal./mole. The latter gives $Ea\sim 145-\frac{1}{2}D(C-H)+X$ leading to $D(C-H)$ in propylene $\geqslant$ 146 kcal./mole. Both values are, of course, impossible.

[10] H. S. Taylor and J. O. Smith, J. Chem. Phys. **8**, 543 (1940).

[11] E. T. Butler and M. Polanyi, Trans. Faraday Soc. **39**, 19 (1943).

[12] A. Shaw and M. Szwarc, unpublished results.

However, on the basis of present thermochemical data, the value of 72 kcal./mole as $D(C-H)$ in propylene leads to the value of 30 kcal./mole for the heat of dissociation of the central C—C bond in diallyl.**** This value is hardly acceptable, and it seems to be too low. To get more information on this subject some crude experiments of pyrolysis of diallyl were performed. No effect was observed on heating diallyl vapor at pressure of 60 mm of Hg and 180°C over a period of 16 hours. There was no increase of pressure, and the vapor could be condensed at −80°C, leaving no non-condensable residue. The pressure observed in this experiment was equal to the calculated value on the basis of the ideal gas law, i.e., there was no appreciable dissociation of diallyl into allyl radicals.

Heating at about 350°C caused some reaction with production of gas, which was not condensable in liquid air (probably H_2). The matter was not pursued further.

In conclusion we can say that this low value for the $D(C-C)$ in diallyl is the important argument against mechanism 1 and at present perhaps the only one.

Turning now to mechanism 2, we can suppose that the chain is probably a very short one. The argument is taken from our study of pyrolysis of isobutene (the following paper), which seems to be a chain process, similar to that outlined in the present paper. In the case of isobutene the maximum chain length is given by the CH_4/H_2 ratio which was found to be about 9. It is plausible to assume that the length of the chain in the decomposition of propylene should be no longer, as the removal of H atom from allyl radical probably requires 12 kcal. more than the removal of CH_3 group from the similar methyl-allyl radical.†

Another argument in favor of a short chain is provided by our experiments with a propylene-diallyl mixture. Diallyl should dissociate into allyl radicals, and if these radicals decompose as demanded by mechanism 2, the rate of reaction should increase very considerably. In fact, the addition of 0.2 percent of diallyl (which is comparable with the percent of decomposition of pure propylene at the temperature of this experiment) caused no appreciable change in the rate of decomposition. This result can be even regarded as an argument against mechanism 2.

If we assume that the chain is short, say about 10, we are able to calculate the difference in energies of activation of processes 1 and 5 from the following expression,

$$E_1-E_5=2.\,RT[\ln.\ (\text{chain length})+\tfrac{1}{2}\ln\cdot 3]$$

which is the straightforward conclusion from mechanism 2. The term $\frac{1}{2}\ln\cdot 3$ comes as a result of three times greater frequency factor for k_1 than for k_5 (on statistical grounds). Thus we find

$$E_1-E_5\sim 11 \text{ kcal./mole},$$
$$E_1+E_5\sim 145 \text{ kcal./mole}$$
(from thermochemical data),

and in result $E_1\sim 78$ kcal./mole. This value corresponds to the frequency factor $2.5\cdot 10^{13}$ for the unimolecular constant corresponding to the first step in the decomposition of propylene, in good agreement with the frequency factors found for toluene and the xylenes,[4] and leads to much more plausible value of 42 kcal./mole for the $D(C-C)$ of the central C—C bond in diallyl. It should be noticed, however, that this calculation of $D(C-H)$ in propylene was based on the approximation $k_2\sim k_6$.

The Reactions between Hydrogen Atoms and Propylene

Both suggested mechanisms of decomposition of propylene assume two reactions between H atoms and C_3H_6, namely,

$$H+CH_3\cdot CH=CH_2\rightarrow H_2+\cdot CH_2-CH=CH_2, \quad (2)$$

$$H+CH_3\cdot CH=CH_2\rightarrow CH_3\cdot+C_2H_4. \quad (3)$$

The variation of CH_4/H_2 ratio with temperature indicates that the energy of activation of (2) is by 2–4 kcal. greater than that of (3). The reaction (3) most probably goes in two steps:

$$H+CH_3-CH=CH_2\rightarrow CH_3-CH_2-CH_2, \quad (A)$$

$$CH_3-CH_2-CH_2\rightarrow CH_3+C_2H_4. \quad (B)$$

The "hot" radical formed in step (A) decomposes easily into CH_3 radical and C_2H_4, as the over-all process is exothermic to an extent of 13 kcal. The attack of H atom on the other end of the double bond seems to be ineffective. The "hot" radical $CH_3\cdot CH\cdot CH_3$ formed by such a process should decompose into its original components, i.e., propylene and an H atom. The decomposition into CH_3 and $CH_2\cdot CH$ seems to be energetically improbable (very likely an endothermic process).

It should be noted that a change of the conditions under which H atoms interact with propylene changes profoundly the ultimate products of reaction. The extraction of H atoms and formation of

**** The heat of formation of gaseous diallyl can be obtained from the heat of combustion of liquid diallyl (Coops, Mulder, Dienske, and Smittenberg, Rec. Trav. Chim. 65, 128 (1946), taking 8 kcal./mole for the heat of vaporization, or from Rossini's heat of formation of *n*-hexane in conjunction with Kistiakowsky's heat of hydrogenation of diallyl. Both methods give the same value.

† While the endothermicity of the reaction $CH_3-CH=CH_2\rightarrow CH_2=C=CH_2+2H$ is 145 kcal., the endothermicity of the reaction $(CH_3)_2:C=CH_2\rightarrow CH_2=C=CH_2+H+CH_3$ is 133 kcal. Since the $D(C-H)$'s in propylene and isobutene are probably very similar, the difference of 12 kcal. should be mainly accounted for by the difference between removal of H from allyl radical and CH_3 from the methyl-allyl radical.

allyl radicals seem to be suppressed very considerably at normal or slightly elevated temperatures, since this reaction needs higher energy of activation than the decomposition into CH_3 and C_2H_4. The study of Rabinovitch, Davis, and Winkler[13] confirms this view. They found CH_4 and C_2H_6 as the main products of reaction between propylene and H atoms produced by Wood-Bonhoeffer technique. This was interpreted by them as a result of a decomposition of a "hot" radical $CH_3 \cdot CH_2 \cdot CH_2 \cdot$ produced by association of C_3H_6 and H. The total balance of products obtained in their investigation leaves no room for the assumption of the reaction (2). For the reason discussed previously, the association of a "hot" radical $CH_3 \cdot CH \cdot CH_3$ is of little importance.

However, an increase of the total pressure increases the probability of stabilization of either of these "hot" radicals by subsequent collision with a third body. This conclusion is born out by results obtained by Moore and Taylor[14] who investigated the mercury photosensitized hydrogenation of propylene. The stabilized radicals mainly dimerize giving C_6H_{14} as the main products of reaction. The formation of "non-hot" association products in mercury photosensitized hydrogenation may be still easier because of the participation of HgH molecules as hydrogenation agents. A collision between HgH and C_3H_6 leads to Hg and C_3H_7 radical and the excess energy can be removed in the form of translational energy.

In discussing the reactions involving the "hot" radicals C_3H_7 we have given the reasons why the formation of a "hot" $CH_3 \cdot CH \cdot CH_3$ radical is not effective. These reasons do not apply to reactions involving "non-hot" C_3H_7 radicals. The investigation of Moore, reported on the 113th meeting of American Chemical Society (April 1948) shows the preferential formation of $CH_3 \cdot CH \cdot CH_3$ radical to that of $CH_3 \cdot CH_2 \cdot CH_2$. The reported product of reaction was $CH_3 \cdot CH(CH_3) \cdot CH \cdot CH_3$ and not *n*-hexane.

[13] B. S. Rabinovitch, S. G. Davis, and C. A. Winkler, Can. J. Research **21B**, 251 (1943).

[14] W. J. Moore and H. S. Taylor, J. Chem. Phys. **8**, 504 (1940).

CONCLUSIONS

The experimental facts reported in this paper lead to the final conclusion that the first step in the thermal decomposition of propylene is the breaking of the molecule into an H atom and an allyl radical. The H atoms react with the excess of propylene giving H_2, CH_4, and C_2H_4. On that basis we could postulate two mechanisms which account for all observed facts. The fate of the allyl radicals was not finally established. Its decomposition into an H atom and an allene molecule is the basis of mechanism 2, while mechanism 1 assumes its removal by disproportionation.

One can assume a mechanism very similar to mechanism 2, in which the first step is the breaking of a propylene molecule into CH_3 and $CH_2{:}CH$ radicals, followed by the same sequence of reactions as postulated in mechanism 2. The argument against this assumption is based on our results obtained in the study of the thermal decomposition of isobutene (following paper). This compound decomposes according to mechanism 2. If the first step were the splitting-off of a CH_3 radical, then the products would not contain any H_2. The presence of hydrogen proves, therefore, the splitting of isobutene molecules into H atoms and $CH_2 \cdot C(CH_3){:}CH_2$ radicals. It is extremely improbable that the initial decomposition of propylene would differ from that of isobutene, and thus we reject the suggested reaction

$$CH_3{:}CH{=}CH_2 \rightarrow CH_3 \cdot + \cdot CH{=}CH_2.$$

The problem of the energy of the C—H bond in propylene would be solved if we could decide between the two mechanisms discussed. Taking into account all the arguments mentioned in the discussion, we are inclined to assume that mechanism 2 with a short chain is the more probable one. On that basis we suggest 78 kcal./mole as the most probable value for $D(C-H)$ in propylene. Further investigations are required, however, before we can reach the final decision.

The Kinetics of the Thermal Decomposition of Isobutene

M. SZWARC
Department of Chemistry, The University of Manchester, Manchester, England
(Received August 5, 1948)

The thermal decomposition of isobutene was found to be a homogeneous gas reaction of the first order. The first-order constant is $0.5 \cdot 10^{13} \exp(67{,}000/RT)$. The products of the decomposition included H_2, CH_4, and allene. The experimental results are explained in terms of a chain mechanism, the initiating step being the decomposition of the isobutene molecule into an H atom and a $\cdot CH_2-C(CH_3)=CH_2$ radical. The most probable value of the D(C−H) in isobutene is 76 kcal./mole. This estimate is based on certain assumptions concerning the frequency factors.

THE aim of this work was to supplement that done on the pyrolysis of propylene. We used the same apparatus and technique as described in the preceding paper. The isobutene was kindly supplied by Messrs. I.C.I., Billingham, and contained over 99 percent of C_4H_8. This product was further purified by a vacuum distillation from a trap at −80°C into one cooled by liquid air. The criterion of purity was that the product recovered from any pyrolysis should give the same rate of decomposition on being pyrolyzed once more. By this standard the distilled isobutene was sufficiently pure (see Table I). The reproducibility of the results was not as good as in the case of propylene, and this was particularly noticeable in experiments performed at lower temperatures (see Table I and Fig. 1).

It was found that the thermal decomposition of isobutene is a homogeneous gas reaction of the first order. Packing of the reaction vessel with silica wool (increasing the surface by factor of 6) caused no change in the rate of decomposition (see Table II and Fig. 1). The reaction was shown to be first order by changing the pressure of isobutene from about 1 mm of Hg up to 20 mm of Hg, the results being summarized in Table III. The variation of the first-order constant with temperature is shown in graph 1, where logk is plotted against $1/T$. This graph contains all the experimental results. The "best" straight line corresponds to an energy of activation of 67 kcal./mole and a frequency factor of 5.10^{12}. The experimental error is about ±4 kcal./mole. Table IV contains all the results not tabulated in the preceding tables.

TABLE I.

Run	Previous pyrolysis	T°C	P·mm Hg	$K \cdot 10^3$ sec.$^{-1}$	
	Temperature round 767°C				$K_{767} \cdot 10^3$ sec.$^{-1}$*
1	Not pyrolyzed	771	8.8	48.9	45.6
2	Not pyrolyzed	771	8.8	47.4	44.1
3	Once pyrolyzed at 770°C	768	9.0	45.6	43.8
4	Once pyrolyzed at 770°C	767	8.7	46.0	46.0
5	Once pyrolyzed at 770°C	767	8.6	43.7	43.7
41	Once pyrolyzed at 790°C	767	9.2	41.8	41.8
42	Once pyrolyzed at 790°C	769	9.0	49.0	44.0
46	Twice pyrolyzed at 790°C	763	9.5	38.8	43.0
47	Twice pyrolyzed at 790°C	762	8.9	45.8	60.5
53	Twice pyrolyzed at 740°C	760	8.5	35.0	43.9
	Temperature round 708°C				$K_{708} \cdot 10^3$ sec.$^{-1}$*
50	Twice pyrolyzed at 740°C	709	8.9	4.7	4.5
51	Twice pyrolyzed at 740°C	708	8.7	5.7	5.7
52	Twice pyrolyzed at 740°C	707	8.6	6.0	6.2
54	3 times pyrolyzed at 740°C	704	8.9	8.0	9.3
55	4 times pyrolyzed at 740°C	706	8.4	6.0	6.5
56	4 times pyrolyzed at 740°C	704	8.5	5.5	6.1
14	3 times pyrolyzed at 770°C	711	8.5	10.0	8.8
15	3 times pyrolyzed at 770°C	711	8.7	9.5	8.3

* This column contains the values of K interpolated to a constant temperature for the sake of comparison.

THE PRODUCTS OF DECOMPOSITION

The decomposition of isobutene produced H_2 and CH_4 in proportions independent of temperature and pressure of C_4H_8. The results of the analysis of H_2+CH_4 mixture are summarized in Table V. The average composition of this mixture was 1 mole of H_2 to 9 moles of CH_4.

The analysis of other products of the pyrolysis was very difficult as the percentage of decomposition was kept extremely low (from about 0.01 percent up to 2 percent) in order to avoid side reactions. The distillation on a Podbielmak type still* revealed that allene was another main product of decomposition. Its quantity suggested that the ratio (H_2+CH_4)/allene was 1:1. The allene fraction was identified by its boiling point (−34°−−35°C) and by its reaction with solution of $HgCl_2$ (white precipitate).

TABLE II. Packed reaction vessel.

Run	T°C	P mm Hg	$K \cdot 10^3$ sec.$^{-1}$	Percent H_2	Percent CH_4
72	725	8.0	14.5	—	—
74	730	8.4	18	—	—
73	732	8.3	22	—	—
75	760	8.5	51	14%	86%
76	793	11.5	155	—	—

* For the distillation we could only use samples of isobutene pyrolyzed twice or three times at higher temperatures.

TABLE III.

Run	T°C	P mm Hg	Time of contact sec.	Percent of decomp.	$K \cdot 10^3$ sec.$^{-1}$	
						$K_{660} \cdot 10^3$ sec.$^{-1}$*
59	660	19.5	0.180	0.023	1.3	1.3
60	660	8.5	0.195	0.033	1.7	1.7
62	657	4.6	0.200	0.036	0.8	0.9
						$K_{688} \cdot 10^3$ sec.$^{-1}$*
31	689	15.2	0.170	0.075	4.4	4.2
29	687	8.7	0.195	0.082	4.2	4.4
30	687	8.8	0.195	0.062	3.2	3.3
32	688	2.9	0.220	0.064	2.9	2.9
33	688	2.8	0.220	0.073	3.3	3.3
						$K_{768} \cdot 10^3$ sec.$^{-1}$*
8	768	13.2	0.160	0.86	54	54
4	767	8.7	0.180	0.83	46	48
5	767	8.6	0.180	0.79	44	46
6	768	2.9	0.210	0.80	38	38
7	769	2.9	0.205	0.78	38	37
						$K_{808} \cdot 10^3$ sec.$^{-1}$*
64	806	8.9	0.185	4.25	230	250
65	808	4.7	0.195	4.30	220	220
68	809	2.8	0.200	3.20	160	155
67	809	1.3	0.215	5.38	250	240

* This column contains the values of K interpolated to a constant temperature for the sake of comparison.

DISCUSSION

The reported facts are against any mechanism of unimolecular type, i.e., based on the assumption that the rate-determining step is the breaking of some bond in the molecule of isobutene, followed by a sequence of rapid reactions between the radicals so created and the undecomposed C_4H_8. The decisive argument is that the observed energy of activation of 67 kcal./mole is too low to be regarded as a dissociation energy of any bond existing in the molecule of isobutene. In addition, the fact that the percentage of CH_4 was so high is by itself a powerful argument against the unimolecular mechanism of the type proposed for the decomposition of propylene. According to this mechanism more H_2 should be produced in the decomposition of isobutene than was observed in the case of propylene. The chance of reaction between H atoms and the H's of the CH_3 groups doubles, while that of addition to the central C decreases as a result of shielding of this atom by the two CH_3 groups. Thus the ambiguity which we encountered in the case of propylene does not exist in the case of isobutene. We can, therefore, safely assume that the pyrolysis of isobutene proceeds according to the following chain mechanism, corresponding to that previously proposed to account for the decomposition of propylene.

$$CH_2=C(CH_3)_2 \rightarrow CH_2=\underset{\displaystyle CH_3}{\underset{|}{C}}-CH_2\cdot + H, \quad (1)$$

$$CH_2=C(CH_3)_2 + H \rightarrow H_2 + CH_2=\underset{\displaystyle CH_3}{\underset{|}{C}}-CH_2\cdot, \quad (2)$$

$$CH_2=\underset{\displaystyle CH_3}{\underset{|}{C}}-CH_2\cdot \rightarrow CH_2=C=CH_2 + CH_3\cdot, \quad (3)$$

$$CH_2=C(CH_3)_2 + CH_3\cdot \rightarrow CH_4 + CH_2=\underset{\displaystyle CH_3}{\underset{|}{C}}-CH_2\cdot, \quad (4)$$

$$CH_3\cdot + \cdot CH_2-\underset{\displaystyle CH_3}{\underset{|}{C}}=CH_2 \rightarrow CH_3-CH_2-\underset{\displaystyle CH_3}{\underset{|}{C}}=CH_2. \quad (5)$$

The reactions (1) and (2) are the chain initiation, the reactions (3) and (4) are the chain propagation and the reaction (5) is the chain termination.**

At this point it should be mentioned that the pyrolysis of isobutene was investigated recently by Rice and Haynes.[1] The experimental results of these authors support in some respect the present findings.

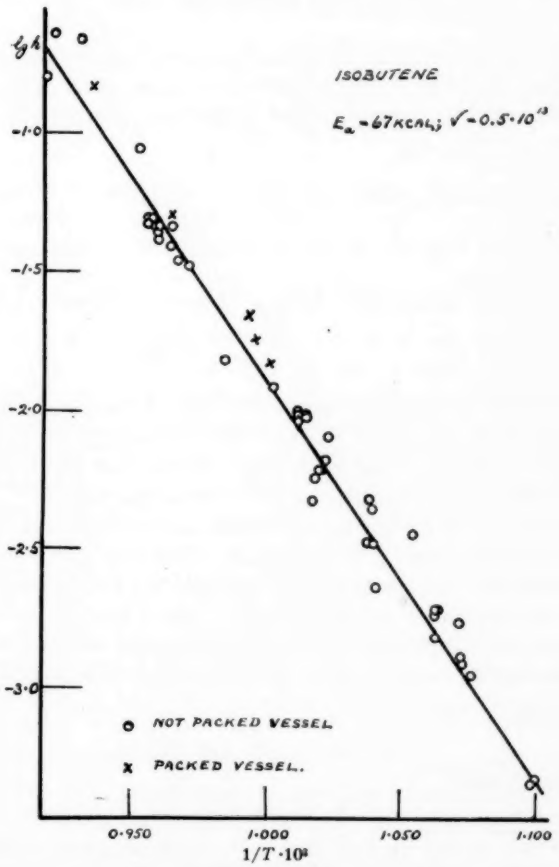

FIG. 1.

** The two other chain terminations can be ruled out in the same way as mentioned in the preceding paper.

[1] F. O. Rice and W. S. Haynes, J. Am. Chem. Soc. 70, 964 (1948).

TABLE IV.

Run	T°C	P mm Hg	Time of contact sec.	Percent decomp.	$K \cdot 10^3$ sec.$^{-1}$
25	636	8.6	0.185	0.009	0.48
26	638	8.5	0.190	0.009	0.46
22	656	8.6	0.170	0.019	1.1
23	659	8.5	0.195	0.025	1.3
24	659	8.4	0.160	0.019	1.2
10	667	8.9	0.185	0.035	1.9
11	668	8.8	0.180	0.034	1.9
12	668	8.6	0.185	0.033	1.8
13	668	8.8	0.180	0.027	1.5
69	675	8.7	0.205	0.082	4.0
20	687	8.8	0.190	0.068	3.6
21	687	8.5	0.195	0.070	3.6
16	711	8.8	0.175	0.160	9.4
17	714	8.6	0.180	0.175	9.7
18	714	8.7	0.165	0.155	9.5
19	714	8.4	0.170	0.155	9.1
28	723	8.6	0.160	0.19	12
27	754	8.7	0.165	0.56	34

TABLE V.

Run	Previous treatment of sample	T°C	P mm of Hg	Percent H_2	Percent CH_4
35	Once pyrolyzed at 690°C	690	8.8	10	90
38	3 times pyrolyzed at 690°C	690	8.9	8	92
39	5 times pyrolyzed at 690°C	690	8.8	10	90
54	3 times pyrolyzed at 740°C	704	8.9	9.5	90.5
55	4 times pyrolyzed at 740°C	706	8.4	11	89
51	2 times pyrolyzed at 740°C	708	8.7	10	90
49	Once pyrolyzed at 740°C	740	8.7	9.5	90.5
53	2 times pyrolyzed at 740°C	760	8.5	10.5	89.5
46	2 times pyrolyzed at 790°C	763	9.5	10	90
41	Once pyrolyzed at 790°C	767	9.2	8	92
3	Once pyrolyzed at 770°C	768	9.0	11	89
8	2 times pyrolyzed at 770°C	768	13.2	12	88
63	4 times pyrolyzed at 740°C	774	8.6	12	88
64	5 times pyrolyzed at 740°C	806	8.9	11	89
68	2 times pyrolyzed at 800°C	809	2.8	13	87

Thus H_2, CH_4, and allene were reported as the products of decomposition, and the ratio of H_2/CH_4 was very close to that found in the present work. From their data we calculated the first-order constant at 790°C as $190 \cdot 10^{-3}$ sec.$^{-1}$,*** while our value at this temperature (interpolated) was $120 \cdot 10^{-3}$ sec.$^{-1}$

In conclusion Rice and Haynes postulated a chain mechanism which differs from that given above only in the initiation steps. The initiation proposed by these authors was

$$CH_2=C(CH_3)_2 \rightarrow CH_3\cdot + CH_2=\dot{C}-CH_3, \qquad (6)$$

$$CH_2=C(CH_3)_2 + CH_2=\dot{C}-CH_3 \rightarrow CH_2=CH-CH_3 + CH_2=\underset{\displaystyle CH_3}{\overset{\displaystyle |}{C}}-CH_2\cdot. \qquad (7)$$

It should be noticed, however, that Rice's mechanism does not account for the formation of H_2, which was found as a product of reaction by Rice and Haynes and in the present investigation.****

Returning to the chain mechanism proposed in the present work, it should be observed that this mechanism accounts for the formation of H_2 as well as for that of CH_4 and allene. The CH_4/H_2 ratio gives the length of the chain. Using the stationary state method we obtain the following expressions:

$$d(H_2+CH_4)/dt \sim [k_1+(k_1\cdot k_3\cdot k_4/k_5)^{\frac{1}{2}}]\cdot(C_4H_8) \sim (k_1\cdot k_3\cdot k_4/k_5)^{\frac{1}{2}}\cdot(C_4H_8);$$

chain length

$$\sim (k_3\cdot k_4/k_1\cdot k_5)^{\frac{1}{2}}.$$

The approximate expression follows from the assumption that k_1 is much smaller than k_3, k_4, or k_5. The expression for $d(H_2+CH_4)/dt$ leads to the energy of activation of $\frac{1}{2}(E_1+E_3+E_4) \sim 69$ kcal./mole, as E_1+E_3 is equal to or slightly greater than 133 kcal., the endothermicity of the reaction:

$$CH_2=C(CH_3)_2 \rightarrow CH_2=C=CH_2+CH_3+H \quad -133 \text{ kcal.}$$

and E_4 is probably about 4 kcal./mole.†

The reactions (4) and (5) are bimolecular reactions which should correspond to about the same collision frequency, while the reactions (1) and (3) are unimolecular decompositions and on theoretical grounds[2] should have frequency factors of the order 10^{13}. Thus the frequency factor for the over-all reaction should be also of the order 10^{13}. In such a way the discussed mechanism accounts for the observed energy of activation and frequency factor.

From the expression for the chain length we obtain ln. (chain length) $= (1/2RT)(E_1-E_3-E_4) - \frac{1}{2}$ ln. 6. The last term arises from the statistical factor of 6 existing in the frequency factor of reaction (1) but not in that of reaction (3). Now, putting for the chain length $CH_4/H_2 = 9$ and for E_4 a value of 4 kcal. (see the previous footnote), we obtain

$$E_1-E_3 \sim 17 \text{ kcal.},$$

while

$$E_1+E_3 = 133 \text{ kcal.} + x,$$

where x is the energy of activation for the reaction (8).

$$CH_2=C=CH_2+CH_3 \rightarrow CH_2=\underset{\displaystyle CH_3}{\overset{\displaystyle |}{C}}-CH_2. \qquad (8)$$

*** We use for this calculation the result obtained in the experiment performed at 790°C, pressure of 9 mm of Hg and time of contact 0.3 sec., as these conditions are similar to those at which we worked.

**** However, see C. D. Hurd and L. K. Eilers, Ind. Eng. Chem. **26**, 776 (1934) and C. D. Hurd and F. H. Blunck, J. Am. Chem. Soc. **59**, 1869 (1937).

† For analogy with the energy of activation for $CH_3+CH_3\cdot CH=CH_2 \rightarrow CH_4+CH_2-CH=CH_2$ see H. S. Taylor and J. O. Smith, J. Chem. Phys. **8**, 543 (1940).

[2] M. Polanyi and E. Wigner, Zeits. f. physik Chemie **A139**, 439 (1928).

Taking for x a reasonable value of 2 kcal. we obtain

$$D(C-H)=E_1=76 \text{ kcal./mole.}$$

This value corresponds to 5.10^{13} as the frequency factor of the unimolecular constant for the first step of the decomposition of isobutene. It would be expected that this factor should be twice as high as that for propylene (from statistical reason), and thus the good agreement between the frequency factors found for toluene, the xylenes,[3] propylene, and isobutene provides some justification for the applied approximations.

[3] M. Szwarc, Nature **160**, 403 (1947); J. Chem. Phys. **16**, 128 (1948).

THE JOURNAL OF CHEMICAL PHYSICS VOLUME 17, NUMBER 3 MARCH, 1949

Vibrational Analysis of the 3400A Triplet-Singlet Emission of Benzene*

HARRISON SHULL**
Department of Chemistry, University of California, Berkeley, California

The triplet-singlet emission of benzene at 3400A in a rigid glass-solution has been obtained and measured more accurately than in previous work. An assignment is proposed accounting for all the important bands observed. The analysis of the vibrational structure indicates the presence of the 703 cm^{-1} b_{2g} fundamental, showing that in the triplet-singlet transition, the triplet level combines in the same manner as a $^1B_{1u}$ state for electric dipole radiation. This will lead to a definite assignment of the symmetry of this triplet level when the theoretical rules for intercombinations in polyatomic molecules are derived. The analysis supports a hexagonally symmetric planar model for this triplet state.

INTRODUCTION

THAT the phosphorescence emission observed from many organic molecules was a transition from a triplet to the ground singlet state of the molecule was suggested by Lewis and Kasha.[1,2] Sklar[3] reported finding a weak absorption in the 3400A region (spectrum shown by Lewis and Kasha[2]) which he attributed to one of the triplet levels predicted in his theoretical calculations. It was suggested that this absorption represented the symmetry allowed transition $^1A_{1g}\rightarrow{}^3E_u^-$ which was predicted at 2120A. Theory, however, predicted an additional transition $^1A_{1g}\rightarrow{}^3B_{1u}$ at 4750A. Inability to find this transition was ascribed to the double forbiddenness of the transition (both spin and symmetry forbidden), whereas the transition $^1A_{1g}\rightarrow{}^3E_u^-$ is spin forbidden only.

A further calculation of the triplet level was made by Goeppert-Mayer and Sklar[4] using the method of anti-symmetrized products of molecular orbitals. Their calculations showed $^3B_{1u}$ as the lowest triplet level, followed in turn at higher energies by $^3E_u^-$ and $^3B_{2u}$. The calculated transition $^1A_{1g}\rightarrow{}^3B_{1u}$ was at 8300A. London[5] recalculated these levels including a number of integrals neglected by Goeppert-Mayer and Sklar. The new calculated transition $^1A_{1g}\rightarrow{}^3B_{1u}$ is at 2760A. It should be noted in this recalculation, the singlet levels are in poor agreement with observation, and the relatively good agreement with the lowest triplet level must be regarded as fortuitous.

It is very unlikely that there is a lower triplet level than that involved in this 3400A transition, since the lowest frequency band of the absorption agrees almost exactly with the highest frequency band of the phosphorescence emission.[1] In general emission in polyatomic molecules in condensed media has been observed only from the lowest level above the ground state of a given multiplicity, even though excitation occurs exclusively in higher levels.[6] It is, therefore, more likely that the singlet-triplet absorption at 3400A and its corresponding emission are to be correlated with the lowest triplet level ($^3B_{1u}$) predicted by theory. Absorption to the higher triplet levels ($^3E_u^-$ and $^3B_{2u}$) is expected to be hidden by the much more intense singlet-singlet bands.

Roothaan and Mulliken[7] have indicated, however, that previously calculated integrals may be sufficiently in error to reverse the position of the

* From the dissertation submitted in partial fulfillment of the requirements for the Degree of Doctor of Philosophy at the University of California at Berkeley.

** Shell Research Fellow in Chemistry 1946–1947. Abraham Rosenberg Fellow in Chemistry 1947–1948. Present address: Department of Physics, University of Chicago, Chicago, Illinois.

[1] G. N. Lewis and M. Kasha, J. Am. Chem. Soc. **66**, 2100 (1944).

[2] G. N. Lewis and M. Kasha, J. Am. Chem. Soc. **67**, 994 (1945).

[3] A. L. Sklar, J. Chem. Phys. **5**, 669 (1937).

[4] M. Goeppert-Mayer and A. L. Sklar, J. Chem. Phys. **6**, 645 (1938).

[5] A. London, J. Chem. Phys. **13**, 396 (1943).

[6] Data on this point are not too convincing in the literature. Further evidence to be published soon has been obtained by Dr. M. Kasha of this laboratory.

[7] C. C. J. Roothaan and R. S. Mulliken. J. Chem. Phys. **16**, 118 (1948).

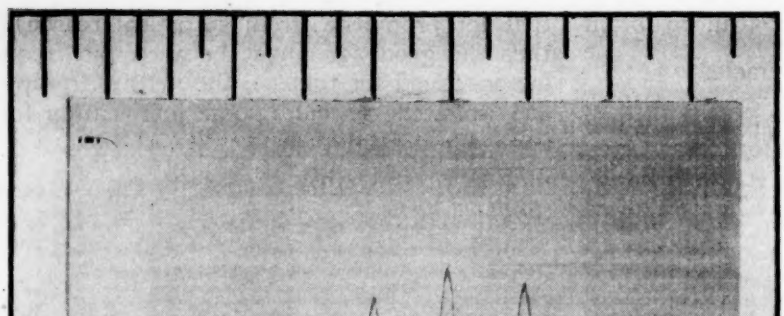

FIG. 1. Microphotometer tracing of the triplet-singlet emission spectrum at a 2× magnification of the frequency scale of the actual spectrum.

$^3B_{1u}$ and $^3B_{2u}$ levels. It is of interest, therefore, to examine the absorption and emission systems to establish definitely the symmetry of this triplet level.

Since the singlet-triplet absorption has been observed only in samples of liquid benzene with at least a 10-cm optical path (ϵ approximately 0.0004), as a series of weak bands superimposed upon the tail of the 2600A singlet-singlet absorption band, little information may be derived from it concerning the triplet state. There is noticeable in this weak absorption a series of four bands with separations of about 900 cm^{-1}, and this progression may be assigned to the totally symmetric frequency in the triplet state. This is the more probable since this vibration has been observed to have a frequency of 992 cm^{-1} in the ground $^1A_{1g}$ state,[8] 923 cm^{-1} in the first excited $^1B_{2u}$ state,[9] and about 965 cm^{-1} in the second excited singlet state.[10] Even the absolute position of this absorption observed in liquid benzene may not be used to locate definitely the 0,0 band, since the emission spectrum has been obtained only in a rigid glass-solution, and the absolute positions of the spectra in the two media are not comparable. Further experiments are in progress in this laboratory to attempt the recording of this absorption band in the same rigid medium in which the phosphorescence emission was obtained. It is to be presumed that the same type of absolute correlation could be obtained through the observation of both the emission and absorption of crystalline benzene. The excellent absorption spectra obtained by Kronenberger[11] with crystalline benzene at 20°K did not include the range of the singlet-triplet absorption, and it is doubtful if large enough single crystals were obtained in this investigation to measure these weak bands.

TABLE I. Observed frequencies of the bands in the 3400A triplet-singlet emission of benzene.

1. 29,470±10 cm^{-1}	10. 25,555
2. 28,784	11. 25,125
3. 28,460	12. 24,933
4. 28,310	13. 24,743
5. 27,891	14. 24,577
6. 27,308	15. 24,149
7. 26,893	16. 23,735
8. 26,308	17. 23,163
9. 25,916	18. 22,900
	19. 21,850

The triplet-singlet emission spectrum of benzene has previously been reported by Lewis and Kasha[1] and Nauman.[12] All spectra in these investigations were obtained with the use of a wide slit. This slit width, 0.3 to 0.5 mm, is too wide even for the moderate dispersion of the medium Hilger quartz spectrograph used and for the general width of the benzene bands. These investigations, designed merely for qualitative considerations, did not

[8] N. Herzfeld, C. K. Ingold, and H. G. Poole, J. Chem. Soc. (London) **1946**, 316.
[9] F. M. Garforth, C. K. Ingold, and H. G. Poole, J. Chem. Soc. (London) **1948**, 491.
[10] G. Nordheim, H. Sponer, and E. Teller, J. Chem. Phys. **8**, 455 (1940).
[11] A. Kronenberger, Zeits. f. Physik. **63**, 494 (1930).
[12] R. V. Nauman, Dissertation, University of California at Berkeley, 1947.

permit accurate analysis because of lack of sufficiently precise calibrations.[13]

EXPERIMENTAL

A new spectrum of the phosphorescence emission of benzene has been obtained using a much narrower slit (0.10 mm) and, consequently, a much longer exposure (30 hours). Figures 1 and 2 show typical tracings of this new benzene spectrum with the frequency scale magnified 2× and 10×, respectively. The bands are arbitrarily numbered from the high frequency end. Band 3 is, of course, less accurately measured, but it is included because of the importance of the first few differences in establishing the analysis. Table I lists the frequencies of all the observed bands.

A sample of very pure benzene, crystallized seven times by the method of Lewis and Kasha,[1] was dissolved in EPA (5 parts absolute ether, 5 parts isopentane, and 2 parts absolute ethyl alcohol) and solidified at liquid nitrogen temperatures. The phosphoroscope was essentially that used by Lewis and Kasha with a small rotating can, quartz dewar, and test tube. The source was a hydrogen arc (National Technical Laboratories No. 2230). The use of a much smaller quartz dewar and test tube (diameter ½ inch) enabled the source and the spectrograph slit to be placed very close to the sample tube, eliminating the use of all quartz lenses. The sample was changed approximately once an hour to avoid emission from possible photo-chemical decomposition products.

The errors mentioned in reference 13 were avoided by superimposing a low pressure mercury calibration spectrum directly upon a portion of the emission spectrum of benzene without moving either the slit or the plate holder. A dispersion curve was made from the calibrating lines for each

TABLE II. Comparison of frequencies observed in the gas phase (see reference 14) and crystal (see reference 11) absorption and fluorescence spectra of benzene.

Assignment	Gas frequency	Solid frequency
$a_{1g}(B_{2u})$	923 cm^{-1}	923 cm^{-1}
$e_g^+(B_{2u})$	3085	3099*
$e_g^+(B_{2u})+2\times e_u^+(B_{2u})$	1000	988
$a_{1g}(A_{1g})$	992	990
$e_g^+(A_{1g})$	606	600

* This value is corrected according to the new interpretation of the B_{2u} frequencies suggested by C. K. Ingold and F. M. Garforth, J. Chem. Soc. (London) **1948**, 417. Better agreement is obtained with this interpretation than with that proposed by the SNST analysis (see reference 14).

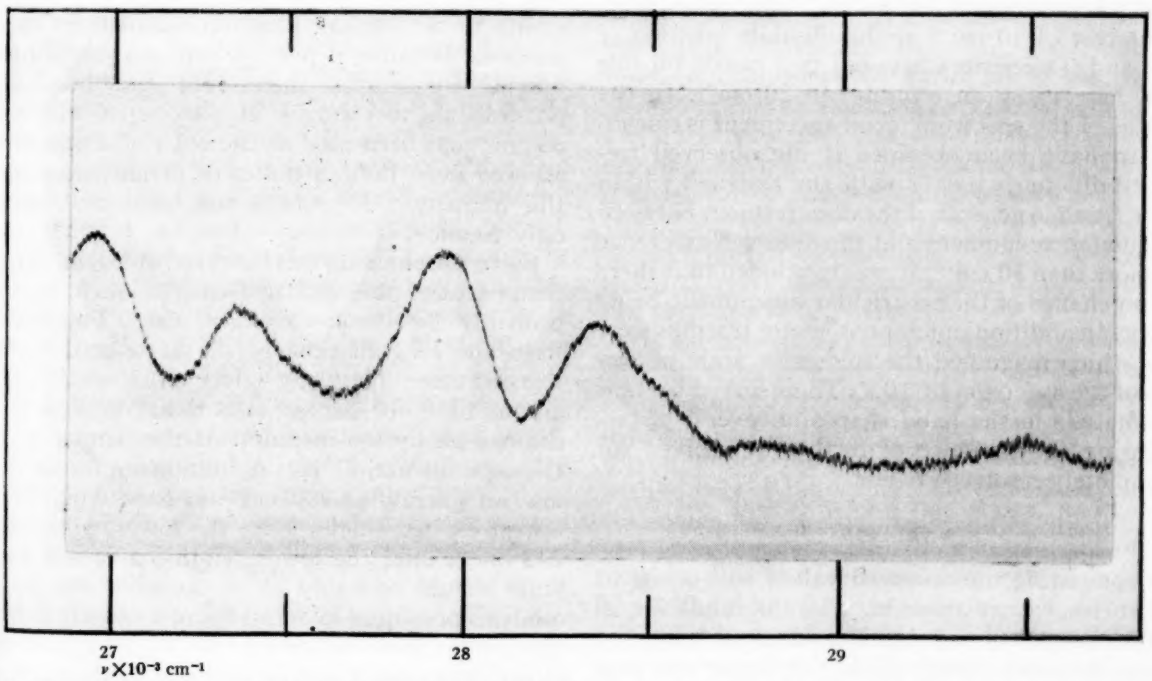

FIG. 2. Microphotometer tracing of the higher energy bands of the triplet-singlet emission spectrum at a 10× magnification of the frequency scale.

[13] It was the general practice to move the plate-holder, narrow the slit and place adjacent to the phosphorescence spectrum that of a low pressure mercury arc. A calibration curve was used common for all plates, and spectra were located with respect to this calibration curve through the use of the mercury lines. This procedure introduced three errors: (1) the movement of the plate-holder may have displaced the observed spectrum with respect to the calibration lines, (2) narrowing the slit displaces the spectrum, and the maxima observed with a wide slit do not coincide with those observed with a narrow one, (3) two successive plates placed in the same plate-holder do not necessarily assume the same curvature, and it is important to use a separate calibration curve for each plate. Previously published spectra and frequencies[1,2,12] may therefore be in error up to perhaps 150 cm^{-1} not withstanding smaller limits of error suggested in these papers.

TABLE III. Data of Halford and Schaeffer (see reference 15) on corresponding infra-red bands of benzene in the vapor, liquid, and solid states close to the melting point.

Vapor	Liquid	Solid	Vapor	Liquid	Solid
671	674	676	1755	1760	1764
779	774	766	1811	1822	1836
1032	1033	1037	1880	1880	1890
1243	1247	1252	1954	1965	1982
1385	1393	1396	2215	2210	2220
1483	1478	1485	2620	2600	2600
1615	1614	1616	3085	3065	3070
1655	1650	1650			

individual plate so that no errors were introduced as a result of change in plate curvature. Each plate was traced several times with a Zeiss recording microphotometer with varying slit widths both through a portion of the spectrum upon which the mercury lines had been superimposed and through a portion in which the calibration lines were absent. Measurements were made upon the tracings by the use of a comparator reading to 0.001 mm, and possessing highly accurate ways for both horizontal and vertical motion. Such accuracy was not at all necessary in this work, however, since the nature of the emission spectrum is such that measurements of the maxima can be made only to about 0.1 mm upon a 2× tracing. This corresponds to an error of 10 cm^{-1} in the absolute position of any band. Differences between two peaks, on this basis, may carry an error up to 20 cm^{-1}. In the analysis of the spectrum, good agreement is considered to have been obtained if the observed frequency difference agrees with the assigned within 30 cm^{-1}, and in general, if the disagreement between a calculated assignment and the observed difference was more than 50 cm^{-1}, it was concluded that there was no chance of that particular assignment being correct. In addition, microphotometer tracings were made which magnified the frequency scale of sections of the spectrum by 10×. These served to show asymmetries in the band shapes in several places, indicating the presence of further unresolved (or incompletely resolved) bands.

ANALYSIS

In comparing the observed values with assigned frequencies, we are assuming that the fundamental frequencies calculated by Ingold *et al.*[8] for the gaseous state are closely applicable to the emission spectrum in a rigid glass-solution at liquid nitrogen temperature. That this is valid is not obvious *a priori*, but several data may be quoted to make it more reasonable. Sponer, Nordheim, Sklar, and Teller[14] in their analysis of the gaseous absorption and fluorescence of benzene also re-examined data obtained by Kronenberger[11] upon the crystal at 20°K. They found the spectrum shifted by 261 cm^{-1}, but typical vibrational differences were found relatively unchanged. Some examples are shown in Table II.

Halford and Schaeffer[15] took the infra-red spectrum of benzene in the solid, liquid, and vapor states close to the freezing point of benzene. Their data may be examined for the effect of state of aggregation upon the vibrational frequency, but not of the temperature, since the latter variable was not changed significantly in this particular investigation. Typical examples of corresponding bands in the three states are assembled in Table III. From inspection of the spectra these may easily be identified as corresponding bands. The differences observed are in most cases hardly more than the errors in the determination of the vapor phase frequencies themselves, involving as they do, the assumption of harmonic vibrations. Halford and Schaeffer conclude that "the molecular vibrations retain their individualities in the condensed phases to a very high degree."

The close agreement of the easily observed totally symmetric frequencies in the phosphorescence emission with that in the gas phase as shown below is a final indication of the validity of using the complete set of gas phase fundamentals in this analysis. Because of possible errors in these fundamental frequencies themselves and because of possible slight changes in passing to the solid, 30 cm^{-1} has been used as the limit of disagreement allowed even though the error in measurement of the frequency differences has been indicated as only 20 cm^{-1}.

Since the emission was observed at liquid nitrogen temperature, the emitting triplet state is most probably in a non-vibrating state. This follows from the long lifetime of the state and the low temperature. The long lifetime, 7 sec.[16] allows ample time for excess vibrational energy to be drained off by the medium. At the temperature of the experiments, 77°K, the Boltzmann factor for as low an energy as 200 cm^{-1} is only 0.02. In the lowest excited singlet state the lowest vibration is 243 cm^{-1},[9] and the lowest vibration in the triplet state should probably be in the same range. The analysis presented in detail below makes it unlikely that such a low vibrational level of the triplet state is involved, and consequently the weakness of the first few bands may not be attributed to a Boltzmann distribution in low vibrational levels of this state. The weakness of bands 1, 2, 3, and any others in this series concealed by the remainder of

[14] Sponer, Nordheim, Sklar, and Teller, J. Chem. Phys. **7**, 207 (1939).

[15] R. S. Halford and O. A. Schaeffer, J. Chem. Phys. **14**, 141 (1946).

[16] D. S. McClure, Dissertation, University of California at Berkeley, 1948.

the spectrum, does set them apart from the remaining bands, and any adequate analysis should have at least a qualitative explanation of this fact. Since it is concluded that the initial state is the lowest vibrational level of the triplet molecule, all differences observed must be characteristic of the ground state. This is an important factor contributing to the simplicity of the spectrum.

A final assumption is made for the purpose of the analysis that the symmetry selection rules for this intercombination transition are the same as for singlet-singlet transitions. That this may not be the case is shown by some examples in diatomic molecules. The use of this assumption will lead, however, to a correct choice of the symmetry of the singlet level which interacts with this triplet level to make the transition observed.

A glance at the spectrum immediately suggests that bands 4, 6, 8, 10 and bands 5, 7, 9 (11 or 12), form two series. Calculation of these differences shows that, excepting 8–10 which will be discussed later, they do indeed fall very nicely into line, and that they correspond to expected series of totally symmetric vibrations. The differences are: 4–6, 1002 cm^{-1}; 6–8, 1000 cm^{-1}; 5–7, 998 cm^{-1}; 7–9, 977 cm^{-1}; 9–12, 983 cm^{-1}. The average of these, 992 cm^{-1}, is to be compared with the a_{1g} fundamental of 992 cm^{-1}. In addition similar differences appear between other bands which may possibly be linked to this vibration, but not in any long series. Examples are: 10–14, 11–15, 13–16, 15–17 with values 978, 976, 1008, 986 cm^{-1} respectively, averaging 987 cm^{-1}. For the further analysis of the spectrum, two possibilities must be considered. Either band 1 is the 0,0 band or it is not the 0,0 band. In the former case, the 0,0 band may be assumed observable either because the transition is permitted under the symmetry selection rules or because the close environment of the rigid medium perturbs the otherwise forbidden transition and makes it weakly observable. First we may consider the assumption that band 1 is the 0,0 band.

Under this assumption, the differences between band 1 and the next few bands must most likely represent fundamental frequencies of the ground state. It is not considered likely that combination frequencies will be important relative to the fundamental vibrations. The 1–2 difference, 686 cm^{-1}, may be ascribed within the above mentioned limits of error either to 671 (a_{2u}) or 703 (b_{2g}). Also 1010 (1–3, less accurately known) is in the region of 970 (e_u^+), 985 (b_{2g}), 992 (a_{1g}), 1010 (b_{1u}), and 1039 (e_u^-). Difference 1–4 of 1160 cm^{-1} is close only to 1178 (e_g^+), and 1–5 of 1579 cm^{-1} is close only to 1596 (e_g^+). Since the latter two bands are each identifiable only with a single fundamental frequency, both of which are of the same symmetry type, and since these two bands are the first two

TABLE IV. Fundamental frequencies of benzene from Ingold (see reference 8) (column 2) and the same plus the 1–2 observed difference of 686 cm^{-1}.

Symmetry	Fundamental Frequency	Fundamental+686
e_u^+	405	1091
e_g^+	606	1292
a_{2u}	671	1357
b_{2g}	703	1389
e_g^-	849	1535
e_u^+	970	1656
b_{2g}	985	1671
a_{1g}	992	1678
b_{1u}	1010	1696
e_u^-	1039	1725
b_{2u}	1110	1796
e_g^+	1178	1864
a_{2g}	1326	2012
e_u^-	1485	2171
e_g^+	1596	2282
b_{2u}	1648	2334
e_g^+	3047	3733
b_{1u}	3060	3746
a_{1g}	3062	3748
e_u^-	3080	3766

of the high intensity group, we are led to the suggestion that the transition is a forbidden one, but appears weakly due to perturbations by the medium, and more strongly when perturbed by vibrations of e_g^+ symmetry.

For combinations with an A_{1g} ground state, only four types of states may be associated with e_g^+ vibrations. These are B_{2u}, B_{1u}, E_u^+, and E_u^-. Furthermore, it may be shown group theoretically that all of these transitions are associated only with g vibrations (a consequence of the electric moment operator having only u characteristics). Hence, if differences 1–4 and 1–5 are to be identified with g vibrations, so must also differences 1–2 and 1–3. This limits the interpretation of difference 1–2 to the 703 (b_{2g}) vibration, and 1–3 to either the 985 (b_{2g}) or 992 (a_{1g}) vibration.

Of the four states mentioned above as associated with e_g^+ vibrations, only two may also be associated with b_{2g} vibrations. These are B_{1u} and E_u^+. Since benzene has an even number of electrons, the wave-function for each state must be symmetric with respect to the plane of the ring. This condition eliminates E_u^+, leaving B_{1u} as the symmetry of the perturbing singlet state.

We must consider now all other reasonable possibilities in order to determine if any of the remainder are as satisfactory in accounting for the first five bands as this one which considers the 1–2 difference as the b_{2g} 703 cm^{-1} fundamental. There is no possible fit if we consider the 1–2 difference as the 671 a_{2u} vibration. For transition to the ground A_{1g} state, this choice would imply that the lowest triplet was perturbed by a state of symmetry E_g^- or A_{1g}. The former state is eliminated because it is antisymmetric to the benzene plane. If A_{1g}, the vibrations allowed would be of symmetrv a_{2u} or e_u^-,

having frequencies of 671 (a_{2u}), 1039, 1485, 3080 (e_u^-). Difference 1–4 of 1160 cm^{-1} can hardly correlate with any of these or with the possibility of 671+992=1663 cm^{-1}. One is led to the conclusion, then, that if band 1 is the 0,0 transition, band 2 is certainly due to the 0,1 transition involving one quantum of 703 cm^{-1} b_{2g}.

We next must examine the possibility that the 0,0 band is not observable because of the forbidden character of the transition. It is then presumed that the spectrum observed is due to perturbation of the symmetry by certain vibrations with resulting violation of the selection rules. The band differences observed should then be found to agree with differences in fundamental frequencies, especially for the first band. In Table IV, therefore, appear all the fundamental frequencies of benzene in column 2, and in column 3 these frequencies plus the observed 1–2 difference of 686 cm^{-1}. Where coincidences are found between column 2 and column 1 there is the possibility that the 0,0 band is as many wave numbers above band 1 as the lower of the two frequencies concerned. This new 0,0 position may then be used for a band analysis in the same manner as when band 1 was considered as the 0,0 band.

Being slightly liberal with the 30 cm^{-1} error suggested, six coincidences are found. Three of these correspond to the impossible situation of a g and a u vibration arising from the same electronic level. These are the coincidences 671 (a_{2u})+686 =1357 with 1326 (a_{2g}); 985 (b_{2g})+686=1671 with 1648 (b_{2u}); 992 (a_{1g})+686=1678 with 1648 (b_{2u}). There remain three coincidences which must be examined in more detail. These are 405 (e_u^+)+686 =1091 with 1110 (b_{2u}); 606 (e_g^+)+686=1292 with 1326 (a_{2g}); 970 (e_u^+)+686=1656 with 1648 (b_{2u}).

First, consider the possibility that the 0,0 band is 405 cm^{-1} above the band 1. Then the frequency differences between the 0,0 band and the first five bands observed are: 405, 1091, 1415, 1565, 1983. The e_u^+ vibration 405 cm^{-1} and the 1110 b_{2u} vibration (1091), imply an electronic state of symmetry B_{1g} or E_g^+. If the latter, the totality of allowed vibrations are 405, 970, 1010, 1039, 1110, 1485, 1648, 3060, 3080. The observed 1415 may be correlated with 405+992=1397, but there is no possible correlation for the 1565 band. 1983 could not possibly be correlated with 1110+992=2102 and this leaves the first two strong bands with no theoretical counterpart. Therefore, an E_g^+ state at this frequency seems out of the question. The B_{1g} symmetry is unsuitable because it does not satisfy the requirement of being symmetric with respect to the molecular plane.

The second case places the 0,0 band 606 cm^{-1} above band 1, and the new differences between this and the observed bands are 606, 1292, 1616, 1766, 2185. Since 606 is of symmetry e_g^+ and 1292 corresponds to 1326 of symmetry a_{2g}, the only symmetry allowing vibrations of these two types is E_u^-. Transitions between E_u^- and A_{1g}, however, are allowed. It seems unlikely that this possibility is correct, for the suggestion of an E_u^- symmetry was arrived at only with the supposition that the transition was forbidden. Even so, the vibrations might also be considered. The totality of allowed vibrations are 606, 849, 992, 1178, 1326, 1596, 3047, 3062. The first three observed differences may be correlated with 606, 1326, 1596, but there are no possibilities for the next one. The combination 849+992=1841 cannot be used for 1766, but 1178+992=2170 agrees well with 2185. Since the first important band is still unaccounted for, and the selection rules do not follow any normal pattern, this is also considered an unlikely possibility.

The final case for consideration places the 0,0 band 970 cm^{-1} above band 1. The new differences then become 970, 1656, 1980, 2130, 2549. If 1656 is the 1648 b_{2u} vibration then the perturbing level is either of symmetry E_g^+ or B_{1g} as in case 1 above and the allowed vibrations are 405, 970, 1010, 1039, 1110, 1485, 1648, 3060, 3080. None of the remaining three bands may be correlated with fundamentals. Difference 1980 is closely 970+992=1962, and 2130 just falls within the range of 1110+992=2102, but 2549 has no counterpart. Hence this analysis is also discarded.

Thus, careful analysis of all the reasonable possibilities shows there is but one satisfactory way of accounting for the first five bands observed. This will henceforth be considered as the correct choice in the following discussion.

Returning to this choice, the 1–2 difference has been settled as corresponding to the 703 b_{2g} vibration. There are two possibilities for the 1–3 difference. As may be seen from the tracings, this is a relatively inaccurately measured shoulder and the value 1010 cm^{-1} could correspond either to the 985 b_{2g} or 992 a_{1g} vibration. The latter might be expected to appear to about the same intensity as the 1 band because of perturbations by the rigid medium. There is no obvious reason why the 985 band should either be present or absent other than its being of appropriate symmetry. Thus it is equally hard to explain why the 606 e_g^+ vibration prominent in the fluorescence and singlet absorption spectra does not appear here at all. Its absence is most logically ascribed to the Franck-Condon principle. Differences 1–4 and 1–5 were explained by the appropriate e_g^+ vibrations, while 6, 7, 8, 9, and 12 were accounted for on the basis of a_{1g} progressions. It would not be surprising if some of the higher bands and shoulders were hard to account for, as there are undoubtedly many bands of varying intensities superimposed, and the max-

ima measured may not accurately represent true maxima of the component bands.

Band 10, however, is moderately sharp and the measurement of its position should be fairly accurate. When the differences between it and preceding bands are considered, no correlation with fundamentals of appropriate symmetry is possible. From the tracing it appears generically to belong to the series 4–6, 6–8, 8–10, but the 8–10 difference is only 753 cm^{-1}, far from the expected 992 cm^{-1}. This band must come from higher combinations. Since it is fairly intense, it is logical to suggest that it is the result of a combination band superimposed upon bands 4, 5, 6, or 7. It is unlikely that such intensity could be gained by superimposing combinations upon the weaker series of bands 1, 2, or 3.

For this reason, a complete survey was made of all binary combination possibilities of benzene. Difference 4–10 is 2755 cm^{-1}, and the combinations within 40 cm^{-1} of this value are

$$1110\ (b_{2u})+1596\ (e_g^+)=2706\ (e_u^+),$$
$$1110\ (b_{2u})+1648\ (b_{2u})=2758\ (a_{1g}),$$
$$1178\ (e_g^+)+1596\ (e_g^+)=2774\ (a_{1g}, a_{2g}, e_g^+).$$

The latter two are of appropriate symmetry for the combination since superimposed upon e_g^+ vibrations may be expected only a_{1g} vibrations (although some other types may possibly appear according to group theory). The last one is the more likely since involved in it are vibrations already known to be excited.

The combinations corresponding to the difference 5–10 of 2336 cm^{-1} are

$$671\ (a_{2u})+1648\ (b_{2u})=2319\ (b_{1g}),$$
$$703\ (b_{2g})+1596\ (e_g^+)=2299\ (e_g^-),$$
$$703\ (b_{2g})+1648\ (b_{2u})=2351\ (a_{1u}),$$
$$849\ (e_g^-)+1485\ (e_u^-)=2334\ (a_{1u}, a_{2u}, e_u^+),$$
$$985\ (b_{2g})+1326\ (a_{2g})=2311\ (b_{1g}),$$
$$992\ (a_{1g})+1326\ (a_{2g})=2318\ (a_{2g}),$$
$$1010\ (b_{1u})+1326\ (a_{2g})=2336\ (b_{2u}),$$
$$1039\ (e_u^-)+1326\ (a_{2g})=2365\ (e_u^-),$$
$$1178\ (e_g^+)+1178\ (e_g^+)=2356\ (a_{1g}, a_{2g}, e_g^+).$$

Only the last one has symmetry a_{1g}, and once again this involves a vibration known to be excited (for band 4).

6–10 has a difference of 1753 cm^{-1} to which correspond the following combinations.

$$405\ (e_u^+)+1326\ (a_{2g})=1731\ (e_u^+),$$
$$606\ (e_g^+)+1110\ (b_{2u})=1716\ (e_u^-),$$
$$606\ (e_g^+)+1178\ (e_g^+)=1784\ (a_{1g}, a_{2g}, e_g^+),$$
$$671\ (a_{2u})+1110\ (b_{2u})=1781\ (b_{1g}),$$
$$703\ (b_{2g})+1039\ (e_u^-)=1742\ (e_u^+).$$

There is once again one of the appropriate symmetry involving e_g^+ vibrations. This time, however, there is involved the 606 vibration which did not appear in the early bands. It can thus be seen that there is no lack of combinations from which to choose, and no certain choice may be made among them.

Particularly suggestive, however, is the combination of two units of 1178 added onto one of 1596 to give band ten, for it is found that two units of 1596 added onto one of 1178, a total of 4370 corresponds fairly well to 4345, the hitherto unexplained 1–11 difference. Allowing 10–14 (978 observed) 11–15 (976 observed), and 15–17 (986 observed) as a_{1g} vibrations, this leaves bands 13, 16, 18, and 19 as yet unaccounted for. Of these 13 and 16 are connected by what is possibly an a_{1g} vibration (1008 observed). The 1–13 difference of 4727 observed is not too far away from three units of 1596 = 4788. Further speculation on these weak bands of uncertain position is not profitable at this time. Table V summarizes the analysis.

DISCUSSION

The analysis leads to the conclusion, therefore, that the 3400A triplet-singlet emission is observed because of mixing with the triplet level of a singlet level of symmetry B_{1u}. This will lead to a definite decision as to the symmetry of the lowest triplet level when the intercombination selection rules are fully understood. At the present time, it is not clear whether B_{1u} singlet states will mix with B_{1u} or B_{2u} triplet states, and a final choice must wait until this point is clarified. In diatomic molecules $^3\Sigma^+$ states act like $^1\Sigma^-$ states when they combine with singlet states, and this situation may also

TABLE V. Proposed assignment of bands for the triplet-singlet emission of benzene at 3400A. In each case the transition is from the 0 vibrational level of the triplet state to the level of the ground state indicated.

Band (x)	Vibrational Level of $^1A_{1g}$ State	Difference $1-x$ Calc'd.	Obs'd
1	0	0	0
2	1 of 703 (b_{2g})	703	686
3	1 of 985 (b_{2g}) or 1 of 992 (a_{1g})	985 or 992	1010
4	1 of 1178 (e_g^+)	1178	1160
5	1 of 1596 (e_g^+)	1596	1579
6	1 of 1178 (e_g^+)+1 of 992 (a_{1g})	2170	2162
7	1 of 1596 (e_g^+)+1 of 992 (a_{1g})	2588	2577
8	1 of 1178 (e_g^+)+2 of 992 (a_{1g})	3162	3162
9	1 of 1596 (e_g^+)+2 of 992 (a_{1g})	3580	3554
*10	1 of 1596 (e_g^+)+2 of 1178 (e_g^+)	3952	3915
*11	1 of 1178 (e_g^+)+2 of 1596 (e_g^+)	4370	4345
12	1 of 1596 (e_g^+)+3 of 992 (a_{1g})	4572	4537
*13	3 of 1596 (e_g^+)	4788	4727
*14	1 of 1596 (e_g^+)+2 of 1178 (e_g^+) +1 of 992 (a_{1g})	4944	4893
*15	1 of 1178 (e_g^+)+2 of 1596 (e_g^+) +1 of 992 (a_{1g})	5362	5321
*16	3 of 1596 (e_g^+)+1 of 992 (a_{1g})	5780	5735
*17	1 of 1178 (e_g^+)+2 of 1596 (e_g^+) +2 of 992 (a_{1g})	6354	6307
18	Not assigned	—	6570
19	Not assigned	—	7620

* Assignment of these bands is less certain.

occur in polyatomic molecules.[17] In that case a B_{1u} singlet state would perturb a B_{2u} triplet state. A B_{2u} assignment for the lowest triplet state would not agree with previous theoretical calculations.[3,4]

Several final points may be brought out. First, the present analysis very nicely accounts for the weakness of the first few bands. The 0,0 band 1 appears only because of perturbations of the medium. Band 2 might be expected to have higher intensity since it involves the addition of a perturbing vibration that makes the transition allowed. That it does not do so may be attributed to the absence of any other nearby electronic level for which the transition moment to the ground state is polarized in the Z direction. Thus the 2600A benzene band's weakness relative to the 2000A band has been attributed to the proximity of the latter to the allowed 1800A $E_u^- \rightarrow A_{1g}$ transition.[10] The observations indicate that the band series observed for both these singlet forbidden bands involve an electric moment in the plane of the ring. No transitions are known at all in which polarization perpendicular to the ring may be expected, nor are any calculated by the molecular orbital treatment. It would seem logical, therefore, to believe that band 2 and possibly the shoulder 3 would not appear at all because of the absence of a suitable transition from which to "borrow," except for the perturbing influence of the medium. This would, therefore, account for the observation that bands 1 and 2 (and possibly 3) are of almost identical intensity. Bands 4 and 5, of course, from this viewpoint are much stronger since in this case there is a nearby electronic transition from which they can borrow some intensity.

This immediately suggests that the fluorescence of benzene should be re-examined under similar conditions in a rigid medium. Sponer, Nordheim, Sklar, and Teller[14] made no mention of finding either the 703 or 985 b_{2g} vibrations, but the plates of Radle and Beck[18] should be re-examined for them. The absence of these vibrations in the gas phase, however, does not preclude their appearance in the rigid medium, where they are much more likely to be found, judging from the phosphorescence analysis above.

Examination of Kronenberger's[11] data on crystalline benzene at liquid hydrogen temperature indicates the possible presence of the b_{2g} vibration which is 985 cm^{-1} in the A_{1g} state but 775 cm^{-1} in the lowest excited singlet state.[9] Assuming the assignment of the 0,0 band at 37,828 cm^{-1},[14] the theoretical position of this b_{2g} vibration would be at 38,603 cm^{-1}. Kronenberger reports a weak band at 38,600 cm^{-1}, which may possibly be thus assigned. There is no evidence of the 703 b_{2g} vibration which drops to 365 cm^{-1} in the excited state. If this assignment were found to be correct, the lowest excited singlet state would have to be redesignated as B_{1u}. The fact that this reported band is much weaker than the forbidden 0,0 band in this transition, however, makes the assignment unlikely.

Redlich and Holt,[19] using a classical analysis upon previous inaccurate data, arrived at the conclusion that their calculations supported a quinoidal model of the triplet state as proposed by Lewis and Kasha.[2] It should be pointed out that the latter proposed a non-planar model while Redlich and Holt's best model was planar. In fact, they definitely ruled out a non-planar model. Part of the evidence for the non-planar model proposed by Lewis and Kasha was the prominent 400 cm^{-1} difference in their data, which they ascribed to the 405 e_u^+ out-of-plane vibration of benzene. The present analysis has shown that a reasonable assignment may be made with the assumption of retention of D_{6h} symmetry in the triplet state. The previous assumptions attributing the weakness of the first few bands to the Franck-Condon principle have been found unnecessary. In view of the success of analyzing the 2600A singlet-singlet absorption and fluorescence bands[14] and, in the present case, the triplet-singlet emission on the basis of hexagonally symmetric excited states, it would seem likely that this configuration is the most probable one.

Sponer, Nordheim, Sklar, and Teller[14] pointed out that in the totally symmetric progressions observed by them in the analysis of the lowest excited singlet state, the usual case was that the second member was the most intense, while the first and third were of about equal intensity but somewhat lower. It is apparent from the tracings that the same is true of the phosphorescence emission spectrum, and the considerations applied by these authors may be applied equally well here. These suggested that the increase in the ring size was of the order of magnitude of 0.1A, showing that despite disturbance of the π bonds, the molecule is rather securely held by its σ-bond framework.

Ingold *et al.*[20] have succeeded in setting up an approximate potential function for the lowest excited singlet state as a result of their assignment of most of the vibrational frequencies of this state. They conclude from consideration of the relationships between force constants and bond lengths that the increase in size for this singlet state is

[17] The author is indebted to Professor R. S. Mulliken for pointing this out.

[18] W. F. Radle and C. A. Beck, J. Chem. Phys. **8**, 507 (1940).

[19] O. Redlich and E. K. Holt, J. Am. Chem. Soc. **67**, 1228 (1945).

[20] F. M. Garforth, C. K. Ingold, and H. G. Poole, J. Chem. Soc. (London) **1948**, 508.

about 2½ percent or 0.04A in the C−C bond. It is likely that the change in size of the molecule in passing to the triplet state is of the same order of magnitude. That there are, however, some fundamental differences in the shape of the lowest triplet and lowest excited singlet states is shown by the prominence of the 1178 and 1596 cm^{-1} e_g^+ vibrations in the triplet emission, whereas the 606 and 1596 e_g^+ vibrations are prominent in the singlet emission.

THE JOURNAL OF CHEMICAL PHYSICS VOLUME 17, NUMBER 3 MARCH, 1949

The Configuration of Real Polymer Chains*

PAUL J. FLORY
Department of Chemistry, Cornell University, Ithaca, New York

(Received August 23, 1948)

The average configuration of polymer molecules in solution is markedly influenced by the obvious requirement, ordinarily disregarded in problems relating to molecular configuration, that two elements of the molecule are forbidden from occupying the same location in space. The influence of spatial "interferences" between different segments of the molecule on its average configuration has been investigated by statistical and thermodynamic methods.

It is shown that if the average linear dimension of a polymer chain is to be taken proportional to a power of the chain length, that power must be greater than the value 0.50 previously deduced in the conventional "random flight" treatment of molecular configuration. This power should approach 0.60 for long chain molecules in good solvents. With increase in size of the solvent molecule, the influence of interference on molecular configuration diminishes, vanishing entirely in the extreme case of a solvent which is also a high polymer. The effect of a heat of interaction between solvent and polymer may also be incorporated quantitatively in the theory. A positive heat of mixing (poor solvent) tends to offset the expansive influence of interference, and the exponent referred to above tends to approach 0.50. The results are of foremost significance in the interpretation of the intrinsic viscosity and its dependence on the polymer constitution and on the solvent. It is pointed out that the spatial dimensions of the irregularly coiled polymer molecule cannot be correlated directly with hindrance to rotation about chain bonds, unless the expansion of the configuration due to interference and the effects of the heat of dilution are first of all taken into account.

INTRODUCTION

THE spatial configuration of randomly coiled chain polymer molecules is customarily treated in the "random flight" approximation, according to which each element, or "segment," of the chain is considered to be free to choose any orientation with respect to its predecessor, independent of the locations of all other segments of the same molecule. Impossible configurations which would require two segments to occupy the same element of volume are not excluded from consideration. The effects of short range "interferences" of this nature between two segments situated in close proximity along the chain are readily taken into account approximately by merely enlarging the effective segment length somewhat, the form of the equation expressing the nature of the chain configurations being unaltered.[1] The influence of long range interferences between remotely related segments of the same chain is not so easily disposed of, however.

The average "density" of polymer within the region occupied by a chain of a thousand segments may be of the order of only one percent. The chance that a given segment will seek to occupy the site occupied by some other remotely connected segment will be relatively rare. It must not be inferred, however, that long range interferences are inconsequential under these conditions. A given "random flight" configuration for the molecule will be acceptable only in case *none* of its segments is assigned to a site occupied by another segment. The probability of compliance with this condition will be of the order of e^{-5} for a molecule of a thousand segments distributed at an average density of one percent. Only a very small fraction of the "random flight" configurations tacitly assumed in previous theories may be realized by the actual chain molecule. Interferences will be fewer on the average in more expanded configurations. Hence, a relatively larger fraction of the latter will be acceptable to the actual polymer chain and the average size of the randomly coiled molecule will be greater than that calculated by the usual procedures.

This fairly obvious influence of interference of actual chain molecules having finite lateral dimensions has been pointed out on various occasions[2-4] in the past, but it has not been investigated quantitatively. Direct treatment of the configuration problem in terms of the space coordinates for

* The greater portion of the theoretical development presented in this paper was carried out during the author's tenure as George Fisher Baker Non-Resident Lecturer in Chemistry at Cornell University for the spring term of 1948.

[1] W. Kuhn, Kolloid Zeits. **87**, 3 (1939).

[2] W. Kuhn, Kolloid Zeits. **68**, 2 (1934).

[3] M. L. Huggins, J. App. Phys. **10**, 700 (1939).

[4] R. Simha, J. Polymer Sci. **3**, 227 (1948).

each segment would be prohibitively difficult indeed. In the present paper an estimate of the effects of intra-chain interferences has been accomplished through the use of statistical methods. These lend themselves also to the taking into account of the effect on the molecular configuration of energy interactions between solvent and polymer. The results of this analysis are directly applicable to the treatment of intrinsic viscosity.

THE INFLUENCE OF LONG RANGE INTERFERENCE ON MOLECULAR CONFIGURATION

Consider a system containing N polymer molecules in a solution so dilute that the interactions between polymer molecules may be disregarded. We shall be concerned with the internal configurations of these molecules, their arrangement relative to one another throughout the solution being unimportant here. Let the state of the system be defined in terms of the numbers N_i of molecules having their ends separated by the distances r_i. Then the total number of internal configurations consistent with the given distribution of chain displacement lengths (r_i) may be written

$$\Omega = N! \prod_i (\omega_i)^{N_i}/N_i!, \tag{1}$$

where ω_i is the total number of configurations available to a chain having the "displacement length" r_i. If there were no interference, the probability W_i of a displacement length between r_i and r_i+dr_i would be given to a satisfactory approximation by the Gaussian function

$$W_i dr_i = (\beta^3/\pi^{\frac{1}{2}}) \exp(-\beta^2 r_i^2) 4\pi r_i^2 dr_i, \tag{2}$$

where

$$\beta^2 = 3/(2Zl^2), \tag{3}$$

Z being the number of segments and l the length of each segment for the "equivalent chain" composed of rigid segments connected by completely flexible bonds.[5] Consequently, in the absence of interference, ω_i would be given by $W_i\omega_0$ where ω_0 is the total number of all configurations available to the chain. Owing to interference, only a fraction f_i of these random flight configurations for the chain displacement length r_i are acceptable. Hence

$$\omega_i = f_i W_i \omega_0, \tag{4}$$

and

$$\Omega = \Omega_0 N! \prod_i (f_i^{N_i} W_i^{N_i}/N_i!), \tag{5}$$

where Ω_0 is the total number of internal configurational arrangements given by

$$\Omega_0 = \omega_0^N.$$

It will be assumed that f_i may be replaced by its average value designated by f. On introducing Stirling's approximation, the logarithm of the relative number of configurations for a given chain displacement length distribution specified by the N_i's then becomes

$$\ln(\Omega/\Omega_0) = N \ln(fN) + \sum_i N_i \ln(W_i/N_i).^6 \tag{6}$$

For the purpose of estimating f, it is convenient to adopt the lattice model customarily employed in treating the configurational statistics of polymer mixtures and their solutions. The volume of a cell of the lattice will be expressed by V, and the number of segments *of this size* in the polymer molecule will be represented by x. These "lattice segments" will not ordinarily be identical with those employed in the specification of the configuration of the chain in space. The latter generally will be larger, depending on the flexibility of the chain and on local steric interactions; i.e., x generally will exceed Z, and $V^{\frac{1}{3}}$ will be less than l. With reference to the lattice scheme, the average random flight chain is represented by a probability distribution of occupied cells within a certain region of the lattice. Since the density distribution will be variable over this region, we may consider a small portion of the region in which the average density is uniform. If there are x_j segments in this volume composed of ν_j cells, the probability that no two of the segments x_j are assigned to the same cell will be

$$f_j = \prod_{i=0}^{x_j-1} (1 - i/\nu_j) \cong \exp(-x_j^2/2\nu_j)$$

from which it follows that

$$\ln f \equiv \sum_j \ln f_j = -\sum (x_j^2/2\nu_j). \tag{7}$$

The summation in Eq. (7) depends on the spatial distribution of segments of the polymer molecule. The exact character of this distribution is difficult to ascertain. Even in the case of a hypothetical

[5] In the approximation that each bond between successive chain atoms is subject to a hindrance potential which is a function of the angle φ of rotation about that bond, and independent of other bond angles, β could be defined in accordance with the results of P. Debye (Report to the Office of Rubber Reserve, April 10, 1945) as follows:

$$\beta^{-2} = (2/3) l_0^2 n' [1+(\cos\varphi)_{Av}]/[1-(\cos\varphi)_{Av}] \times [1+\cos\theta]/[1-\cos\theta],$$

where l_0 is the length of a valence bond of the chain, n' is the number of chain bonds, and θ is the fixed valence angle (e.g. 109.5°). In general, polymer chains will not conform to this approximation (see subsequent discussion). Hence, the hypothetical chain of simply connected units, as referred to above and in other publications, is preferred here, notwithstanding the fact that the exact magnitude of l (and correspondingly of Z) remains beyond the scope of the treatment.

[6] If $f=1$ corresponding to no interference, and if the chain displacement length distribution is the most probable one specified by $N_i = NW_i$, W_i being given by Eq. (2), then $\Omega/\Omega_0 = 1$.

random flight chain, the distribution of segments about the center of gravity (unlike the chain displacement length distribution) cannot be expressed in closed form. The distribution for a real polymer chain, in addition to being expanded as a result of chain segment interference, probably will be distorted as well; the average concentration of segments near the center may be diminished relative to their concentration in outlying regions of the distribution.

Since the value of the sum in Eq. (7) is not critically dependent on the precise nature of the spatial distribution of segments, a satisfactory evaluation may be secured by arbitrarily expressing the average density of segments at a distance s from the center of gravity by a Gaussian function

$$W'(s)=(\beta'/\pi^{\frac{1}{2}})^3\exp(-\beta'^2s^2)4\pi s^2, \tag{8}$$

where the parameter β' is to be assigned a value such that the mean square distance, $\langle s^2\rangle=3/2\beta'^2$, of the segments from the center of gravity shall coincide with that for the actual distribution. For a random flight chain Debye[7] has shown that $\langle s^2\rangle=\langle r^2\rangle/6$ where r represents the distance between chain ends. According to Eqs. (2) and (3), $\langle r^2\rangle=Zl^2$. Hence,

$$\langle s^2\rangle=Zl^2/6$$

for the hypothetical random flight chain. Linear dimensions of the actual distribution of segments will be increased owing to the influence of long range interference by a factor designated by α. Hence, for a real polymer molecule

$$\langle s^2\rangle=\alpha^2Zl^2/6,$$

from which it follows that

$$\beta'^2=9/\alpha^2Zl^2. \tag{9}$$

Equation (9) specifies the value of β' which fulfills the requirement that the Gaussian distribution (8) shall yield the correct value for $\langle s^2\rangle$.

The number x_j of segments in a spherical shell of radius s_j and thickness Δs will be given by

$$x_j=xW'(s_j)\Delta s,$$

and the number of lattice cells in the same volume by

$$\nu_j=4\pi s_j^2\Delta s/V.$$

Substituting these expressions in Eq. (7) and evaluating the corresponding integral from $s_j=0$ to ∞,

$$\ln f=-Vx^2\beta'^3/2^{5/2}\pi^{3/2}$$
$$=-(27/2^{5/2}\pi^{3/2})Vx^2/(\alpha lZ^{1/2})^3. \tag{10}$$

Letting the length l' of the lattice segment equal $V^{\frac{1}{3}}$ and noting that $xl'=Zl$, the above relationship may be written

$$\ln f=-CZ^{\frac{1}{2}}/\alpha^3, \tag{11}$$

where

$$C=(27/2^{5/2}\pi^{3/2})(l'/l) \tag{12}$$
$$\cong(l'/l). \tag{12'}$$

It is obvious from the nature of the problem treated above that the actual average distribution of segments in space may be replaced by a uniform distribution of the x segments within a sphere of radius R_e so chosen as to give the required result.[8] The summation in Eq. (7) over the equivalent sphere is simply $x^2/2\nu$, where

$$\nu=(4\pi/3)R_e^3/V.$$

Hence,

$$\ln f=-3Vx^2/8\pi R_e^3.$$

Comparing this result with Eq. (10), the radius of the equivalent sphere is found to be given by

$$R_e=(\pi/2)^{1/6}(1/3)^{2/3}\alpha lZ^{1/2}$$
$$=0.52\alpha lZ^{1/2}\cong\alpha lZ^{1/2}/2. \tag{13}$$

Thus, R_e is very nearly half the root-mean-square distance between chain ends. This is about the same size as the equivalent sphere found by Debye and Bueche[9] to represent the hydrodynamic interaction of the chain with solvent in the limit of unperturbed velocity distribution ("free draining" chain) through the molecule.

In calculating the interference within the randomly coiled molecule according to the above procedure, no account is taken of the fact that segments comprising the molecule are connected to one another, and hence that these segments must occupy a contiguous set of lattice cells. The expectancy for the occurrence of a segment in a cell immediately adjacent to a cell known to be occupied has been tacitly assumed to equal the average concentration of segments at the given distance from the center of gravity. Actually, this expectancy is greater than the average concentration since the segment which occupies the given cell must be adjoined by two other segments of the same chain (assuming, of course, that the segment in question is not a terminal segment). Thus, the knowledge that a given cell is occupied by a polymer chain segment enhances the likelihood that other nearby cells are also occupied. "Short range" interferences between segments separated by only a few intervening segments are largely neglected in the above calculation. For this reason, Eqs. (10) and (11) must not be construed as

[7] P. Debye, J. Chem. Phys. **14**, 636 (1946).

[8] This procedure is similar to that employed recently by Debye in the treatment of the hydrodynamic interaction of the polymer molecule with the solvent. The writer applied a similar simplification to the treatment of the thermodynamic behavior of dilute polymer solutions. (See reference 15.)

[9] P. Debye and A. M. Bueche, J. Chem. Phys. **16**, 573 (1948).

indicative of the *total* interference within the randomly coiled molecule. In this connection it should be noted that as a result of the above averaging procedure the interference according to Eq. (11) for a chain of $2Z$ segments is less than that for two chains of Z segments, i.e., $f_{2Z} > f_Z^2$. Obviously, the total interference for the chain of $2Z$ segments must exceed that for the separate chains.

The consequences of this deficiency of the above treatment are by no means as disastrous as might be supposed, for we are concerned here merely with that part of the total interference which is dependent on the volume occupied by the molecule; i.e., only the "long range" interferences between segments belonging to remotely connected portions of the chain are appreciably affected by moderate degrees of expansion of the average configuration. For this purpose, Eq. (11) appears to afford a legitimate approximation.

It remains to evaluate the second term on the right of Eq. (6). In the absence of interference the most probable chain displacement length distribution would be defined by

$$N_i = NW(r_i),$$

where $W(r_i)$ is the probability distribution (W_i) given by Eq. (2). The increase in the effective average volume of the randomly coiled molecule brought about by interference presumably will be accompanied by a similar distortion of the chain displacement length distribution. If this is the case, this distribution for the actual molecule can be expressed as follows

$$N_i = NW(r_i/\alpha),$$

or

$$N_i dr_i = N(\beta^3/\pi^{\frac{1}{2}}) \exp(-\beta^2 r_i^2/\alpha^2)(4\pi/\alpha^3) r_i^2 dr_i. \quad (14)$$

Thus, it is assumed that the distribution over r_i is uniformly shifted by the same factor α as applies to the average radial distribution of segments about the center of gravity. Substituting from Eq. (14) for N_i and from (2) for W_i in the latter term of Eq. (6)

$$\sum N_i \ln(W_i/N_i) = N \ln(\alpha^3/N) - N(4\beta^5/\alpha^3\pi^{\frac{1}{2}})(1-1/\alpha^2)\sum_{r_i} \exp(-\beta^2 r_i^2/\alpha^2) r_i^4 dr_i.$$

Replacing the summation by the value of the corresponding integral over r_i from 0 to ∞,

$$\sum N_i \ln(W_i/N_i) = N \ln(\alpha^3/N) - 3N(\alpha^2-1)/2. \quad (15)$$

Substituting Eqs. (11) and (15) in (6) and expressing the results as an entropy $S(\alpha)$,

$$S(\alpha)/k = \ln(\Omega/\Omega_0) = N[-CZ^{\frac{1}{2}}/\alpha^3 + 3 \ln\alpha - 3(\alpha^2-1)/2]. \quad (16)$$

The equilibrium expansion factor α for which $S(\alpha)$ is a maximum, obtained by differentiating and equating to zero, is specified by the relationship

$$\alpha^5 - \alpha^3 = CZ^{\frac{1}{2}}. \quad (17)$$

TREATMENT OF THE INTERACTION OF THE POLYMER MOLECULE WITH SOLVENT AS A SWELLING PHENOMENON

It is apparent from inspection of Eq. (16) and from its derivation that the last two terms correspond to the entropy of elastic deformation of a system of independent polymer chains subjected to uniform dilution. The first term can be shown to correspond to an entropy of dilution. Thus, the above treatment resembles that previously applied to the problem of swelling of cross-linked network structures.[10] The influence of long range interference on the average configuration of a system of independent polymer molecules dispersed in an abundance of solvent may, in fact, be treated as a swelling phenomenon. One may adopt the view that the polymer segments tend to dilute themselves with more solvent in order to achieve a higher entropy of mixing. This process of dilution of the segments is accompanied by an adverse expansion of the polymer chain configurations. Equilibrium is obtained when the attendant opposing forces are in balance. The influence of a heat of mixing of segments with solvent may be included in logical fashion. The following distinction from the problem of swelling in network structures must be borne in mind, however. The individual polymer chains are independent of one another in the present problem, whereas in the swelling of a network structure the ends of the chain elements are required to meet at the network junctions.[10]

The entropy of dilution of a system of polymer segments combined in a single continuous structure may be written[11,12]

$$\Delta S_{dil}/k = -n \ln v_1, \quad (18)$$

where n is the number of solvent molecules and v_1 is their volume fraction in that system. The entropy of elastic deformation of the molecule is given by

$$\Delta S_{el}/k = 3 \ln\alpha - 3(\alpha^2-1)/2, \quad (19)$$

derivation of which is obvious from the treatment given in the preceding section.[13] The effect of a

[10] P. J. Flory and J. Rehner, Jr., J. Chem. Phys. **11**, 521 (1943).

[11] M. L. Huggins, J. Phys. Chem. **46**, 151 (1942); Ann. N. Y. Acad. Sci. **43**, 1 (1942).

[12] P. J. Flory, J. Chem. Phys. **10**, 51 (1942).

[13] W. Kuhn, R. Pasternak and H. Kuhn, Helv. Chim. Acta **30**, 1705 (1947), have deduced Eq. (19) in an equivalent, though less direct, manner. They have applied it to the treatment of swelling of network structures, overlooking the fact that it does not take into account the requirement that the chain ends must meet at the network junctions. While Eq. (19) is applicable to the treatment of independent chains,

heat of mixing of polymer and solvent may be introduced through use of an expression of the van Laar form

$$\Delta H = Bx V v_1,$$

where B is the cohesive energy density constant characteristic of a given solvent-polymer pair. Employing the conventional procedure

$$\Delta H/kT = \mu x v_1, \tag{20}$$

where μ is defined as

$$\mu = BV/kT, \tag{21}$$

which differs from the usual definition of μ in that the volume V of the lattice cell replaces the molar volume of the solvent.

Combining Eqs. (18), (19) and (20), there is obtained for the free energy of dilution

$$\Delta F/kT = n \ln v_1 + \mu x v_1 + 3(\alpha^2-1)/2 - 3\ln\alpha. \tag{22}$$

Adopting the previously employed equivalent sphere within which the polymer segments are considered to be uniformly distributed

$$n = [(4\pi/3)R_e^3 - xV]/x_s V,$$

where x_s is the number of lattice cells occupied by a molecule of solvent. In this way, the effect of the size of the solvent molecule is included. Substituting from Eq. (13) for R_e, and using the previous substitutions $V^{\frac{1}{2}} = l'$ and $xl' = Zl$,

$$n = (x/x_s)(x\alpha^3/2CZ^{\frac{1}{2}} - 1), \tag{23}$$

where C is defined by Eq. (12), or to a satisfactory approximation by Eq. (12′). Similarly,

$$v_1 = nx_s/(nx_s + x) = 1 - 2CZ^{\frac{1}{2}}/x\alpha^3. \tag{24}$$

Substituting these expressions for n and v_1 in Eq. (22) and expanding the logarithmic term in series

$$\Delta F/kT = -(1/x_s)(x - CZ^{\frac{1}{2}}/\alpha^3 - \cdots) + \mu(x - 2CZ^{\frac{1}{2}}/\alpha^3) + 3(\alpha^2-1)/2 - 3\ln\alpha. \tag{25}$$

Terms beyond the first two in the series expansion may be neglected. On equating to zero the derivative of ΔF with respect to α, there is obtained

$$C(1/x_s - 2\mu)Z^{\frac{1}{2}} = \alpha^5 - \alpha^3 \tag{26}$$

which replaces Eq. (17) of the previous development. Equation (26) reduces to (17) for the case: $x_s = 1$ and $\mu = 0$.

If the solvent and polymer mix without heat effect, $\mu = 0$ and

$$CZ^{\frac{1}{2}}/x_s = \alpha^5 - \alpha^3. \tag{26′}$$

an additional term (given by $-(3/2)\ln\alpha$ for a tetrafunctionally connected network) must be included in the elastic entropy of dilution of a network structure.

If the solvent is itself polymeric such that x_s is very large, the term on the left approaches zero and α approaches unity. Thus, a polymer molecule situated in a medium consisting of other polymer molecules of the same kind, or in a medium of unlike polymer molecules with which it mixes athermally, will occupy spatial configurations coinciding with those calculated in the random flight approximation, undistorted by interference effects. To understand the basis for this deduction, it is necessary to observe that while an expansion of the dissolved molecule decreases its interference with itself, "interference" with surrounding polymer molecules is correspondingly increased. Expansion of the molecule achieves no net improvement in the configurational freedom of the system as a whole. This deduction is important for it justifies use of the random flight approximation in the treatment of concentrated polymer systems, e.g., in the treatment of rubber elasticity.

If the solvent is of low molecular weight, x_s may be set equal to unity. It is preferable, however, to express the relationship (26) as follows:

$$C_1(1 - 2\mu_1)Z^{\frac{1}{2}} = \alpha^5 - \alpha^3, \tag{27}$$

where

$$C_1 = C/x_s \quad \text{and} \quad \mu_1 = \mu x_s.$$

It is to be noted that μ_1 ($= BV_1/RT$ where V_1 is the molar volume of the solvent) is the analog of the μ defined in previous treatments of polymer solvent interactions.[11,12,14] The present μ_1 may not be numerically equivalent to the μ deduced from thermodynamic measurements on the same polymer-solvent system. In particular, the value of μ_1 applicable here should not correspond to the μ obtained from thermodynamic measurements on *dilute* solutions.[15] The former applies to the energy interaction of an individual polymer molecule with its immediate environment; the energy contribution to the latter depends on the over-all polymer concentration in quite a different manner owing to the discontinuous nature of the solution.[15] Furthermore, the latter μ contains contributions from sources other than the interaction energy.[15]

It has often been suggested[3,12,16] that an endothermic heat of interaction between solvent and polymer should cause the randomly arranged polymer chain to contract so that it occupies a smaller volume. This expectation is abundantly confirmed by the lower intrinsic viscosity values observed in poorer solvents. Similarly, in good solvents configurations for which there are fewer polymer-to-polymer contacts will be preferred, and the molecule will therefore choose larger configurations. The

[14] P. J. Flory, J. Chem. Phys. **12**, 425 (1944).
[15] P. J. Flory, J. Chem. Phys. **13**, 453 (1945).
[16] T. Alfrey, A. Bartovics, and H. Mark, J. Am. Chem. Soc. **64**, 1557 (1942).

present theory gives quantitative form to these ideas. If μ_1 is positive (but less than $\frac{1}{2}$),[17] the value of the expansion factor is diminished according to Eq. (27). If μ_1 is negative, representing a favorable heat of mixing, α is increased.

The interaction energy term obviously could have been introduced in the treatment given in the preceding section. The effect of the size of the solvent is not so easily incorporated in that development. To indicate the manner in which it would enter, it may be sufficient to point out that a solvent comprised of more than one segment may assume any one of a number of internal configurations; i.e., its situation is no longer specified by merely assigning it a location in the lattice. The interference term cannot be expressed in terms of the polymer molecule alone, for the arrangement of the polymer molecule affects the configurations available to the solvent molecules. The total configurations available to the system as a whole must be considered. In this way the influence of solvent size as expressed in Eq. (26) may be deduced.

DISCUSSION

The exact value to be assigned to C, or to C_1, cannot be deduced from theory because of the difficulty of bridging the gap between the actual polymer chain in solution on the one hand and the idealized chain model composed of Z segments arranged in the hypothetical lattice on the other. In general l' will be less than l. Values of C in the range from 0.1 to 1.0 are anticipated, depending on the cross-sectional dimensions of the chain and its flexibility. For a very high polymer, Z will be of the order of 10^4. Hence, $\alpha^5-\alpha^3$ may assume values of the order of 10 to 100, corresponding to $\alpha=1.7$ to 2.5 for high polymers in athermal solvents. The predicted influence of long range interference on the dimensions of the random polymer chain is by no means trivial, therefore.

The factor α may be incorporated directly in previous formulas expressing the dimensions of polymer molecules in terms of bond angles and the potential energy function associated with rotation about the bonds. Thus, the mean square distance between the ends of a tetrahedrally bonded chain may be expressed approximately as follows:[5,18,19]

$$\langle r^2\rangle \cong 2\alpha^2 l_0^2 n'(1+\langle\cos\varphi\rangle)/(1-\langle\cos\varphi\rangle), \quad (28)$$

where l_0 is the length of each bond, n' is the number of bonds and φ represents the angle of rotation about a bond measured from the trans (or planar zig-zag) configuration, $\langle\cos\varphi\rangle$ indicating the average value of the cosine. Alternatively, this may be expressed in terms of the equivalent hypothetical freely jointed chain as follows:

$$\langle r^2\rangle = \alpha^2 l^2 Z, \quad (29)$$

where compliance with Eq. (28) together with the condition $Zl=n'l_0$ would require that l and Z be related to l_0 and n' as follows

$$l = 2l_0(1+\langle\cos\varphi\rangle)/(1-\langle\cos\varphi\rangle),$$

and

$$Z = (n'/2)(1-\langle\cos\varphi\rangle)/(1+\langle\cos\varphi\rangle).$$

Dimensions of high polymer molecules in solution, as deduced from the angular dissymmetry of scattered light, are known to be appreciably larger than would be calculated assuming free rotation about every bond and neglecting the interference effect.[9,20] Debye and Bueche[9] noted for example that the value of $\langle r^2\rangle^{\frac{1}{2}}$ deduced from light scattering dissymmetry measurements on a polystyrene of molecular weight 10^6 was $3.5(\langle r^2\rangle_0)^{\frac{1}{2}}$, where $\langle r^2\rangle_0$ represents the mean square distance between the ends of a chain possessing free rotation and devoid of interference; according to Eq. (28), $\langle r^2\rangle_0 = 2l_0^2 n'$. If the difference between the observed $\langle r^2\rangle$ and $\langle r^2\rangle_0$ is to be ascribed entirely to hindrance to free rotation, it follows from Eq. (28) that the average value of $\cos\varphi$ must be 0.85 corresponding to $\varphi=\pm 32°$. In terms of the freely jointed hypothetical chain (Eq. (29))

$$\langle r^2\rangle_{\text{obs.}}/\langle r^2\rangle_0 = \alpha^2 l/2l_0. \quad (30)$$

If $\alpha=1$, the result of Debye and Bueche requires that $l/l_0=24$, i.e., the equivalent chain must consist of about twelve structural units. This seems unreasonably large to be attributed entirely to hindered rotation.

Recent calculations by Taylor[21] show that the potential barrier to free rotation about the bonds of a polymethylene chain is capable of accounting for an increase in linear dimension by a factor of only 1.5 to 2.0. The phenyl substituents of polystyrene doubtless increase the hindrance to free rotation. Some of these steric interactions may oppose the planar zig-zag arrangement of adjacent chain atoms, however, and it does not follow that the average of $\cos\varphi$ will be much increased by the presence of bulky substituents. Short range interferences between nearby, but not consecutive, units will increase the length of the chain somewhat. It seems unlikely, however, that the aggregate influence of hindrance to free rotation about the carbon-

[17] Precipitation probably will set in for values of the μ_1 near $\frac{1}{2}$. It is readily seen that as $1-2\mu_1$ approaches zero, Eq. (27) acquires multiple solutions in α. At $\mu_1=\frac{1}{2}$, solutions are $\alpha=1$ and 0. The indicated collapse of the molecule will be preceded by mutual interaction of polymer molecules resulting in the formation of a new phase.

[18] W. J. Taylor, J. Chem. Phys. **15**, 412 (1947).

[19] H. Kuhn, J. Chem. Phys. **15**, 843 (1947).

[20] P. M. Doty, W. A. Affens, and B. H. Zimm, Trans. Faraday Soc. **42B**, 66 (1946).

[21] W. J. Taylor, J. Chem. Phys. **16**, 257 (1948).

carbon single bonds, steric interactions between substituents, and short range interferences may be sufficient to account for the observed disparity between $\langle r^2\rangle$ and $\langle r^2\rangle_0$. This difficulty disappears if α is assigned a value in the range predicted above. The length l of the equivalent segment (see Eq. (30)) then assumes a reasonable value, and extraordinary hindrance to free rotation need not be postulated. In any event, molecular dimensions should not be related directly to chain stiffness; the effect of long range interference on the molecular dimensions must first of all be taken into account. It is important to note that whereas l in Eq. (29) (or l_0 and the function of $\langle\cos\varphi\rangle$ in Eq. (28)) should be independent of molecular weight, α increases with the chain length.

In the above discussions both the polymethylene chain model with hindered rotation (Eq. (28)) and the hypothetical freely jointed chain (Eq. (29)) have been employed. Clearly the short range steric interactions—steric interactions between substituents and what have been called short range interferences—are too complex to justify literal application of Eq. (28); in particular, the potential energy associated with rotation about a given bond will depend also on the rotation angle prevailing for other nearby bonds. Interpretation of chain configurations in terms of the hypothetical freely jointed equivalent chain (Eq. (29)) widely used by Kuhn is to be preferred.

The expansion in chain configuration resulting from long range interference is also of importance in the interpretation of the viscosities of dilute polymer solutions. Kuhn[2] long ago pointed out that solvent within the domain of an irregularly coiled polymer molecule of sufficient size would move with the molecule when the dilute solution is subject to shear.[22] In effect, then, the molecule and associated solvent would behave like an Einstein sphere and the specific voscosity of the solution should be 2.5 times the total *effective* volume of all these spheres. Translated to intrinsic viscosity expressed in $(g/cc)^{-1}$

$$[\eta]=2.5(4\pi/3)R_e^3/M, \tag{31}$$

where R_e is the radius of the equivalent sphere.[23] For the random flight chain R_e will be proportional to $M^{\frac{1}{2}}$. Hence, the intrinsic viscosity should be proportional to $M^{\frac{1}{2}}$. However, Kuhn[2,22] recognized that the "volume filling effect" (equivalent to long range interference) would increase the molecular configuration dimension, and for reasons not made clear he concluded that the augmentation in the effective volume could be introduced as a factor proportional to a low power of M. He suggested, therefore, that the intrinsic viscosity should depend on the molecular weight according to the relationship[2]

$$[\eta]=KM^a, \tag{32}$$

where a lies in the range from 0.6 to 0.9. This conclusion regarding the exponent a appeared to be contradicted by such experimental data as were available at that time (1934) but it has since proved to be remarkably correct.

The recent treatments of the hydrodynamic interaction of a randomly coiled polymer molecule with the solvent medium advanced by Debye and Bueche[9] and by Kirkwood and Riseman[24] in effect permit the factor 2.5 to be replaced by a function (designated by φ in the D-B treatment) representing the effective permeation of the flowing solvent through the domain of the polymer chain. Making this replacement in Eq. (31) and substituting from Eq. (13) for R_e,

$$\begin{aligned}[\eta]&=\text{const.}(l^3Z^{\frac{1}{2}}/M)\alpha^3\varphi\\&=\text{const.}(l^3/M_0)Z^{\frac{1}{2}}\alpha^3\varphi,\end{aligned} \tag{33}$$

where M_0 is the molecular weight per segment and φ varies with chain length, approaching an upper limiting value (2.5 in the D-B treatment) for sufficiently long chains. Debye and Bueche,[9] and also Kirkwood and Riseman,[24] attribute the almost universal apparent dependence of intrinsic viscosity (in a good solvent) on a power of the chain length which is greater than one-half to the variation of the hydrodynamic factor φ with M.

According to Eqs. (26), or (27), α in a good solvent should approach proportionality to $Z^{1/10}$ in the high molecular weight range. As the molecular weight decreases, or if a poorer solvent is used, the dependence of α on Z must be approximated by a lower power of Z. Hence, the product $Z^{\frac{1}{2}}\alpha^3$ in Eq. (33) should vary as Z raised to a power between 0.5 and 0.8, being near the upper limit in a good solvent if the chain length is great. Virtually all reliable experimental results on the relationship of intrinsic viscosity to molecular weight require a values for Eq. (32) which are in this range. This fact together with other experimental observations to be discussed elsewhere[25] lead to the conclusion that the hydrodynamic factor φ is substantially independent of M within the molecular weight range ordinarily covered; apparently φ approaches

[22] See also W. Kuhn, and H. Kuhn, Helv. Chem. Acta. **26**, 1394 (1943).

[23] The equivalent sphere entering into Eq. (31) may differ in size from that employed above in the treatment of the interference effect. Actually they are similar in size, although the use of the same symbol R_e here and above is not meant to imply that they are identical. For present purposes it is sufficient to note that the one R_e should be proportional to the other.

[24] J. G. Kirkwood and J. Riseman, J. Chem. Phys. **16**, 565 (1948).

[25] T. G. Fox, Jr. and P. J. Flory, to be published.

its upper limit for negligible solvent flow permeation of the equivalent sphere. The difference between the value of a observed to apply in Eq. (32) and 0.50 should be ascribed primarily to the influence of long range interference and to the heat of dilution of the polymer segments with solvent molecules.

At sufficiently low molecular weights the decrease in φ with further decrease in chain length must become significant. On the other hand, α^3 varies as Z raised to a power which diminishes as the chain length becomes small (see above). The dependences of these two factors (φ and α^3) on Z are such as to compensate (partially at least) one another so as to preserve the empirical relationship (32) with a fixed exponent a down to lower molecular weights than would be possible if either of the two factors alone entered in Eq. (33).

THE JOURNAL OF CHEMICAL PHYSICS VOLUME 17, NUMBER 3 MARCH, 1949

Theory of the Thermal Diffusion of Electrolytes in a Clusius Column

GEORGE GUTHRIE, JR., J. NORTON WILSON,* AND VERNER SCHOMAKER
*Gates and Crellin Laboratories of Chemistry, California Institute of Technology, Pasadena, California***

(Received August 30, 1948)

A theory is presented which accounts approximately for the apparently anomalous difference between the thermal diffusion coefficients of an ion in the presence and in the absence of other electrolytes; the theory is based on the existence of an electric field parallel to the thermal gradient in the electrolyte as a consequence of the variation in mobility among the various ions present. It is pointed out also that some data on the behavior of electrolytes in a Clusius column are at variance with the Debye exponential law concerning the steady-state distribution of solute.

AN apparent anomaly in the thermal diffusion of electrolytes was reported by Gillespie and Breck[1] and by Hirota[2] in 1941. In experiments with the Clusius column[3] these workers found that one[4] of a mixture of two electrolytes was transported into the upper reservoir, contrary to its behavior when it was the only solute; the other electrolyte of the mixture was transported as usual into the lower reservoir, but to a greater extent than when it was the only solute. Prior to this work no instances of the thermal diffusion of an electrolyte against the temperature gradient had been recorded in the literature.

A similar but less striking effect has long been known to occur in the ordinary diffusion of mixtures of electrolytes:[4,5] the more mobile of two mixed electrolytes diffuses more rapidly, the less mobile more slowly, than each diffuses alone. Vinograd and McBain[6] accounted for the effect quantitatively in terms of an electrostatic field set up by the diffusion of ions of different mobilities. It occurred to one of us (G.G.) that the results of Gillespie and Breck and of Hirota could be similarly explained. We present herewith approximate treatments of the behavior of the mixed electrolytes in the pure Soret effect and in the Clusius column; the analysis accounts approximately for the anomalies referred to above.

THE SORET EFFECT

Let the thermal gradient lie along the x axis. At the steady state the flux f_i of the i'th ionic species across any plane in the solution normal to x will vanish, i.e.

$$f_i = -D_i dc_i/dx - D_i' c_i dT/dx + \nu_i u_i c_i E = 0 \quad (1)$$

where D_i is the ordinary diffusion coefficient, D_i' is the thermal diffusion coefficient, c_i is the concentration in equivalents per unit volume, u_i is the equivalent mobility, ν_i is the sign of the ionic charge, and E is the local field postulated to arise from the difference in ionic mobilities. Let us substitute $RTu_i = FD_i$, where F is the Faraday; multiply Eq. (1) by ν_i/D_i and sum over all ions. Applying the approximate neutrality condition $\sum \nu_i dc_i/dx = 0$ we obtain

$$(EF/RT)\sum c_i = (dT/dx)\sum \nu_i c_i D_i'/D_i, \quad (2)$$

and

$$\frac{d \ln c_i}{dx} = \left(-\frac{D_i'}{D_i} + \frac{\nu_i \Sigma \nu_i c_i D_i'/D_i}{\Sigma c_i} \right) \frac{dT}{dx}. \quad (3)$$

For non-electrolytes the Soret coefficient, σ, is equal to the ratio $-D'/D$. We shall call this ratio for individual ions the intrinsic Soret coefficient σ_i^*.

* Shell Development Company, Emeryville, California.
** Contribution No. 1222.
[1] L. J. Gillespie and S. Breck, J. Chem. Phys. 9, 370 (1941).
[2] K. Hirota, Bull. Chem. Soc. (Japan) 16, 232 (1941).
[3] K. Clusius and G. Dickel, Naturwiss. 26, 546 (1938).
[4] In these experiments the two electrolytes have a common ion.
[5] T. Graham, Phil. Trans. Roy. Soc. (London) 805 (1850); J. W. McBain and C. R. Dawson, J. Am. Chem. Soc. 56, 52 (1934).
[6] J. R. Vinograd and J. W. McBain, J. Am. Chem. Soc. 63, 2008 (1941).

The observed Soret coefficient σ_i for an ion in an electrolyte is therefore

$$(d\ \ln c_i/dx)(dx/dT)=\sigma_i=\sigma_i^*-\nu_i\sum\nu_i c_i\sigma_i^*/\sum c_i. \quad (4)$$

For a single electrolyte AX this becomes

$$\sigma_{AX}=\sigma_A=\sigma_X=1/2(\sigma_A^*+\sigma_X^*). \quad (5)$$

For a mixture of electrolytes AX and BX

$$\begin{aligned}\sigma_A&=\sigma_{AX}+[c_B/(c_A+c_B)](\sigma_{AX}-\sigma_{BX})\\ \sigma_B&=\sigma_{BX}+[c_A/(c_A+c_B)](\sigma_{BX}-\sigma_{AX}).\end{aligned} \quad (6)$$

Equations (6) predict effects of the type observed by Gillespie and Breck and by Hirota. The electrolyte which has the higher Soret coefficient alone will have an enhanced Soret coefficient in the mixture; that with the lower Soret coefficient alone will have a diminished coefficient in the mixture and may even have the sign of its coefficient reversed if the difference between σ_{AX} and σ_{BX} is sufficiently great. Unfortunately no data are available for a direct test of these equations.

THERMAL DIFFUSION WITH CONVECTION

In the Clusius column a thermal gradient is maintained between two parallel vertical walls set close together; a convection current is thereby superimposed on the thermal diffusion current and the solute diffusing to the cold wall is carried to the bottom of the column and concentrated there.

Let the vertical coordinate be y with origin at the bottom of the column of height h. Let the temperature gradient be parallel to the coordinate x with origin mid-way between the walls, separated by a distance $2a$.

A material balance for an element of volume of height dy and unit width extending normal to the y axis from $x=0$ to $x=a$ leads at the steady state to

$$-D_i\partial c_i/\partial x-D_i'c_i\partial T/\partial x+\nu_i D_i c_i FE_x/RT$$
$$-\int_0^a v_y(x)[\partial c_i(x)/\partial y]dx=0 \quad (7)$$

where v_y is the vertical component of the convection current and all concentrations unless otherwise specified refer to the values at $x=0$. Effects of diffusion arising from $D\partial c/\partial y$ have been neglected as small compared to $v_y\partial c/\partial y$.

Since $\partial c/\partial y$ is not likely to vary markedly with x, we may to a good approximation replace the integral in (7) with $a\bar{v}_y\partial c/\partial y$ where $\bar{v}_y$ is the mean velocity of the convection current between $x=0$ and a.

The field E may be evaluated as before in any one of several ways; the accuracy and convenience of the result depends on which of the terms is eliminated in the summation. We choose to eliminate $\sum\nu_i\partial c_i/\partial y$ and obtain

$$\frac{FE}{RT}=\frac{\Sigma\nu_i D_i\partial c_i/\partial x+(\partial T/\partial x)\Sigma\nu_i D_i'c_i}{\Sigma D_i c_i} \quad (8)$$

whence

$$a\bar{v}_y\partial c_i/\partial y=-\left(D_i\partial c_i/\partial x-\frac{\nu_i D_i c_i\Sigma\nu_i D_i\partial c_i/\partial x}{\Sigma D_i c_i}\right)$$
$$-\frac{\partial T}{dx}\left(D_i'c_i-\frac{\nu_i D_i c_i\Sigma\nu_i D_i'c_i}{\Sigma D_i c_i}\right). \quad (9)$$

A consideration of the divergence of the flux in a volume element of cross section $dydx$ at $x=0$ indicates that $\partial c_i/\partial x$ at $x=0$ is small. To a fair approximation we may set $(\partial c_i/\partial x)_0$ equal to $\varphi c_i\sigma_i dT/dx$ for all ions, where φ is a constant lying between zero and unity and σ_i is defined by Eq. (4). This relation has been shown by de Groot[7] to hold approximately in the thermal diffusion of non-electrolytes in the Clusius column. Substitution of this approximation in (9) by means of Eq. (3) leads to

$$\frac{\partial c_i}{\partial y}=\frac{-(1-\varphi)dT/dx}{a\bar{v}_y}\left(D_i'c_i-\frac{\nu_i D_i c_i\Sigma\nu_i D_i'c_i}{\Sigma D_i c_i}\right). \quad (10)$$

Equation (10) can be integrated for the case of a single electrolyte, AX, if the dependence on y[8] of the mobilities, thermal diffusion coefficients, and average convection velocity can be neglected. Application of the conservation condition

$$\int_0^h c\,dy=hc_0,$$

where c_0 is the initial concentration of electrolyte, then leads to

$$R_{AX}=\ln(c_b/c_t)_{AX}=\left(\frac{c_b-c_t}{c_0}\right)_{AX}$$
$$=K_{AX}h\left(\frac{D_A'u_X+D_X'u_A}{u_A+u_X}\right) \quad (11)$$

where R is called the enrichment. The quantities c_b and c_t are respectively the concentrations at the bottom and top of the column; K_{AX} is a constant whose magnitude depends on the dimensions of the apparatus and on the density, thermal expansion coefficient, and viscosity of the solution.

[7] S. R. de Groot, *L'Effet Soret* (N.V. Noord-Hollandsche Utgevers Maatschappij, Amsterdam, 1945), p. 107.

[8] The dependence on y either may be explicit or may be implicit through dependence on c.

TABLE I.

Solution	Ion	Expt.	Enrichment c_b/c_t Theory	Soret*	$(c_b-c_t)/c_0$ Expt.	Theory	Observer
1 N HCl	H^+, Cl^-	1.22					Hirota**
1 N NaCl	Na^+, Cl^-	1.047					
1 N NH_4Cl	NH_4^+, Cl^-	1.010					
0.5 N HCl	H^+	1.34	1.43[a,c]	1.32			
0.5 N NaCl	Na^+	0.97	0.95[a,c]	0.97			
0.5 N HCl	H^+	1.42	1.51[a,c]	1.34			
0.5 N NH_4Cl	NH_4^+	0.89	0.88[a,c]	0.89			
1 N HCl	H^+, Cl^-	9.4			1.60		Gillespie and Breck
1 N $FeCl_2$	Fe^{++}, Cl^-	1.30			0.23		
1 N HCl	H^+	39.	72. [a,c]	25.	1.90	4.30[a,c]	
1 N $FeCl_2$			296. [a,d]			2.74[a,d]	
			20.4 [b,c]			3.01[b,c]	
			36.4 [b,d]			2.74[b,d]	
	Fe^{++}	0.92	0.40[a,c]	0.48	−0.10	−0.92[a,c]	
			0.55[a,d]			−0.52[a,d]	
			0.55[b,c]			−0.59[b,c]	
			0.62[b,d]			−0.44[b,d]	

* Enrichment assumed proportional to effective Soret coefficient.
** All measurements by Hirota listed above were made after his column had been running for two hours. The two-hour values did not differ greatly from the equilibrium values in these cases for which both were obtained; e.g. for 1 N NaCl, 1 N NH_4Cl and 1 N HCl the equilibrium values were respectively 1.048, 1.010, and 1.25 as compared to values of 1.047, 1.010 and 1.22 at two hours.
[a] Using $R=\ln(c_b/c_t)$.
[b] Using $R=(c_b-c_t)/c_0$.
[c] Approximate integration, Eq. (13).
[d] Exact integration, Eq. (14).

In the integration of Eq. (10) for a mixture of two electrolytes, AX and BX, it is convenient to substitute $c_X=c_A+c_B$, and to substitute for the expressions in u_iD_j' in terms of the quantities $R_{ij}'=R_{ij}K_m/K_{ij}$. Equation (10) becomes for this case

$$-\frac{\partial c_A}{\partial y}=\frac{c_A}{h}\left\{\frac{(u_A+u_X)R_{AX}'c_A+[(u_A+u_X)(u_B+u_X)R_{AX}'-u_A(u_B+u_X)R_{BX}']c_B/u_X}{(u_A+u_X)c_A+(u_B+u_X)c_B}\right\}. \tag{12}$$

A similar expression for $\partial c_B/\partial y$ is obtained by interchanging the subscripts A and B.

These expressions can be integrated approximately if the fraction in curly brackets is assumed to be constant, giving

$$R_A=\frac{[(u_A+u_X)R_{AX}']c_A+[(u_A+u_X)(u_B+u_X)R_{AX}'-u_A(u_B+u_X)R_{BX}']c_B/u_X}{(u_A+u_X)c_A+(u_B+u_A)c_B} \tag{13}$$

and the corresponding expression for R_B. When the enrichments are great enough to invalidate this approximation, an exact integration may be made. Variables may be separated in terms of the parameter, $V=c_A/c_B$. Integration of dV/dy and dc_B/dV yields

$$-\frac{y+y_0}{h}=\frac{u_X(u_A-u_B)\ln(1+V)}{(u_A+u_X)(u_B+u_X)(R_{AX}'-R_{BX}')}+\frac{u_X\ln V}{(u_A+u_X)(R_{AX}'-R_{BX}')} \tag{14}$$

and

$$\ln kc_B=\frac{[u_A(u_B+u_X)R_{BX}'-u_B(u_A+u_X)R_{AX}']\ln(1+V)+u_X(u_B+u_X)R_{BX}'\ln V}{(u_A+u_X)(u_B+u_X)(R_{AX}'-R_{BX}')}$$

where y_0 and k are integration constants determined by the ratio and absolute magnitudes of the initial concentrations respectively. The limits of integration y_t and y_b are determined by the relation $y_t-y_b=h$.

In obtaining Eq. (12) from Eq. (11) it has been assumed that the quantities u and D' for each ion are constant. This assumption is justified even approximately only if the solutions of AX, BX, and of the mixture have the same ionic strength. Fortunately, this requirement is met in the experiments of Hirota. For dealing with more complicated situations such as are presented by the experiments of Gillespie and Breck a more complex equation corresponding to Eq. (12) can be obtained in which the values u and D' corresponding to the different

ionic strengths enter specifically. The variations in mobilities with ionic strength can be predicted fairly well, but no adequate theory appears to be available for the prediction of variations in D'.

APPLICATION TO EXPERIMENT

The experimental enrichments obtained by the authors cited are compared in Table I with the values predicted by means of Eqs. (13), (14), with substitution of the concentrations corresponding to the initial composition of the solutions, of mobilities corresponding to infinite dilution and a temperature midway between those of the hot and cold walls and of $R_{AX}'=R_{AX}$ and $R_{BX}'=R_{BX}$. We have presented the results of the approximate integration, Eq. (13), for all of the experiments. The more exact integration, Eq. (14), was computed only for the experiments of Gillespie and Breck, in which the enrichments were large. In this computation K_m was assumed equal to K_{AX}; this may be only a rough approximation.

In the data presented by Gillespie and Breck, $\ln c_b/c_t$ *does not equal* $(c_b-c_t)/c_0$ for single electrolytes; that is, the variation of concentration with height is not purely exponential as predicted by Eq. (11). This complication may contribute to the disagreement between these data and the approximate theory presented here. It is not possible to choose at this time between the substitution of $\ln c_b/c_t$ and $(c_b-c_t)/c_0$ for the enrichment R. For the experiments of Gillespie and Breck we have made calculations using both values. It will be seen that the agreement is much better with Hirota's data, as is to be expected from the arguments given above.

It also may be mentioned that the results obtained by Gillespie and Breck and by Hirota can be accounted for by assuming that the enrichments of the various ions are proportional to their corrected Soret coefficients as given by Eq. (6). The enrichments computed on the basis of this assumption are given in column 3 of Table I; we are unable to present a detailed explanation for their excellent agreement with the experimental results, although the result perhaps may be a natural consequence of the small separations obtained together with good equilibration along the temperature gradient.

APPENDIX

The Apparent Distribution of Solute in Gillespie and Breck's Column

Evidence will now be presented which suggests that the concentration of solute at the steady state in Gillespie and Breck's apparatus approximates more closely a linear dependence on the vertical coordinate than the exponential dependence which was predicted by Debye[9] and which also follows from the treatment presented here.

TABLE II.

Solution	$\frac{c_b-c_t}{c_0}$	c_b/c_t		
			Calculated	
	Expt.	Expt.	Linear	Exponential
0.5 M $FeCl_2$	0.22	1.29	1.25	1.25
0.5 M $BaCl_2$ Ba^{++} +1 M HCl H^+	0.44	1.64	1.57	1.55
	1.06	3.9	3.26	2.88
1 M HCl	1.60	9.4	9.0	4.95
1 M HCl +0.5 M $FeCl_2$ H^+	1.90	39.	39.	6.69

Applying the conservation condition to a column without reservoirs as used by Gillespie and Breck we have for the exponential distribution,

$$c=U(x)\exp(\alpha y),$$

the consequence

$$(c_b-c_t)/c_0=\ln(c_b/c_t) \qquad (14)$$

where c_0 is the initial concentration.

For a linear distribution of concentration up the column,

$$c=U(x)(1+\beta y),$$
$$(c_b-c_t)/c_0=2(c_B/c_t-1)/(c_B/c_t+1). \qquad (15)$$

The experimental values of $(c_b-c_t)/c_0$ and c_b/c_t, which were both reported by Gillespie and Breck, are presented in Table II together with the values of c_b/c_t calculated by means of Eqs. (14) and (15) from the experimental values of $(c_b-c_t)/c_0$. The results shown in Table II indicate that the distribution of solute up the column is certainly not exponential and may be roughly linear.

We are unable to account for the apparently linear distribution; a function linear in y is not a valid solution for the differential equation which applies to a column in which only laminar convection occurs. Possibly in Gillespie and Breck's apparatus v_y varied appreciably with y. It is quite possible, also, that the apparent agreement with a linear distribution is purely coincidental; indeed, some of their data appear to require a dependence of c on y whose curvature is of the opposite sign from that of the exponential.

ACKNOWLEDGMENT

The authors wish to express their appreciation to Professor J. G. Kirkwood and to Professor Leverett Davis, Jr., for helpful discussions and advice.

[9] P. Debye, Ann. d. Phys. **36**, 284 (1939).

Burning Velocities of Butadiene-1,3 with Nitrogen-Oxygen and Helium-Oxygen Mixtures*

ELMER J. BADIN, JOSEPH G. STUART, AND ROBERT N. PEASE
Department of Chemistry, Princeton University, Princeton, New Jersey
(Received September 7, 1948)

Burning velocities of nitrogen-oxygen-butadiene-1,3 and helium-oxygen-butadiene-1,3 have been measured at atmospheric and reduced pressures. At atmospheric pressure the ratio of 3.7:1 for the maximum burning velocities was obtained for helium compared to nitrogen as the inert gas. Reduction of pressure caused an increase then a decrease in burning velocity for helium-oxygen-butadiene-1,3. The maximum value of the burning velocity occurred at 300 mm pressure. Calculations of the equilibrium concentrations of H, O, and OH for the gas mixtures used have been made. Assuming that the controlling factor in the burning velocity is the back-diffusion of H-atoms, good agreement between calculated and experimental burning velocity ratios is obtained.

INTRODUCTION

ACCORDING to Tanford's theory[1] of burning velocity, the substitution of helium for the nitrogen of air should increase the burning velocity because (1) a higher temperature will be attained with consequent increase in atom and radical concentrations, and (2) a higher diffusion coefficient will result. In addition the linear burning velocity should be increased by diminishing the pressure. A comparison of bunsen-type flames of butadiene-1,3 with ordinary air and with a corresponding helium-oxygen mixture has been made in this laboratory with the expected results.

In addition to the burning velocity measurements, the concentrations of the radicals H, O, and OH have been calculated from thermodynamic data. These calculations have been made to show that back-diffusion of H-atoms from the flame front into unburned gas is the controlling factor in determining the burning velocity. This has previously been shown to be true for carbon monoxide-hydrogen mixtures[1] and is the basis of the burning velocity theory of Tanford.

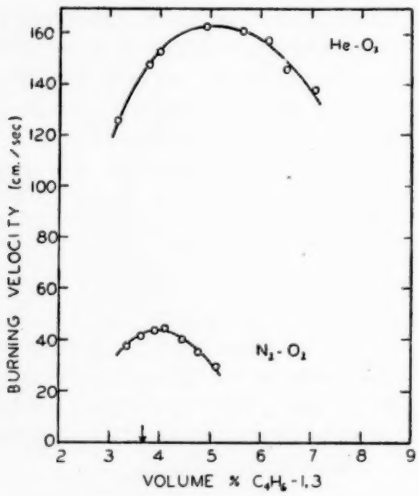

FIG. 1. Burning velocities of butadiene-1,3 (6.66-mm I.D. quartz mantled burner; atmospheric pressure).

EXPERIMENTAL METHOD

Gas mixtures were made up by means of flow meters and fed to a silica burner which was enclosed in a large mantle to exclude secondary air and to permit reduction of pressure.

Two cathetometers, one mounted for measuring vertical distances and one mounted for measuring horizontal distances, were used for measuring the dead space, flame cone height, and cone base diameter. A second "projection method" was used

TABLE I. Burning velocities of nitrogen-oxygen-butadiene-1,3 and helium-oxygen-butadiene-1,3 at atmospheric pressure (6.66-mm I.D. quartz large mantled burner).

Oxidant rate (1/min.)*	C_4H_6-1.3 rate (1/min.)*	Vol. % C_4H_6-1.3	Flame base diam. (mm)	Flame height (mm)	Burning velocity (cm/sec.)
Helium-oxygen:					
12.9	0.35	2.86	lower limit		
	0.39	3.18	6.80	14.7	126
	0.47	3.81	6.70	12.8	148
	0.55	4.02	6.70	12.5	153
	0.62	4.95	6.70	11.7	163
	0.72	5.70	6.70	11.8	161
	0.78	6.16	6.70	12.3	157
	0.83	6.51	6.70	13.4	146
	0.91	7.10	6.80	14.8	138
	0.99	7.79	upper limit		
Nitrogen-oxygen					
4.00	0.121	2.93	lower limit		
	0.139	3.36	7.6	14.85	37.9
	0.151	3.64	7.4	13.80	41.9
	0.163	3.92	7.2	13.55	43.9
	0.171	4.10	7.2	13.50	44.3
	0.187	4.48	7.4	14.50	40.3
	0.200	4.76	7.6	16.15	35.4
	0.216	5.13	7.8	18.70	29.9
	0.277	5.38	upper limit		

* Rates at 25°, 760 mm pressure. Stoichiometric mixture—3.68 vol. % C_4H_6.

* The work described in this paper was done in connection with Contract NOrd 7920 with the United States Naval Bureau of Ordnance, as coordinated by the Applied Physics Laboratory, The Johns Hopkins University. Acknowledgment is also due Dean H. S. Taylor, who has general supervision of this project.

[1] C. Tanford and R. N. Pease, J. Chem. Phys. **15**, 431, 433, 861 (1947).

TABLE II. Burning velocities of butadiene-1,3 in nitrogen-oxygen and helium-oxygen at reduced pressures (10.55-mm quartz burner).

Pressure (mm Hg)	Flow rates* Oxidant	Flow rates* C_4H_6-1,3	Volume % C_4H_6-1,3	Cone areas (cm²) (1)**	(2)***	(3)†	Burning velocities (cm/sec.) (1)**	(2)***	(3)†
Helium-oxygen:									
180	14.0	0.40	2.79	2.09	1.43	1.98	115	168	121
180	14.0	0.61	4.16	1.67	1.49	1.54	146	163	158
180	14.0	0.74	5.04	1.97	1.63	2.02	125	151	122
180	14.0	0.83	5.62	2.67	2.41	2.87	92.6	102	86.1
300	14.0	0.39	2.69	1.72	1.64	1.65	139	146	146
300	14.0	0.47	3.28	1.32	1.48	1.50	183	163	161
300	14.0	0.60	4.09	1.35	1.51	1.44	180	161	169
300	14.0	0.73	4.92	1.97	1.85	1.56	125	133	157
450	14.0	0.36	2.50	1.95	1.89	2.11	123	127	115
450	14.0	0.41	2.85	1.63	1.63	1.68	147	147	142
450	14.0	0.86	5.76	2.12	2.06	2.10	117	120	118
450	14.0	0.96	6.41	3.15	2.92	3.04	79.1	85.4	81.9
Nitrogen-oxygen:									
300	14.0	0.50	3.43	4.34	4.38	4.11	55.7	55.0	58.8
300	14.0	0.54	3.68	4.31	4.07	4.23	56.2	59.7	57.3
300	14.0	0.66	4.47	5.15	5.06	5.09	47.4	48.3	48.0
450	14.0	0.53	3.63	4.88	4.98	5.04	49.6	48.6	48.2
450	14.0	0.61	4.19	6.79	4.80	4.92		50.8	53.7

* All flow rates are given at the pressure indicated in liters per minute.
** The height and diameter at the base of the flame determined by cathetometer and the area determined by

$$A = \pi r(r^2+h^2)^{\frac{1}{2}}.$$

*** Dimensions determined by projection and area calculated as in (1).
† Dimensions determined by projection, area calculated by dividing the flame outline into frustums of cones and making a summation of the surface area using ½ (sum of the perimeters) (slant height) to determine the area of each frustum.

for determining the flame dimensions. In this method, a light-tight box fitted with a transparent screen at the end was mounted directly behind the flame. An 80-mm diameter, 100-mm focus double convex lens was mounted in the box so that the flame was just outside the focus. In this way an inverted real image of the stationary flame was cast on the screen and traced on a thin piece of paper. A beam of light was used to obtain a projection of the burner tube of known outside dimension. By using an enlargement factor, it was possible to determine all the flame dimensions including the dead space. The method was essentially that used by Garsyth, Forsyth, and Townend.[2]

Three methods were used for determining the cone areas:

TABLE III. Calculated radical concentrations for butadiene-1,3 flames in helium-oxygen and nitrogen-oxygen (stoichiometric composition: 3.68 percent butadiene-1,3).

Inert gas	Total pressure (atm.)	Burning velocity (expt.) (cm/sec.)	Calculated equilibrium flame temperature (°K)	Radical concentrations (atm.) H	O	OH
N_2	1	43	2380	0.00088	0.00086	0.0039
He	1	143	2660	0.00430	0.00470	0.0115
N_2	½	53	2350	0.00057	0.00057	0.00233
He	½	179	2600	0.00264	0.00273	0.00600

[2] Garsyth, Forsyth, and Townend, The Institute of Fuel, p. 175 (1945).

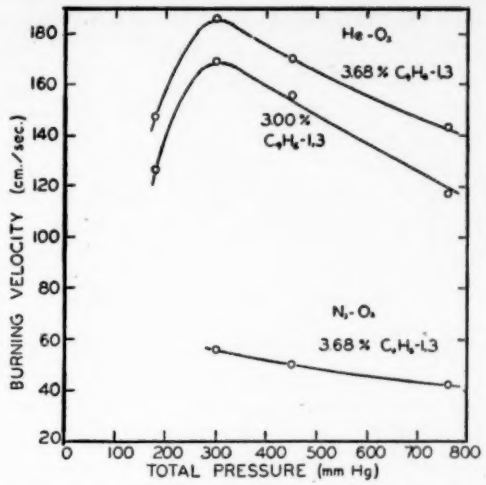

FIG. 2. Variation of burning velocity of butadiene-1,3 with pressure (cathetometer measurements; points at 760-mm, 6.66-mm burner; other values using 10.55-mm burner).

(1) Calculation using base diameter and flame height on the basis of an ideal cone from the cathetometer measurements.
(2) Calculation as in (1) with measurements taken from the projected image instead of the cathetometer measurements.
(3) Calculation from the projected image by obtaining the lateral areas of frustums into which the projected image was divided.

Burning velocities were calculated using the method of Gouy[3] where

$S = V/A$.
S = burning velocity in cm per sec.
V = volume feed rate of flow in cm³ per sec. at the operating pressure.
A = flame cone area in cm² calculated from $\pi r(r^2+h^2)^{\frac{1}{2}}$.

Data for areas and burning velocities (V/A in cm per sec.) calculated by the above three methods are collected in Table II. In each case burning velocities were based on the outer cone areas. At the lower pressures the reaction zone appears to become thicker. If burning velocities had been based on the inner cone border or an intermediate border, somewhat larger burning velocities would have resulted.

TABLE IV. Comparison between experimental and calculated burning velocity ratios.

	$\frac{He}{N_2}$ expt.	$\frac{He}{N_2}$ calc.	$\frac{1 \text{ atm.}}{\frac{1}{2} \text{ atm.}}$ expt.	$\frac{1 \text{ atm.}}{\frac{1}{2} \text{ atm.}}$ calc.
Total pressure, 1 atm.	3.3	3.2	—	—
Total pressure, ½ atm.	3.4	3.1	—	—
Inert gas, N_2	—	—	0.81	0.88
Inert gas, He	—	—	0.80	0.90

[3] Gouy, Ann. Chim. Phys. 18, 1 (1879).

To determine burning velocities at atmospheric pressure a 6.66-mm I.D. mantled (25-mm I.D. mantle) quartz burner was used.

Butadiene-1,3 was obtained from the Matheson Company. Helium-oxygen mixtures were obtained from the American Oxygen Company. By gas analyses the helium-oxygen mixture contained about 21 percent oxygen (analysis of several tank mixtures).

RESULTS AND DISCUSSION

In Table I and Fig. 1 data are shown for burning velocities of helium-oxygen-butadiene-1,3 and nitrogen-oxygen-butadiene-1,3 for a 6.66-mm burner. From these data it can be seen that the ratio of the maximum value for helium as compared with nitrogen is 3.7:1 corresponding to values of 163 and 44.3 cm/sec. There is, thus, a striking increase produced in the burning velocity when helium is substituted for nitrogen.

Data at reduced pressures (a 10.55-mm diameter burner was used so that lower pressures might be attained) are shown in Table II. The variation of burning velocity with pressure has been plotted (see Fig. 2) from values obtained from graphs of the data in Tables I and II for the composition 3.68 vol. percent and 3.00 percent butadiene-1,3. For helium-oxygen this correlation indicates an increase in burning velocity with decrease in pressure down to 300 mm. Below this pressure the burning velocity of helium-oxygen-butadiene-1,3 mixtures decreases.

Higher flame speeds in "helium air" have been observed in methane combustion by Coward and Jones.[4] As they point out, the lower heat capacity of helium results in a higher flame temperature. This is borne out by the calculated values given Table III.

The concentrations of H, O, and OH have also been calculated from the thermodynamic data and are included in Table III. It will be noted that the increase in equilibrium H-atom concentration at either pressure on substituting helium for nitrogen roughly parallels the increase in burning velocity. Assuming that the controlling factor is the back-diffusion of H-atoms from the flame front into unburned gas, an approximate solution indicates that the burning velocities should be given by[1]

$$u = A(c_0 D)^{\frac{1}{2}}$$

where A = a coefficient depending on mixture composition; c_0 = equilibrium H-atom concentration at flame temperature; and D = coefficient of diffusion for H-atoms into unburned gas. This equation is roughly obeyed (Table IV) when account is taken of the somewhat greater diffusibility into "helium air." The higher flame velocities at lower pressures follow from the increase in diffusion coefficients (greater mean free path).

[4] Coward and Jones, J. Am. Chem. Soc. 49, 386 (1927).

THE JOURNAL OF CHEMICAL PHYSICS VOLUME 17, NUMBER 3 MARCH, 1949

An Electrostatic Theory of the Potential Barriers Hindering Rotation around Single Bonds

EDWIN N. LASSETTRE AND LAURENCE B. DEAN, JR.*
Department of Chemistry, The Ohio State University, Columbus, Ohio
(Received September 16, 1948)

A number of simplifying hypotheses concerning the distribution of molecular electrons are discussed. On the basis of these hypotheses, the contribution of electrostatic forces to the interaction energy between two non-adjacent covalent bonds in a molecule has been estimated by expansion of the electrostatic potential in inverse powers of the distance. The expansion is carried as far as the quadrupole term. A discussion is given of the magnitudes to be expected for quadrupole moments of covalent bonding distributions. It is found that the electrostatic interactions, when extended to the quadrupole approximation, are sufficient to account for potential barriers hindering internal rotation in ethane, methylamine, methyl alcohol and dimethylacetylene. Using reasonable assumptions concerning the distribution of unshared electron pairs, the unsymmetrical configuration of hydrogen peroxide is found to be stable, in agreement with experiment. Extension of the treatment to the more complex molecules propane, isobutane, and neopentane indicates that the interaction between non-adjacent groups is not negligible. A relation between bond quadrupole moments and interatomic distance is given, and possible refinements to the treatment are discussed.

IT is the purpose of this paper to describe a theory, based on the electrostatic interaction of bonding charge distributions, which accounts for the main features of the observations on hindered rotation in several substances.[1] The theory seems attractive because (i) it is sufficiently general to include a large class of compounds, (ii) it can be developed in a simple and straightforward way from the generally accepted ideas concerning the distribution of molecular electrons, (iii) its application does not require a very detailed knowledge of the electron distributions, (iv) it is applicable to other phenomena which involve the interaction of oriented charge distributions, and (v) those empirical parameters which characterize the distributions are clearly and accurately defined and suggest other means by which the theory can be experimentally tested.

For the sake of simplicity a number of specific hypotheses concerning the distribution of molecular electrons are required. For the most part, these are generally accepted, at least as approximations. Nevertheless, it seems worth while to list and discuss each hypothesis, both in order to indicate the direction of development of the theory and to call attention to a number of sources of possible error which will probably be taken into account in a more refined theory. The hypotheses are as follows:

(a) *The molecular electrons are grouped into shared pairs, unshared pairs, and inner shell electrons.*

(b) *A single bond charge distribution consists of a shared pair of electrons and a unit positive charge at each nucleus.* Positive charges are grouped with negative in order to provide an electrically neutral distribution. This simplifies the subsequent calculations. Obviously, the interaction of two distributions having a common nucleus cannot be treated in this manner. Such interactions never enter, however, into the calculation of potential barriers hindering internal rotation. The case of unshared pairs is treated in a later section.

(c) *A single bond charge distribution is cylindrically symmetric with respect to the internuclear axis.* This hypothesis simplifies the calculations considerably, as can be seen by considering ethane. In this substance, the interaction of the electrons of the C−H bond with those of the C−C bond need not be evaluated, since it does not change as the methyl groups are rotated relative to each other. The hypothesis of cylindrical symmetry is in accord with the results of approximate wave mechanical calculations. The effect of departure from cylindrical symmetry was considered by Gorin, Walter, and Eyring,[2] who concluded that the effect was small.

(d) *Two single bond charge distributions which have no common atom do not significantly overlap.* The interacting distributions which are involved in the calculation of potential barriers are considerably removed from each other. In the case of ethane, the distances involved are indicated by Fig. 1, in which two C−H bonds and the connecting C−C bond are shown. This arrangement constitutes the closest possible approach which can be achieved by rotation of one methyl group with respect to the other. Contour lines of constant charge density are also shown in the figure. These were computed from a localized molecular orbital (see Section II), so constructed as to give the proper C−H bond dipole moment. In Fig. 2, contour lines are shown for a "normal" covalent bond (see Section II). Both of these are, of course, very rough approximations and have only qualitative significance. It seems clear that the two C−H distributions do not overlap very much, and the hypothesis of negligible overlapping seems more reasonable than any alternative now available. If overlapping is negligible, then exchange interactions are also negligible.

(e) *The electrostatic potential of a single bond charge distribution is sufficiently well characterized by its dipole and quadrupole moments, calculated relative to an origin midway between the nuclei.* The hypothesis is certainly valid at sufficiently large distances from the distribution, but may introduce considerable error when used in calculating the interaction between distributions as close as the C−H bonds in ethane, which are typical. That the distributions be non-overlapping is not sufficient to insure validity of this hypothesis. We have formulated the problem of calculating the electrostatic potential of the distribution provided by a localized molecular orbital and evaluated a few of the integrals,

* University Fellow—1947–48.

[1] A brief description of preliminary work on ethane has been reported previously. J. Chem. Phys. **16**, 151 (1948). See also J. Chem. Phys. **16**, 553 (1948) where an error is corrected.

[2] E. Gorin, J. Walter, and H. Eyring—J. Am. Chem. Soc. **61**, 1876 (1939).

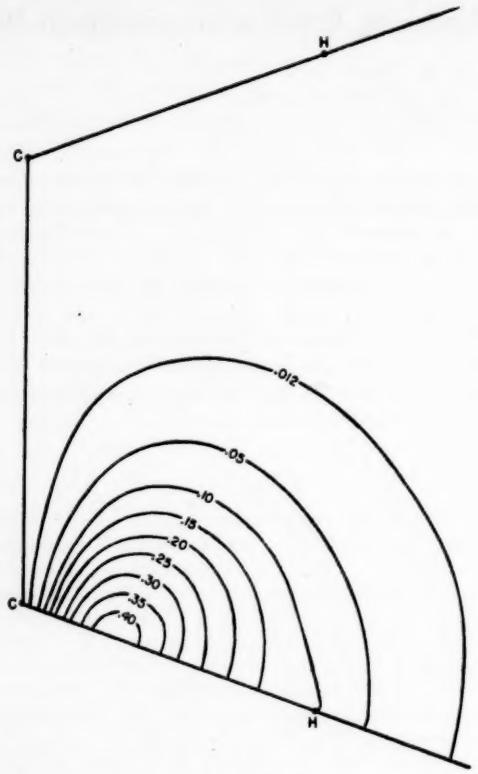

FIG. 1. Charge density contours for the C−H bond computed from a localized molecular orbital which leads to the proper dipole moment. Charge densities are in atomic units.

but concluded that the distribution was too rough an approximation to justify the labor involved in a complete calculation. The chief justification for this hypothesis must, therefore, lie in its success in accounting for the observed facts concerning hindered rotation by means of quadrupole moments which have *reasonable magnitudes*. The magnitudes of bond quadrupole moments are further considered in Section IIC. The origin of coordinates affects the accuracy of this approximation, especially when applied at close distances. A point midway between the nuclei has been chosen because it seems reasonable and is definitely fixed when the molecular configuration is known. A more suitable choice of origin could be made if the bond distributions were exactly known. This origin is, however, midway between the nuclei if the atoms of the bond are alike and is probably not far removed even when the atoms are unlike. The matter is further discussed in Section VI.

(f) *The charge distributions are unchanged, except in orientation, on internal rotation which preserves bond angles and interatomic distances.* Polarization and other deformation is therefore neglected. The chief justification for this lies in the fact that other investigators have been unable to account for a substantial contribution to potential barriers from this source. A more refined theory would take this factor into consideration.

Application of these hypotheses to the calculation of potential barriers requires a general theory of interaction of static charge distributions. Such a theory has been treated by several authors.[3] Since, however, the present application is largely dependent on the results of numerical calculations, it is very important that all terms be accurately defined in order to avoid error. For this reason, a treatment is included.

[3] See, e.g., H. Marganau, Rev. Mod. Phys. **11**, 1 (1939) and references there given.

II. INTERACTION OF STATIC CHARGE DISTRIBUTIONS

In calculating the energy of interaction of two static charge distributions, it is convenient to first calculate the electrostatic field of one distribution and then to compute the energy of a second distribution when placed into the field of the first. The electrostatic field of a cylindrically symmetric distribution can be very easily calculated by means of expansion in series of spherical harmonics. In the case of a general distribution, oriented in an arbitrary way, there is some advantage in using Cartesian coordinates together with a vector and matrix notation. This procedure is followed below. Since the development is similar in many respects to that of Marganau,[3] the details of algebraic manipulation are, for the most part, omitted.

A. Electrostatic Potential

Consider a system of point charges, the nth charge having magnitude q_n and placed at the terminus of the position vector $\mathbf{r}_n$. The electrostatic potential of the distribution at $\mathbf{r}$ is then

$$U(\mathbf{r})=\sum_n [q_n/(|\mathbf{r}-\mathbf{r}_n|)].$$

The extension to a continuous charge distribution is obvious. If $|\mathbf{r}_n|<|\mathbf{r}|$, each term of the sum can be expanded in a Maclaurin series. We thus obtain

$$U(\mathbf{r})=(q/r)+(\boldsymbol{\mu}\cdot\mathbf{r}/r^3)+(\mathbf{r}\cdot\Phi\mathbf{r}/2r^5)+\cdots. \quad (1)$$

Here $q=\sum_n q_n$ is the net charge of the system, $\boldsymbol{\mu}=\sum_n q_n\mathbf{r}_n$ is the dipole moment vector, and Φ is the quadrupole moment matrix with elements

$$\phi_{xx}=\sum_n q_n(3x_n^2-r_n^2), \quad \phi_{yy}=\sum_n q_n(3y_n^2-r_n^2),$$
$$\phi_{zz}=\sum_n q_n(3z_n^2-r_n^2),$$
$$\phi_{xy}=\phi_{yx}=3\sum_n q_n x_n y_n, \quad \phi_{xz}=\phi_{zx}=3\sum_n q_n x_n z_n,$$
$$\phi_{yz}=\phi_{zy}=3\sum_n q_n y_n z_n.$$

In all subsequent applications, only electrically neutral charge distributions are considered, hence, $q=0$. When transformed to principal axes Φ is diagonal and, since $\phi_{xx}+\phi_{yy}+\phi_{zz}=0$, only two of the three principal moments are independent.

The case of a distribution with an n-fold rotation axis ($n\geqslant 3$) is of particular interest and simplicity. In this case, the dipole moment vector is parallel to the axis of symmetry and two of the principal

quadrupole moments are equal. Let the unique quadrupole moment be $2P$; then the other two moments are $-P$ and $-P$. Let α, β, γ be unit vectors in the direction of the principal axes, γ being the unique axis. Then $\Phi\alpha=-P\alpha$, $\Phi\beta=-P\beta$, $\Phi\gamma=2P\gamma$. Any vector $\mathbf{S}$ can be expressed as a linear combination of α, β, γ as follows:

$$\mathbf{S}=a\alpha+b\beta+c\gamma,$$

where $a=\mathbf{S}\cdot\alpha$, $b=\mathbf{S}\cdot\beta$, $c=\mathbf{S}\cdot\gamma$. It can be readily shown by means of these relations that

$$\Phi\mathbf{S}=-P\mathbf{S}+3P\gamma(\mathbf{S}\cdot\gamma). \tag{2}$$

Since both γ and μ are parallel to the axis of symmetry, we can choose γ parallel to μ or

$$\gamma=\mu/\mu. \tag{3}$$

If $\mathbf{S}$ is replaced by $\mathbf{r}$ in Eq. (2), then

$$\mathbf{r}\cdot\Phi\mathbf{r}=-Pr^2+3P(\gamma\cdot\mathbf{r})^2$$

and the electrostatic potential becomes

$$U=[\mu\cos\theta/r^2]+\tfrac{1}{2}P[(3\cos^2\theta-1)/r^3]+\cdots, \tag{4}$$

where $\cos\theta=\gamma\cdot\mathbf{r}/r$. This result can be obtained in a much simpler way, but the method used here is very convenient when applied to the more complex problem of the interaction of two cylindrically symmetric charge distributions, which is treated in a later section. The unusual simplicity of this case is due not only to equality of quadrupole moments, but also to the fact that μ is parallel to the unique principal quadrupole axis. It is particularly to be noted that, to this degree of accuracy, the electrostatic potential is characterized by two parameters, μ and P. The former is, of course, the dipole moment, while the latter will be referred to as the quadrupole moment of the distribution. For future reference, the value of P in the case of a distribution consisting of both point charges and continuously distributed charge of density ρ is given below:

$$P=\sum_n q_n(r_n^2-3x_n^2)+\int(r^2-3x^2)\rho d\tau. \tag{5}$$

In this formula the z axis is along the unique principal axis, while x and y are perpendicular to this axis.

B. Interaction between Distributions

If U_1 is the electrostatic potential of one distribution and a second distribution of charge density ρ_2 is placed in its field, the interaction energy is

$$V(\mathbf{R})=\int U_1(\mathbf{R}+\mathbf{r})\rho_2 d\tau. \tag{6}$$

Here $\mathbf{R}$ is a position vector from the origin of the first distribution to the origin of the second, and $\mathbf{r}$ is a vector from the origin of the second to an arbitrary point. The integral extends over all values of $\mathbf{r}$. We suppose that the charge density of distribution 1 does not overlap that of 2. Hence, $\nabla^2U_1=0$ in the region 2. Now expand $U_1(\mathbf{R}+\mathbf{r})$ in a Taylor series around $\mathbf{r}=0$ and subtract $(r^2/6)\nabla\cdot\nabla U_1(\mathbf{R})=0$ from the result, and we obtain, on integrating term by term,

$$V(\mathbf{R})=q_2U_1(\mathbf{R})+\mu_2\cdot\nabla U_1(\mathbf{R})+\tfrac{1}{6}\nabla\cdot(\Phi_2\nabla U_1(\mathbf{R}))+\cdots. \tag{7}$$

Here q_2, μ_2, and Φ_2 are the net charge, dipole moment vector, and quadrupole moment matrix of distribution 2. They are defined in the same way as the corresponding quantities of Section IA. To complete the derivation, we utilize Eq. (1) and let $q_1=0$, $q_2=0$. After performing the differentiations, we get

$$V(\mathbf{R})=[\mu_1\cdot\mu_2/R^3]-[3(\mu_1\cdot\mathbf{R})(\mu_2\cdot\mathbf{R})/R^5]+[(\mu_2\cdot\Phi_1\mathbf{R}-\mu_1\cdot\Phi_2\mathbf{R})/R^5]-[5/2R^7][(\mathbf{R}\cdot\Phi_1\mathbf{R})(\mu_2\cdot\mathbf{R})-(\mathbf{R}\cdot\Phi_2\mathbf{R})(\mu_1\cdot\mathbf{R})]+[1/3R^5][\tfrac{1}{2}\nabla\cdot(\Phi_1\Phi_2\mathbf{R})-(5/R^2)\mathbf{R}\cdot\Phi_1\Phi_2\mathbf{R}+(35/4R^4)(\mathbf{R}\cdot\Phi_1\mathbf{R})(\mathbf{R}\cdot\Phi_2\mathbf{R})]. \tag{8}$$

In this expression, the first, second, and third lines give the dipole-dipole, dipole-quadrupole, and quadrupole-quadrupole interactions, respectively. In these expressions μ_1, Φ_1 are the vector dipole moment and the quadrupole moment matrix of distribution 1, while μ_2, Φ_2 are the corresponding quantities for distribution 2. The vector $\mathbf{R}$ is directed from 1 to 2. We note in passing that the dipole vector is directed from the center of negative charge to the center of positive charge.

Equation (8) is applicable, in general, to the interaction of two arbitrary charge distributions, although it is rather complex. If each of the two distributions is cylindrically symmetric, the interaction takes a much simpler form, which can be obtained by making use of the results of Section A. Let $\mathbf{S}$ be an arbitrary vector. Since both distributions 1 and 2 are cylindrically symmetric, we obtain for $\Phi_1\mathbf{S}$ and $\Phi_2\mathbf{S}$ two equations of the same form as (2).

$$\Phi_1\mathbf{S}=P_1[-\mathbf{S}+3\gamma_1(\gamma_1\cdot\mathbf{S})], \tag{9}$$

$$\Phi_2\mathbf{S}=P_2[-\mathbf{S}+3\gamma_2(\gamma_2\cdot\mathbf{S})]. \tag{10}$$

In these equations P_1 and P_2 are the quadrupole

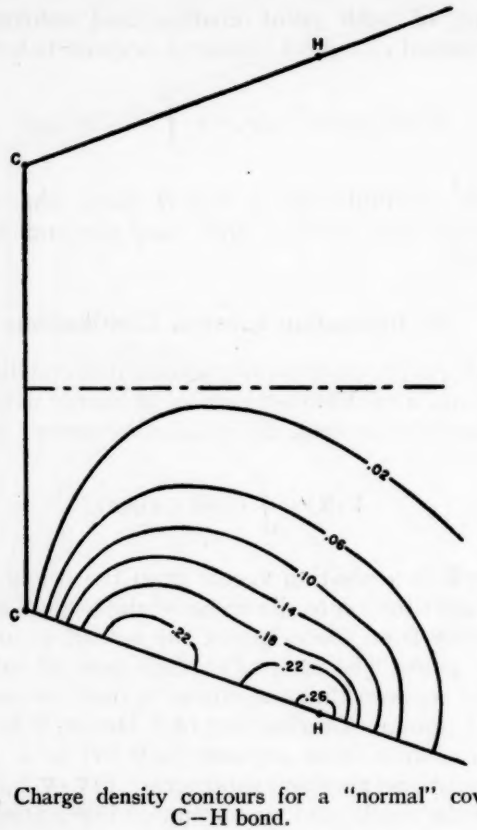

FIG. 2. Charge density contours for a "normal" covalent C−H bond.

moments of the two distributions, and γ_1, γ_2 are unit vectors in the directions of the respective unique principal axes. By means of these relations Eq. (8) can be expressed in terms of convenient variables. Consider, for example, the term $\mu_2\cdot\Phi_1\mathbf{R}$. Using (9) with **S** replaced by **R**, we find

$$\mu_2\cdot\Phi_1\mathbf{R}=P_1[-\mu_2\cdot\mathbf{R}+3(\mu_2\cdot\gamma_1)(\gamma_1\cdot\mathbf{R})]. \quad (11)$$

However, both distributions are cylindrically symmetric and, hence, γ_1, μ_1 are parallel to the symmetry axis and, hence, to each other and similarly for γ_2, μ_2. Therefore,

$$\begin{aligned}\gamma_1&=\mu_1/\mu_1,\\ \gamma_2&=\mu_2/\mu_2.\end{aligned} \quad (12)$$

Using these relations (11) becomes

$$\mu_2\cdot\Phi_1\mathbf{R}=\mu_2P_1[-\gamma_2\cdot\mathbf{R}+3(\gamma_2\cdot\gamma_1)(\gamma_1\cdot\mathbf{R})]. \quad (13)$$

It is convenient to introduce three angles defined as follows in terms of scalar products:

$$\gamma_1\cdot\mathbf{R}=R\cos\theta,\quad \gamma_2\cdot\mathbf{R}=R\cos\gamma,\quad \gamma_1\cdot\gamma_2=\cos\theta'.$$

In terms of these variables (13) becomes

$$\mu_2\cdot\Phi_1\mathbf{R}=\mu_2P_1R(3\cos\theta\cos\theta'-\cos\gamma). \quad (14)$$

In precisely the same way, every term in Eq. (8) can be expressed in terms of the four variables R, $\cos\theta$, $\cos\gamma$, $\cos\theta'$. The final result is as follows:

$$\begin{aligned}V=(\mu_1\mu_2/R^3)&[\cos\theta'-3\cos\theta\cos\gamma]\\ &+(1/R^4)\{\mu_2P_1[(3\cos\theta\cos\theta'-\cos\gamma)\\ &-(5/2)\cos\gamma(3\cos^2\theta-1)]\\ &-\mu_1P_2[(3\cos\gamma\cos\theta'-\cos\theta)\\ &-(5/2)\cos\theta(3\cos^2\gamma-1)]\}\\ &+[P_1P_2/3R^5][(35/4)(3\cos^2\theta-1)\\ &\times(3\cos^2\gamma-1)+5(3\cos^2\theta-1)\\ &+5(3\cos^2\gamma-1)+\tfrac{3}{2}(3\cos^2\theta'-1)\\ &-45\cos\theta\cos\gamma\cos\theta'+5]. \quad (15)\end{aligned}$$

The application of this equation is somewhat tedious, but is quite straightforward. It is particularly important that the terms of each type, dipole-dipole, dipole-quadrupole, quadrupole-quadrupole have in common the fact that they are products of a constant factor by a *known function of angle and distance.* In this respect, the interaction of cylindrically symmetric charge distributions has unusual simplicity.

C. Approximate Quadrupole Moments

The dipole moments for many bonds are known as the result of investigations of dielectric constants. Quadrupole moments have not been measured, however, except in the case of molecular hydrogen.[4] In applying Eq. (15), we use the results of observation to calculate P and, hence, some estimate of the orders of magnitude of bond quadrupole moments must be available in order to avoid the possibility of gross error. In this section we shall first obtain an approximate upper limit to the quadrupole moments of single bonds and then use localized molecular orbitals to obtain rough estimates of the moments for single, double and triple bonds. The results, although inaccurate, are of some use as indication of orders of magnitude.

The discussion of quadrupole moments is somewhat simplified by introducing the following three quantities

$$\Theta_{xx}=\sum_n q_n{x_n}^2+\int x^2\rho d\tau,$$

$$\Theta_{yy}=\sum_n q_n{y_n}^2+\int y^2\rho d\tau,$$

$$\Theta_{zz}=\sum_n q_n{z_n}^2+\int z^2\rho d\tau.$$

For cylindrically symmetric distributions $\Theta_{xx}=\Theta_{yy}$ and

$$P=\Theta_{zz}-\Theta_{xx}.$$

In the case of a covalent bond, the two discrete positive charges lie on the z axis and the electrons

[4] Norman F. Ramsey, Phys. Rev. **58**, 190 (1940).

are continuously distributed. The sums in the above formulas then extend over the positive charges, while the integrals extend over the negative charge distribution and are negative since ρ is negative. In the case of Θ_{zz} the sum over nuclei vanishes since the charges lie on the z axis. Therefore, Θ_{zz} is negative. Next consider the problem of obtaining an *upper limit* to P. Clearly, an upper limit to Θ_{zz} is obtained under such circumstances that the z coordinates of the negative charges vanish; i.e., this charge lies in the x, y plane. In this case, only the sum over nuclei remains and, if the interatomic distance is R, then $\Theta_{zz}=R^2/2$ in atomic units. This suggests the classical model in which both electrons move at opposite extremities of the diameter of a circular orbit whose plane is perpendicular to the line of centers and which bisects the line of centers. If λ is the radius of the orbit, then the x coordinates of the two electrons are $\lambda\cos\varphi$ and $\lambda\cos(-\varphi)$. After averaging over φ, we obtain

$$\Theta_{xx}=-\lambda^2.$$

An upper limit to P is obtained when Θ_{xx} is as negative as possible, and this is achieved at $\lambda=\infty$. This result, however, is not of much value and, hence, some other reasonable estimate must be made. For this purpose we consider that the two bonded nuclei are at equilibrium with respect to repulsion by each other and attraction by the electrons. If the effective charge on each nucleus is $+1$, equilibrium is attained when $\lambda^2=3(R/2)^2$. If the effective nuclear charges are greater, the factor 3 is replaced by a smaller number.[5] Since only an upper limit is required, only the case of unit charges is considered. This gives finally

$$P=(R^2/2)+\tfrac{3}{4}R^2=(5/4)R^2$$

as the approximate upper limit. Obviously, numerous objections can be raised to this result and, in fact, no finite upper limit exists in the strictest mathematical sense. Nevertheless, the distribution treated is so extreme that any quadrupole moment obtained empirically which exceeds the above value or even closely approaches it must be regarded with suspicion. For the H−H, C−H, and C−C bonds, R (in atomic units) is 1.40, 2.07, and 2.92, respectively. The corresponding limits are 2.5, 5.4, and 10.6.

In order to obtain a more reliable estimate of the orders of magnitude of quadrupole moments, account must be taken of the continuous distribution of negative charge. For this purpose localized molecular orbitals, which are expressed as linear combinations of atomic orbitals, can be used. These considerations are extremely crude and must be regarded as examples of familiar distributions rather than theoretical calculations of bond quadrupole moments.

Let ψ_C and ψ_H be normalized atomic orbitals for carbon and hydrogen, respectively, and let σ_{H-H}, σ_{C-H}, σ_{C-C} designate localized molecular orbitals for the H−H, C−H, and C−C bonds, respectively. Then

$$\sigma_{H-H}=A(\psi_{H_1}+\psi_{H_2}),$$
$$\sigma_{C-H}=a\psi_C+b\psi_H,$$
$$\sigma_{C-C}=B(\psi_{C_1}+\psi_{C_2}),$$

where A, B, a, b are constants. The normalizing condition $\int\sigma^2 d\tau=1$ determines A and B completely and provides one relation between a and b. As the carbon atomic orbital, we take the product of a radial factor, obtained from Slater's[6] functions and screening constants, by an angular factor equal to Pauling's tetrahedral orbital.[7] Since there are two electrons per bond, the charge density contributed by electrons is $\rho=-2\sigma^2$.

With the use of σ_{C-H} and Eqs. (16), Θ_{zz} and Θ_{xx} have been calculated for several values of a/b. The integrals were evaluated in the usual way by transformation to spheroidal coordinates. Since no new integrals were encountered, the details of the calculations are omitted. The results are given in Table I. It is to be noted that both positive and negative values of Θ_{zz} are obtained, but the magnitudes are small. The values of P are positive in all cases and change but little with change in a/b. The type of charge density represented by σ_{C-H} has already been discussed in connection with Figs. 1 and 2, which show contour lines for the cases $a/b=5.75$ and $a/b=1$, respectively. The former corresponds to a distribution with proper dipole moment (at least in magnitude), while the latter is the molecular orbital analog of a "normal" covalent bond. The dipole moment for each distribution has also been calculated and is given in column 5. That such a large value of a/b is required to give the correct bond dipole moment is somewhat disturbing and does not inspire great confidence in the accuracy of this approximation. The large dipole moment for the "normal" bond is also difficult to reconcile with current views on bond dipole moments. It seems possible that neglect of polarization of the hydrogen orbital is responsible for the large moments. Significant polarization of the hydrogen orbitals is found in the wave mechanical treatment of the hydrogen molecule ion and very probably should also be taken into account in other substances as well. Neither the direction nor magnitude of error in the calculated quadrupole moment is immediately obvious. Nevertheless, the results serve a useful purpose in indicating the order of magnitude of the moment.

[5] Niels Bohr, Phil. Mag. 26, 857 (1913).

[6] John C. Slater, Phys. Rev. 36, 57 (1930).

[7] Linus Pauling, *Nature of the Chemical Bond* (Cornell University Press, Ithaca, New York, 1940), p. 86.

The values of Θ_{zz}, Θ_{xx}, and P calculated for the C−C bond from σ_{C-C} are given in Table II. It is to be noted that Θ_{zz} is positive and has a considerable magnitude. This arises because both carbon orbitals are of such a type as to cause accumulation of electrons between the nuclei. The effect is illustrated by the contour diagram of Fig. 3. The quadrupole moment P is again positive. For later use the quadrupole moment of H_2 has also been computed from σ_{H-H}. These results are also included in Table II. In this case, Θ_{zz} is negative, while P is again positive. In view of all of the above results, it seems probable that P is positive, in general, for single bonds.

In the case of multiple bonds, the electrons in π-orbitals must also be considered. The π-orbitals can again be approximately represented as linear combinations of atomic orbitals of carbon. The atomic orbitals are taken as products of radial functions of the Slater type with angular factor corresponding to p atomic orbitals. The symmetry axes of the atomic orbitals are, of course, at right angles to the line of centers. Tetrahedral orbitals were used for the σ-bonds in both double and triple bonds. This is not strictly accurate, but suffices for these order of magnitude estimates. Moments calculated in this way for both the double and triple bond are given in Table II. The triple bond is cylindrically symmetric, whereas the double bond is not, as indicated by the fact that $\Theta_{xx} \neq \Theta_{yy}$.

Several points suggested by the foregoing treatment which will be used in the following sections may be briefly summarized as follows: (a) single covalent bonds have large quadrupole moments, (b) any quadrupole moment for a single bond which is greater than $5R^2/4$ is unreasonable, (c) the quadrupole moments of single bonds are positive, (d) the triple bond charge distribution is cylindrically symmetric, but the double bond distribution is not.

That the quadrupole moments obtained empirically in the following sections have reasonable magnitudes can be further verified by using the moments to calculate the diamagnetic susceptibilities of anisotropic hydrocarbons. This work will be discussed in a later paper.

TABLE I. Calculated moments for C−H bond.

a/b	$-\Theta_{zz}$	Θ_{xx}	P	μ (Debye)
1.0	1.72	−0.28	1.44	−2.30
1.5	1.64	−0.06	1.58	−1.51
2.0	1.58	0.05	1.64	−0.98
4.0	1.48	0.18	1.65	0.03
5.75	1.44	0.19	1.63	0.40

III. APPLICATION TO SYSTEMS HAVING ONE INTERNAL DEGREE OF ROTATIONAL FREEDOM

In order to test the theory, a number of simple molecular systems have been examined by means of numerical calculation, the results of which are discussed in the following sections. The succession of molecules treated is such that unshared electron pairs replace covalent bonds step by step. The effect of unshared electron pairs in hindering rotation is thereby illustrated.

A. Ethane

The results of applying these methods to ethane have been previously reported,[1] but were not described in any detail. In considering ethane, only the interaction between C−H bonds in one methyl group with those of the other methyl group need be considered. The unique principal axes of the quadrupoles are along the line of centers. The unit vectors γ_1 and γ_2 along the unique axes are directed from carbon to hydrogen. These vectors are necessarily parallel or antiparallel to μ_1 and μ_2, respectively, depending on whether the dipole moment is directed from carbon to hydrogen or *vice versa*. Since it would obviously be troublesome to change the definitions (12) to take both cases into account, the practice of making the magnitudes of μ_1 and μ_2 either positive or negative has been adopted. If μ_1 is negative in (12), then obviously γ_1 is antiparallel to μ_1 and, hence, all of the various possibilities can be taken account of correctly by means of changing signs. Let **C** be a unit vector along the C−C bond axis. If φ be the dihedral angle between the plane of γ_1, **C** and the plane of γ_2, **C**, the various distances and angles can easily be shown to have the following form:

$$\begin{aligned} \cos\theta' &= 8/9\,\cos\varphi - \tfrac{1}{9}, \\ R\cos\theta &= -R\cos\gamma = [(4h/9)(\cos\varphi - 1)] - [R_0/3], \\ R^2 &= R_0^2 + [(4h^2/9)(1-\cos\varphi)]. \end{aligned} \tag{16}$$

Here h is the C−H interatomic distance, C is the C−C interatomic distance and $Ro = C + (h/3)$. All bonds were assumed to be tetrahedral, and in the numerical calculations atomic units were used throughout. In these units $h = 2.07$ and $C = 2.915$. In angstrom units $h = 1.09$ and $C = 1.54$. Using these formulas and Eq. (15), the interaction energies for the three C−H bonds of one methyl group with the three of the other methyl group were calculated for both the staggered (D_{3d}) and eclipsed (D_{3h}) configurations.

The difference in energies is the barrier hindering rotation (V_0). In atomic units

$$V_0 = V(eclipsed) - V(staggered) = 0.3066\times10^{-2}\mu^2 + 1.8536\times10^{-3}\mu P + 0.8987\times10^{-3}P^2,$$

where μ and P are the dipole and quadrupole moments of the C−H bond.** If V_0 is positive, the staggered configuration has lower energy and therefore is the stable configuration, while if V_0 is negative, the eclipsed configuration is stable. The expression on the right-hand side can be regarded as a quadratic form in two variables (μ, P). This form can easily be shown to be positive definite and, hence, is positive for all real values of μ and P. We conclude that the staggered configuration is stable, no matter what the magnitudes or signs of μ and P may be.

It is known from other considerations that $\mu=\pm 0.158$ atomic unit (± 0.4 Debye). Using these values and the observed barrier (2750 cal.),[8] the quadrupole moments can be calculated. In this way we obtain $P=2.03$ if μ is positive and 2.35 if μ is negative. It should be mentioned that, in solving the quadratic equation for P, two roots are obtained, one positive and the other negative. Since we have concluded previously that the bond quadrupole moments are always positive, the negative roots were discarded.

In Section IIC, an upper limit of 5.4 was estimated for the C−H bond. Both of the above moments lie well below this value and, hence, do not seem unreasonable in this respect. The C−H bond moment calculated in Section IIC by means of a molecular orbital is 1.63. Both of the empirical moments are somewhat higher than this, but are of the same order of magnitude. That the direction of deviation is reasonable is indicated by the fact that the *accurate* quadrupole moment for H_2 (0.442)[9] is 30 percent higher than the *approximate* moment (0.34 —see Table II). Not only do the deviations of the empirical C−H bond moments from the approximate moments agree in *direction* with those for H_2, but even the *magnitude* (+25 percent if μ is positive and +44 percent if μ is negative) of the deviations are comparable, especially in the case of positive dipole moment.

An important point concerning ethane remains. In the experimental determination of the ethane barrier, the interaction energy was assumed to have the form

$$V=V(staggered)+(V_0/2)(1+\cos 3\varphi). \quad (17)$$

The experimental barrier for ethane ($V_0=2750$ cal.) is therefore dependent on the accuracy with which this function represents the interaction energy. On the basis of the dipole-quadrupole model, this functional dependence is explicitly obtained and is obviously different in form from (17). Nevertheless, (17) constitutes a rather good approximation. This has been established by calculating the interaction energy from Eq. (15) as a function of φ, using Eqs. (16). The results are given in Table III and, for comparison, the same interactions computed from (17) are included. The agreement between (17) and (15) is surprisingly close. It is therefore concluded that calculation of quadrupole moments from the observed barrier is self-consistent, since the dipole-quadrupole model leads to a dependence on angle which is practically indistinguishable from (17).

The net interaction between methyl groups in ethane is one of repulsion for all values of φ, as is evident from Table III. However, the interaction between individual bonding distributions may be either attraction or repulsion, depending on the value of φ. This is illustrated by Fig. 4, in which the energy of interaction of one C−H bond of one methyl group with one bond of the other group is shown as a function of φ. The separate dipole-dipole, dipole-quadrupole, and quadrupole-quadrupole energies are also given in the same figure. The quadrupole-quadrupole interaction is much the largest and, hence, an inverse fifth-power dependence on distance is indicated.

It is interesting that an inverse fifth-power dependence on distance was found empirically by Aston, Isserow, Szasz, and Kennedy.[10] These authors attributed the barriers to repulsion between hydrogens, however, and, hence, the results cannot be directly compared with the present theory which provides for dependence on orientation of the distributions as well as on the distance.

The predominance of the quadrupole-quadrupole interaction is of considerable interest because it indicates at once that substantial barriers hindering rotation are to be expected in all substances similar to ethane. This arises because the quadrupole moments of single bonds are always expected to have considerable magnitudes whether the atoms of the bond are alike or not. In this respect quadrupole and dipole moments are very different, since the latter vanish when the atoms of the bond are alike and are widely different in magnitude for other bonds.

If both signs for the C−H bond dipole moment are used, two alternative sets of empirical bond quadrupole moments are obtained from potential barrier data. It has been found that energy *differ-*

** The numerical work has been checked by means of a calculation in which Eq. (8) is employed directly and all calculations carried through in Cartesian coordinates. The results agree accurately with those quoted above. Six significant figures have been carried in all numerical work, both in order to avoid error caused by large cancellations and since high powers of the distances appear. The bond distances and angles are obviously not known with any such accuracy, and one significant figure has been dropped in reporting the results of numerical calculations.

[8] G. B. Kistiakowsky, J. R. Lacher, and F. Stitt, J. Chem. Phys. **7**, 289 (1939).

[9] H. M. James and A. S. Coolidge, Astrophys. J. **87**, 447 (1938).

[10] Aston, Isserow, Szasz, and Kennedy, J. Chem. Phys. **12**, 336 (1944).

TABLE II. Calculated moments for C−C, C=C, C≡C, and H−H bonds.

Bond	$-\Theta_{xx}$	$-\Theta_{yy}$	Θ_{zz}	P
C−C	1.43	1.43	2.36	3.79
C=C	5.07	2.63	1.15	—
C≡C	6.28	6.28	0.08	6.36
H−H	2.09	2.09	−1.75	0.34

ences calculated from these two sets did not differ significantly in a variety of cases. No clear-cut decision between these alternatives can be reached on the basis of calculations thus far performed. Since it is inconvenient to calculate and report both sets, we have preferred to adopt the usual convention that hydrogen is positive and, hence, μ is positive. This alternative seems a little more likely from the foregoing comparison of C−H and H−H bond moments. The possibility of a negative dipole moment is not excluded, however.

B. Methyl Amine

Methyl amine differs from ethane in that the nitrogen atom contains an unshared electron pair. In considering electrostatic interactions which involve the unshared pair, it is convenient to consider a neutral distribution consisting of the pair of electrons and two of the positive charges on the nitrogen nucleus. The nitrogen nucleus is taken as the origin of coordinates. As a guide in treating the problem, it is useful first to consider the distribution of molecular electrons in accordance with the qualitative ideas of Pauling.[11] The bonding in methyl amine must be such as to lead to minimum energy for the molecule. We consider first, and in turn, two extreme situations. In the first case, minimum energy for the bonding electrons is the predominant factor. This is achieved when the three bonding orbitals on nitrogen are tetrahedral. This, however, leaves only a tetrahedral orbital to be occupied by the unshared pair, and the distribution has cylindrical symmetry around the fourth tetrahedral direction. In the second extreme case, the energy of the unshared electron pair is the predominant factor. In this case, the pair occupies an s orbital on nitrogen and the distribution has spherical symmetry. The final distribution is a compromise between these extremes such that the total energy is a minimum. These considerations are, of course, very rough, and in what follows we shall not use them in any quantitative way. Instead we shall suppose only that the unshared pair is distributed with cylindrical symmetry. Its symmetry axis is fixed with respect to the NH_2 group and rotates with that group. Equation (15) can now be applied to show that the interaction of the unshared pair with the methyl group does not change as the NH_2 group is rotated around the C−N bond. Consider first the interaction of one C−H bond with the unshared pair. Let **R** be drawn from the C−H bond to the origin of the pair; i.e., the nitrogen nucleus. Then two of the variables (R and $\cos\theta$) do not change on rotating the NH_2 group, but the other two ($\cos\theta'$ and $\cos\gamma$) do change. Let the angle of rotation be φ. Then the interaction energy can be readily shown to have the form

$$V(\varphi)=A_0+A_1\cos\varphi+A_2\cos^2\varphi,$$

where A_0, A_1, A_2 depend on the bond angles, interatomic distances, moments, and the angle between the symmetry axis of the pair and the C−N bond, but do not depend on φ. The total interaction of the pair with all three bonds of the methyl group is

$$V(\varphi)+V(\varphi+120°)+V(\varphi+240°)=3A_0+\tfrac{3}{2}A_2.$$

This expression, however, is independent of φ and, hence, the interaction of the unshared pair does not change on rotation and does not contribute to a barrier hindering rotation. The simplicity of this case is due to trigonal symmetry of the methyl group. Under these conditions, the barrier will be entirely determined by the interaction of N−H and C−H bonds.

On this basis, the barrier can be calculated, using Eq. (15), by methods very similar to the ethane calculation. The C−H bond dipole (μ_1) and quadrupole (P_1) moments, the N−H bond dipole (μ_2) moment, and the interatomic distances are given in Table IV. For convenience, all bond angles are assumed to be tetrahedral. Interaction energies have been calculated for both the eclipsed and staggered configurations for several values of the N−H bond quadrupole moment (P_2). In all cases, the staggered configuration has the lower energy. In column 6 of Table IV, the difference $V(eclipsed) - V(staggered)$ is given. The quadrupole moments appear in column 1 and the separate dipole-dipole, etc., energies are given in columns 2, 3, 4, and 5. The quadrupole-quadrupole interaction is again predominant. The entries in column 6 are to be compared with the observed barriers hindering rotation

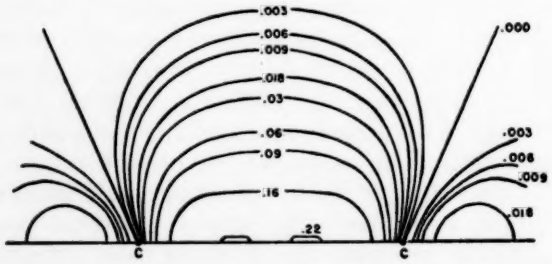

FIG. 3. Charge density contours for the C−C bond calculated from a localized molecular orbital.

[11] See reference 7, Chapter III.

around the C−N bond. Two values for this barrier have been reported. Aston, Siller, and Messerly obtained a barrier of 3000 cal./mole as the result of a calorimetric study,[12] while Aston and Doty calculated a barrier of 1520 cal./mole as the result of a spectroscopic study.[13] Table IV has been constructed in such a way as to cover the range included by these two values in steps of 500 cal. The quadrupole moment required to account for a 3000-cal. barrier is 2.42. The upper limit to the N−H bond moment estimated by means of the method of Section II is 4.6. Since this considerably exceeds all of the moments given in Table V, it provides no basis for excluding the high barrier. It is probable that the actual barrier can be accounted for by means of the dipole-quadrupole model with reasonable quadrupole moments and without contribution from the unshared pair. The probable barrier for this substance will be further discussed in Section V.

C. Methyl Alcohol

The oxygen atom in methyl alcohol contains two unshared pairs. If the distribution of each pair has cylindrical symmetry, the two symmetry axes being different in general, then, because of the trigonal symmetry of the methyl group, the interaction of each unshared pair with the methyl group is unchanged on rotation around the C−O bond. This can be proved in precisely the same manner as for methyl amine. The barrier hindering rotation is then due entirely to interaction of the O−H bond with the C−H bonds of the methyl group. The calculation can be carried out in the same manner as for ethane and methyl amine. All moments except the quadrupole moment of the O−H bond are known and, hence, calculations are again made for several values of this moment. The differences $V(eclipsed) - V(staggered)$ are given in column 6 of Table V. The bond quadrupole moments are given in column 1. The interatomic distances and the remaining moments are also given in the table. All bond angles were assumed to be tetrahedral. The quadrupole-quadrupole interaction is again predominant. The values in column 6 are to be compared with the observed barrier. The potential barrier hindering rotation in methyl alcohol was calculated from calorimetric data by Crawford,[14] who obtained 3400 cal./mole. A spectroscopic study by Koehler and Dennison[15] led to a barrier of 1340 cal./mole. The subject has been reviewed recently by French and Rasmussen,[16] who repeated Crawford's calculation,

[12] J. G. Aston, C. W. Siller, and G. H. Messerly, J. Am. Chem. Soc. **59**, 1743 (1937).
[13] J. G. Aston and P. M. Doty, J. Chem. Phys. **8**, 743 (1940).
[14] Bryce L. Crawford, Jr., J. Chem. Phys. **8**, 744 (1940).
[15] J. S. Koehler and D. M. Dennison, Phys. Rev. **57**, 1006 (1940).
[16] F. A: French and R. S. Rasmussen, J. Chem. Phys. **14**, 389 (1946).

TABLE III. Interaction of methyl groups in ethane. $V(\varphi) - V(60)$ in kcal., $\mu = +0.158$ a.u., $V(60) = 14.2$ kcal., $\mu = -0.158$ a.u., $V(60) = 29.0$ kcal.

φ	0	10	20	30	40	50	60
$\mu = +0.158$	2.750	2.563	2.052	1.361	0.677	0.182	0.000
$\mu = -0.158$	2.750	2.563	2.051	1.360	0.676	0.182	0.000
$(V_0/2)(1+\cos 3\varphi)$	2.750	2.566	2.062	1.375	0.688	0.184	0.000

using more recent physical constants, and obtained the barrier 2360 cal./mole. They also pointed out that other thermodynamic data which seem equally reasonable lead to essential agreement with the spectroscopic barrier of 1340 cal./mole or less. We have varied the O−H bond quadrupole moment over such a range as to include both of these values. By means of the method of Section II, the upper limit to the O−H bond moment is estimated as 4.1. The moment required to provide a barrier of 2360 calories is 3.56 atomic units. This approaches the upper limit too closely to seem reasonable. On the other hand, the quadrupole moment required to account for a barrier of 1340 cal./mole is 1.822, which seems more reasonable. Since this latter barrier has considerably stronger experimental support than does the 2360 barrier, it appears that the theory is supported by this result. As will be indicated later, a barrier even lower than 1340 would not be unreasonable.

The interaction energy in methyl alcohol has been computed for several other values of φ in order to test the accuracy with which a formula of the form (17) fits the dependence on angle. The agreement is good, and it must be concluded that (17) is an accurate approximation in this case.

D. Hydrogen Peroxide

The two previous examples, methyl alcohol and methyl amine, constitute cases in which the un-

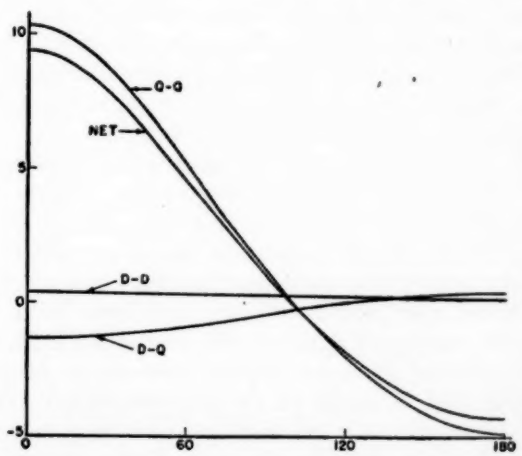

FIG. 4. Energy of interaction of a C−H bond in one methyl group with one in the other methyl group of ethane as a function of the angle of rotation. The *cis* position comes at $\varphi = 0°$

shared electron pairs play no role in hindering rotation because of trigonal symmetry of the methyl group. In one respect, this is fortunate, since the study of these substances provides a convenient means of empirically calculating the N−H and O−H bond quadrupole moments from observed potential barriers without interference from unshared pairs. At the same time, these substances provide no information concerning the distribution of unshared electron pairs, and it is of interest, therefore, to consider an example in which the methyl group is replaced by one of lower symmetry. A simple substance of this type is hydrogen peroxide, and its equilibrium configuration is discussed below in some detail.

The hydrogen peroxide molecule is known to have a permanent dipole moment and to be non-planar. The dihedral angle between hydroxyl groups has been estimated by various investigators and probably lies between 100° and 110°. If the only important interactions were those between O−H bonding distributions, the equilibrium dihedral angle would be 180°, contrary to experiment. It seems evident, therefore, that the interaction between unshared electron pairs must play an important role in determining the equilibrium arrangement.

In order to proceed, it is necessary to consider further the distribution of unshared electron pairs. In this case, as with methyl amine, some progress can be made by applying Pauling's ideas. The two extremes cases are (a) that the bonding orbitals are tetrahedral, thus leading to the strongest bonds and placing the unshared pairs in each of the two remaining tetrahedral orbitals, and (b) that one unshared pair occupies the orbital of lowest energy ($2s$) and leaves the three $2p$ orbitals for the other unshared pair and two bonds. The actual distribution is a compromise which is probably considerably nearer to (b) than to (a), since, in oxygen, the $2s$ orbital has much lower energy than does $2p$. We have chosen the symmetry axes and dipole moments so as to accord with (b), recognizing, however, that the choice is extreme and may require modification. The explicit hypotheses used in calculation are as follows: (i) one unshared pair is distributed with spherical symmetry; (ii) the second unshared pair is distributed with cylindrical symmetry; (iii) the axis of symmetry is perpendicular to a plane which contains the oxygen atom and two atoms which are bonded to it; (iv) each distribution consists of an unshared pair and two positive charges from the oxygen nucleus; (v) the dipole moment of each distribution is zero. As before, the origin of each distribution is taken at the oxygen nucleus. Only one unshared pair on each oxygen need be considered, since the other has spherical symmetry.

The interactions which must be considered in treating H_2O_2 are those between the two O−H bonds, between the O−H bonds and the unshared pairs on opposite oxygens, and finally that between an unshared pair on each oxygen. By hypothesis the unshared pairs have no dipole moments and, hence, their interaction involves only the quadrupole term of (15). The interaction energy is

$$V\text{pair} = (3Q^2/2R^5)(\tfrac{1}{2}+\cos^2\varphi). \qquad (18)$$

Here Q is the quadrupole moment of the unshared pair, R is the interatomic distance of the O−O bond, and φ is the dihedral angle between two planes containing the O−H groups and intersecting along the O−O bond. When $\varphi=0$, the hydroxyl groups are in the *cis* position. It is obvious that V is a minimum when $\varphi=\pi/2$, no matter what the magnitude or sign of Q may be. The interaction tends, therefore, to stabilize the configuration in which the dihedral angle is 90°. The energy of interaction between an O−H bond and the unshared pair on the opposite oxygen has the form $A+B\cos^2\varphi$, where A and B are independent of φ. This term must have either a maximum or a minimum when $\varphi=\pi/2$, depending on the magnitudes and signs of the various moments and the interatomic distances which determine B.

The combined influence of all effects is best shown by means of numerical calculation. Since neither quadrupole moment is known with any accuracy, the interaction energies have been calculated for several combinations of moments. The quadrupole moment for the unshared pair calculated from a $2p_z$ atomic orbital of the Slater type is -1.16 atomic unit. Only negative values for this moment have been used. The results of the calculations are given in Table VI. The first column contains the bond quadrupole moment, the second contains the quadrupole moment of the unshared pair, while the next five contain the energies of interaction at various angles referred to the *trans* position as zero. In the eighth column the dihedral angles for which the energy is a minimum are given. These angles were obtained by graphical interpolation and may be in error by one or two degrees. The depth of the minimum is indicated in column 9, while the energy of the *trans* configuration is given for reference in column 10. It seems remarkable that the equilibrium dihedral angle varies only in the range from 94° to 113° for such wide variations in the quadrupole moments. In all cases, there are two maxima, a high one in the *cis* position and a lower one in the *trans* position. Zumwalt and Giguère have investigated a band system of hydrogen peroxide in the near infrared[17] and concluded that φ is greater than 95° and that there are two potential maxima, one high and the other low. It seems evident that our hypotheses concerning the distribution of molecular electrons

[17] L. R. Zumwalt and P. A. Giguère, J. Chem. Phys. 9, 458 (1941).

are sufficient to account for all of the known facts concerning the equilibrium configuration and internal rotation of hydrogen peroxide using quadrupole moments of reasonable magnitudes.

In order to obtain information concerning the unshared pair on the nitrogen atom of the amino group, it is necessary to consider a substance in which the unshared pair plays a role in determining the equilibrium configuration. Such a substance is hydrazine. If the unshared pair were distributed with spherical symmetry, the equilibrium configuration of the NH_2 groups would be determined entirely by the interaction of N—H bonds. From Eq. (15) it follows that the *trans* position of the amino groups is the stable one. This configuration, however, leads to zero dipole moment for the molecule, which is in contradiction to experiment. If our model is to be applicable, it follows that the unshared pair must depart significantly from spherical symmetry. Stated in terms of Pauling's approximate model, the unshared pair is distributed in a manner which lies between an atomic s orbital and a tetrahedral orbital. This factor may ultimately require consideration in the case of H_2O_2 also. A quantitative calculation has not been made.

The equilibrium configuration of hydrogen peroxide was predicted correctly some years ago by Penney and Sutherland[18] as the result of a straightforward, although approximate, wave mechanical treatment. They also considered the case of hydrazine and predicted an unsymmetrical arrangement which accounts rather well for its dipole moment. A detailed quantitative comparison of their treatment with that used here cannot be made, since they begin from different points. In a qualitative way, however, this treatment differs from theirs in that we have neglected some of the exchange interactions and have approximated to the Coulomb integrals by means of expansion in inverse powers of the distance, thus introducing dipole and quadrupole terms. However, we have attempted to avoid explicit use of atomic orbital approximations except for qualitative purposes. All of the interactions treated here also occur in their treatment, although in somewhat disguised form. Even the departure from spherical symmetry of the unshared pair on nitrogen is included by them by considering the combination of two states for the nitrogen atoms whose configurations are s^2p^3 and sp^4. The two treatments differ, therefore, chiefly in the types of approximations involved and especially in that we have applied, systematically and empirically, a model which has been deliberately reduced to its simplest form and which must be refined as the result of comparison with experiment.

[18] W. G. Penney and G. B. B. M. Sutherland, J. Chem. Phys. 2, 492 (1934).

TABLE IV. Methylamine barrier for various quadrupole moments. C—H bond: $\mu_1=0.158$ a.u., $P_1=2.03$ a.u., $R=2.07$ a.u. N—H bond: $\mu_2=0.517$ a.u., $R=1.91$ a.u. C—N bond: $R=2.78$ a.u.

P_2	D_1-D_2 kcal.	D_1-Q_2 kcal.	D_2-Q_1 kcal.	Q_1-Q_2 kcal.	Net kcal.
0.97	0.12	0.09	0.37	0.92	1.50
1.45	0.12	0.13	0.37	1.38	2.00
1.93	0.12	0.18	0.37	1.83	2.50
2.42	0.12	0.22	0.37	2.29	3.00

E. Dimethyl Acetylene

The treatment of dimethyl acetylene is of interest chiefly because it indicates the effect of increasing the distance between methyl groups. The potential barrier for this substance was investigated by Osborne, Garner, and Yost,[19] who found it too small to measure. Assuming, as discussed in Section II, that the triple bond is cylindrically symmetric, the entire barrier is due to the interaction between methyl groups. Using the same method as for ethane and the accepted interatomic distances, we have calculated this barrier and find 31 cal./mole. This is negligible, in complete agreement with experiment, and provides additional confirmation for the model.

IV. MORE COMPLEX EXAMPLES. THE INTERACTION OF NON-ADJACENT GROUPS

In all of the preceding examples for which experimental potential barriers are available, the potential function $V=(V_0/2)(1+\cos 3\varphi)$ has been assumed in interpreting the experimental data. Since the dipole-quadrupole theory leads to a potential function which approximates very closely to the above form, the use of observed potential barriers for the calculation of approximate quadrupole moments is at least self-consistent. In the class of compounds to be discussed next, this self-consistency no longer prevails, since the potential barriers are ordinarily calculated from experimental data (usually thermodynamic) on the basis of the assumption that only adjacent groups interact significantly. It will appear shortly that this assumption is not consistent with

TABLE V. Methyl alcohol barrier for various quadrupole moments. C—H bond: $\mu_1=0.158$ a.u., $P_1=2.03$ a.u., $R=2.07$ a.u. O—H bond: $\mu_2=0.596$ a.u., $R=1.815$ a.u. C—O bond: $R=2.70$ a.u.

P_2	D_1-D_2 kcal.	D_1-Q_2 kcal.	D_2-Q_1 kcal.	Q_1-Q_2 kcal.	Net kcal.
1.07	0.08	0.06	0.19	0.57	0.90
1.82	0.08	0.10	0.19	0.97	1.34
3.56	0.08	0.20	0.19	1.89	2.36

[19] D. Osborne, C. Garner, and D. M. Yost, J. Chem. Phys. 8, 131 (1940).

the present theory. The work of Pitzer[20] on propane has already indicated appreciable interaction between methyl groups. Since quadrupole moments are not available for the C−C bond, it is most convenient to proceed first by assuming the validity of the hypothesis in order to calculate an approximate moment and then by using the moment to show by numerical calculation that a contradiction arises. Despite the uncertainty concerning the C−C bond moment, certain interesting conclusions concerning equilibrium configurations can be obtained.

We consider first the case of propane, for which the barrier per methyl group has been found to be 3400 cal./mole.[20] Using Eq. (15), the interaction energy has been computed for the arrangement in which both methyl groups are staggered (*ss*) and also when both are eclipsed (*ee*). The terms staggered and eclipsed refer to the orientation of each methyl group with respect to the immediately adjacent group, not with respect to each other. The difference between the two energies is as follows:

$$V(ee)-V(ss)=0.4861\times10^{-2}\mu^2 +3.4722\times10^{-3}P_H\mu-0.2242\times10^{-3}P_c\mu +1.4745\times10^{-3}P_H^2+0.3853\times10^{-3}P_HP_c. \quad (19)$$

Here P_H, P_c are the quadrupole moments of the C−H and C−C bond, respectively, and μ is the dipole moment of the C−H bond. In the calculations, all bond angles were assumed to be tetrahedral and the same interatomic distances as for ethane were used. Atomic units are used throughout. The assumption of tetrahedral bond angles is very probably inaccurate. Since, however, experimentally determined bond angles are not available for some substances and are subject to considerable experimental error in others, this procedure is probably as satisfactory as any other. In any case, it greatly simplifies the numerical calculations.

If the values of $P_H=2.03$ and $\mu=0.158$ are used in Eq. (19), then P_c must be 4.77 in order that $V(ee)-V(ss)$ be equal to twice the barrier per methyl group. This will certainly be the case if the interaction between methyl groups makes a negligible contribution to the barrier and may be approximately true in any case. The moment (P_c) obtained in this way is considerably less than the upper limit of Section II and is positive. Moreover, it exceeds the approximate moment calculated from molecular orbitals by 26 percent, which is in the same direction and has nearly the same magnitude as that found for the H−H and C−H bonds. Therefore, the bond quadrupole moment seems quite reasonable.

The separate interaction energies are also of interest and are given in Table VII. The contributions of the interaction of the methyl groups with (a) the methylene group, (b) the C−C bonds, and (c) each other are tabulated separately. These are further subdivided into dipole-dipole, dipole-quadrupole, and quadrupole-quadrupole interactions. The interaction between methyl groups, although significant, is not predominant. The interaction between adjacent groups contributes 86 percent of the barrier; the remainder is a result of the methyl-methyl interaction.

Using the above value of P_c, the difference between the energies of the completely eclipsed and completely staggered configurations of isobutane and neopentane can be easily calculated, since no new interactions appear. The energy differences per methyl group are given in Table VIII. The observed barriers are also included for comparison. The agreement between calculation and experiment is excellent, and the essential correctness of the above analysis might seem to be conclusively confirmed. This was, in fact, our first conclusion, but a more penetrating investigation reveals the inconsistencies which were referred to earlier. The difficulties are strikingly revealed by the treatment of neopentane, and we therefore proceed to a more detailed discussion of this substance.

The energies of all the configurations of neopentane in which the various methyl groups are staggered and eclipsed in every possible way have

TABLE VI. Hydrogen peroxide. O−H bond: $\mu=0.596$ a.u., $R=1.815$ a.u. O−O bond: $R=2.760$ a.u.

P	Q	$V(0)-V(180)$ kcal.	$V(90)-V(180)$ kcal.	$V(100)-V(180)$ kcal.	$V(110)-V(180)$ kcal.	$V(120)-V(180)$ kcal.	φ_{min}	$V(\min)-V(180)$ kcal.	$V(180)$ kcal.
1.40	−1.00	8.18	−4.03	−4.44	−4.27	−3.80	100°	−4.44	5.91
	−1.20	8.18	−6.73	−7.07	−6.66	−5.82	96°	−7.10	9.05
	−1.40	8.18	−9.90	−10.16	−9.46	−8.21	94°	−10.22	12.90
1.60	−1.00	10.51	−2.76	−3.36	−3.38	−3.10	106°	−3.45	5.44
	−1.20	10.51	−5.39	−5.93	−5.70	−5.07	99°	−5.93	8.66
	−1.40	10.51	−8.49	−8.94	−8.43	−7.39	96°	−8.98	12.59
1.80	−1.00	13.27	−1.32	−2.15	−2.37	−2.31	113°	−2.40	4.83
	−1.20	13.27	−3.87	−4.64	−4.62	−4.22	105°	−4.70	8.12
	−1.40	13.27	−6.89	−7.58	−7.29	−6.49	100°	−7.60	12.13

[20] Kenneth S. Pitzer, J. Chem. Phys. **12**, 310 (1944).

been calculated. The results are given in the first four rows of Table IX. All are referred to the completely staggered configuration as the zero of energy. The symbol $V(seee)$ designates the energy of the configuration in which one methyl group is staggered, while the other three are eclipsed, etc. These results are not significantly changed by using the alternative set of moments corresponding to negative μ. The net energy of the configuration with one methyl group eclipsed and the other three staggered is negative with respect to the completely staggered arrangement (see column 4). Obviously, therefore, the completely staggered arrangement is not the stable one, since eclipsing one methyl group lowers the energy. The reason for this unexpected result will be evident from columns two and three, which give the interaction energy between methyl groups and C−C bonds, and interaction of the methyl groups with each other, respectively. The energies in column two rise steadily as the methyl groups are successively eclipsed and, hence, if the interaction of methyl groups with each other were neglected, the completely staggered configurations would be stable. From column three, it is evident that the methyl-methyl interactions are by no means negligible and they are, in fact, responsible for this unexpected result. In considering these results, it must be remembered that the energies given in Table IX are *differences*. The actual magnitudes of the methyl-methyl interactions are considerably less than the methyl to C−C interactions, but, whereas the latter tend to cancel on rotating one methyl group into the eclipsed position, the former do not cancel to as great an extent. It follows from the above that the completely staggered configuration is not the one of minimum energy, because of the interaction of methyl groups with each other. Moreover, the value of P_c which is required in order to stabilize the staggered configuration is considerably greater than the upper limit given in Section II. It is therefore concluded that the effect is real, if the dipole quadrupole model is valid. There remains the problem of determining the configuration of minimum energy. If the configuration with one methyl group eclipsed and the other three staggered were to be the stable configuration, it would virtually prove the dipole quadrupole model to be invalid, since such an unsymmetrical configuration could hardly have escaped detection. Therefore, we have calculated the interaction energy for two other configurations in which all four methyl groups were simultaneously rotated in the same sense through 30° and 35°, respectively, with respect to the completely eclipsed configuration. (A rotation through 60° leads to the completely staggered configuration.) The energies are given in the last two rows of Table IX. The configuration obtained by a 30° rotation has the lowest energy of any listed in the table. Although a rigorous proof is lacking, it seems likely that the configuration of minimum energy is one in which all methyl groups are symmetrically rotated through an angle which does not differ greatly from 30°. The point group symmetry of neopentane would then be T instead of T_d for the staggered arrangement.

TABLE VII. Propane: $V(ee)-V(ss)$. C−H bond: $\mu=0.158$ a.u., $P=2.03$ a.u., $R=2.07$ a.u. C−C bond: $\mu=0$, $P=4.77$ a.u. $R=2.915$ a.u.

	$D-D$ kcal.	$D-Q$ kcal.	$Q-Q$ kcal.	Net kcal.
Methyl-methylene	0.06	0.50	3.09	3.65
Methyl −C−C	0.00	−0.11	2.34	2.23
Methyl-methyl	0.01	0.20	0.71	0.92
Net	0.08	0.59	6.13	6.80

Calculations for propane and isobutane analogous to those for neopentane are shown in Tables X and XI, respectively. The results in these two cases are less clear-cut, since several configurations have nearly equal energies. It seems likely, and is in accord with the tabulated energies, that the staggered configuration is stable for propane, while, in isobutane, the methyl groups are symmetrically rotated through an angle greater than 35°. No theoretical method for the exact location of the minima is immediately available and a more thorough numerical exploration does not seem worth while.

In conclusion, it seems obvious that, if the dipole quadrupole theory of the origin of potential barriers is valid, the interaction between non-adjacent groups cannot be safely ignored. Since the existing potential barriers were deduced from experimental data by assuming the contrary, they are not directly comparable with the energy differences computed here. To remedy this deficiency requires the recalculation of thermodynamic functions on a basis which takes all interactions into account. Such an investigation will no doubt be somewhat elaborate and has not been undertaken.

It is finally of some interest to consider how the results of Table VIII are altered when the staggered configuration is replaced by that of minimum energy. The results are shown in Table XII. The close agreement between the energy differences and

TABLE VIII.

Hydrocarbon	n	$(1/n)[V(e)-V(s)]$ kcal.	Observed barrier kcal.
Ethane	1	2.75	2.75
Propane	2	3.40	3.40
Isobutane	3	4.06	3.87[a]
Neopentane	4	4.73	4.70[b]

[a] J. G. Aston, R. M. Kennedy, and S. C. Schumann, J. Am. Chem. Soc. 62, 2059 (1940).
[b] Kenneth S. Pitzer, Chem. Rev. 27, 39 (1940).

TABLE IX. Neopentane.

	Methyl-C−C kcal.	Methyl-methyl kcal.	Net kcal.
$V(eeee)-V(ssss)$	13.38	5.55	18.92
$V(seee)-V(ssss)$	10.03	−5.36	4.67
$V(ssee)-V(ssss)$	6.69	−9.92	−3.23
$V(ssse)-V(ssss)$	3.34	−8.13	−4.79
$V(30)-V(ssss)$	6.56	−13.88	−7.32
$V(35)-V(ssss)$	4.83	−11.95	−7.11

the measured potential barriers no longer holds for isobutane and neopentane. This is, of course, to be expected as the result of the foregoing discussion. It seems entirely clear, however, that the interactions are of the proper magnitude to account for the hindering of rotation, and improved agreement may well be obtained when a more detailed analysis of the experimental data becomes available.

V. RELATION OF QUADRUPOLE MOMENTS TO INTERATOMIC DISTANCES

It would be useful to have a method of estimating unknown quadrupole moments. A relation of the type needed is suggested by the quadrupole moments calculated from localized molecular orbitals. Calculations are available for three single bonds, H−H, C−H, and C−C. A graph of these moments against the squares of the corresponding interatomic distances is shown in Fig. 5. A fourth point corresponding to the carbon-carbon triple bond is also included, its quadrupole moment being divided by three. All four points fall very near to a straight line. A similar graph of experimental quadrupole moments is shown in Fig. 6, in which the moments of H−H, C−H, and C−C bonds are shown *vs.* R^2 and lie on a straight line. The first of these moments comes from the James and Coolidge calculation, while the other two are those calculated from potential barrier data as previously discussed. It is interesting, although probably not significant, that extrapolation of the straight line to zero interatomic distance gives the sign and approximate magnitude of the expected moment for an unshared electron pair. Figure 6 can be used for the estimation of unknown moments. The chief uncertainty lies in the C−C quadrupole moment, which was obtained in the previous section by means of a rather arbitrary procedure. In the absence of more accurate information, however, these results have been used. A correction can be made as soon as more accurate moments become available.

TABLE X. Propane.

	Methyl-methylene kcal.	Methyl-C−C kcal.	Methyl-methyl kcal.	Net kcal.
$V(ee)-V(ss)$	3.65	2.23	0.92	6.80
$V(es)-V(ss)$	1.82	1.11	−2.71	0.23
$V(30)-V(ss)$	1.80	1.09	−2.31	0.58
$V(35)-V(ss)$	1.33	0.80	−1.99	0.15

TABLE XI. Isobutane.

	Methyl-C−H kcal.	Methyl-C−C kcal.	Methyl-methyl kcal.	Net kcal.
$V(eee)-V(sss)$	2.73	6.69	2.77	12.19
$V(ees)-V(sss)$	1.82	4.46	−4.50	+1.78
$V(ess)-V(sss)$	0.91	2.23	−5.42	−2.28
$V(30)-V(sss)$	1.35	3.28	−6.94	−2.31
$V(35)-V(sss)$	1.00	2.42	−5.97	−2.56

In Section III the potential barriers hindering rotation in methyl amine and methyl alcohol were calculated for several values of the bond moments. The N−H and O−H bond moments obtained by interpolation from Fig. 6 are 1.56 and 1.35, respectively. The corresponding calculated potential barriers are 2.11 kcal. for methyl amine and 0.99 kcal. for methyl alcohol. In the light of our present, and rather meager, knowledge, these constitute the probable contributions of dipole-quadrupole potentials to the barriers hindering rotation in these substances. The calculated barrier for methyl amine lies between the two conflicting experimental values 1.52 and 3.00 kcal., while in the case of methyl alcohol the calculated barrier is slightly less than the probable measured barrier of 1.34 kcal. In view of both the experimental and theoretical uncertainties involved, these discrepancies are not regarded as serious.

VI. ACCURACY OF THE THEORY

No reliable estimate of error can be obtained except by empirical test. Nevertheless, the implications of the model used can be made clearer by means of further discussion of the electrostatic potentials of cylindrically symmetric distributions. For this purpose a few general results concerning the potentials of such distributions are needed. These are given largely without proof, since they are easily obtainable from standard potential theory.

The electrostatic potential of a cylindrically symmetric charge distribution at a point R, θ, φ external to a sphere containing all the charge is

$$U=\sum_m \beta_m[P_m(\cos\theta)/R^{m+1}].$$

TABLE XII.

Hydrocarbon	n	$(1/n)[V(\max)-V(\min)]$ kcal.
Ethane	1	2.75
Propane	2	3.40
Isobutane	3	4.90
Neopentane	4	6.58

Here

$$\beta_m = \int r^m P_m(\cos\theta)\rho d\tau + \sum_n q_n r_n^m P_m(\cos\theta_n),$$

P_m is the mth Legendre polynomial, and ρ is the charge density. The discrete point charges, which lead to the sum in β_m, must lie on the axis of symmetry. The approximation previously used involves the neglect of terms higher than $m=2$. It is obvious from (20) that the approximation becomes more accurate as R becomes larger. It may be accurate, however, even if R is small, provided that the moments $\beta_3, \beta_4, \cdots$ are sufficiently small. It will appear shortly that the distances of approach used here are so close that the higher order moments must be small in order that the theory be accurate. Before discussing this point, however, it is worth while to note that β_3 can be made to vanish by properly selecting the origin of coordinates, at least in favorable cases. In order to proceed with the last objective, it is necessary to discuss the moments further.

The first four moments, expressed in terms of Cartesian coordinates, are

$$\beta_0 = \int \rho d\tau,$$

$$\beta_1 = \int z\rho d\tau,$$

$$\beta_2 = \tfrac{1}{2}\int (3z^2 - r^2)\rho d\tau,$$

$$\beta_3 = \tfrac{1}{2}\int z(5z^2 - 3r^2)\rho d\tau.$$

The summation over discrete charges has been omitted for brevity. In order to illustrate the required property, consider another expansion around a new origin lying on the symmetry axis and such that the point (x, y, z) becomes $(x, y, z-a)$ in the new system. Let $\beta_0', \beta_1', \cdots$ be the moments calculated relative to the new origin. Then

$$\beta_0' = \beta_0,$$

$$\beta_1' = \beta_1 - a\beta_0,$$

$$\beta_2' = \beta_2 - 2a\beta_1 + a^2\beta_0,$$

$$\beta_3' = \beta_3 - 3a\beta_2 + 3a^2\beta_1 - a^3\beta_0,$$

$$\vdots$$

$$\beta_m' = \sum_{l=0}^{m} \binom{m}{l} \beta_l (-a)^{m-l},$$

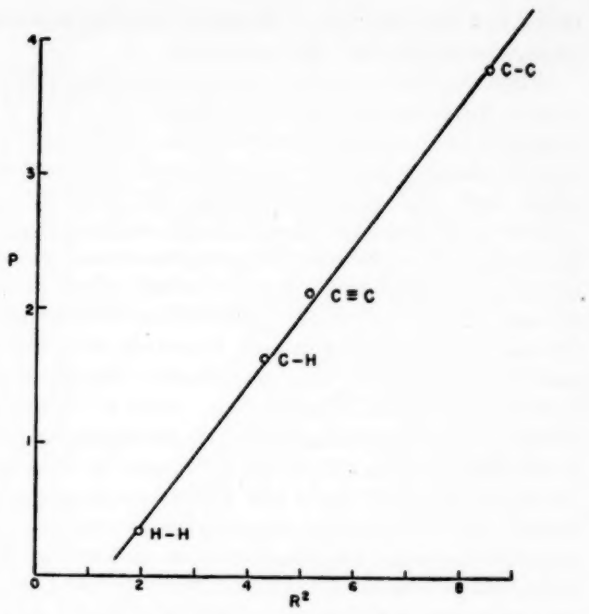

FIG. 5. The relation between calculated bond quadrupole moments (P) and the squares of the bond distances (R^2). Moments are those calculated from approximate localized molecular orbitals. Atomic units are used.

where $\binom{m}{l}$ is a binomial coefficient. Hence, the new moments are expressed in terms of the old and the shift in origin. It is evident that, if all moments of

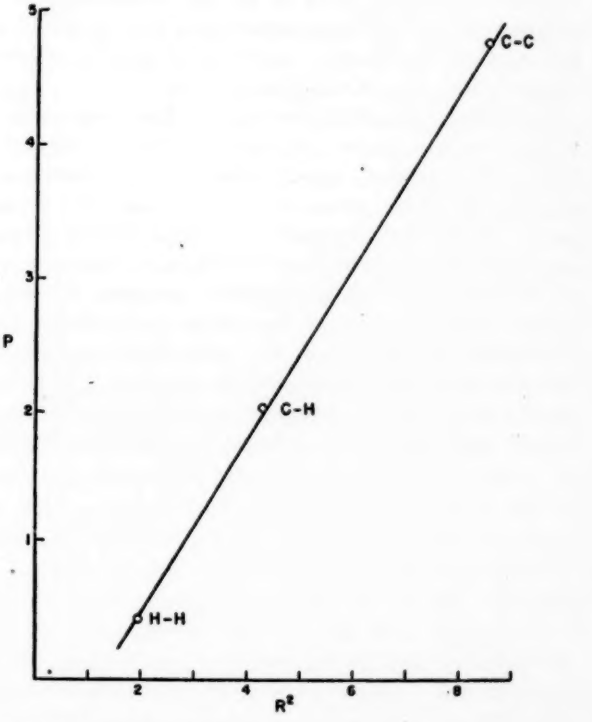

FIG. 6. The relation between observed quadrupole moments (P) and the squares of interatomic distances (R^2). Atomic units are used.

order less than m vanish, then β_m is invariant to a change in origin, but not otherwise.

When the above results are applied to single bond charge distributions, β_0 must vanish, since the distribution is electrically neutral. The dipole moment β_1 will vanish when the two atoms of the bond are alike, but not otherwise except by accident. It follows that the dipole moment is independent of the choice of origin under all circumstances, and the quadrupole moment (β_2) is invariant when $\beta_1=0$, but not otherwise. Strong evidence has been brought forward for large quadrupole moments of covalent bonds and, hence, it may be assumed that β_3 is not invariant for such distributions. Since β_3 is not invariant, it is convenient to select the origin in such a way that it vanishes. If the two atoms of the bond are equivalent and the origin is halfway between the nuclei, then ρ is an even function of z and all of the odd moments vanish. In particular, β_3 vanishes for this choice of origin. If the atoms are not the same, an origin can be chosen if the moments β_1, β_2, β_3, are known with respect to any origin. This can be done by setting $\beta_3'=0$ and solving for a in the above formula.

If this choice of origin is made, then Eq. (15) is accurate up to and including the inverse fifth power of the distance. Otherwise, an additional term appears in the inverse fifth power interaction which involves both β_1 and β_3 (dipole-octupole interaction). In practice, our information concerning the distribution is not sufficient to permit a calculation of origin, except for bonds between like atoms and, hence, all calculations have been arbitrarily referred to the midpoint of the line of centers.

It has been mentioned earlier that the present theory is inaccurate unless the moments of order higher than two are small. This point can be readily demonstrated by means of calculations on a simple point charge distribution. The distribution chosen corresponds to ethane, but with both electrons of each C—H bond placed midway between C and H nuclei. The energies of the staggered and eclipsed configuration can then be calculated *exactly* by summing the interactions of the charges. The difference $V(eclipsed)-V(staggered)$ obtained in this way is 1.35 kcal. On the other hand, for this distribution, $\mu=0$ and $P=2.14$ and, hence, the approximate equation (15) can be applied to the same distribution. This leads to the approximate result $V(eclipsed)-V(staggered)=2.59$ kcal. which is almost twice as great as the exact value. This distribution is therefore not sufficiently well characterized by its dipole and quadrupole moments. Since the interatomic distances and angles used are precisely the same as for ethane and the approximate result is in error by almost 100 percent, it is evident that, in general, the distances of approach are too close for (15) to be an acceptable approximation for *arbitrary* charge distributions. Our hypothesis that bonding distributions be sufficiently well characterized by their dipole and quadrupole moments implies that the higher moments are actually small. The above point charge distribution is obviously not that which prevails in ethane and, hence, our previous considerations are not rendered invalid and, in fact, the close agreement with experiment seems to confirm the model and, hence, the implication of small moments of order higher than two. The hypothesis of a dipole quadrupole model therefore has more far reaching implications than might appear at first sight.

Finally, it must be admitted that empirical success for the theory is not sufficient to *guarantee* that higher moments are small, since a number of other approximations concerning the symmetries and polarizabilities of distributions have been made. Cancellation of errors could occur which make the dipole quadrupole theory applicable even though the higher moments are rather large. This possibility seems somewhat remote, but cannot be rigorously excluded. It would obviously be desirable to treat the problem exactly, and this could be done if the charge distributions were known. Such, however, is not the case and some approximation must be adopted in order to progress at all. Despite its shortcomings, this procedure has the virtue of clarity and simplicity and, above everything else, it leads to agreement with experiment. In the process, the quadrupole moments of bonding distributions can be deduced and the theory can be tested in a more conclusive way when experimentally determined moments become available.

THE JOURNAL OF CHEMICAL PHYSICS VOLUME 17, NUMBER 3 MARCH, 1949

The Effect of Droplet Size on Surface Tension

RICHARD C. TOLMAN
California Institute of Technology, Pasadena, California

(Received September 23, 1948)

The effect of droplet size on surface tension is given theoretical consideration with the help of results of the Gibbs thermodynamic theory of capillarity and of previous results of the author as to the sign and magnitude of superficial densities. It is concluded that surface tension can be expected to decrease with decrease in droplet size over a wide range of circumstances. In addition, approximate figures are obtained for the rate at which such decreases may be expected. The decreases become significant for very small drops. The results are of interest in view of the important role of surface tension in determining the behavior of small droplets.

I. INTRODUCTION

IT is the purpose of this article to give brief theoretical consideration to the effect of droplet size on the surface tension between a liquid droplet and the vapor with which it is in equilibrium. The investigation will be carried out on the basis of the Gibbs[1] theory of surface tension, with the help of recent conclusions as to the location of the Gibbs surface of tension,[2] and as to the sign and order of magnitude of surface densities referred thereto.[3] The results of the present consideration can be important when we wish to understand the behavior of very small droplets and will be used for this purpose in proposed later work.

A certain amount of previous theoretical consideration has already been given to the problem at hand. Gibbs[4] himself came to the general conclusion that the effect of radius of curvature on surface tension would be small in typical cases until we get to very small radii. This conclusion will be maintained by the present work. Bakker,[5] on the other hand, gave thermodynamic arguments to prove that the surface tension between droplets and vapor composed of a single substance would be absolutely constant down to the smallest radii. This conclusion, nevertheless, cannot be maintained using the Gibbs definitions of surface tension and of the radius of the surface of tension, regarded in the present article as appropriate. Keenan[6] has recently concluded that the surface tension of a drop of liquid can be expected to decrease with decrease in radius. This conclusion was derived, however, by treating the drop and its vapor as though they were actually separated by a third entity, "a thin film of the same material in some 'surface state,'" a concept which does not readily permit exact definition and quantitative application. Rice[7] has more recently stated the conclusion that one-component, two-phase systems can be in equilibrium at a given temperature only at one definite pressure, but that the effect of increase in pressure—if this were possible—would be in a direction to lead to increase in surface tension. This conclusion is based, however, on a theory of surface tension which is not adequate for the treatment of curved surfaces (cf. reference 2, §8), and the conclusion should not be regarded as providing grounds for believing that an increase in surface tension would accompany the increase in vapor pressure and correlated decrease in droplet radius which are actually possible under equilibrium conditions. The treatment given in the present paper will lead to the conclusion that surface tension can be expected in typical cases over a wide range of circumstances to decrease with decrease in droplet radius, and will provide roughly approximate quantitative information as to the rate at which such decrease may be expected to take place.

Direct experimental measurements of the effect of droplet size on surface tension will not be readily obtainable, especially since the theoretical effects become important only for very minute drops. Direct experiments have been made, however, on the surface tension of thin films of soap solution by Rheinhold and Rücher.[8] Estimating the thickness of such films by their colors, these experiments were taken as indicating substantially constant values of surface tension down to a thickness of about 5×10^{-6} cm, followed for thinner film first by observed decreases in surface tension which could

[1] J. Willard Gibbs, *Collected Works* (Longmans Green and Company, New York, 1928) Vol. I, p. 219 ff.
[2] R. C. Tolman, J. Chem. Phys. **16**, 758 (1948).
[3] R. C. Tolman, J. Chem. Phys. **17**, 118 (1949).
[4] See the conclusion expressed by Gibbs at the bottom of page 232, reference 1. Note also the further conclusion of Gibbs, pp. 254–5, that the radius r of the surface of tension, the surface tension, and the work W needed to form a droplet from its vapor would simultaneously reach the value zero, even though the physical inhomogeneity might not itself vanish at that point. This conclusion, if actually meaningful, applies to droplets beyond the range of smallness with which we shall be concerned.
[5] G. Bakker, *Handbuch der Experimentalphysik* (Akad. Verlags., Leipzig, 1928), Vol. 6, p. 434.
[6] J. H. Keenan, *Thermodynamics* (John Wiley and, Sons, Inc., New York, 1941), pp. 440, 441, 479, 482, 483.
[7] O. K. Rice, J. Chem. Phys. **15**, 333 (1947).
[8] Rheinhold and Rücher, Phil. Trans. Roy. Soc. **177**, 627 (1886).

reach several percent, and then later by inferred increases in surface tension which would explain the known stability of black portions of film of thickness 1.1 to 1.2×10^{-6} cm, in contact with thick portions of film. These findings were taken by Sir J. J. Thomson[9] as evidence for his assumption that the surface tension of water droplets would pass through a minimum followed by one or more maxima on going to smaller and smaller droplets. However, attention must be forcibly called to the difference between films of soap solution and droplets formed from a pure substance. The behavior of the films must be strongly affected, and indeed perhaps mainly determined, by the soap adsorbed at the surface of the film. The presumable importance of the role played by the soap is confirmed by the great difference in the behavior of old and freshly prepared soap solutions which was actually found in the experiments of Rheinhold and Rücher (see reference 8, p. 658). Under the circumstances, an important part of our empirical interest must actually lie in the indirect verification of theoretical results if they prove successful in explaining important features of the phenomena of droplet behavior in laboratory apparatus, in engineering appliances, and in the earth's atmosphere.

II. DERIVATION OF RELATION BETWEEN σ AND r

Our derivation[10] of an expression for the dependence of surface tension σ on droplet radius r will be based on equations provided by the theory of Gibbs. We shall be concerned with the effect of changes in radius on surface tension in the case of droplets and vapor composed of a single substance maintained at some given constant temperature.

In accordance with the general equation of Gibbs (reference 1, Eq. (508); reference 2, Eq. (69)) for the dependence of surface tension on the variables that determine it, we can write for the dependence of surface tension on potential, in the case of a one-component, two-phase system maintained at constant temperature, the relation

$$d\sigma = -\Gamma d\mu, \tag{2.1}$$

where Γ is the superficial density of matter at the boundary between the two phases—computed with respect to the surface of tension—and μ is the Gibbs potential for the fluid in the homogeneous portions of either of the two phases.

Furthermore, in accordance with the general equation of Gibbs (reference 1, Eq. (98); reference 2, Eq. (6.10)) for the dependence of the pressure of a homogeneous phase on its state, we can also write, in the present special case, for any isothermal change which preserves equilibrium between the phases,

$$d\mu = dp'/\gamma' = dp''/\gamma'', \tag{2.2}$$

where p' and p'' are the pressures and γ' and γ'' the densities of fluid in the liquid and in the vapor phase. We note that the relation between dp' and dp'' agrees with the familiar condition of LeChatelier[11] on the changes in pressures needed to maintain equilibrium between phases.

Finally, in accordance with the Gibbs deduction (reference 1, Eq. (500); reference 2, Eq. (6.2)) of the Kelvin relation between pressure difference and curvature, we can write

$$p' - p'' = 2\sigma/r \tag{2.3}$$

as an expression connecting the pressures p' and p'', inside a droplet and its surrounding vapor, with the surface tension σ and radius r of the droplet. In applying Eqs. (2.2) and (2.3) to very small droplets, it is to be noted that p' and γ' are to be taken as the pressure and density for a large mass of internal phase in a condition at the temperature of interest to give the same value of μ as that of the vapor (cf. Gibbs, reference 1, p. 253), and it is also to be noted that σ and r are to be taken as the values of surface tension and radius for the surface tension of the droplet (cf. reference 2, §7). This now completes what is needed for the derivation of the desired expression.

Substituting the two equations given by (2.2) into (2.1), we can write

$$d\sigma = -(\Gamma/\gamma')dp' = -\Gamma(dp''/\gamma'') \tag{2.4}$$

which, by rearrangement, gives us

$$d\sigma = -(\Gamma/\gamma' - \gamma'')d(p' - p'') \tag{2.5}$$

as an expression for the dependence of surface tension, at constant temperature, on the pressure difference between the interiors of the two phases.[12] By differentiating the expression for pressure difference given by (2.3), and substituting in (2.5), we obtain

$$d\sigma = -[\Gamma/(\gamma' - \gamma'')]d(2\sigma/r)$$

or

$$(1/\sigma)(d\sigma/dr) = [2/r^2][\Gamma/(\gamma' - \gamma'')]/[1 + [2/r][\Gamma/(\gamma' - \gamma'')]] \tag{2.6}$$

as the desired expression for the dependence of surface tension σ on radius r, when we have equi-

[9] See J. J. Thomson and G. P. Thomson, *Conduction of Electricity through Gases* (Cambridge University Press, Cambridge, 1928), 3rd edition, Vol. I, p. 329.

[10] It will be noted that the development given in this section and in Section 4 is in part a specialization and in part an extension of a treatment given by Gibbs on page 232, reference 1.

[11] H. LeChatelier, Zeits. f. physik. Chemie 9, 335 (1892).

[12] Equation (12.5) is identical with Gibbs' Eq. (578), *Equilibrium of Heterogeneous Substances*, reference 1, for the case of constant temperature.

librium at a given temperature in a one-component system between a liquid droplet and its vapor.

Although the relation given by (2.6) has been derived for droplets and vapor composed of a single pure substance, we may also be interested in the behavior of droplets and vapor in the presence of an additional permanent gas such as air. In this connection, it may be remarked that methods similar to the foregoing can also be used to treat a multicomponent system consisting of a liquid droplet in the presence of added gases as well as in contact with its own vapor. Under the assumption that all the gases present can be treated as perfect and that the partial pressures of the added gases are kept constant, it then proves possible to derive an equation for the dependence of surface tension on radius of exactly the same form as (2.6), provided we now interpret the quantities Γ, γ', and γ'' as the superficial density referred to the surface of tension, and as the volume densities in the two phases, which would be assumed by the substance forming the droplet in the presence of the added gases. It may also be remarked that the measurements of Richards and Carver[13] on the slight lowerings of surface tension resulting from the presence of air, and the measurements of Kundt[14] with gases at higher pressures, have shown that we may expect, in general, only small effects on capillary phenomena from the presence of indifferent permanent gases at pressures in the neighborhood of one atmosphere. In the light of this discussion, we shall be able to take the relation given by (2.6) as appropriate for applications either in the absence or presence of some indifferent gas at low pressure.

III. INTERPRETATION OF THE QUANTITY $\Gamma/(\gamma'-\gamma'')$

In order to apply our expression for the dependence of surface tension σ on droplet radius r, as given by (2.6), we must first consider the significance of the quantity $\Gamma/(\gamma'-\gamma'')$, where Γ is the superficial density of fluid at the boundary of the droplet, computed with respect to the surface of tension, and γ' and γ'' are the volume densities of the fluid in the interior of the liquid and vapor phases.

In accordance with its original introduction (see reference 1, p. 224; reference 2, Eq. 6.8), the superficial density Γ may be defined as the difference —per unit area of dividing surface—between the actual amount of fluid in our two-phase system and the amount which it would contain if the liquid and vapor phases retained uniform densities to the Gibbs surface of tension as the dividing surface between the phases. Hence, if $c=1/r$ is the curvature of the surface of tension and x is a variable measuring radial distances therefrom in the direction from liquid to vapor, we can evidently write for Γ the expression

$$\Gamma=\int_{-a}^{0}(\gamma-\gamma')(1+cx)^2dx+\int_{0}^{b}(\gamma-\gamma'')(1+cx)^2dx, \quad (3.1)$$

where the limits of integration at $x=-a$ and $x=b$ are taken sufficiently distant from the surface of tension at $x=0$, so that the fluid has reached substantially the same condition at those points as in the contiguous homogeneous phases.

In addition to the surface of tension, we shall also find it useful to consider a dividing surface located so as to make the value of superficial density vanish when computed with respect thereto. If $x=\delta$ denotes the location of this new surface, measured in the radial direction from the surface of tension at $x=0$, we can then evidently write

$$\begin{aligned}0&=\int_{-a}^{\delta}(\gamma-\gamma')(1+cx)^2dx+\int_{\delta}^{b}(\gamma-\gamma'')(1+cx)^2dx\\&=\int_{-a}^{0}(\gamma-\gamma')(1+cx)^2dx+\int_{0}^{\delta}(\gamma-\gamma')(1+cx)^2dx\\&\quad+\int_{0}^{b}(\gamma-\gamma'')(1+cx)^2dx-\int_{0}^{\delta}(\gamma-\gamma'')(1+cx)^2dx. \quad (3.2)\end{aligned}$$

Substituting (3.2) from (3.1) we obtain

$$\begin{aligned}\Gamma&=\int_{0}^{\delta}(\gamma'-\gamma'')(1+cx)^2dx\\&=(\gamma'-\gamma'')(\delta+c\delta^2+\tfrac{1}{3}c^2\delta^3), \quad (3.3)\end{aligned}$$

and dividing through by $(\gamma'-\gamma'')$ and replacing the curvature c by the reciprocal of the radius r of the surface of tension, we can then write

$$\Gamma/(\gamma'-\gamma'')=\delta[1+(\delta/r)+\tfrac{1}{3}(\delta^2/r^2)] \quad (3.4)$$

as the desired expression to be used in interpreting the quantity $\Gamma/(\gamma'-\gamma'')$, which appears in our expression (2.6) for the change in surface tension

[13] T. W. Richards and E. K. Carver, J. Am. Chem. Soc. **43**, 827 (1921).
[14] A. Kundt, Ann. d. Physik **12**, 538 (1881).

with radius. In accordance with this result, the quantity $\Gamma/(\gamma'-\gamma'')$ depends on the distance δ from the surface of tension to the dividing surface for which the superficial density of fluid vanishes, and depends also on the ratio of δ to the radius of curvature r of the surface of tension.

For plane surfaces of separation, the radius of curvature r goes to infinity, and the relation given by (3.4) reduces to

$$\Gamma/(\gamma'-\gamma'')=\delta. \tag{3.5}$$

In previous work concerned with the case of plane surfaces, we have computed values of $\Gamma/(\gamma'-\gamma'')$ for several fluids at 20°C and for water over a range of temperatures from 10° to 50°C. The figures obtained for $\Gamma/(\gamma'-\gamma'')$ were found to be positive in sign, with values running from 0.96 to 3.5×10^{-8} cm, corresponding to a range of from 0.25 to 0.6 times the figure for intermolecular distances in the liquid phase involved. (See reference 3, Tables IV and V.) It was clear that the method of computation was not sufficiently reliable so that the calculated values for $\Gamma/(\gamma'-\gamma'')$ could be taken as exact. Nevertheless, it was concluded that the values were of the correct sign and of the correct order of magnitude. Furthermore, it is in accord with a reasonable picture of the structure of the "liquid face," at the boundary between liquid and vapor phases, to expect values of the order of a molecular diameter or an appreciable fraction thereof, for the distance from the surface of tension where changes in curvature alone do not require work out to a dividing surface so located as to make the superficial density of fluid vanish when computed with respect thereto.

For curved surfaces of separation, it is evident, from the form of (3.4) and from the small values obtained for $\delta=\Gamma/(\gamma'-\gamma'')$ in the case of plane surfaces, that $\Gamma/(\gamma'-\gamma'')$ can be expected to remain nearly constant until we get to quite small droplets. When we go to very minute droplets, however, it is evident from (3.4) that we must expect the value of $\Gamma/(\gamma'-\gamma'')$ to change, in the first place for the definite reason that the terms δ/r and $\delta^2/3r^2$ will no longer be negligible compared to unity, and in the second place because we cannot expect the value of δ itself to be strictly independent of droplet size. In the application made in the next section, we shall allow for the effect of the terms δ/r and $\delta^2/3r^2$, but shall treat δ as a constant. At the present stage of theory, we could hardly hope to make a reliable computation of the dependence of δ on droplet size, but can conclude that δ will be reasonably constant over a wide range of droplet sizes since it measures the distance between two surfaces whose separation is presumably closely connected with intermolecular distances in the liquid.

IV. APPLICATION OF RELATION BETWEEN σ AND r

We are now ready to apply our expression for the dependence of surface tension on radius as given by (2.6). Substituting the expression for $\Gamma/(\gamma'-\gamma'')$ given by (3.4), we have

$$\frac{1}{\sigma}\frac{d\sigma}{dr}=\frac{[2\delta/r^2][1+(\delta/r)+\frac{1}{3}(\delta^2/r^2)]}{1+[2\delta/r][1+(\delta/r)+\frac{1}{3}(\delta^2/r^2)]} \tag{4.1}$$

for the rate of change of surface tension σ with droplet radius r. And integrating from $r=\infty$ corresponding to a plane surface to any radius of interest $r=r$, we can write

$$\log\frac{\sigma}{\sigma_0}=\int_\infty^r\frac{[2\delta/r^2][1+(\delta/r)+\frac{1}{3}(\delta^2/r^2)]}{1+[2\delta/r][1+(\delta/r)+\frac{1}{3}(\delta^2/r^2)]}dr, \tag{4.2}$$

where σ_0 is the surface tension for a plane surface of separation between the two phases of a one-component fluid system and σ is the surface tension at the same temperature for the surface of a droplet of the fluid of radius r.

Neglecting the terms δ/r and $\delta^2/3r^2$ in comparison with unity, and treating δ as a constant, the integral on the right-hand side can be readily evaluated to give the simple result

$$\sigma/\sigma_0=1/(1+2\delta/r). \tag{4.3}$$

Allowing for the effect of the terms δ/r and $\delta^2/3r^2$ and still treating δ as a constant, an explicit expression can be obtained for the integral on the right-hand side of (4.2), which is, however, too complicated in form to be immediately transparent. Hence, it is more illuminating to give the results obtained by numerical quadrature.

In Table I we present the numerical results obtained. The first column lists the values of δ/r considered, the second column lists the corresponding values of $1/(1+2\delta/r)$ giving the computed ratio σ/σ_0 neglecting the change of $\Gamma/(\gamma'-\gamma'')$ with radius, and the final column lists the values of σ/σ_0 computed by treating δ as constant but without neglecting the terms δ/r and $\delta^2/3r^2$ in comparison with unity. It will be noted from the table that the values of surface tension σ decrease with decrease in droplet radius r, in accordance with the positive sign which we have found for the superficial density Γ referred to the Gibbs surface of tension. It will also be noted, by comparing the values in the second and third columns of the table, that the terms δ/r and $\delta^2/3r^2$, which are added to unity in the complete expression (4.2) for σ/σ_0, have an increasingly important effect in augmenting the lowering of surface tension as we go to smaller and smaller droplets.

In accordance with the table and with the expression given by (4.3), it will be appreciated

TABLE I. Change in surface tension with radius.

δ/r	$[1+(2\delta/r)]^{-1}$	σ/σ_0	δ/r	$[1+(2\delta/r)]^{-1}$	σ/σ_0
0	1	1	0.4	0.56	0.52
0.01	0.98	0.98	0.5	0.50	0.46
0.02	0.96	0.96	0.6	0.45	0.41
0.05	0.91	0.91	0.7	0.42	0.36
0.1	0.83	0.83	0.8	0.38	0.33
0.2	0.71	0.70	0.9	0.36	0.30
0.3	0.63	0.60	1.0	0.33	0.28

that a decrease in surface tension below that for a plane surface must be expected as soon as we go to a droplet of any finite radius. Nevertheless, to obtain for example a lowering of surface tension of 4 percent, we should have to go to a value of 0.02 for δ/r, and hence, taking δ as of the order of 10^{-8} cm, to a value of the order of 10^{-6} cm for the diameter of the droplet. Consequently, direct experimental measurement of decrease in surface tension with decrease in droplet size does not appear probable. Furthermore, existing measurements of surface tension made by methods involving the use of drops of appreciable sizes can be taken as furnishing values of surface tension which apply to plane surfaces within the limits of experimental error.

Although no significant lowering of surface tension can be expected for a drop of appreciable size, it will be seen from the table that we can expect very significant lowerings when we go to small enough droplets. Thus we have a decrease of 30 percent even for a droplet where the radius of the surface of tension is still five times as great as the distance from that surface to a dividing surface so located as to make the computed superficial density of fluid equal to zero. We regard the disclosure of such great changes in surface tension, within the range of droplet sizes where we might expect our results to be reasonably valid, as quite important owing to the pronounced role of surface tension in determining the behavior of small droplets.

V. CONCLUDING REMARKS

It is presumable that we can place less and less confidence on the results given for surface tension lowering in Table I as we go to smaller and smaller droplets. We must reach this conclusion for several reasons.

In the first place, in evaluating the integral on the right-hand side of our expression (4.2) for the ratio σ/σ_0, we have treated δ as constant with the same values for droplets of any size as for the plane surfaces where we have previously obtained approximate values for this quantity (reference 3). The reasons for treating as reasonably constant over a wide range of droplet sizes have already been expressed. Nevertheless, it is clear that δ can be expected to vary appreciably when we go to droplets small enough.[15]

In the second place, it will be noted, in the case of the expression for superficial density given by (3.1), that we have made use of an equation which assumes the possibility of employing integrals, with respect to the distance x from the surface of tension, that extend from a lower limit at $x=-a$ in the liquid where the properties of the fluid would become substantially identical with those for a large mass of liquid having the same value for the Gibbs potential μ as that for the vapor. It will also be recalled that integrals with the same kind of lower limit have been employed (see references 2 and 3) in the previous work which has led to our theoretical structure. In the case of sufficiently small droplets, however, it is evident that no such lower limit would be possible inside the actual droplet. Hence, we have another reason why results of quite different character might be obtained for very minute droplets.

Finally, a remark must be made with regard to the general nature of the method of investigation which has been adopted. It is certainly appropriate to use the concept of surface tension and the methods of thermodynamics in investigating the behavior of a fluid system composed of homogeneous phases of large volume meeting in a transition layer of large area. As we consider smaller and smaller droplets of liquid phase, however, the concept of surface tension and the previously satisfactory thermodynamic methods seem less and less appropriate. Indeed it will ultimately seem more satisfactory to continue the investigation using the concept of forces exerted by individual molecules and the more detailed methods of molecular mechanics. This, however, is a different task from the one set for this paper.

In view of the foregoing discussion, it is clear that we can place less and less reliance on the numerical values given in Table I as we go to smaller and smaller droplets. Nevertheless, we can presumably place considerable reliance on the figures where the radius r of the surface of tension of the droplet is sufficiently large compared with the distance δ characterizing the internal structure of the transition layer as previously discussed. As a consequence we are led to the final tentative conclusion that we can expect very appreciable decreases in surface tension with decrease in droplet size to take place within the range where our methods of treatment are still appropriate.

[15] It is interesting to suggest the possibility that δ might ultimately change sign and thus lead to a minimum of surface tension as assumed by Sir J. J. Thomson (see reference 9). It seems probable, however, that the surface of tension would continue to lie inside the dividing surface, which makes superficial density vanish, so long as we stay within a range of droplet sizes where we feel comfortable in applying the methods used above.

THE JOURNAL OF CHEMICAL PHYSICS VOLUME 17, NUMBER 3 MARCH, 1949

The Statistical Mechanical Theory of Surface Tension

JOHN G. KIRKWOOD AND FRANK P. BUFF
The Gates and Crellin Laboratories of Chemistry, California Institute of Technology, Pasadena, California

(Received September 30, 1948)

A general statistical mechanical theory of interfacial phenomena is developed and expressions are derived relating the surface tension and other superficial thermodynamic functions to the potential of intermolecular force and molecular distribution functions. On the basis of a reasonable approximation to the superficial density of molecular pairs, the Lennard-Jones potential and the Eisenstein-Gingrich radial distribution function, the surface tension, surface energy, and the superficial density of matter, referred to the surface of tension, are calculated for liquid argon at 90°K and compared with experiment. The positive value which is obtained for the superficial density, referred to the surface of tension, confirms the results of Tolman's quasi-thermodynamic theory and leads to the conclusion the surface tension of small drops decreases with increasing curvature.

I.

THE most recent statistical mechanical analysis of the relation between surface tension and the intermolecular forces acting at an interface between two fluid phases is due to R. H. Fowler.[1] However, as in earlier and more primitive analyses of the problem, Fowler introduces, almost at the beginning, the approximation of a mathematical surface of density discontinuity between the two phases. The formulation of a general theory of surface tension, free from this simplification will be presented here. Following the deduction of a general expression for surface tension in terms of the potential of intermolecular force and molecular distribution functions, the use of the mathematical surface of density discontinuity for the purpose of approximate calculation will be discussed.

In the formulation of the theory we shall need two molecular distribution functions, $\rho^{(1)}(\mathbf{R})$ and $\rho^{(2)}(\mathbf{R}_1, \mathbf{R}_{12})$, the statistical mechanical theory of which will be presented in Section II. The singlet density $\rho^{(1)}(\mathbf{R})$ specifies the average number of molecules $\rho^{(1)}dv$ in volume element dv at a point $\mathbf{R}$ in the fluid. The doublet or pair density $\rho^{(2)}(\mathbf{R}_1, \mathbf{R}_{12})$ specifies the average number of molecular pairs $\rho^{(2)}dv_1dv_{12}$, one member of which is situated in volume element dv at point $\mathbf{R}_1$ and the other in dv_{12} at point $\mathbf{R}_{12}$ in the relative configuration space of the pair. The pair correlation function $g^{(2)}(\mathbf{R}_1, \mathbf{R}_{12})$ is defined by the relation,

$$\rho^{(2)}(\mathbf{R}_1, \mathbf{R}_{12}) = \rho^{(1)}(\mathbf{R}_1)\rho^{(1)}(\mathbf{R}_2)g^{(2)}(\mathbf{R}_1, \mathbf{R}_{12}). \quad (1)$$

In the interior of an homogeneous fluid phase, say α, $\rho_\alpha^{(1)}$ is independent of $\mathbf{R}$ and the correlation function $g^{(2)}(R_{12})$ depends only on the pair distance R_{12} and is identical with the radial distribution function of the theory of liquids.

We now consider a heterogeneous system consisting of two fluid phases α and β separated by a plane transition zone. We select an arbitrary Gibbs[2] dividing surface in this zone and define a rectangular coordinate system (x, y, z) with the dividing surface as the (x, y) plane and z axis parallel to the normal to the dividing surface directed from phase α to phase β. From the molecular point of view, a plane transition zone implies that the density $\rho^{(1)}(z)$ depends only on z and that the density $\rho^{(2)}(z_1, R_{12})$ depends only on z_1 and $\mathbf{R}_{12}$. The analysis of curved phase boundaries and the definition of the surface of tension will be reserved for treatment in a later article.

Instead of attempting to determine surface free energy as the isothermal work of formation of unit area of interface, according to the thermodynamic definition, we find that the mechanical definition of surface tension in terms of the stress transmitted across a strip of unit width, normal to a Gibbs dividing surface, offers the most direct approach to a molecular theory.* The stress acting in the x direction across such a strip in the (y, z) plane of unit width in the y dimension and extending from $-l/2$ to $+l/2$ in the z dimension, where l is a macroscopic length large relative to the range of intermolecular forces, would have the value $-pl$, resulting from the uniform normal pressure p acting in both phases α and β, if there were no interfacial contribution. The tension γ, in excess of the contribution $-pl$ as a result of the uniform normal pressure, acting across the strip is, according to the mechanical definition, the interfacial tension of the phase boundary. Thus we may write,

$$\gamma = \sum_z + \int_{-l/2}^{l/2} p dz, \quad \int_{-l/2}^{l/2} p dz = pl, \quad (2)$$

[1] R. H. Fowler, Proc. Roy. Soc. **A159**, 229 (1937).

[2] J. W. Gibbs, Collected Works (Longmans Green and Company, 1928), Vol. I, p. 219.

* This point of view resembles that of G. Bakker, Kapillarität u. Oberflächenspannung, Wien-Harms' Handbuch der Experimentalphysik VI (1928).

where $\sum_x$ is the actual stress acting across the strip. For $\sum_x$, we may write

$$\sum_x = -kT\int_{-l/2}^{l/2}\rho^{(1)}(z)dz+\sum_x', \tag{3}$$

where the first term arises from momentum transport and the second term $\sum_x'$ is the intermolecular force transmitted across the strip.

According to the statistical mechanical theory of homogeneous fluid phases,[3] the pressure p may be expressed in two equivalent forms,

$$\begin{aligned} p&=kT\rho_\alpha^{(1)}-(1/6)\int R_{12}(dV/dR_{12})\rho_\alpha^{(2)}(R_{12})dv_{12},\\ p&=kT\rho_\beta^{(1)}-(1/6)\int R_{12}(dV/dR_{12})\rho_\beta^{(2)}(R_{12})dv_{12}\end{aligned} \tag{4}$$

where $V(R_{12})$ is the potential of intermolecular force** acting between a pair of molecules separated by a distance R_{12}. If we define densities $\rho_{\alpha\beta}^{(1)}$ and $\rho_{\alpha\beta}^{(2)}$ with respect to an arbitrary Gibbs dividing surface in the following manner,

$$\begin{aligned} &\rho_{\alpha\beta}^{(1)}=[1-A(z)]\rho_\alpha^{(1)}+A(z)\rho_\beta^{(1)},\\ &\rho_{\alpha\beta}^{(2)}=[1-A(z)]\rho_\alpha^{(2)}+A(z)\rho_\beta^{(2)},\\ &A(z)=0, \quad z<0,\\ &A(z)=1, \quad z\geqslant 0,\end{aligned} \tag{5}$$

where $A(z)$ is the unit step function, we may evidently express p in the form,

$$p=kT\rho_{\alpha\beta}^{(1)}-\tfrac{1}{6}\int R_{12}\frac{dV}{dR_{12}}\rho_{\alpha\beta}^{(2)}dv_{12} \tag{6}$$

which will presently be useful. We remark that $\rho_{\alpha\beta}^{(1)}$ and $\rho_{\alpha\beta}^{(2)}$ are the densities which would exist in the hypothetical heterogeneous system possessing the properties of the homogeneous phase α to the left and those of the homogeneous phase β to the right of the arbitrary Gibbs dividing surface.

We now proceed to determine $\sum_x'$, the contribution to the actual stress acting across the strip, arising from intermolecular forces. A molecule 1 situated at a point $\mathbf{R}_1$ below the (y, z) plane experiences a force $\nabla_{R_{12}}V(R_{12})$ from a molecule 2 situated at a point $\mathbf{R}_1+\mathbf{R}_{12}$ above the (y, z) plane. Thus the average force exerted by molecules in a volume element dv_{12} above the (y, z) plane on those in a volume element dv_1 below the plane is

$$\rho^{(2)}(z_1, R_{12})\nabla V(R_{12})dv_1dv_{12},$$

with a component $d\sum_x'$ in the x direction given by

$$d\sum_x'=\mathbf{e}_x\cdot\nabla V(R_{12})\rho^{(2)}(z_1, \mathbf{R}_{12})dv_{12}dv_1, \tag{7}$$

where $\mathbf{e}_x$ is a unit vector in the x direction. Integration over all configurations $\mathbf{R}_1$ below the (y, z) strip and over all configurations $\mathbf{R}_{12}$ above the strip leads to the result,

$$\begin{aligned}\sum_x'=\int_{-l/2}^{+l/2}\int_{-\frac{1}{2}}^{+\frac{1}{2}}\int_{-\infty}^{0}\int_{-x_1}^{\infty}\int_{-\infty}^{+\infty}\int_{-\infty}^{+\infty}\frac{x_{12}}{R_{12}}\frac{dV}{dR_{12}}\\ \times\rho^{(2)}(z_1, \mathbf{R}_{12})dy_{12}dz_{12}dx_{12}dx_1dy_1dz_1,\end{aligned} \tag{8}$$

which, after partial integration with respect to x_1, and extension of the residual integration over x_{12} to the interval $-\infty\leqslant x_{12}\leqslant+\infty$ by virtue of the symmetry requirement that the integrand be an even function of x_{12}, becomes

$$\sum_x'=\tfrac{1}{2}\int_{-l/2}^{+l/2}\int\frac{x_{12}^2}{R_{12}}\frac{dV}{dR_{12}}\rho^{(2)}(z_1, \mathbf{R}_{12})dv_{12}dz. \tag{9}$$

Substitution of Eq. (9) into Eq. (3) yields the desired expression for the total stress $\sum_x$, normal to the strip,

$$\begin{aligned}\sum_x&=-\int_{-l/2}^{l/2}p'(z)dz,\\ p'(z)&=kT\rho^{(1)}(z)-\tfrac{1}{2}\int\frac{x_{12}^2}{R_{12}}\frac{dV}{dR_{12}}\rho^{(2)}(z, \mathbf{R}_{12})dv_{12}.\end{aligned} \tag{10}$$

We remark that $p'(z)$ reduces to the macroscopic pressure given by Eq. (4) in the interior of either phase α or β, when $\rho^{(1)}$ and $\rho^{(2)}$ become independent of z and $\rho^{(2)}$ depends only on the scalar distance R_{12}. Substitution of the expression (10) into Eq. (2) and passage to the limit $l\to\infty$, yields for the surface tension γ,

$$\gamma=\int_{-\infty}^{\infty}[p-p'(z)]dz, \tag{11}$$

where p is the uniform normal pressure determined by the equation of state of either phase and $p'(z)$ is given by the second of Eqs. (10). Equation (11) resembles a relation recently obtained by Tolman on thermodynamic grounds.[4] However, it should be pointed out that $p'(z)$ cannot without approximation be identified with the macroscopic pressure of the fluid appropriate to the density $\rho^{(1)}(z)$, as surmised by Tolman. Instead, the molecular theory underlying Eq. (10) is necessary for the determination of $p'(z)$.

[3] J. G. Kirkwood, J. Chem. Phys. **14**, 180 (1946).

** We restrict ourselves here to one component systems composed of molecules for which the potential of intermolecular force has the form, $\sum_{i<k}V(R_{ik})$. For a more general intermolecular force containing terms depending on the coordinates of more than two molecules, distribution functions $\rho^{(n)}$ for $n>2$ would enter explicity into the theory.

[4] R. C. Tolman, J. Chem. Phys. **16**, 758 (1948).

Combining Eqs. (6) and (10), we obtain,

$$p-p'(z)=-kT\rho_s^{(1)}(z)+\tfrac{1}{2}\int\frac{x_{12}^2}{R_{12}}\frac{dV}{dR_{12}}\rho_s^{(2)}(z,\mathbf{R}_{12})dv_{12}, \tag{12}$$

$$\rho_s^{(1)}(z)=\rho^{(1)}(z)-\rho_{\alpha\beta}{}^{(1)},$$

$$\rho_s^{(2)}(z,\mathbf{R}_{12})=\rho^{(2)}(z,\mathbf{R}_{12})-\rho_{\alpha\beta}{}^{(2)},$$

where $\rho_s^{(1)}$ and $\rho_s^{(2)}$ are the excess singlet and pair densities reckoned relative to the arbitrary Gibbs dividing surface. Substitution of Eq. (12) into Eq. (11) and inversion of the order of integration leads to the final result of our analysis,

$$\gamma=-\Gamma_s^{(1)}kT+\tfrac{1}{2}\int\frac{x_{12}^2}{R_{12}}\frac{dV}{dR_{12}}\Gamma_s^{(2)}(\mathbf{R}_{12})dv_{12},$$

$$\Gamma_s^{(1)}=\int_{-\infty}^{+\infty}\rho_s^{(1)}(z)dz, \tag{13}$$

$$\Gamma_s^{(2)}=\int_{-\infty}^{+\infty}\rho_s^{(2)}(z,\mathbf{R}_{12})dz,$$

where $\Gamma_s^{(1)}$ is the superficial density of the Gibbs thermodynamic theory and $\Gamma_s^{(2)}$ is the superficial pair density, which does not appear explicitly in the thermodynamic theory. Since Eqs. (12) and (13) are evidently independent of the choice of dividing surface, this surface may be chosen to make $\Gamma_s^{(1)}$ vanish, if desired. The expression for the surface tension γ then reduces to the second term of Eq. (13). Of greater physical significance is the surface of tension. By an analysis of curved interfaces which will not be given here, we find that the Gibbs dividing surface coincident with the surface of tension is determined by the condition.

$$\int_{-\infty}^{+\infty}z[p-p'(z)]dz=0. \tag{14}$$

Equation (14) is identical in form with Tolman's[4] condition in the limit of zero curvature of the phase boundary, with the difference that $p'(z)$ is not to be considered as thermodynamically defined, but is to be calculated according to molecular theory by Eq. (10).

The generalization of Eq. (13) to a multicomponent system is easily achieved with the result,

$$\gamma=-\sum_{\sigma=1}^{\nu}{}^{\sigma}\Gamma_s^{(1)}kT+\tfrac{1}{2}\sum_{\sigma,\kappa=1}^{\nu}\int\frac{x_{12}^2}{R_{12}}\frac{dV_{\sigma\kappa}}{dR_{12}}{}^{\sigma\kappa}\Gamma_s^{(2)}(\mathbf{R}_{12})dv_{12}, \tag{15}$$

where the sums extend over the ν components of the system, ${}^{\sigma}\Gamma_s^{(1)}$ is the superficial singlet density of component σ, and ${}^{\sigma\kappa}\Gamma_s^{(2)}$ is the superficial pair density for pairs of type $\sigma\kappa$.

The use of Eqs. (13) and (15) for purposes of calculation requires a consideration of the molecular theory of the densities $\rho^{(1)}(z)$ and $\rho^{(2)}(z,\mathbf{R}_{12})$, with which we shall be concerned in Section II.

II.

The theory of liquids, either in the formulation of Kirkwood[5] or in the formulation of Born and Green[6] leads to a set of integro-differential equations for the densities $\rho^{(n)}$ in the configuration space of subsets of n molecules, which form a part of a larger closed system composed of N molecules. The equations of Born and Green prove to be the most convenient for the study of the densities $\rho^{(n)}$ in the neighborhood of a phase boundary. They are most conveniently derived from the well-known relations,[5]

$$\nabla_\sigma\log\rho^{(n)}(\mathbf{R}_1,\cdots\mathbf{R}_\sigma\cdots\mathbf{R}_n)=\beta^{(n)}\langle\mathbf{F}_\sigma\rangle_{Av};\qquad\sigma=1,\cdots n,$$

$$\rho^{(n)}\,{}^{(n)}\langle\mathbf{F}_\sigma\rangle_{Av}=\int\nabla_\mu V(R_{\sigma\mu})\times\rho^{(n+1)}(\mathbf{R}_1\cdots\mathbf{R}_\sigma\cdots\mathbf{R}_n,\mathbf{R}_\mu)dv_\mu+\beta\sum_{\substack{\kappa=1\\\neq\sigma}}^{n}\nabla_\kappa V(R_{\sigma\kappa})\rho^{(n)}(\mathbf{R}_1\cdots\mathbf{R}_n), \tag{16}$$

$$\rho^{(n)}=[N!/(N-n)!]p^{(n)},\quad\beta=1/kT,$$

where $p^{(n)}$ is the probability density in configuration space of a specified subset, and ${}^{(n)}\langle\mathbf{F}_\sigma\rangle_{Av}$ is the mean intermolecular force acting on molecule σ of the set, averaged over the residual phase space of the set $N-n$, canonically distributed. From Eqs. (16), we obtain at once the Born-Green system of integro-differential equations,

$$\nabla_\sigma\rho^{(n)}(\mathbf{R}_1,\cdots\mathbf{R}_n)=\beta\sum_{\substack{\kappa=1\\\neq\sigma}}^{n}\nabla_\kappa V(R_{\sigma\kappa})\rho^{(n)}(\mathbf{R}_1\cdots\mathbf{R}_n)+\beta\int\nabla_\mu V(R_{\sigma\mu})\rho^{(n+1)}(\mathbf{R}_1,\cdots\mathbf{R}_\sigma\cdots\mathbf{R}_n,\mathbf{R}_\mu)dv_\mu. \tag{17}$$

We now define a set of superficial densities $\rho_s^{(n)}$ by the relations

$$\rho_s^{(n)}(z_1,\mathbf{R}_{12},\cdots\mathbf{R}_{1n})=\rho^{(n)}(z_1,\mathbf{R}_{12}\cdots\mathbf{R}_{1n})-\rho_{\alpha\beta}{}^{(n)},$$

$$\rho_{\alpha\beta}{}^{(n)}=[1-A(z_1)]\rho_\alpha{}^{(n)}(\mathbf{R}_{12}\cdots\mathbf{R}_{1n})+A(z_1)\rho_\beta{}^{(n)}(\mathbf{R}_{12}\cdots\mathbf{R}_{1n}), \tag{18}$$

[5] J. G. Kirkwood, J. Chem. Phys. **3**, 300 (1935).
[6] M. Born and H. S. Green, Proc. Roy. Soc. **A188**, 10 (1946); H. S. Green, *ibid.* **189**, 103 (1947).

with respect to the arbitrary Gibbs dividing surface, appropriate to a plane transition zone between two fluid phases α and β, regarding all densities $\rho^{(n)}$ as functions of the position $\mathbf{R}_1$ of an arbitrarily selected molecule of the set n and of the positions $\mathbf{R}_{12}, \cdots \mathbf{R}_{1n}$ of the other molecules of the set relative to the reference molecule 1. Equation (18) generalizes the definitions of the superficial densities $\rho_s^{(1)}$ and $\rho_s^{(2)}$ given in Eq. (12). We then find by Eqs. (17) that the superficial densities $\rho_s^{(n)}$ satisfy the set of integro-differential equations,

$$\begin{aligned}\nabla_\sigma \rho_s^{(n)} &= \mathbf{e}_z \delta(z_1)\delta_{\sigma 1}(\rho_\alpha^{(n)} - \rho_\beta^{(n)}) \\ &+\beta \sum_{\substack{\kappa=1 \\ \neq\sigma}}^{n} \nabla_{R_{\sigma\kappa}} V(R_{\sigma\kappa}) \rho_s^{(n)} \\ &+\beta \int \nabla_{R_{\sigma\kappa}} V(R_{\sigma\mu}) \\ &\times \rho_s^{(n+1)}(\mathbf{R}_1, \mathbf{R}_{12} \cdots \mathbf{R}_{1n}, \mathbf{R}_{1\mu}) dv_\mu,\end{aligned} \tag{19}$$

$$\nabla_\sigma \rho_s^{(n)} = \left[\nabla_{R_1} \rho_s^{(n)} - \sum_{\kappa=2}^{n} \nabla_{R_{1\kappa}} \rho_s^{(n)}\right]\delta_{\sigma 1} + (1-\delta_{\sigma 1}) \nabla_{R_{1\sigma}} \rho_s^{(n)}.$$

The first of Eqs. (19) has the form,

$$\frac{d\rho_s^{(1)}(z_1)}{dz_1} = (\rho_\alpha^{(1)} - \rho_\beta^{(1)})\delta(z_1) + \beta \int \frac{z_{12}}{R_{12}} \frac{dV}{dR_{12}} \rho_s^{(2)}(z_1, \mathbf{R}_{12}) dv_{12}, \tag{20}$$

and the second of Eqs. (19), determining $\rho_s^{(2)}$ is similar but more complicated. Since the equation for $\rho_s^{(n)}$ involves $\rho_s^{(n+1)}$, the exact solution of Eqs. (19) requires consideration of densities $\rho_s^{(n)}$ for all subsets n of the total number of molecules N comprising the system. For purposes of calculation, it is therefore expedient to close the system of equations for some small n_0 by means of a suitable approximation.

We will now use Eq. (20) to eliminate $\Gamma_s^{(1)}$ from Eq. (13) and for the calculation of $\Gamma_s^{(1)}$ relative to the surface of tension, the position of which is determined by Eq. (14). In preparation for these tasks we define the z_1-moments of $\rho_s^{(1)}$ and $\rho_s^{(2)}$ as follows,

$$\begin{aligned}[\Gamma_s^{(1)}]_\nu &= \int_{-\infty}^{+\infty} z_1^\nu \rho_s^{(1)}(z_1) dz_1, \\ [\Gamma_s^{(2)}]_\nu &= \int_{-\infty}^{+\infty} z_1^\nu \rho_s^{(2)}(z_1, \mathbf{R}_{12}) dz_1,\end{aligned} \tag{21}$$

not all of which need to exist. These moments are evidently the coefficients of $(ik)^\nu/\nu!$ in the expansions of the respective Fourier transforms,

$$\begin{aligned}L^{(1)}(k) &= \int_{-\infty}^{+\infty} e^{ikz_1} \rho_s^{(1)}(z_1) dz_1, \\ L^{(2)}(k) &= \int_{-\infty}^{+\infty} e^{ikz_1} \rho_s^{(2)}(z_1, \mathbf{R}_{12}) dz_1.\end{aligned} \tag{22}$$

Taking Fourier transforms of both sides of Eq. (20), we obtain the relations,

$$\begin{aligned}-ikL^{(1)}(k) &= \beta \int \frac{z_{12}}{R_{12}} \frac{dV}{dR_{12}} L^{(2)}(k, \mathbf{R}_{12}) dv_{12};\ \kappa \neq 0 \\ \rho_\beta^{(1)} - \rho_\alpha^{(1)} &= \beta \int \frac{z_{12}}{R_{12}} \frac{dV}{dR_{12}} \Gamma_s^{(2)}(\mathbf{R}_{12}) dv_{12}, \\ [\Gamma_s^{(1)}]_\nu &= -\frac{\beta}{\nu+1} \int \frac{z_{12}}{R_{12}} \frac{dV}{dR_{12}} [\Gamma_s^{(2)}]_{\nu+1} dv_{12}.\end{aligned} \tag{23}$$

Use of Eqs. (23) in Eqs. (13) and (14) leads to the following expressions for the surface tension γ and the position z_0 of the surface of tension in the coordinate system selected, entirely in terms of the moments $[\Gamma_s^{(2)}]_\nu$ of the superficial pair density.

$$\begin{aligned}\gamma &= \int \frac{1}{R_{12}} \frac{dV}{dR_{12}} \left\{ z_{12}[\Gamma_s^{(2)}]_1 + \frac{x_{12}^2}{2}[\Gamma_s^{(2)}]_0 \right\} dv_{12}, \\ z_0 &= \frac{1}{2\gamma} \int \frac{1}{R_{12}} \frac{dV}{dR_{12}} \{x_{12}^2[\Gamma_s^{(2)}]_1 + z_{12}[\Gamma_s^{(2)}]_2\} dv_{12}.\end{aligned} \tag{24}$$

If z_0 is reckoned relative to the Gibbs dividing surface which makes $\Gamma_s^{(1)}$ vanish, the invariant superficial density Γ_s^*, relative to the surface of tension is evidently given by,

$$\Gamma_s^* = z_0(\rho_\beta^{(1)} - \rho_\alpha^{(1)}). \tag{25}$$

In order to use Eqs. (24) and (25) for purposes of approximate calculation, we will attempt to construct a first approximation to $\rho_s^{(2)}$ without undertaking the more difficult task of solving the higher members of Eqs. (19). We return to Eq. (1), specialized for the case of a plane interfacial zone,

$$\rho^{(2)} = \rho^{(1)}(z_1)\rho^{(1)}(z_1+z_{12}) g^{(2)}(z_1, \mathbf{R}_{12}) \tag{26}$$

and select the Gibbs dividing surface which makes $\Gamma_s^{(1)}$ vanish as the plane of reference for the calculation of $\rho_s^{(2)}$ and its moments. Restricting ourselves to a liquid phase α in equilibrium with a vapor phase β, we now shrink the physical transition zone to a mathematical surface coincident with the Gibbs

dividing surface. In this approximation, designated as that of zero order, we have

$$\begin{aligned} \rho^{(1)}(z) &= \rho_\alpha^{(1)} && z \leqslant 0 \\ &= 0 && z > 0 \end{aligned} \qquad (27)$$

$$g^{(2)}(z_1, \mathbf{R}_{12}) = g_\alpha^{(2)}(R_{12}); \quad z_1 \leqslant 0,$$

where $g_\alpha^{(2)}(R_{12})$ is the radial distribution function of the homogeneous liquid phase α. From Eqs. (12), (26), and (27), we thus obtain,

$$\rho_s^{(2)}(z_1, \mathbf{R}_{12}) = -\rho_\alpha^{(1)2} g_\alpha^{(2)}(R_{12})[1 - A(z_1)]A(z_1 + z_{12})$$

$$\begin{aligned} A(z) &= 0 \quad z < 0 \\ &= 1 \quad z \geqslant 0 \end{aligned} \qquad (28)$$

$$[\Gamma_s^{(2)}]_\nu = (-1)^{\nu+1} \frac{z_{12}^{\nu+1}}{\nu+1} \rho_\alpha^{(1)2} g_\alpha^{(2)}(R_{12}); \quad z_{12} \geqslant 0$$

$$= 0 \quad z_{12} < 0,$$

as zero order approximations to $\rho_s^{(2)}$ and its moments, referred to the Gibbs dividing surface making $\Gamma_s^{(1)}$ vanish in zero order. First approximations to the moments $[\Gamma_s^{(1)}]_\nu$ can be obtained, if desired, by use of the zero order moments $[\Gamma_s^{(2)}]_\nu$ of Eq. (28) in Eq. (23), but we will not discuss them here.

Substitution of the moments $[\Gamma_s^{(2)}]_\nu$ of Eq. (28) into the first integral of Eqs. (24) yields the following approximation to the surface tension γ,

$$\gamma = \frac{\pi \rho_\alpha^{(1)2}}{8} \int_0^\infty R^4 \frac{dV}{dR} g_\alpha^{(2)}(R) dR. \qquad (29)$$

Eq. (29) is identical with Fowler's expression for the surface tension at an interface between a liquid phase and a vapor phase of negligible density, which was based upon the same approximation to the pair density $\rho_s^{(2)}$ as that employed here. However, Fowler's analysis was quite different from our own, and he failed to obtain the general expressions for surface tension, Eqs. (13) and (15) of Section I. Since he attempted to determine surface free energy as one half the work of adhesion between two columns of liquid phase of unit cross section, he was forced to introduce the approximation of mathematical surfaces of discontinuity almost at the beginning.

The Gibbs surface density of internal energy, E^s, is evidently given by,

$$E^s = \tfrac{1}{2} \int V(R_{12}) \Gamma_s^{(2)}(\mathbf{R}_{12}) dv_{12}. \qquad (30)$$

Unlike the surface tension, this quantity is not independent of the choice of the Gibbs dividing surface. For the one component system, it is conventional to refer it to the dividing surface making $\Gamma_s^{(1)}$ vanish. Using Eq. (28), we find that E^s is given by

$$E^s = -\frac{\pi}{2} \rho_\alpha^{(1)2} \int_0^\infty R^3 V(R) g_\alpha^{(2)}(R) dR \qquad (31)$$

in zero order approximation.

From the second of Eqs. (24), determining the position of the surface of tension, Eq. (25) and Eq. (28), we find

$$\Gamma_s^* = \rho_\alpha^{(1)} \delta$$

$$\delta = \frac{4}{15} \frac{\int_0^\infty R^5 \frac{dV}{dR} g_\alpha^{(2)}(R) dR}{\int_0^\infty R^4 \frac{dV}{dR} g_\alpha^{(2)}(R) dR} \qquad (32)$$

as the zero order approximation to Γ_s^*, the invariant superficial density of matter, referred to the surface of tension. Although negative values of Γ_s^* are not excluded, it is found that Eq. (32) generally leads to positive values of Γ_s^*, in agreement with the calculation of Tolman[7] by his quasi-thermodynamic method. As Tolman points out in a forthcoming article, a positive value of Γ_s^* implies that the surface tension γ must decrease with increasing curvature of the interface, a fact of much significance in the mechanism of nucleation and growth of embryos of vapor phase into small droplets under conditions of super-saturation.

III.

Equations (29), (31), and (32) are in a form allowing relatively simple calculation of the thermodynamic observables, γ, E^s, and Γ_s^* from the potential of intermolecular force $V(R)$ and the radial distribution function $g_\alpha^{(2)}(R)$ of the liquid phase. We will undertake calculations in the approximation represented by these equations for liquid argon, using the Lennard-Jones potential,

$$V(R) = \frac{8.62 \times 10^{-8}}{R^{11.4}} - \frac{1.11 \times 10^{-10}}{R^6} \qquad (33)$$

as modified by Rushbrooke[8] in accordance with the calculations of Corner, where V is expressed in ergs and R in Angstrom units. For information concerning the radial distribution function, $g_\alpha^{(2)}(R)$, we employ the data of Gingrich and Eisenstein.[9]

[7] R. C. Tolman, J. Chem. Phys. in this issue.

[8] G. S. Rushbrooke, Proc. Roy. Soc. Edinburgh 60, 182 (1940); J. Corner, Trans. Faraday Soc. **35**, 711 (1939).

[9] A. Eisenstein and N. H. Gingrich, Phys. Rev. 62, 261 (1942).

We need to calculate two types of integral for use in Eqs. (29), (31), and (32),

$$B_\nu = \int_0^\infty R^\nu (dV/dR) g_\alpha^{(2)}(R) dR,$$
$$D_\nu = \int_0^\infty R^\nu V(R) g_\alpha^{(2)}(R) dR \tag{34}$$

on which we have two experimental controls, the equation of state, Eq. (4) and the well-known expression for the molar energy of vaporization.

$$p = \rho_\alpha^{(1)} kT - (2\pi/3)\rho_\alpha^{(1)2} B_3,$$
$$\Delta E_v = -2\pi N \rho_\alpha^{(1)} D_2. \tag{35}$$

We find that the relations (35) cannot be immediately satisfied with the Lennard-Jones potential and Eisenstein-Gingrich experimental radial distribution function, since the integrals B_ν are very sensitive to the form of the first peak of $g_\alpha^{(2)}(R)$. In fact, without adjustment, the wrong sign is obtained for B_3 which determines the cohesive contribution to the pressure arising from intermolecular forces. We therefore turn to an analytical approximation,

$$g_\alpha^{(2)}(R) = (a_1/R)^s \exp[(a_m/a_1)^t - (a_m/R)^t] \qquad 0 \leqslant R \leqslant a, \tag{36}$$
$$\doteq 1 \quad a_1 < R$$

to the first peak of the radial distribution function which we have found useful in our investigation of transport processes. Since the other factors in the integrands of Eqs. (34) are of short range for small ν, the first peak plays a dominant role and it is adequate to approximate $g_\alpha^{(2)}(R)$ by unity for distances greater than a_1.

It was found expedient to determine the parameters a_1 and t from the experimental data of Eisenstein and Gingrich and then to adjust the remaining parameters s and a_1 to satisfy Eqs. (35) with the experimental values of p and ΔE_v. By this procedure, we find for liquid argon at 90° in equilibrium with the saturated vapor,

$$a_1 = 4.50\text{A} \quad t = 14,$$
$$a_m = 3.55\text{A} \quad s = 7.00. \tag{37}$$

TABLE I. The integrals B_ν and D_ν.

D_2	B_4	B_5
-4.03×10^{-12} ergs A^2	8.82×10^{-12} ergs A^4	1.20×10^{-10} ergs A^5

TABLE II. The surface tension, surface energy, and invariant superficial density of matter of argon at 90°K.

	γ(dynes/cm)	E^s(dynes/cm)	Γ_s^*(g/cm²)
Theory	14.9	27.2	4.99×10^{-8}
Experiment*	11.9	35	

* See reference 11.

The radial distribution function corresponding to this choice of parameters has its first peak at 3.73A and the first coordination number, obtained by integration under this peak is 8.1, both in good agreement with the experimental values.

In Table I we present the values of the necessary integrals B_ν and D_ν, calculated with the aid of the $g_\alpha^{(2)}(R)$ of Eq. (36) and the constants given in Eq. (37). Values of the surface tension γ, the superficial density of energy,[10] E^s, and the invariant superficial density of matter Γ_s^*, reckoned relative to the surface of tension have been calculated by means of Eqs. (29), (31), and (32) and the integrals of Table I. The results of the calculation are presented in Table II. The theoretical values of the surface tension and surface energy compare favorably with the measurements of Baly and Donnan,[11] which to our knowledge have not been repeated by later workers. The surface of tension lies at a distance δ of 3.63A below the Gibbs dividing surface making $\Gamma_s^{(1)}$ vanish and Γ_s^* has the same sign and magnitude as the superficial densities estimated by Tolman for other liquids on the basis of his quasi-thermodynamic theory. More accurate results than those presented here could be obtained by carrying out calculations, at great expenditure of labor, to higher orders of approximation. However, it appears that the zero order approximation employed here is reasonably good and that significant changes in magnitude or sign can scarcely be expected in the higher orders of approximation.

We wish to acknowledge our indebtness to the late Professor Richard C. Tolman for many stimulating discussions out of which this investigation grew. Although we greatly regret that death prevented him from reading the manuscript of this article, we are happy to be able to confirm by means of molecular theory the conclusions reached by Tolman on the basis of his quasi-thermodynamic theory.

[10] Similar calculations of the superficial density of energy have been made by A. Harasima, Proc. Phys. Math. Soc. Japan **22**, 825 (1940) and G. Jura, J. Phys. and Coll. Chem. **52**, 40 (1948).

[11] Baly and Donnan, J. Chem. Soc. **81**, 907 (1902); G. Rudorf, Ann. d. Physik **29**, 751 (1909).

Letters to the Editor

THIS section will accept reports of new work, provided these are terse and contain few figures, and especially few halftone cuts. The Editorial Board will not hold itself responsible for opinions expressed by the correspondents. Contributions to this section should not exceed 600 words in length and must reach the office of the Managing Editor not later than the first of the month preceding that of the issue in which the letter is to appear. No proof will be sent to the authors. The usual publication charge ($4.00 per page) will not be made and no reprints will be furnished free.

A Study of Metallic Electrodes Prepared by Sublimation

B. C. BRADSHAW
Signal Corps Engineering Laboratories, Fort Monmouth, New Jersey
January 20, 1949

A NUMBER of attempts have been made to prepare solid metals in a strain-free condition and to use them as reversible electrodes. A few authors have succeeded in preparing pure strain-free single crystals of zinc.[1] At least one paper by Clayton and Vosburgh[2] records the preparation of reversible zinc electrodes by careful annealing of a large piece of zinc. The latter authors compared their annealed electrodes to both surface amalgamated zinc and to saturated zinc amalgam. Silver chloride electrodes which are reversible have been prepared by reducing silver oxide thermally.[3] The silver thus formed is in the form of a very finely divided spongy crystalline mass.

The following is an account of a study of electrodes prepared by evaporating zinc in vacuum. Pure zinc metal was vacuum sublimed on platinum wire set in the end of glass tubes. The zinc was deposited on the electrodes in the form of very finely divided loosely adhering crystals.

The electrodes, thus prepared, were placed in a dilute solution of pure zinc chloride saturated with basic zinc carbonate: air being rigidly excluded. Several sets of these cells were made at different times and the electromotive force measured. They usually agreed among themselves to within 25 to 30 microvolts. Very seldom did the difference exceed 70 microvolts. These cells were found to be stable for longer than eight weeks. The electrodes were not injured by storing in distilled water after they had been removed from a zinc chloride solution. However, when the same electrodes were reused return to equilibrium was slow—probably due to zinc chloride which was not washed out of the crystal aggregates. Cells using freshly prepared electrodes came to equilibrium almost at once.

The results so far obtained strongly indicate that zinc electrodes prepared in this way are free from strain and are reversible. It is hoped that this may be a general property of crystals formed in this way.

[1] F. H. Getman, J. Phys. Chem. **35**, 2749 (1931).
[2] Clayton and Vosburgh, J. Am. Chem. Soc. **58**, 2013 (1936).
[3] Jones and Baeckström, J. Am. Chem. Soc. **56**, 1524 (1934).

Isotope Effect in the Rupture of Carbon-Carbon Bonds in Propane-1-C^{13}

JACOB BIGELEISEN
Brookhaven National Laboratory, Upton, Long Island, New York
January 7, 1949

RECENT experiments have shown a significant isotope effect in the rupture of carbon-carbon bonds in propane-1-C^{13} by electron impact[1] as well as in thermal cracking.[2] It is difficult to understand the isotope effects in the thermal cracking experiments in terms of some of the proposed mechanisms for the reaction. Thus such experiments may lead to a better understanding of the detailed mechanism. The isotope effect, 8 percent greater frequency of rupture of $C^{12}-C^{12}$ than $C^{12}-C^{13}$ at ten percent cracking (14 percent for infinitesimal cracking[3]), is sufficiently large to permit a detailed investigation of the isotope effects.

The pyrolysis of propane is probably a chain reaction, and the over-all isotope effect in the depletion of propane as well as in the formation of individual products is the result of several consecutive and competing reactions. For a detailed interpretation of the mechanism, it is necessary to know the isotope effects in the various elementary reactions. To this end I have calculated an upper limit for the ratios of the rate constants in the rupture of the C−C bonds in propane according to the following reactions

$$C^{12}H_3-C^{12}H_2-C^{12}H_3 \xrightarrow{k_1} C^{12}H_3+C^{12}H_3C^{12}H_2, \quad (1)$$

$$C^{12}H_3-C^{12}H_2-C^{13}H_3 \xrightarrow{k_2} C^{13}H_3+C^{12}H_3C^{12}H_2, \quad (2)$$

$$C^{12}H_3-C^{12}H_2-C^{13}H_3 \xrightarrow{k_3} C^{12}H_3+C^{13}H_3C^{12}H_2. \quad (3)$$

The ratios of the rate constants $k_1/2k_2$ and $k_1/2k_3$ have been calculated by using an approximate equation derived[4] by the application of the statistical mechanical treatment of isotopic molecules[5] to the statistical treatment of absolute rates.[6] The approximate equations for the ratios of the rate constants are

$$\frac{k_1}{2k_2}=\left\{\frac{m_2^*}{m_1^*}\right\}^{\frac{1}{2}}\{1+\Sigma_i{}^{3n-6}G(u_i)\Delta u_i-\Sigma_i{}^{3n^1-6}G(u_i\ddagger)\Delta u_i\ddagger\}, \quad (4)$$

$$\frac{k_1}{2k_3}=\left\{\frac{m_3^*}{m_1^*}\right\}^{\frac{1}{2}}\{1+\Sigma_i{}^{3n-6}G(u_i)\Delta u_i-\Sigma_i{}^{3n^1-6}G(u_i\ddagger)\Delta u_i\ddagger\}. \quad (5)$$

The function $G(u)$ has been previously defined;[5] m^* is the effective mass of the activated complex along the reaction coordinate; $\Delta u_i=(hc/kT)(\omega_{1i}-\omega_{2i})$; and ‡ is a property of the activated complex.

For the calculation of an upper limit to the isotope effect in the C−C bond rupture we assume that the skeletal vibrations are reduced to zero in the activated complex, and the remaining vibrations of the molecule are unaffected. That is, we assume that the activated complex consists of two essentially free methyl groups and one free methylene group. In such a model we should take into account that the C−H bonds will be stronger in the free methyl and methylene groups than in propane. Since this reduces the isotope effect, and the model of the activated complex is artificially chosen to give an upper limit, we shall neglect this effect.

The normal vibrations of propane have not yet been completely analyzed,[7] and it is not possible to treat the skeletal vibrations independently of the rocking vibrations.[8,9] Therefore the skeletal vibrations have been approximated using the force constants $k_{C-C}=4.03\times10^5$ dynes/cm and $k_\sigma=0.36\times10^5$ dynes/cm. This set of force constants gives a slightly better fit to the experimental data than those used by Abonen.[10] For convenience in calculation, the isotope effect in the skeletal vibrations is calculated for the molecule $C^{13}H-C^{12}H-C^{13}H$, and the vibrational isotope effect divided by 2. Thus the right-hand brackets in Eqs. (4) and (5) become $(1+1/2(G(u_1)\Delta u_1+G(u_2)\Delta u_2+G(u_3)\Delta u_3))$. The values of ω and $\Delta\omega$ calculated with the above force constants are

	ω	$\Delta\omega$
ω_1	918	14.6
ω_2	375	9.8
ω_3	1053	13.6

The ratios of the effective masses are calculated according to a recent treatment given by Slater.[11] In a unimolecular decomposition of a polyatomic molecule, the effective mass is the reduced mass of the two atoms connected in the bond being broken. The results of the calculation of an upper limit

of the isotope effect in the rupture of C−C bonds in propane are given in Table I.

TABLE I.

T°K	$k_1/2k_2$	$k_1/2k_3$
300	1.043	1.023
400	1.034	1.014
500	1.030	1.010
800	1.024	1.004

If one assumes that the various ion fragments smaller than $C_3H_8^+$ formed in the electron bombardment experiments arise from the decomposition of the latter, and that the skeletal vibrations of the ion are the same as those in the molecule (actually they should be smaller and thus the isotope effects somewhat reduced), then the isotope effects in the electron bombardment should be the same as those given in Table I. The significant discrepancy is that the ratio $k_1/2k_3$ found experimentally[1] is less than unity. A similar discrepancy exists in the ions formed from deutero-methane. It is difficult to see how any mechanism which treats the production of ions as a rate process will remove this discrepancy. If one postulates that the C−H force constants are sufficiently greater in the above model of the activated complex than in the parent ion to reduce $k_1/2k_3$ below unity, then $k_1/2k_2$ will be sufficiently lower than the experimental value to give this procedure much weight.

[1] Beeck, Otvos, Stevenson, and Wagner, J. Chem. Phys. **16**, 255 (1948).
[2] See reference 1, p. 993.
[3] J. Bigeleisen, unpublished calculations.
[4] J. Bigeleisen, presented at the Brookhaven conference on kinetics, December 1, 1948.
[5] J. Bigeleisen and M. G. Mayer, J. Chem. Phys. **15**, 261 (1947).
[6] For a discussion of the statistical treatment of absolute rates see S. Glasstone, K. J. Laidler, and H. Eyring, *The Theory of Rate Processes* (McGraw-Hill Book Company, Inc., New York, 1941).
[7] See Gerhard Herzberg, *Infrared and Raman Spectra of Polyatomic Molecules* (D. Van Nostrand Company, Inc., New York, 1945), pp. 359 ff.
[8] J. Bigeleisen, unpublished calculations.
[9] L. Friedman and J. Turkevich, unpublished infra-red spectra of the deutero-propanes.
[10] C. A. Ahonen, J. Chem. Phys. **14**, 625 (1946).
[11] N. B. Slater, Proc. Roy. Soc. **194**, 112 (1948).

Dissociation Schemes of N_2, P_2, As_2, Sb_2, and Bi_2*

L. GERÖ AND CATHERINE FONÓ
University for Technical and Economic Sciences, Budapest, Hungary
January 3, 1949

THE results in the NO spectrum which lead to a new dissociation scheme of NO[1-3] make the revision of the N_2 dissociation energy also necessary. The re-examination of the observed dissociation phenomena in N_2 and N_2^+ yields, according to Schmid and Gerö,[1,2] a dissociation scheme for N_2 in which the $N_2(^1\Sigma_g^+)$ ground state dissociates into $^2D+^2D$ atoms. The bond energy of the molecular ground state and the dissociation energy counted from the $^4S+^4S$ atomic term combination are given in the first line of Table I.

TABLE I.

	Bond energy, cm^{-1} energy height of $^2D_{3/2}+^2D_{3/2}$	Dissociation energy, cm^{-1} energy height of $^4S+^4S$
$N_2(^1\Sigma_g^+)$	78,750	40,350
$P_2(^1\Sigma_g^+)$	44,600	21,870
$As_2(^1\Sigma_g^+)$	34,540	13,360
$Sb_2(^1\Sigma_g^+)$	25,220	8,200
$Bi_2(^1\Sigma_g^+)$	15,860	−6,980

A review of the available experimental material for P_2, As_2, Sb_2, and Bi_2, in the light of this dissociation scheme of N_2, results in new dissociation schemes for these molecules, according to which the molecular ground states are also formed from $^2D+^2D$ atoms. The corresponding values of bond energies and dissociation energies are included in Table I.

In the P_2 spectrum the observed predissociation effects,[4] at the $v'=10$, $J'=58$ and $v'=11$, $J'=34$ levels of the $^1\Sigma_u^+$ state give, with the limiting curve method, $51{,}965\pm25$ cm^{-1} for the energy height of the predissociation limit. The dissociation scheme is obtained by identifying this limit with the energy height of the $^2D+^2P$ atomic term combination. The $^4S+^4S$ atomic term combination is slightly above the energy height of the last observed vibrational level of the $P_2(^1\Sigma_g^+)$ ground state at 21,830 cm^{-1} with $v''=32$, explaining in this way the interruption of the observed bands at this vibrational quantum number.

In As_2 the given dissociation scheme can be obtained by ascribing the observed predissociation effects[5] in the neighborhood of 42,700 cm^{-1} to the effect of the $^2D+^2P$ term combinations. The splitting of these atomic term combinations makes it possible to explain the interruption of the bands from the B level with $v=8$ at 42,824 cm^{-1} by the effect of the $^2D_{5/2}+^2P_{3/2}$ term combination, the interruption of the bands from the A level with $v=9$ at 42,578.7 cm^{-1} by the effect of $^2D_{3/2}+^2P_{3/2}$, the predissociation effects of the A, $v=8$ and B, $v=6$ levels by the effect of $^2D_{5/2}+^2P_{1/2}$, and the interruption of the bands from the C level with $v=0$ at 42,006 cm^{-1} by the effect of the $^2D_{3/2}+^2P_{1/2}$ atomic term combination. The energy height of the $^2D_{3/2}+^2D_{3/2}$ term combination is in good agreement with the extrapolated 31,726 cm^{-1} bond energy value of the ground state. The interruption of the observed bands with the $v=70$ level of the $X(^1\Sigma_g^+)$ ground state at 24,085 cm^{-1} can be explained by the presence of the $^4S+^2D_{3/2}$ atomic term combination at this energy height, whereas the energy height of the $^4S+^4S$ atomic term combination is between the $v=34$ and $v=35$ vibrational levels of the ground state, and in Fig. 1 of Almy and Kinzer's first paper, one can observe a sudden weakening of the intensity in this region.

The values given for Sb_2 result from attributing the predissociation effect observed by Naudé[6] at 2842A = 35,200 cm^{-1} to the $^2D_{3/2}+^2P_{3/2}$ atomic term combination.

In Bi_2, in identifying the predissociation effect[3] of the C level at 37,026 cm^{-1} with the energy height of the $^2D_{3/2}+1_{1/2}$ atomic term combination, the $^4S+5_{1/2}$ term combination yields as convergence limit for the bond energy of the C level 2490 cm^{-1}, whereas the value calculated by Almy and Sparks is 2500 cm^{-1}. In the neighborhood of the predissociation effect at the D level at 42,485 cm^{-1} and of the slightly higher convergence limit of this level, the atomic term combinations are so numerous as a result of this coordination that one cannot decide which of them is responsible for the effects. The bond energy of the ground state counted from the $^2D_{3/2}+^2D_{3/2}$ term combination is 15,860 cm^{-1}, the bond energy of the B state counted from the $^2D_{5/2}+^2P_{1/2}$ term combination is 12,375 cm^{-1}. Almy and Sparks calculate by extrapolation for the bond energy of the ground state 14,900 cm^{-1}, while linear extrapolation would give 23,100 cm^{-1}; for the bond energy of the B state they calculate 11,516 cm^{-1}, the linear extrapolated value being 14,600 cm^{-1}.

The dissociation schemes of PO, AsO, SbO, and BiO should also show a corresponding analogy with that of NO, though there are much less available data for these molecules. According to the NO dissociation scheme of Schmid and Gerö,[1-3] the $NO(X\,^2\Pi)$ ground state dissociates into $N(^3D)+O(^3P)$ atoms with a bond energy of 53,800 cm^{-1}. The analogous term combination should also correspond to the convergence limit of the ground states of PO, AsO, SbO, and BiO. This view is fairly well supported by the increasing spin splitting of the $X\,^2\Pi$-ground states of these molecules which is 120.9 cm^{-1} for NO, 224 cm^{-1} for PO, 1024 cm^{-1} for AsO, 2272 cm^{-1} for SbO. These are comparable with the spin splitting of the corresponding ^2D terms which are 7 cm^{-1} for N, 14.6 cm^{-1} for P, 322.2 cm^{-1} for As, 1341.6 cm^{-1} for Sb, 4019 cm^{-1} for Bi,

but could hardly be understood if the molecular ground states dissociated into ^4S atoms and $O(^3P)$.

In the case of AsO we can identify the $As(^2D)+O(^3P)$ atomic term combination with the energy height of the observed predissociation effect[8] at approximately 39,900 cm^{-1}, this value also yielding the bond energy of the AsO ground state. For PO an interpolation between the values for NO and AsO yields for this bond energy 43,000 cm^{-1}. The corresponding approximate values for SbO and BiO result in 37,000 cm^{-1} and 35,000 cm^{-1} from a vibrational extrapolation of the levels of the ground state. All these bond energy values lie between the corresponding bond energy of the N_2, P_2, As_2, Sb_2, and Bi_2 molecules and the 40,990 cm^{-1} bond energy of O_2.

* This manuscript is published posthumously as Dr. Gerö is deceased.
[1] R. F. Schmid and L. Gerö, Csillagászati Lapok **6**, 101 (1943).
[2] R. Schmid and L. Gerö, Matematikai és Természettudományi Értesitö **62**, 408, 416 (1943).
[3] L. Gerö and R. Schmid, Proc. Phys. Soc. **60**, 533 (1948).
[4] G. Herzberg, Ann. d. Physik (5) **15**, 677 (1932).
[5] G. M. Almy and G. D. Kinzer, Phys. Rev. **47**, 721 (1935); **52**, 814 (1937).
[6] S. M. Naudé, Phys. Rev. **45**, 280 (1934).
[7] G. M. Almy and F. M. Sparks, Phys. Rev. **44**, 365 (1933).
[8] F. A. Jenkins and L. A. Strait, Phys. Rev. **47**, 136 (1935).

The Thermodynamic Properties of Activated Complexes

E. BRUNNER
Shell Development Company, Emeryville, California
October 4, 1948

THE standard free energy of activation, $\Delta F\ddagger$, is currently introduced into the theory of rate processes by the definition[1]

$$\Delta F\ddagger = -RT \log K\ddagger. \tag{1}$$

$K\ddagger$ is regarded as the equilibrium constant for the activated complex and is related to the rate constant k by

$$k = (kT/h)K\ddagger. \tag{2}$$

The other thermodynamic properties of the activated complex are defined analogously. However, the frequency kT/h enters the theory of rate processes in a conventional rather than in a significant way. This circumstance severely limits the usefulness of the thermodynamic quantities so defined; for, although the thermodynamic properties of the activated complexes of different reactions of the same order might be compared with each other, they cannot be significantly compared with the thermodynamic quantities for complete processes, in the definitions of which the conventional frequency kT/h does not enter.

To obtain Eq. (2), the rate constant is first factored as follows:[1]

$$k = (1/\delta)(kT/2\pi m^*)^{\frac{1}{2}} K_c, \tag{3}$$

where m^* is the mass associated with the reaction coordinate, δ is the length of the pass in the potential energy hypersurface that defines the activated complex, and K_c is the equilibrium constant for the activated complex defined in the ordinary way. Then that part of the phase integral over the region of phase space representing the system as an activated complex that arises from integration over the reaction coordinate and its conjugate momentum, is factored out of K_c, leaving the quotient $K\ddagger$. The phase integral is calculated in the usual way with the result

$$K_c = (\delta/h)(2\pi m^* kT)^{\frac{1}{2}} K\ddagger. \tag{4}$$

Equation (2) follows from (3) and (4). The conventional character of kT/h in the present theory is revealed by this derivation, for kT/h involves the weight factor used in forming the averages of statistical mechanics, and physical significance can never be ascribed to the weight factors used in forming averages, but only to their ratios.

It is possible, with the help of Eq. (3), to introduce thermodynamic properties for the activated complex that do not involve the conventional frequency kT/h, the definition for the standard free energy of activation being, for example,

$$\Delta F_c = -RT \log K_c. \tag{5}$$

It is suggested that the quantities defined in this way may prove more useful than those as currently defined. The proposed quantities are less convenient for purposes of tabulation than those as currently defined, for they involve the quantities δ and m^* that one may not always know, but they would seem to offer greater scope for the formulation of significant relationships. The proposed definitions are applicable only to those cases in which a reasonably definite value of δ exists (whether or not it be known). But in the opposite cases—in those cases, namely, in which the pass in the potential energy hypersurface that defines the activated complex is not sufficiently long and flat and does not fall sufficiently steeply at the ends to determine a reasonably definite value for δ—one may seriously doubt that the activated complex partakes sufficiently of the nature of an ordinary molecule, with thermodynamic properties of its own, to make any definition for its thermodynamic properties other than misleading.

[1] Glasstone, Laidler, and Eyring, *The Theory of Rate Processes* (McGraw-Hill Book Company, Inc., New York, 1941), Chapter 4.

The Correlation between Viscosity and Energy of Vaporization

E. BRUNNER
Shell Development Company, Emeryville, California
October 4, 1948

THE following equation has been proposed[1] as an approximate relation between the viscosity, η, of a liquid and its energy of vaporization, ΔE_v:

$$\eta = \frac{h}{v} e^{\Delta E_v/\alpha RT}. \tag{1}$$

Here v represents the molecular volume of the liquid and α is an empirical constant. The occurrence of Planck's constant in this relation, in such a way that it cannot be removed by altering the value of α, is surprising, for neither viscosity nor vaporization is ordinarily regarded as a quantum effect.

Equation (1) is obtained from the equation

$$\eta = \frac{h}{v} e^{\Delta F\ddagger/RT}, \tag{2}$$

of the rate process theory of flow by an argument that the free energy of activation for flow might be expected to be some fraction of the energy of vaporization. However, $\Delta F\ddagger$ cannot be significantly compared with an ordinary thermodynamic quantity, such as ΔE_v, that does not involve the conventional frequency kT/h.[2] The occurrence of Planck's constant in Eq. (1) simply calls attention to this fact.

Although the argument that the free energy of activation for flow should be a fraction of ΔE_v cannot apply to the quantity $\Delta F\ddagger$, it conceivably might apply to the quantity ΔF_c as defined in reference 2. The relation between $\Delta F\ddagger$ and ΔF_c is readily found to be $\Delta F\ddagger - \Delta F_c = RT \log\{\delta/h(2\pi m^* kT)^{\frac{1}{2}}\}$, so that Eq. (2) can be written

$$\eta = \frac{\delta}{v}(2\pi m^* kT)^{\frac{1}{2}} e^{\Delta F_c/RT}. \tag{3}$$

The quantities m^* and δ are defined in reference 2.

In order to obtain an equation analogous to (1) that might be compared with experiment, we have not only to replace ΔF_c by a fraction $\Delta E_v/\beta$ of the energy of vaporization but also to replace m^* and δ by observed quantities. We may

reasonably replace m^* by the molecular mass m, and at least as a rough approximation we may suppose that δ is for all liquids the same fraction $bv^{\frac{1}{3}}$ of the mean molecular distance. Making these substitutions we get for comparison with experiment:

$$\eta = b\frac{(2\pi mkT)^{\frac{1}{2}}}{v^{\frac{1}{3}}}e^{\Delta E_v/\beta RT}. \quad (4)$$

Equations (1) and (4) were compared with the experimental data for 67 liquids. The quantity h in Eq. (1) was treated as an adjustable empirical constant. A least squares solution with respect to $\log\eta$ gave the following values for the parameters: $\alpha=2.84$, $h=1.41\times10^{-26}$ erg sec., $\beta=3.26$, $b=0.075$. The value found for α does not differ greatly from the value 2.45 obtained by Eyring and collaborators by restraining h to be Planck's constant. The value found for b does not seem inconsistent with its interpretation as the fraction of the mean molecular distance to be ascribed to the activated complex, although the interpretation of the length δ is not so clear in the case of a flowing liquid as in the case of a chemical reaction, where it may be related to a feature of the in principle calculable potential energy hypersurface.

The root mean square deviations of the common logarithm of η as calculated for the 67 liquids by Eqs. (1) and (4) were 0.250 and 0.189, respectively. The precision with which these equations represent the experimental data is accordingly not great. In view of the complexity of the liquid state and the consequent obscurity that surrounds the quantities δ and ΔF_e, one may hesitate to ascribe much significance to the fact that Eq. (4) represents the data appreciably better than does Eq. (1); but it is satisfying that, of the two equations, the one whose form does not suggest that viscosity is a quantum phenomenon and whose derivation seems the more nearly understandable, does represent the data at least as well as the other.

[1] Glasstone, Laidler, and Eyring, *The Theory of Rate Processes* (McGraw-Hill Book Company, Inc., New York, 1941), pp. 491–493.
[2] E. Brunner, "The thermodynamic properties of activated complexes," J. Chem. Phys. **17**, 347 (1949).

Effect of Limiting Summation over Vibrational Levels on Calculations of Thermodynamic Properties

HAROLD W. WOOLLEY
National Bureau of Standards, Washington, D. C.
January 3, 1949

A NUMBER of laboratories are engaged in computing thermodynamic functions for simple polyatomic molecules by direct summation over the vibrational levels. The writer has had occasion to inquire as to the error introduced by stopping such summations at too low a total vibrational energy. The result for the simple case of harmonic oscillators may be of interest to readers contemplating such calculations.

For a single harmonic oscillator, the summation over all levels gives $Q_H=(1-e^{-hc\omega/kT})^{-1}$, and if levels above W wave numbers are omitted, the partition function as calculated will be $Q=Q_H(1-e^{-hcW/kT})$. In an actual computation, one might be tempted to assume that essentially the same relative error would be introduced in the case of a polyatomic molecule by stopping the summation when the combined energy of its several assumed harmonic oscillators has reached the value W. While such a relation between errors could be expected if the summation included all levels for which the energy of each component oscillator was less than W, actual summations would scarcely be carried out with such an irregular total energy of cut-off. With a uniform energy of cut-off, the situation is somewhat less favorable.

The proper estimate may be made readily by noting that the summations are made over the points of a hyperlattice, using only points in the positive domain of v_i's, limited by the hyperplane $E=\sum_{i=1}^{n}\omega_i v_i$. The number of modes of vibration is n, so that each component of any degenerate frequency is to be counted. The portion of hyperspace thus bounded has the "volume" $V=\frac{E^n}{n!\Pi_i\omega_i}$, so that the number of states between E and $E+dE$ is $dV=\frac{E^{n-1}dE}{(n-1)!\Pi_i\omega_i}$. The summation over states above $E=W$ is then given approximately by

$$\frac{1}{(n-1)!\Pi_i\omega_i}\int_W^\infty e^{-hcE/kT}E^{n-1}dE=\Pi_i\left(\frac{kT}{hc\omega_i}\right)\cdot e^{-y}\sum_{m=0}^{n-1}\frac{1}{m!}y^m,$$

where $y=hcW/kT$. With Q_H representing the result of complete summation for all levels of the oscillators, the partition function actually obtained using levels only up to $E=W$ will be

$$Q=Q_H(1-\rho e^{-y}),$$

where $\rho=\sum_{m=0}^{n-1}\frac{1}{m!}y^m$. In regard to calculations for very high temperatures ($y\ll1$), it is of interest that ρ, the multiplier of e^{-y}, is composed of the early terms of the power series development for e^y. For the moderate temperatures for which calculations are made, e^{-y} is made small by making y of the order of magnitude of a sizeable integer. Under these conditions ρ becomes a considerable magnitude.

The approximate effect on the thermodynamic functions due to neglect of high levels is readily expressed in terms of the effect for a single oscillator. For the single harmonic oscillator with levels cut off at W wave numbers, the error would be

$$\Delta(-F^0/RT)_1=\ln(1-e^{-y})\simeq-e^{-y},$$

where $y=hcW/kT$,

$$\Delta(H^0/RT)_1=-ye^{-y}/(1-e^{-y}),$$

and

$$\Delta(C_p^0/R)_1=-y^2e^{-y}/(1-e^{-y})^2.$$

For a system of n modes of vibration with levels cut off at W wave numbers

$$\Delta(-F^0/RT)_n=\Delta(-F^0/RT)_1\cdot\rho$$

$$\Delta(H^0/RT)_n=\Delta(H^0/RT)_1\cdot\left(\frac{1-e^{-y}}{1-\rho e^{-y}}\right)\frac{y^{n-1}}{(n-1)!},$$

and

$$\Delta(C_p^0/R)_n=\Delta(C_p^0/R)_1\cdot\left(\frac{1-e^{-y}}{1-\rho e^{-y}}\right)^2\left[\frac{y^{n-1}}{(n-1)!}-\frac{y^{n-2}}{(n-2)!}\right],$$

approximately, for $n>1$.

In Table I, a few rough values are given to compare the cut-off error for a molecule with four vibrational degrees of freedom ($n=4$) with that for a single degree of freedom

TABLE I. Effect of cut-off on thermodynamic functions for harmonic oscillators (for one and for four vibrational modes).

Boltzmann factor e^{-y}	$\Delta(-F^0/RT)_n$ $(n=1)$	$(n=4)$	Ratio
10^{-4}	0.0001	0.0183	183
10^{-5}	0.00001	0.0033	333
10^{-6}	0.000001	0.00055	550
	$\Delta(H^0/RT)_n$		
e^{-y}	$(n=1)$	$(n=4)$	Ratio
10^{-4}	0.0009	0.12	133
10^{-5}	0.000115	0.029	255
10^{-6}	0.000014	0.0061	440
	$\Delta(C_p^0/R)_n$		
e^{-y}	$(n=1)$	$(n=4)$	Ratio
10^{-4}	0.0085	0.77	91
10^{-5}	0.0013	0.25	189
10^{-6}	0.00019	0.07	344

($n=1$). The four degrees of freedom might, for example, be for two non-degenerate vibrations and one doubly degenerate vibration. It is seen that for the molecule with four vibrational modes, the summation would have to extend above the point where the Boltzmann factor is 10^{-6} in order to avoid introducing an error in C_p^0 as large as 0.1 cal. deg.$^{-1}$ mole^{-1}, because of the presence of a multiplying factor in excess of 300. The situation would be modified appreciably in the case where effects of anharmonicity were included, so that the present results do not apply quantitatively for that case.

In conclusion, it should be noted that the multiplying factors for the errors increase very rapidly in passing to molecules with a larger number of atoms.

Salt Effects on Ionic Equilibria

A. R. Olson and T. R. Simonson
University of California, Berkeley, California
January 11, 1949

ABOUT three months ago, we submitted a paper concerning the effects of salts on the rates of ionic reactions in aqueous solution for publication in this journal. In this paper we demonstrated that for a reaction between ions of like sign, the specific rate does not depend upon the ionic strength of the solution. It does depend upon the concentrations and characters of the ions of sign opposite to that of the reactants.

As a logical consequence of this fact, we could expect to find that an equilibrium between ions of the same sign would also be independent of the ionic strength. We now announce that this has been experimentally proved to be so.

The equilibrium studied is $Fe^{+++}+H_2O \rightleftarrows FeOH^{++}+H^+$, in dilute perchloric acid solution (about $0.002M$). The absorption spectra of Fe^{+++} and of $FeOH^{++}$ are sufficiently different in the region $\lambda=3500$A to $\lambda=2500$A so that concentration changes can easily be observed even at high dilution (about $3\times10^{-4}M$ in iron), by the use of a quartz spectrophotometer. It was found that the addition of $NaClO_4$ and $La(ClO_4)_3$ produced identical shifts of equilibrium for identical normalities and that the addition of $NaClO_4$ produced a much greater change than did the addition of $La(ClO_4)_3$ of such an amount as to result in the same ionic strength. The lanthanum solution in each case was about $0.003M$. In every experiment the shift was such as to cause an increase in the Fe^{+++} concentration.

It is obvious that if these experiments are independently verified, it will be necessary to restudy the Debye-Hückel approach to the calculation of the acitivity coefficients of ions. The details of these experiments will be submitted for publication soon.

Note on the Coefficient of the Term $\Pi\beta_k^{n_k}$ in the Cluster Integral b_l in Mayer's Condensation Theory

Tzu-Ching Huang*
Department of Chemistry, National Tsing Hua University, Peiping, China
January 5, 1949

THE cluster integral b_l in Mayer's Condensation Theory is the integral over the configuration space of l particles of a sum of products of functions f_{ij} between the particles i and j.[1] It can be analyzed into a sum of products of irreducible integrals β_k's, where β_k is defined as the integral over the configuration space of $k+1$ particles, multiplied by a normalization factor.[2] Thus b_l can be written as follows:

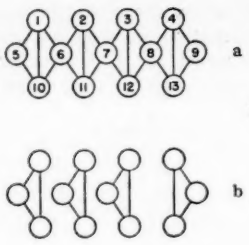

FIG. 1.

$$b_l=\frac{1}{l!}\sum_s K_s\prod_k(k!\beta_k)^{n_k}, \tag{1}$$

$$\Sigma k n_k=l-1,$$

in which n_k is the power with which β_k occurs in the term b_l, and K_s is the coefficient to be determined. Using a physical picture of "bolting the frames," Mayer and Harrison obtained the following result,[3]

$$K_s=\frac{1}{l^{2-n}}\frac{l!}{\prod_k(k!)^{n_k}n_k!}. \tag{2}$$

The meaning of n will be given later. The following derivation of Eq. (2) is essentially based upon the idea of Mayer and Harrison, but it does get rid of "frames," "bolts," "washers," etc. and is therefore quite simple.

A singly connected cluster can be transformed into a number of more-than-singly connected clusters by removing one molecule away from the former. (The terms "singly connected cluster" and "more-than-singly connected cluster" have been clearly defined in Mayer and Mayer's book.[4]) Thus, by taking molecule 8 away from Fig. 1a, the singly connected cluster is changed into four more-than-singly connected clusters (Fig. 1b), and by taking molecule 5 away from Fig. 2a, the singly connected cluster is changed into five more-than-singly connected clusters (Fig. 2b). Let n be the total number of more-than-singly connected clusters formed from a singly connected cluster of l molecules. Then

$$\Sigma n_k=n. \tag{3}$$

Let L_s be the number of ways of placing the numbered molecules into the more-than-singly connected clusters, and M_s be the number of ways of joining together these clusters to form a singly connected cluster. Since there are l ways of removing one molecule, K_s in Eq. (1) becomes

$$K_s=(1/l)L_sM_s. \tag{4}$$

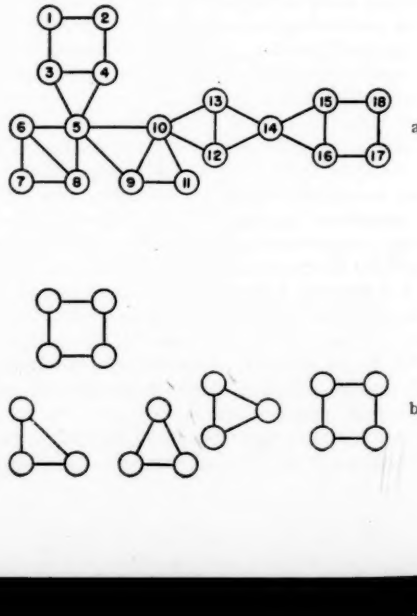

FIG. 2.

[1] J. E. Mayer, J. Chem. Phys. 5, 67 (1937).
[2] J. E. Mayer and P. G. Harrison, J. Chem. Phys. 6, 87 (1938).
[3] See reference 2, p. 94.
[4] See reference 1, p. 337.

The value of L_s is

$$L_s=[l!/(\Pi_k(k!)^{n_k}n_k!)], \quad (5)$$

since the permutation between the molecules with in each more-than-singly connected cluster and the permutation between clusters of identical number of molecules do not lead to new arrangements.

To find M_s, we notice that there are always $n-1$ molecules common to n more-than-singly connected clusters. If a molecule joins up p clusters, it is counted as $p-1$ molecules. Thus in Fig. 1, $n=4$ and $n-1=3$, namely, molecules 6, 7, and 8. In Fig. 2, $n=5$ and $n-1=4$, namely, molecules 5, 10, and 14, molecule 5 being considered as two molecules since it connects up three clusters. Since there are $n-1$ molecules common to the more-than-singly connected clusters and since the singly connected cluster can be formed by putting in any one of the l molecules, it follows

$$M_s=l^{n-1}. \quad (6)$$

If we put Eqs. (5) and (6) into Eq. (4), we get Eq. (2). From Eq. (3), we see that

$$l^n=\prod_k l^{n_k}. \quad (7)$$

Substituting Eq. (7) into Eq. (2) and putting the result in Eq. (1), we obtain finally

$$b_l=\frac{1}{l^2}\sum_{n_k}\prod_k\frac{(l\beta_k)^{n_k}}{n_k!}, \quad (8)$$

$$\Sigma_k k n_k=l-1\cdot$$

* On leave of absence at the California Institute of Technology, Pasadena, California.

[1] J. E. Mayer and M. G. Mayer, *Statistical Mechanics* (John Wiley & Sons, Inc., New York, 1940), p. 280, Eq. (13.5).
[2] See reference 1, p. 287, Eq. (13.25).
[3] See reference 1, pp. 455–459.
[4] See reference 1, pp. 285–288.

Vibrational Fine Structure in the Absorption Spectra of Uranyl and Plutonyl Ions in Aqueous Solution*

M. KASHA
Department of Chemistry, University of California, Berkeley, California
January 17, 1949

THE absorption spectrum of uranyl ion, UO_2^{++}, in aqueous solution at 25°C is unusual in several respects. Uranium in its hexavalent oxidation state has no 5*f* electrons, so that the weak and narrow absorption bands (characteristic of transitions within the *f* shell) which occur in the solution spectra of U(*III*) and U(*IV*) are absent. However, the electronic transition corresponding to the absorption band centering about 4100A is forbidden as is evident from the low value of the max. molar absorption coefficient ($\epsilon=8.5$), and is further distinguished by a discrete, though diffuse, regular vibrational structure (Fig. 1, upper part). The band separations of 11 peaks have a mean value of 724 cm^{-1} for the solution spectrum, which must correspond to the 710-cm^{-1} interval found in the absorption spectrum of crystalline uranyl salts.[1] In the fluorescence spectrum of uranyl salts[2] the main intervals are 860 cm^{-1} and are ascribed to the totally symmetric vibration of the O−U−O molecule, for which a Raman shift of 865 cm^{-1} is observed.[3,4] The 710-cm^{-1} frequency is for the vibration of the molecule in its electronically excited state corresponding to the 865-cm^{-1} vibration of the molecule in its ground electronic state. A recent comparison of the uranyl vibrational data has been made by Freymann.[5]

It is known from chemical evidence that the Pu(*VI*) ion is oxygenated and probably has the formula PuO_2^{++}. Hence it seemed possible that a band analogous to the uranyl absorption band described above could be found also in the spectrum

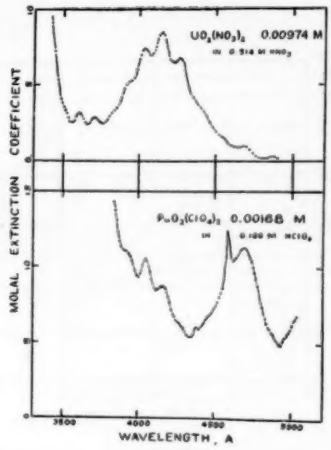

FIG. 1. A section of the absorption spectra of uranyl and plutonyl ions in aqueous solution, showing diffuse vibrational fine structure.

of plutonyl ion in solution. The absorption spectrum of aqueous plutonyl ion is very complex, consisting of many weak and exceptionally narrow bands throughout the visible and adjacent spectral regions. Nevertheless, the expected absorption band with vibrational-like fine structure was found in the 3900–4300A region for a solution of Pu(*VI*) in 0.1*M* perchloric acid (Fig. 1, lower part). The same structure is seen somewhat less distinctly in the spectrum of Pu(*VI*) in nitric acid solution,[6] but is obscured in the spectrum of hydrochloric acid solutions of Pu(*VI*), owing to strong absorption in the same region by Pu(*VI*)-chloride-complexes.

Starting with the 3940A band of PuO_2^{++}, successive frequency intervals of 690, 710, 725 cm^{-1} are found, giving a mean value of 708 cm^{-1}, which must correspond to a O−Pu−O vibration in an electronically excited state of plutonyl. A study of the Raman spectrum of plutonyl ion should reveal a frequency shift corresponding to this vibration in the ground state; it should have a value of about 830 cm^{-1}, analogous to the totally symmetric uranyl vibration frequency.

* Abstracted from a report to be published in the *Plutonium Project Record, National Nuclear Energy Series*, Atomic Energy Commission Documents MDDC-591 and MDDC-892, July 1946, Oak Ridge, Tennessee.

[1] A. C. S. van Heel, Commun. Phys. Lab. Univ. Leiden **187**, 3 (1938).
[2] B. S. Satyanarayana, J. Mysore Univ. **4**, 57 (1943).
[3] G. K. T. Conn and C. K. Wu, Trans. Faraday Soc. **34**, 1483 (1938).
[4] B. S. Satyanarayana, Proc. Ind. Acad. Sci. **A15**, 414 (1942).
[5] M. Freymann, J. de phys. et rad. **9**, 158 (1948).
[6] This has been confirmed recently by R. H. Betts and B. G. Harvey, J. Chem. Phys. **16**, 1089 (1948).

Difference in the Recoil Energy of the Br^{80} Isomers Following Neutron Capture

PAUL P. CAPRON, EDGARD CRÈVECOEUR, AND MAURICE FAES
Institut Interuniversitaire de Physique Nucléaire, Université de Louvain, Louvain, Belgium
January 18, 1949

FOR Br^{80} (18 min.) and for Br^{80} (4.5 hr.) W. H. Hamill and R. R. Williams[1] have found 0.08 and 0.00 as values for the ratio k_6/k_7 where k_6 and k_7 are defined, according Eqs. (1) and (2):

$$HBr+n\xrightarrow{k_6}HBr^*, \quad (1)$$

$$HBr+n\xrightarrow{k_7}H+Br^*. \quad (2)$$

This result is in agreement with experiments we are going to describe briefly, showing that the complex nucleus emits γ-rays in cascade so that the recoil energy of the Br^{80} (18 min.) nucleus is smaller than the recoil energy of the Br^{80} (4.5 hr.) nucleus. As a consequence of this, the probability of molecular dissociation is different and also the charge and the nature of the produced ions.

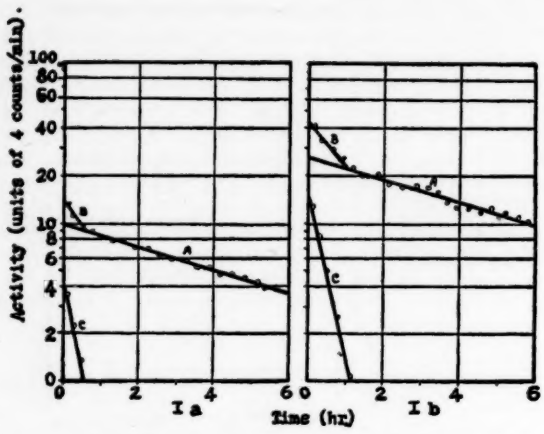

FIG. 1. Isomeric filiation: Ia—Without electric field. Ib—With electric field on the anode. A. Bromine—4.5-hr. activity. B. Bromine—17.4-min. and 4.5-hr. activities. C. Bromine—17.4-min. activity.

TABLE I.

T	Theoretical	$R_0{}^T$ In CBr_4 solid	In C_6H_5Br liquid	Collected on gold plates in C_6H_5Br liquid		
				With field an.	With field cath.	Without field
15 min.	33.26	35.8				
30 min.	26.54	26.3				
45 min.	21.72	19.5				
60 min.	18.20			9.5	11.4	7.34
120 min.	10.83	10.1				
360 min.	4.86		4.78	1.7	1.1	1.1
96 hr.	2.92			0.7	0.5	

If we take into account a difference of 86 kev[2] between the ground state (18 min.) and the metastable state (4.5 hr.), we find by a semi-empirical formula[3] that the binding energy of the $Br^{79}(n,\gamma)Br^{80}$ process is 7.24 Mev for the Br^{80} (18 min.) and 7.154 Mev for the Br^{80} (4.5 hr.). If the full binding energy is emitted as a single γ-ray, the recoil energy would be Er(18 min.)=351 ev and Er(4.5 hr.)=343 ev. It is well known that this is highly improbable and that the emission is rather in cascade.[4] If the isomers come from the same capture level, the recoil energy will be the same if the first γ-rays are identically emitted as these determine principally the recoil. Experiments show it is not true.

In a first series of experiments in liquid C_6H_5Br we confirmed the results obtained by one of us[5] showing separation of the isomers in the electric field during the isomeric transition. After irradiation of 15 hours, the solution is submitted to an electric field (210 volts/cm) for three hours, the electrodes used are gold plates, 2 cm apart. Three hours after irradiation all the Br (18 min.) directly formed had gone, and the Br (18 min.) collected on the plates is produced by isomeric filiation. The same experiment made without a field shows clearly that the effect is amplified with a field and that the Br^{80} (18 min.) is specially collected on the anode. Examples are in Fig. 1.

In a second series of experiments we have studied the primary reaction of the formation of the two isomers of Br^{80} by measuring for different periods of irradiation the ratio of the activity of the two isomers:

R=activity (18 min.)/activity (4.5 hr.).

(a) The total activities produced in CBr_4 solid and C_6H_5Br liquid are independent of the recoil effect.

(b) The activities collected on plates immerged in C_6H_5Br liquid with an electric field are, however, dependent upon the recoil effect and the charge of the ions.

If we call T the period of irradiation and t the time from the end of the irradiation, one finds for the ratio:[6]

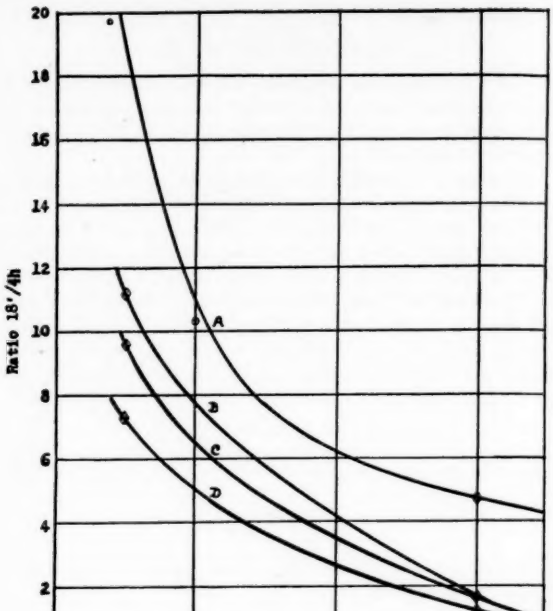

FIG. 2. A. Theoretical curve—experimental point: ○ with CBr_4 solid; ◇ with C_6H_5Br liquid. B. Collected on gold plates with electric field: cathode. C. Collected on gold plates with electric field: anode. D. Collected on gold plates without electric field.

$$R_t{}^T=\frac{\sigma_c(18\text{ min.})b_T e^{-\lambda_2 t}}{\sigma_c(4.5\text{ hr.})(\lambda_1/\lambda_2-\lambda_1)\{a_T{}^T e^{-\lambda_1 t}-b_T e^{-\lambda_2 t}\}} \quad (3)$$

with $t=0$, and T large Eq. (3) reduce to Eq. (4):

$$R_0{}^T=\frac{\sigma_c(18\text{ min.})}{\sigma_c(4.5\text{ hr.})}\cdot\frac{(1-e^{-\lambda_2 T})}{(1-e^{-\lambda_1 T})}=R^\infty\frac{1-e^{-\lambda_2 T}}{1-e^{-\lambda_1 T}}, \quad (4)$$

where λ_2 and λ_1 are the radioactive constants for Br^{80} (18 min.) and Br^{80} (4.5 hr.); σ_e are the capture cross sections and $R^\infty=2.92$.

Table I and Fig. 2 show the results of the experiments.

The results show clearly that the isomers are not collected on the electrodes in the ratio of their formations. The capture cross sections of these isomers are in the ratio 2.92 to 1 at the advantage of the Br^{80} (18 min.). Indeed, less (18 min.) are collected on the electrodes. These results show also that it is difficult to get a clear idea of the nature of the ions.

We know that the ratio of the capture cross sections varies with the energy of the incident neutrons[7] and we may find an explanation if we assume that from a single capture level the first and most energetic γ-ray determine the recoil and the cascade leading to one of the isomeric states. For example, we can imagine that the γ-ray of 0.35 of the available energy (the most probable)[4] will give the Br^{80} (18 min.) state, while the γ-ray 0.6 of the available energy is three times less probable giving Br^{80} (4.5 hr.). The authors know that many other explanations are possible and for this reason experiments must be made where the recoil effect will be studied in gaseous form at low pressure. Working with radioactive bromine (4.5 hr.) we expect to measure the charge of Br^{80} (18 min.) at birth from the isomeric transition. These experiments are in progress.

[1] W. H. Hamill and R. R. Williams, J. Chem. Phys. **16**, 1171 (1948).
[2] A. Berthelot, Ann. de physique **19**, 117 (1944).
[3] Clark Goodman, *The Science of Nuclear Power* (1947), p. 77.
[4] H. A. Bethe, Rev. Mod. Phys. **9**, 233 (1937).
[5] Paul Capron, G. Stokkink, and M. van Meersche, Nature **157**, 806 (1946).
[6] Paul Capron and G. Stokkink, Bull. Acad. Roy. Belg. **32**, 266 (1946).
[7] Paul Capron, Bull. Acad. Roy. Belg. **27**, 524 (1941).